IN VITRO MODELLING OF HUMAN MICROGLIAL ALTERATIONS ASSOCIATED WITH ALZHEIMER'S DISEASE AND POLYGENIC RISK

A thesis submitted for the degree of

Doctor of Philosophy (PhD)

by

Elisa Salis

2022

Alla mia dolcissima Nonna Maria

ABSTRACT

It is increasingly clear that Alzheimer's Disease (AD) presents with a strong genetic component. Recent Genome Wide Association Studies (GWAS) uncovered a huge number of polymorphisms associated with the disease which cumulative effect can be captured by the calculation of the polygenic risk score (PRS). PRS allows the identification of those at the highest and lowest risk of disease, opening new avenues for the understanding of the neurodegenerative processes and protective mechanisms. Samples collected from individuals identified at the extremes of the score can be used to generate stem cells models to investigate molecular mechanisms of the disease on the induced pluripotent stem cell (iPSC)-derived models such as microglial-like cells. In the first part of this study, a cohort of cryopreserved peripheral blood mononuclear cells (PBMC) samples collected from individuals originally sampled for GWAS and identified to have with high or low PRS for AD were used. These samples, collected more than 10 years ago resulted to have suboptimal quality, requiring several protocols and attempts to recover viability and cell number. One of these methods resulted in the successful reprogramming of several samples into iPSCs and their extensively characterisation.

One of the most interesting discovery of recent GWAS is the novel R522 variant located in the *PLCG2* gene which encode for the phospholipase Cγ2 enzyme, mainly expressed in microglia cells. To set the ground for functional studies, two different iPSCs-derived microglia differentiation protocols were tested and characterisations were carried out. Moreover, phenotypic characterization of iPSCs-derived cortical neurons and astrocytes were completed. iPSCs-derived cortical neurons were used to established neuronal-microglia co-culture system; iPSCs-derived astrocyte were used to prepare the astrocyte-conditioned medium (ACM) used to feed cells. PLCγ2^{R522} variant has been associated with decreased risk of developing late onset AD, and it represents the first classically drug-targetable

molecule identified in LOAD genetic studies. Results of this study show that a model of iPSCs-derived microglia-like cells harbouring the PLCG2^{R522} SNP displays an altered neuroinflammatory response upon several different stimuli, such as LPS, oAβ, zymosan and ATP/ADP, in comparison to the common PLCG2^{P522} variant. Different outputs were analysed , including the secretion of cytokines (IL-6, TNF, GCSF, IL10), the possible involvement of NLRP3 inflammasome (IL1β), the levels of NO and the calcium response. Taken together the results support the hypothesis of a protective role of PLCγ2^{R522} variant in the context of AD, via reducing the neuro inflammatory burden in response to several stimuli.

ABBREVIATIONS

Aβ	Amyloid β
oAβ	Amyloid β oligomers
AAVS1	Adeno-associated virus integration site 1
ABI3	Abelson-interactor gene family member 3
ACM	Astrocyte Conditioned Media
AD	Alzheimer's disease
ADGC	AD Genetics Consortium
ADP	Adenosine diphosphate
AGM	Aorta-gonad mesonephros
ANOVA	Analysis of variance
APC	Astrocyte precursor cells
APLAID	Autoinflammation PLCγ2-associated antibody deficiency and immune dysregulation
ApoE	Apolipoprotein E
APP	Amyloid precursor protein
ATP	Adenosine triphosphate
BDNF	Brain-derived neurotrophic factor
BMDM	Bone-marrow derived macrophages
BMP4	Bone morphogenetic protein 4
Ca^{2+}	Calcium ion
CCL	Chemokine (C-C motif) ligand
CD	Cluster of differentiation

CHARGE	Cohorts or Heart and Aging Research in Genomic Epidemiology
Cl^-	Chloride ion
CLU	Clusterin
CNS	Central nervous system
CNTF	Ciliary neurotrophic factor
CNV	Copy Number Variation
CR1	Complement receptor type 1
CRISPR	Clustered regularly interspaces short palindromic repeats
CSF	Cerebral spinal fluid
CX3CR1	CX3C chemokine receptor 1 (or fractalkine receptor)
DAG	Diacylglycerol
DAMPs	Damage-associated molecular patterns
DAP12	DNAX-activating protein of 12 kDa
DMEM	Dulbecco's Modified Eagle Media
EADI	European AD Initiative
EB	Embryoid Body
EGF	Epidermal growth factor
EMP	Erythro-myeloid progenitors
ER	Endoplasmic reticulum
ESCs	Embryonic stem cells
FAD	Familial AD
FBS	Fetal Bovine Serum
FDA	Food and Drug Administration
FITC	Fluorescein Isothiocyanate

FLK1	Fetal Liver Kinase 1 (also VEGF Receptor)
FLT3	Fms-like tyrosine kinase 3
G-CSF	Granulocyte colony-stimulating factor
GDNF	Glial-derived neurotrophic factor
GERAD	Genetic and Environmental Risk in Alzheimer's Disease Consortium
GFAP	Glial fibrillary acidic protein
GM-CSF	Granulocyte Macrophage Colony Stimulating Factor
GWAS	Genome-wide association studies
HEK	Human Embryonic Kidney 293
HSC	Haematopoietic stem cell
IBA-1	Ionised Calcium-Binding Adapter Molecule 1
ICC	Immunocytochemistry
IFN-γ	Interferon γ
IGAP	International Genomics of Alzheimer's Project
IL	Interleukin
IP_3	Inositol-1,2,3-trisphosphate
iPSCs	Induced Pluripotent Stem Cells
K^+	Potassium ion
KDR	Kinase Insert Domain Receptor
KO	Knockout
L-EPC	Late-outgrowth endothelial progenitor cells
LIF	Leukemia inhibitory factor
LMPs	Lympho-myeloid progenitor
LOAD	Late-onset Alzheimer's disease

LPS	Lipopolysaccharide
MAF	Minor allele frequency
MAPT	Microtubule associated protein tau
MCI	Mild Cognitive Impairment
M-CSF	Macrophage Colony Stimulating Factor
MOI	Multiplicity of infection
mRNA	Messenger RNA
NFIA	Nuclear factor I-A
NFκB	Nuclear factor kappa-light-chain-enhancer of activated B cells
NFTs	Neurofibrillary tangles
NLRP3	NOD-Like Receptor family Pyrin domain 3
NO	Nitric oxide
NOS	Nitric oxide synthases
NPC	Neuronal progenitor cell
OR	Odd Ratio
PAMPs	Pathogen-associated molecular patterns
PB	Peripheral Blood
PBMC	Peripheral blood mononuclear cells
PHA-P	Phytohaemagglutinin
PICALM	Phosphatidylinositol Binding Clathrin Assembly Protein
$PI(4,5)P_2$	Phosphatidylinositol-4,5-bisphosphate
PKC	Protein Kinase C
PLAID	PLCγ2-associated antibody deficiency and immune dysregulation
PLCG2	Phospholipase C Gamma 2

PRR	Pattern recognition receptor
PRS	Polygenic risk score
PSEN	Presenilin
PTMs	Post-translational modifications
P2RX	Purinergic receptor P2X
P2RY	Purinergic receptor P2Y
RNASeq	RNA Sequencing
ROS	Reactive oxygen species
RT	Room Temperature
RUNX1	Runt Related Transcription Factor 1
SAD	Sporadic Alzheimer's Disease
SCF	Stem Cell Factor
SeV	Sendai Virus
SNP	Single nucleotide polymorphism
TCR	T cell receptor
TGF-β	Transforming Growth Factor β
TLRs	Toll Like Receptors
TMEM119	Transmembrane protein 119
TNF	Tumour necrosis factor
TPO	Thrombopoietin
TREM2	Triggering Receptor Expressed on Myeloid Cells 2
VEE	non-infectious Venezuelan equine encephalitis virus
VEGF	Vascular Endothelial Growth Factor
WES	Whole-exome sequencing

WGS	Whole-genome sequencing
WHO	World Health Organization
WT	Wild-type
YS	Yolk sac

TABLE OF CONTENTS

ACKNOWLEDGMENTS

I would like to thank my supervisors Julie and Nick for giving me the opportunity of doing my PhD. I have learned and growth lots both personally and professionally, neither of which would have been possible if you didn't open the door of your labs and gave me the chance to prove myself. A special thanks to Georgina, whose guidance and honesty helped me to overcome the toughest time of this experience. Thank you for always having time to listen to me and finding the right words to put me back on track. And last, but not least, a huge thanks to Phil, who took me on board and adopted me in his group to guide me till the end with the new project.

I would also like to thank the GW4 BioMed Doctoral Training Partnership and the Medical Research Council (MRC) for funding my PhD studentship and Prof. Lesley Jones for her mentorship and her invaluable advices along the way.

This experience would have not been the same without my labmates and all the DRI bunch of amazing people. A special thanks to Nina, Emily, Beth, Elena, Dina, Nikoleta, Meghan, Jincy and Hazel. I could not be more grateful of having you with me in this crazy adventure. And thank you to Olena, for your friendship and support (both practical and mental) in the reprogramming challenge.

Un ringraziamento speciale va ai miei genitori e a mio fratello Riccardo per il loro supporto incondizionato, nonostante la distanza. Senza di voi questo traguardo non sarebbe stato possibile. Saro' per sempre grata per i tanti sacrifici fatti e la fiducia riposta in me. E a voi, amiche mie sparse per l'Italia e non solo: le lunghe videochiamate piene di risate, pianti e sfoghi mi hanno salvata in piu di un'occasione.

Y gracias a Jose, por ser mi roca desde el principio. Gracias por escucharme, por soportarme y para tener la habilidad de hacer salir el sol en dias oscuros.

1 Introduction

1.1 Alzheimer's Disease

1.1.1 Alzheimer's Disease: a modern plague

Alzheimer's Disease (AD) is the most common neurodegenerative disorder and accounts for more than 80% of dementia cases in people over 65 years old (Kumar et al., 2015). It is estimated that over 50 million people live with dementia worldwide, with the potential for this to increase to 152 million by 2050(C., 2018).

In its first stages, it is characterized by a significant and progressive memory loss as the hippocampus preferentially degenerates. As the pathology progresses and reaches the amygdala, the affected person experiences emotional instability and behavioural changes, exhibiting a range of psychological problems. Later in the disease, speech and motor functions deteriorate, hallucinations and seizures may emerge affecting the person's ability to perform everyday activities (Graham et al., 2017, Lane et al., 2018). Disease-modifying treatments are not available yet. Current medications approved by the U.S Food and Drug Administration (FDA) focus on temporarily improving symptoms and delaying the development of the disease. These include acetylcholine esterase inhibitors (donepezil, galantamine and rivastigmine), which are prescribed in the early stages of the disease, and NMDA-type glutamate receptor inhibitors (memantine) which are given in the moderate to severe stage of AD. For these reasons, AD is recognized by the World Health Organization (WHO) as a global health priority since this condition represents a great burden not only for the patients and their families, as the gradual decline leads to a slow deterioration of quality of life, but also for public health due to the large cost of care(Lane et al., 2018, Black et al., 2018). Therefore, there is an incredible need of developing new therapeutic options. In June 2021, the FDA approved Aducanumab, an amyloid beta-directed monoclonal antibody that specifically targets aggregates forms of amyloid beta (Aβ). The approval of this drug, however, is still controversial considering the ambiguous clinical trial results

surrounding its efficacy. The FDA required the pharmaceutical company producer of the drug, Biogen, to perform follow-up studies to see if the drug helps treat the symptoms of Alzheimer's.

The first description of the disease dates back to 1907 when Alois Alzheimer reported the case of a 51-year-old woman, Auguste Deter, who was under his care at the state asylum in Frankfurt (Bondi et al., 2017). He observed intracellular neurofibrillary tangles (NFTs) and extracellular amyloid plaques in the postmortem brain that then became the two hallmarks of the disease. The plaques are mainly made up of small toxic peptides known as Amyloid Beta (Aβ) 40 and Aβ42, which are cleavage products of the amyloid precursor protein (APP), a type I transmembrane protein. The neuronal intracellular tangles are primarily composed of paired helical filaments consisting of hyper-phosphorylated tau (Hardy and Selkoe, 2002).

1.1.2 Genetics of Alzheimer's Disease

AD can be generally classified into two categories: early onset AD and late-onset AD(Tellechea et al., 2018). Early onset AD is typically diagnosed in individuals who develop symptoms before the age of 65(Efthymiou and Goate, 2017). It is estimated that it accounts for 5-6% of the cases of AD, and within the group there is a majority of cases which have been found with polygenic component. Around 1% of early onset AD show a heritability of ~90% and is therefore given the definition of "familial form" of AD (FAD)(Wingo et al., 2012). This form of early onset AD is caused by highly penetrant mutations in three genes: *Amyloid precursor protein* (*APP)*, *Presenilin 1* (*PSEN1)* and *Presenilin 2* (*PSEN2)*, resulting in the differential cleavage of APP and consequent production of several forms of Aβ peptide (Fig. 1.2b) (Sims and Williams, 2016, Zhu et al., 2015). Evidence from these cases led to the formulation of the "amyloid cascade hypothesis", which suggests that Aβ deposition is the initial event in AD pathology (Hardy and Allsop, 1991). This hypothesis led the research field and drug discovery companies to investigate AD molecular mechanisms from an Aβ-centric perspective for the past 30 years, in

order to develop potential drugs to target Aβ(Ricciarelli and Fedele, 2017). However, the large number of unsuccessful clinical trials of anti-Aβ therapies and β- and γ-secretase inhibitors strongly challenged this view (Doody et al., 2014, Salloway et al., 2014, Honig et al., 2018).

The vast majority of AD cases are sporadic with late onset AD (LOAD) which present similar clinical and pathological features of early onset AD, but patients develop symptoms after the age of 65(Efthymiou and Goate, 2017). This is the most common form of the disease and has an estimated heritability of 56-79% (Sims and Williams, 2016), but the high polygenicity of LOAD makes the comprehension of the genetic component much more difficult than the familial form (Van Cauwenberghe et al., 2016). The strongest genetic risk factor for late onset AD is *Apolipoprotein E* (*APOE)*, on chromosome 19, which was identified over 25 years ago (Corder et al., 1993). It exists in three polymorphic alleles – ε2, ε3 and ε4, which are formed from two point mutations within exon 4(Schmid et al., 2019). Disease risk is dose-dependent: people carrying one copy of ε4 allele (ApoE ε3/ε4) show a 3-fold increase of risk of developing AD in comparison to people carrying two ε3 alleles. E3 is the most common isoform and is considered the standard neutral allele for the general population. People homozygous for the ε4 allele (ApoE ε4/ε4) show a 12- fold increased risk of disease development(Corder et al., 1993). In contrast, ApoE ε2, is the rarest allele and it confers a small protective effect(Liu et al., 2013). Even though ApoE contribution to the disease has been extensively studied, the underlying mechanism connecting this gene with AD remains poorly understood.

1.1.2.1 Genome- wide association study and common variants

The complexity of the genetic architecture of AD is becoming increasingly clear thanks to the advent of genome-wide association studies (GWAS). GWAS allow scientists to investigate association between a disease or trait of interest, and virtually all loci in the human genome(Lord et al., 2014). The first novel genetic association was identified in 2009, when variants within the *CR1*, *CLU* and *PICALM*

loci were associated with AD(Harold et al., 2009, Lambert et al., 2009). Since then, GWAS have identified over 60 common risk loci with genome-wide significance ($P < 5 X 10^{-8}$)(Wightman et al., 2021). These common variants (minor allele frequency [MAF] > 0.01)(Naj et al., 2021) have a generally small effect size (odds ratios 1.2) and are often located in intergenic or intronic regions(Grozeva et al., 2019). The identification of the high number of genetic variants known today is due to broad international collaboration within the field, including the Genetic and Environmental Risk in AD (GERAD), the European AD Initiative (EADI), the Cohorts or Heart and Aging Research in Genomic Epidemiology (CHARGE) and the AD Genetics Consortium (ADGC). These mentioned consortia joined to form the International Genomics of Alzheimer's Project (IGAP), which has identified numerous novel GWAS loci(Witoelar et al., 2018, Kunkle et al., 2019a, Lambert et al., 2013). Another recent publication combined data from various databank, to arrive at an overall samples size of 455000 individuals, confirming previous reported loci but also highlighting nine additional loci(Jansen et al., 2019). This common effort of the scientific community, together with decreasing sequencing costs and the increase in sample size, will allow the discovery of more associations in the near future.

1.1.2.2 Rare variants and missing heritability

GWAS have been extremely powerful in identifying trait-associated common variants, which are the variants widely available in the genotyping chips used for GWAS(Lord et al., 2014). It is established, however, that the data from GWAS still do not explain a large proportion (approximately 60%) of the genetic variance of sporadic LOAD(Grozeva et al., 2019). Undoubtedly, new common variants will be discovered with more powerful GWAS; however, most likely this will not explain the full heritability. The remaining heritability of AD can be explained in several ways: rare coding variants ([MAF] ≤ 0.01), non-coding and regulatory variations and epigenetic variants(Lord et al., 2014). The identification or rare variants has proved to be difficult(Grozeva et al., 2019). The power of association testing between a single nucleotide polymorphism (SNP) and disease decreases as the

MAF of the variant decreases(Lord et al., 2014); this means that larger sample sizes will be required in order to detect rare variants associated with the disease.

The main technology for detection of rare variants has been DNA sequencing, either whole- genome sequencing (WGS) or whole-exome sequencing (WES). WGS can be still expensive when conducted on large cohorts, and data handling and storage can be difficult(Lord et al., 2014). WES is distinct from WGS by sampling bases in the protein-coding regions of the genome (the exome). This has the advantage that any identified association can be easily tested with *in silico, in vitro* and *in vivo* models most likely having an appreciable functional effect(Grozeva et al., 2019). Another approach is represented by exome-wide microarrays, which check for variants selected from whole-exome sequencing(Sims et al., 2020). The limitation of this technology is in the fact that it can test only variants that are already known. This approach was used by Sims and colleagues who identified novel coding variants in *PLCG2*, *ABI3* and *TREM2*(Sims et al., 2017). This is important because, despite the small statistical effects, these variants show important biological effects(Magno et al., 2019, Maguire et al., 2021). Finally, selecting extreme phenotypes can help with rare variant discovery, considering these people will most likely be enriched for rare disease-causing variants. For AD specifically, this would mean selecting extremely severe cases or early-onset vs extremely old individuals that are cognitively healthy(Lord et al., 2014)

Identifying rare variants is of paramount importance, considering they generally have a larger effect size on AD risk than common variants.

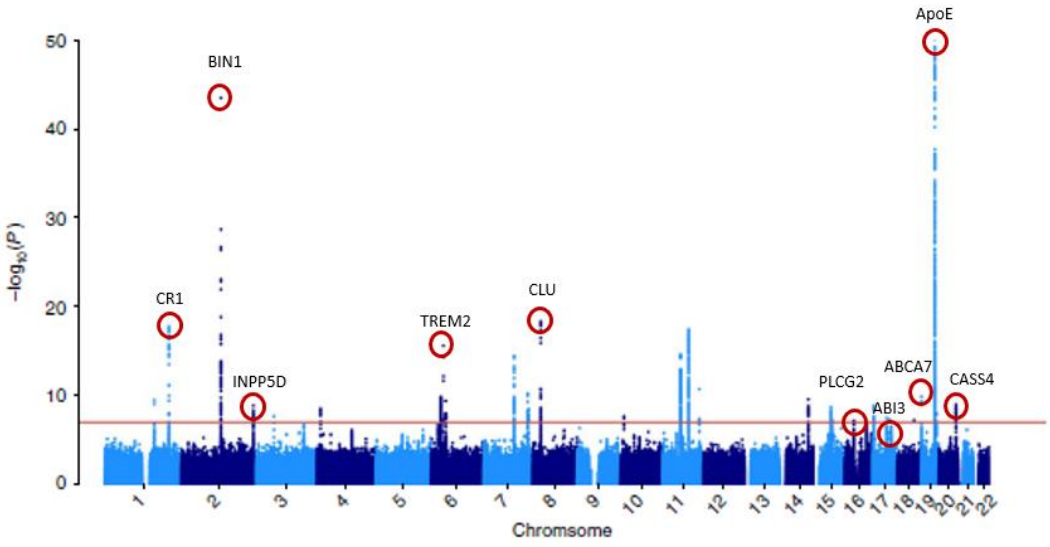

Figure 1.1 – Manhattan Plot showing common and rare variants discovered in recent GWAS – Table adapted from Bertram and Tanzi, 2020

1.1.2.3 Pathway Analysis

The location of the majority of the discovered variants is in non-coding elements of the genome, making it difficult to move from genetic association to biological meaning(Sims et al., 2020). Methods to investigate strong signals in specific sets of genes have helped in identifying possible pathways involved in risk mechanisms. Specifically, these approaches have pointed the attention of researchers towards the evidence that immune system, but also endocytosis and cholesterol metabolism, are strongly implicated in the contribution of AD risk(2015). Moreover, Kunkle and colleagues published one of the largest genome-wide association meta-analysis, including 94.437 individuals who had been diagnosed with late-onset AD. They confirmed 20 previous LOAD risk loci and identified 5 new loci. Pathway analysis of these loci confirms previous finding implicating lipid metabolism and immunity; moreover, they highlight the possible involvement of tau protein and APP metabolism. These results show that genetic variants commonly associated with early-onset autosomal dominant AD might affect LOAD

as well(Kunkle et al., 2019b). Further studies will be needed to confirm the biological meaning of these genetic findings.

1.1.2.4 Polygenic Risk Score

As seen so far, AD is a polygenic disorder with joint contribution from multiple genetic loci. Except for few loci, such as *APOE* and *TREM2*, each disease-associated allele has an estimated effect ranging from 1.1 to 2.1 odds ratio, having a relatively small individual contributions to the disease risk. However, when the susceptibility of all these loci is considered as cumulative, it is possible to predict an AD diagnosis. This cumulative effect can be captured by the polygenic risk score (PRS), which takes into consideration not only all the relevant association discovered by GWAS but also those genetic loci which are hypothesized to lie below the genome-wide significance threshold ($P<5x10^{-8}$)(Sims et al., 2020). It has been shown that, when this approach is taken, and weak effect loci are included in the analysis, the explained heritability increases(Lee et al., 2013). Moreover, the enrichment remains significant, even if strong effect loci such as *APOE* are excluded(Escott-Price et al., 2019).

Several methods for PRS calculation exist(Baker and Escott-Price, 2020). Escott-Price and colleagues created the Cardiff PRS using logistic regression analysis in order to establish predictive values such as sensitivity and specificity (proportion of correctly predicted cases and controls, respectively), positive and negative predictive values (PPV and NPV, probability of having or not having the disease in case of positive or negative result) and area under the curve (AUC)(Escott-Price et al., 2015). They firstly observed that the inclusion of the PRS of 20 genome-wide significant SNPs to the score of APOE ε4 alone (Sensitivity = 0.60; Specificity= 0.75; AUC= 0.69), considerably increased the accuracy of the model (Sensitivity = 0.67; Specificity = 0.67; AUC = 0.72). The predictive accuracy showed an important positive change when AD-associated SNPs with $P<0.05$ were added, and gradually improved when more SNPs with P-values up to $P\leq0.5$ were considered. The best model was achieved when sex and age were included as predictors (Sensitivity =

0.71; Specificity = 0.71; AUC = 0.78). The authors also investigated the prediction accuracy of the model, which inform about the percentage of predicted patients who present with the disease, and on the other hand, the percentage of predicted healthy individuals who are actually controls. This measure is affected by prevalence of the disease in the population; AD being an aged-related pathology, the disease prevalence changes depending on age. The authors showed that at given sensitivity/specificity values, increased prevalence corresponds to increased PPV. This predictive power can be further enhanced if the sample examined is limited to polygenic extremes, and more specifically, the more extreme the cut-off, the more precise was the predictive value. For individuals with 2 standard deviations above the mean, having extreme PRS – the prediction for the diagnosis is highly accurate, reaching 84% in pathology-confirmed samples(Escott-Price et al., 2017). This means that PRS is a tool that offers a great advantage, giving the possibility to identify the individuals at highest risk of developing the disease, early in life. Individuals at the extreme of the polygenic score will be those that can be identified with a higher degree of confidence that either will or will not develop the disease. Furthermore, PRS offers then the possibility of investigating individuals at the extremes by creating, for example, induced pluripotent stem cell (iPSC; as discussed later) and performing functional studies to better understand the pathological pathways. Finally, PRS could be useful in the recruitment of participants into clinical trials by selecting the most and least likely to develop AD, increasing the statistical power of the studies. PRS alone, however, shouldn't be used as predictor of the disease, considering that there isn't yet a unique methodology to calculate it, AD is influenced as well by environmental factors which are not included in the model as of today and PRS is calculated using population-level datasets that are usually predominantly made up of one ethnicity(Baker and Escott-Price, 2020).

1.1.3 Mechanisms of Alzheimer's Disease

The main pathological hallmarks of AD are Aβ plaques and Neurofibrillary Tangles (NFTs). These two characteristic traits are accompanied by gliosis and

inflammation, neuronal loss, and major synaptic changes(Itagaki et al., 1989, Iqbal et al., 2016, Katsumoto et al., 2018, Terry et al., 1991).

1.1.3.1 Amyloid Beta

Aβ protein is the predominant component found in the AD-associated amyloid plaques, which have been extensively studied for the past 30 years(Paroni et al., 2019). It is produced by cleavage of the type I transmembrane protein APP (Figure 1.2)(O'Brien and Wong, 2011). The processing of APP is dependent on three proteolytic enzymes (α-, β- and γ-secretase) and it can be divided into two pathways: the non-amyloidogenic and the amyloidogenic. The non-amyloidogenic pathway involves firstly the cleavage of the full-length APP by α-secretase, which produces the sAPPα ectodomain released outside the cell membrane, and a second fragment of 83 amino acid, the C-terminal APP fragment (α-CTF or C83), which is retained in the plasma membrane. The C83 domain can be further cleaved by the γ-secretase, which releases the p3 fragment (24aa) into the extracellular space, whereas the rest of the protein, called APP intracellular domain (AICD) remains in the cytoplasm(Zhang et al., 2011). The amyloidogenic pathway, instead, involves sequential cuts by β-secretase followed by γ-secretase cut. β-secretase cut releases the sAPPβ ectodomain, leaving at the plasma membrane a 99 amino acid APP carboxy-terminal fragment (β-CTF or C99). The latter can be further cleaved by γ-secretase in different positions, generally every three residues from the C-terminal, to release tripeptide co-products(Bhattarai A Fau - Devkota et al.) (Fig. 1.2B). Among these species, the most abundant are Aβ42 and Aβ40. Aβ42 is the form which shows a higher propensity for aggregation, and it is the major species found in the amyloid plaques(Iwatsubo et al., 1994). Aβ monomers at physiological concentrations are considered non-toxic; however, they can rapidly aggregate into various species of unstable toxic oligomers. These can further aggregate to short irregular protofibrils, and finally elongate into insoluble fibres and finally form amyloid plaques(Hampel et al., 2021). Extensive studies have been carried out in order to understand the most neurotoxic form of Aβ, and currently the scientific consensus is that soluble oligomers, rather than insoluble fibrils, are

the most neurotoxic(Sengupta et al., 2016). A study conducted on Tg2576 mice with plaque pathology, showed no memory impairment in the absence of oligomers(Lesné et al., 2008). On the other hand, the presence of oAβ led to cognitive deficits in absence of amyloid plaque(Gandy et al., 2010). Finally, supporting this hypothesis that large aggregate are not essential to cognitive impairment, there is evidence of individuals with AD with minimal presence of Aβ plaques(Monsell et al., 2015).

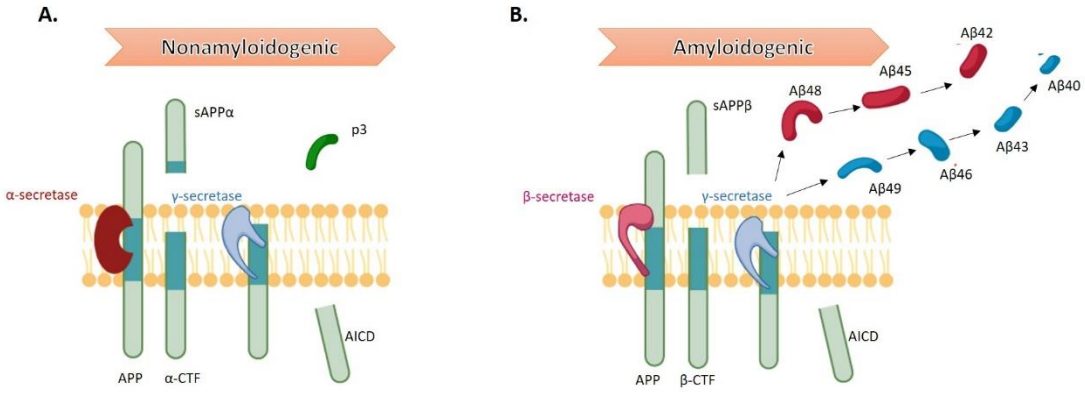

Figure 1.2 – Schematic representation of APP processing. A. Nonamyloidogenic and **B.** amyloidogenic processing of APP involving α-secretase followed by ϒ-secretase and BACE1 followed by ϒ-secretase, respectively, are shown. Both processes generate soluble ectodomains (sAPPα and sAPPβ) and intracellular C-terminal fragments (AICD). (Image adapted from O'Brien et al., 2011).

1.1.3.2 Tau

The second most important pathological hallmark in the development of AD are NFTs. NTFs are abnormal accumulations of Tau protein which are found inside the neurons(Naseri et al., 2019). Tau protein is encoded by the *microtubule associated protein tau* (*MAPT)* gene, which is highly expressed in neurons and localized mainly in axons, where it is an important regulator of axonal transport(Dixit et al., 2008). Tau promotes the polymerization and stability of microtubules by binding to microtubules through its C-terminal region, which contains the microtubule-

binding domain(Weingarten et al., 1975). The *MAPT* gene can generate six different tau isoforms in the human brain due to alterative splicing(Goedert et al., 1989). These isoforms differ by the presence or absence of two 29 amino acid amino-terminal inserts encoded by exons 2 and 3 that are referred as 0N, 1N, 2N tau, and they contain either three (3R) or four (4R) microtubule-binding repeats (3R and 4R tau)(Goedert et al., 1989) at the C-terminal domain of the protein. In a healthy human brain, the 3R and 4R isoforms are found in a 1:1 ratio. Altered *MAPT* pre-messenger RNA (mRNA) splicing results in imbalanced 3R:4R tau ratios. It is still unclear how this altered tau ratio affects AD pathology, however, several studies showed that AD brains have a general increase of 4R tau expression(Ginsberg et al., 2006). Moreover, as previously stated, Tau uses its C-terminal region to bind microtubules, the same region where the 4R repeats are found. It has been shown that 4R tau isoforms lead to a higher ability to promote microtubule assembly when compared with 3R tau isoforms(Lee et al., 1989).

Tau protein is subject to various forms of post-translational modifications (PTMs) such as phosphorylation, acetylation, glycosylation, nitration, glycation and ubiquitination. These PTMs regulate tau function and have been shown to contribute to the pathogenesis of AD(Ramesh et al., 2020). Phosphorylation of Tau is probably one of the most studied PTMs. Tau protein has 85 potential sites for phosphorylation; more than 47 are found in the proline-rich domain(Tapia-Rojas et al., 2019). It is believed that Tau hyperphosphorylation is an early event in AD progression, because high levels of phosphorylated tau correlate with cognitive impairment and are found in the CSF of AD patients at early stages of the disease(Buerger et al., 2006). For these reasons, phosphorylated tau has been proposed as biomarker for AD diagnosis. Finally, Tau hyperphosphorylation, possibly as result of impaired activity or expression of tau kinases and/or phosphatases, leads to the dissociation of the protein from microtubules. This leads to consequent enhancement of tau aggregation from monomeric forms into oligomers, fibrils, filaments and finally NFTs.

1.1.3.3 Glia and neuroinflammation

An additional hallmark of AD, which has been overlooked for many years, is neuroinflammation. Neuroinflammation presents with proliferation and activation of both microglia and astrocytes, the two main glial cell types in the brain. Recent GWAS have discovered a high number of risk genes associated with AD, which are mainly expressed in microglial cells, such as *TREM2, DAP12, CD33*, *Phospholipase C gamma 2 (PLCG2)* and many more(Hansen et al., 2018). In early stages of the disease, microglial activation is believed to be protective, while these cells engulf and destroy secreted Aβ oligomers (oAβ) (Fan et al., 2017). Moreover, microglial activation can be beneficial for neuronal repair by secreting neurotrophic factors such as glial-derived neurotrophic factor (GDNF) and brain-derived neurotrophic factor (BDNF)(Szepesi et al., 2018). The problems arise when microglial activation is sustained over time, becoming harmful for neuronal cells. Specifically, when activated, microglia release a number of proinflammatory cytokines, such as IL-1β, IL-6, tumor necrosis factor (TNF), as well as enhancing oxidative stress by inducing the generation of reactive oxygen species (ROS). Moreover, when hyperactivated, microglia can damage synaptic function by overstimulating the phagocytosis of synapses through pruning mechanisms(Hong et al., 2016). Finally, neuroinflammation can lead to the worsening of Aβ accumulation, when the uptake and clearance of oligomers is impaired(Hickman et al., 2008). For these reasons, chronic microglial activation is believed to be extremely harmful in AD onset and progression, and a general effort in the scientific community in recent years focused on understanding this hallmark. The involvement of microglia cells in AD pathology will be further examined in the 1.2.5 paragraph: Microglia and neuroinflammation in AD.

1.2 Microglia

1.2.1 Microglia origins

The two main groups of cells found in the brain are neurons and glia. Neuronal cells are responsible for propagation of action potentials, releasing

neurotransmitters and forming the neuronal networks important for the transmission of information across the central nervous system (CNS). Glial cells, which consist of macroglia and microglia, perform important tasks in the maintenance of brain homeostasis. The macroglia subgroup, which are developmentally and functionally distinct from microglia, comprises astrocytes, oligodendrocytes and ependymal cells(Ramirez-Exposito and Martinez-Martos, 1998).

Microglia are the innate immune cells of the CNS and comprise between 5 to 12% of the total cell population, depending on the brain region(Lawson et al., 1990). From a developmental point of view, neuronal cells and macroglia share a neuroectoderm origin. On the other hand, microglia derive from primitive myeloid progenitors(Ginhoux et al., 2010). The origin of microglia, however, has been the centre of debate for decades.

In 1913, Santiago Ramon y Cajal described microglia cells as the “third element of the nervous system” to discriminate them from neurons and macroglia(García-Marín et al., 2007). It was then Pio del Rio-Hortega, a student of Ramon y Cajal, who clearly determined that microglia comprise a group of cells within the CNS distinct from neuronal and astrocytic cells, based on observations of their morphological and functional differences. In 1932, he coined the phrase “microglia cells”(del Rio-Hortega, 1932) .

Rio-Hortega was the first to theorise that microglia cells were derived from a mesodermal origin. However, the main school of thought at the time believed in a shared neuro-ectodermal origin with other glial cells(Kitamura et al., 1984, Hao et al., 1991, Fedoroff et al., 1997). In 1982, Murabe and Sano observed morphological homologies between macrophages and microglia(Murabe and Sano, 1983) but it was only later that immunohistochemical studies confirmed this finding by revealing macrophage-specific markers, such as CD11b and F4/80 in mice microglia(Perry et al., 1985) and their equivalents in human microglia(Akiyama and McGeer, 1990). The myeloid origin of microglia was then undoubtedly established.

1.2.2 Microglia originate from precursors which arise during primitive haematopoiesis

It then took 20 years to overcome the next accepted dogma that tissue-resident macrophages were constantly replaced by bone marrow-derived monocytes(Hoeffel and Ginhoux, 2015). Despite seeming true for dermal, gut and heart macrophages, this model was not accurate for all cases.

Haematopoiesis in mammalian embryos consists of two main waves. These waves, which are differentially regulated, show distinct lineage potentials. From murine studies, the primitive wave begins in the extraembryonic yolk sac (YS) from embryonic age 7.5 (E7.5) and gives rise to nucleated erythroblasts and some macrophages (Figure 1.3). The definitive wave, which occurs later in the development starting from E8.5, comprises a transient definitive stage that produces erythro-myeloid progenitor cells (EMPs) and lympho-myeloid progenitor (LMPs) and a definitive stage that gives rise to hematopoietic progenitors, which appear in the aorta-gonads and mesonephros (AGM) region. These lead to the generation of pre-hematopoietic stem cells (pre-HSCs) and mature HSC, which colonize the fetal liver around E10.5 before establishing definitive haematopoiesis (Figure 1.3)(Jagannathan-Bogdan and Zon, 2013).

The fact that microglia originated from the YS was first proposed in 1999(Alliot et al., 1999). Two elegant fate-mapping studies confirmed such an observation(Ginhoux et al., 2010, Schulz et al., 2012). The first study traced the trajectory of the YS-derived cells using an inducible $Runx1^{Cre}$ mouse line(Ginhoux et al., 2010). In Schulz et al., the authors observed that microglia cells were derived from YS- precursors expressing MCSF-R already present between E8.5 and E9.5(Schulz et al., 2012). Kierdorf et al., pushed the understanding of microglial origin further, highlighting an earlier time point (E8.0) for the emergence of microglia progenitors(Kierdorf et al., 2013). Specifically, they identified three independent populations in the early YS at this stage: maternally derived $CD45^{-}$ c-Kit^{-} cells and $CD45^{+}$ c-Kit^{-} cells, neither of which contribute to the microglia pool

population, and finally CD45^{-} c-Kit^{+} EMPs, which make up the real microglia precursors. They showed that these precursors go through developmental stages, which involve the upregulation of CD45 marker first, via Kit$_{low}$ CX3CR1^{-} immature A1 cells to finally mature into Kit^{-} CX3CR1^{+} A2 cells. The maturation of these EMPs takes place during their journey to the developing CNS where they seed and colonise the tissue. Importantly, the authors clarified the role of PU.1 and Irf8 transcription factors during microgliogenesis, both important to induce maturation of c-Kit+ EMPs to A2 mature cells(Kierdorf et al., 2013).

The body of literature focusing on microglial origin, alongside the origin of the other tissue-resident macrophages, has rapidly increased since then(Gomez Perdiguero et al., 2015, Hoeffel et al., 2015, Sheng et al., 2015, Mass et al., 2016). These fate mapping studies uncovered that almost all tissue resident macrophages first appear during embryonic haematopoiesis. Despite this shared early origin, first-wave-derived macrophages are replaced by YS-derived c-Myb^{+} EMPs which are formed during the second wave, with the only exception of microglia cells. These YS-derived precursors, migrate to the fetal liver before reaching their final destination represented by non-CNS tissues(Hoeffel et al., 2015). In contrast to microglia, tissue-resident macrophages go through a monocytic intermediate stage. The main current hypothesis is that microglia are completely first-waved derived. However, a recent study performed on mouse lines showed a microglia Hoxb8 positive subgroup, a marker rarely found in the YS and, on the contrary, predominant in the fetal liver(Chen et al., 2010). Further studies will be necessary to unravel the remaining doubts.

In the adult organism, tissue-resident macrophage are populations that are able to maintain themselves by self-renewal and with minimal contribution from circulating monocytes(Ginhoux et al., 2010, Schulz et al., 2012). Microglia represent the most long-lived population of all myeloid cells. The estimated turnover rate of circulating monocytes is few hours, whereas in the case of microglia is 8-41 months, depending on the brain region(Lawson et al., 1992, Füger

et al., 2017). In the case of depletion from the CNS, however, microglia are able to rapidly repopulate the tissue forming typical cell clusters, suggesting that new microglia are derived from residual cells(Huang et al., 2018, Bruttger et al., 2015).

Understanding the origin and the development of macrophages and microglia cells in particular has two important reasons. First of all, it helps the design of new *in vitro* models such as iPSCs-derived microglia. And secondly, the growing interest in the therapeutic potential of microglia cells strongly relies on a deeper understanding of their origins.

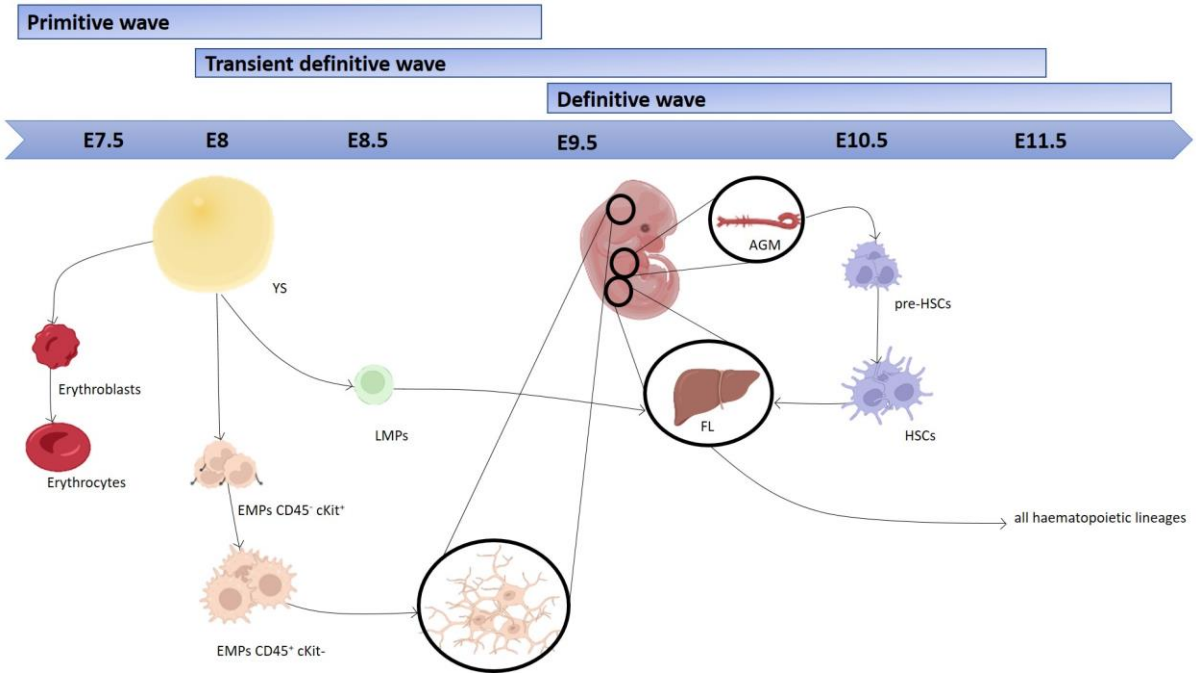

Figure 1.3 – Schematic representation of ontogeny of the hematopoietic system and origin of microglia (Image taken from Hoeffel et al., 2015). Hematopoietic development proceeds in three waves named primitive, transient definitive and definitive. Each wave produces several hematopoietic progenitors, which are shown in the figure together with their site of origin. The primitive wave produces erythroblasts that mature to erythrocytes. Around E8, from the YS arise erytro-myeloid pregenitors (EMPs) that mature to CD45-cKit+ and subsequently to CD45+ cKit- that invade the embryo and migrate to the brain where they differentiate into microglia cells. The transient definitive wave generated other EMPs and lympho-myeloid progenitors (LMPs) that migrate into the fetal liver. Finally, the definitive wave generates pre-HSCs, which mature into HSCs, which again travel to the liver. After E11.5 will remain the principal hematopoietic organ in

the embryo prior their migration to the spleen and the bone marrow. (Image adapted from Hoeffel et al., 2015 and Canu et al., 2021

1.2.3 Microglia identity and the importance of the brain environment

The CNS represents a unique environment, separated from the rest of the body by a tight blood brain barrier. Studies performed on cultured microglia have uncovered the great influence that the brain milieu has on these cells. Transcriptomic analysis of both mouse and human microglia isolated from brain tissues and cultured *in vitro* revealed significant changes in gene expression when compared with freshly isolated cells. Notably, these changes were observed as early as 6 hours of culturing, and lasted for the following 7 day time course. Gene ontology analysis revealed the upregulated genes were particularly enriched for inflammation and stress responses pathways, whereas downregulated genes were enriched for immune cell functions and signalling(Gosselin et al., 2017). The peculiar disruption in gene expression observed by Gosselin and colleagues further revealed the great influence the brain environment has on microglia identity(Gosselin et al., 2017). They discovered that a significant subset of genes, which are upregulated during development (in particular when YS-macrophage colonise the brain and become fetal microglia), were down regulated when the cells were cultured *in vitro.* This suggests that a substantial part of the changes observed in culture derive from a loss of signals occurring in the brain. Other evidence of the importance of the CNS environment comes from an observation by Bohelen and colleagues who transplanted cultured microglia cells into microglia-deficient mice. The transplantation led to cultured microglia quickly regaining their typical gene profile in vivo(Bohlen et al., 2017).

The brain environment is not only important to keep the unique microglial signature; physical contact with other CNS cells is crucial for the correct homeostatic function of microglia cells. Neurons, for example, express factors which play important roles in maintaining microglia cells in a resting state, such as

CD200 and CX3CL1. CD200 is a glycoprotein found on neuronal cell membranes that interacts with CD200R receptor expressed on microglia cells. This receptor-ligand interaction keeps microglia in a ramified and inactive state(Wang et al., 2007, Hoek et al., 2000). CX3CL1 is another neuronal factor, synthesized also by endotheliocytes of brain capillaries, which signals through CX3CR1 receptor and plays a role in preventing microglia activation and neuroinflammation(Cardona et al., 2006, Lee et al., 2010). Loss of connections with other cells of the CNS leads to the activation of microglia, promoting chronic inflammation and release of pro-inflammatory cytokines.

Interaction between microglia and neurons is constant and reciprocal. Microglia play important roles in brain development by actively pruning, engulfing, and eliminating synaptic structures(Crotti and Ransohoff, 2016, Schafer et al., 2012). They facilitate the growth of neuronal network by secreting important factors, such as BDNF, nerve growth factor (NGF) and insulin-like growth factor (IGF-1)(Kettenmann et al., 2011).

Both the origin of microglia, and the environment that they are surrounded by, are crucial for the development of their unique identity. Different studies tried to engraft bone marrow derived myeloid cells into the CNS, resulting in only limited expression of microglia genes. In conclusion, both YS-origin and strong cues from the CNS play vital roles in determining microglial specification, and this is an important aspect to be taken into consideration when designing *in vitro* experiments.

1.2.4 Microglia functions in the developing and adult healthy brain

Considering that microglia cells persist in the brain from the embryonic state throughout adulthood, they adapt their functional ability according to the specific stage of the brain development. Specifically, during early developmental phases and first days post birth, microglia are intensively involved in tissue remodelling processes, being an active player in the establishment of the neuronal

architecture(Frost and Schafer, 2016). This includes the ability to remove non-functional synapses in a process named synaptic pruning, and to remodel synaptic circuits(Wake et al., 2013) and modulate neuronal wiring(Squarzoni et al., 2014). Finally, they are capable of prompting neurogenesis by supporting mechanisms like survival, proliferation and maturation of neuronal progenitor cells (NPCs) and neurons.

In the adult brain, microglia have been considered for a long time to be in a constant quiescent state, with little involvement in any function in homeostatic conditions(Prinz et al., 2019). This belief was overturned with the work of two distinct groups in 2005(Davalos et al., 2005, Nimmerjahn et al., 2005). Nimmerjahn and colleagues used an EGFP-CX3CR1 mouse model to demonstrate that microglia in the healthy adult CNS constantly survey the environment by continuously moving their cellular processes, without disrupting the surrounding neuronal architecture(Nimmerjahn et al., 2005). In the same year, another group used two-photon imaging of CX3CR1-GFP mice, showing that microglia cells move their processes, without moving their cell bodies, towards the site of injury with the aim of forming a physical barrier to protect the healthy tissue(Davalos et al., 2005). Interactions with neighbouring cells and microglial spatial distribution are strictly regulated resulting in a tile-like network(Kettenmann et al., 2013, Askew et al., 2017). This mosaic distribution is maintained during the scanning process, avoiding contact between processes of neighbouring microglia(Nimmerjahn et al., 2005). Extensive studies are still underway to understand which factors regulate this default motility and morphology; however, neurotransmitters, purinergic receptors and ion channels, amino acids, glycolipids and inorganic substances have been proposed(Tremblay et al., 2011). Supporting evidence of the active nature of homeostatic microglia is the expression of genes that sense changes in the milieu, endogenous ligands and microbes, generally referred as the “microglia sensome”(Hickman et al., 2013). Interestingly, it has been shown that aging affects this strictly regulated mosaic organisation, resulting in a decrease in microglia process mobility and an increase in cell soma motility(Hefendehl et al., 2014);

moreover, the branching of processes was observed to be reduced, which leads to reduced area of surveillance: this may be partly responsible for the deterioration of homeostatic function(Spittau, 2017, Davies et al., 2017, Bisht et al., 2016). Finally, up-regulation of microbe-recognition genes and genes involved in neuroprotection are also observed during aging(Hickman et al., 2013).

One of the main functions of microglia cells is phagocytosis, a receptor-mediated process that leads to the removal of cellular debris. It consists of recognition and engulfment into membrane protrusions (called phagosomes) of debris, dying neurons or aggregates of misfolded proteins, such as Aβ. Phagosomes then fuse with lysosomes where terminal digestion and degradation takes place(Tremblay et al., 2011). This process is essential for the maintenance of tissue homeostasis and the rapid clearance of apoptotic cells prevents any secondary necrosis and resulting inflammation(Chan et al., 2006). Sierra and colleagues showed how in the hippocampal subgranular layer, phagocytic microglia quickly remove dying NPCs in a non-inflammatory way, allowing the remaining cells to complete differentiation into granule cells(Sierra et al., 2010).

1.2.5 Microglia and Neuroinflammation in AD

For many years, the AD research landscape was dominated by the theory that disease onset and progression were driven by Aβ and tau misprocessing. However, emerging evidence, especially from genetic studies as discussed above, is pointing to inflammation as actively driving the pathogenesis of AD, rather than as a passive consequence of the appearance of senile plaques and NFTs. Understanding the role of neuroinflammation in CNS disorders might help us to treat or delay the onset of neurodegenerative diseases.

1.2.5.1 DAMPs and PAMPs

Several stimuli, such as neuronal death or protein aggregates, act as triggers to activate a microglia innate immune response. The detection of these specific triggers is mediated via receptors which are able to recognize damage-associated

molecular patterns (DAMPs) or pathogen-associated molecular patterns (PAMPs)(Heneka et al., 2015).

In the context of AD, for example, the inflammatory reaction is partly activated by the binding of microglia cell surface receptors to soluble oAβ and fibrils(Bamberger et al., 2003, Paresce et al., 1996, Liu et al., 2005). Stewart and colleagues demonstrated that upon binding of Aβ to CD36, Toll like receptors 4 (TLR4) and TRL6 receptors, microglia become activated and secrete proinflammatory cytokines and chemokines. Conversely, when these receptors are ablated in an *in vitro* model, Aβ-induced cytokine and chemokine production is decreased and amyloid accumulation inside the cells is interrupted(Stewart et al., 2010, El Khoury et al., 2003).

Aβ phagocytosis and degradation is also carried out by microglia under physiological conditions; the migration of these cells towards the site of the lesion therefore represents a physiological reaction(Sondag et al., 2009). Following receptor binding, microglia start to engulf oligomers and fibrils via phagocytosis(Heneka et al., 2015). Impaired microglia phagocytic function is thought to be one of the causes of inefficient clearance of Aβ, in late onset AD. Hickman and colleagues showed that despite microglia recruitment in early stages of the disease being neuroprotective and leading to Aβ clearance, as the disease develops, Aβ deposition results in sustained proinflammatory cytokine production and, as a consequence, the downregulation of genes involved in Aβ clearance, such as CD36. This, in turn promotes Aβ accumulation, supporting neurodegenerative processes(Hickman et al., 2008).

Recent studies, moreover, have implicated microglia-mediated synapse removal in the development of the disease. Normally, this activity, known as synaptic pruning, is confined during early stages of brain development; however, it can be reactivated in aging or in disease (Rajendran and Paolicelli, 2018). This process is known to involve proteins of the complement cascade, such as C1q and CR3 receptor. C1q localizes at the synapses, and it is thought to tag them to be engulfed

by microglia cells. CR3 receptor, is localized instead on the microglia branches, and it is thought to mediate the phagocytosis of tagged synapses. More evidences are required to elucidate the mechanism by which the re activation of microglia synaptic pruning impact and enhance the neurodegenerative process (Gomez-Arboledas et al., 2021). This is of particular relevance because the worsening of the symptoms during AD progression correlates with synapses loss, more than with amyloid burden(Sheng et al., 2012).

Once again, genetics also support the hypothesis of impaired microglial function: rare mutations in TREM2 and CD33 microglia receptors have been shown to increase risk of AD. TREM2 mediates clearance of neuronal debris via phagocytosis(Hsieh et al., 2009) and is thought to be a receptor for oAβ(Zhao et al., 2018); a rare SNP (R47H) located in the extracellular domain of the receptor increases the risk of developing the disease(Guerreiro et al., 2013). Finally, a rare mutation on CD33, another microglia receptor involved in Aβ clearance, has been reported to reduce Aβ phagocytosis by peripheral macrophages and increase Aβ deposition in the brains of carriers(Bradshaw et al., 2013).

1.2.5.2 Microglia terminology

For a long time, microglia activation has been explained with terminology specific to peripheral macrophage polarization, specifically M1 and M2. Briefly, classically activated macrophages (M1) were demonstrated to secrete inducible nitric oxide synthase (iNOS), resulting in possible damage for the surrounding tissue. This represents a pro-inflammatory phenotype. Alternative activated macrophages (M2), instead, express arginase; this represents an anti-inflammatory phenotype.

New evidence based on transcriptomic and proteomic profiles, regional heterogeneity and diversity of functions from early embryonic life to old age challenged this simplified vision, suggesting that microglia do not follow the M1-M2 dichotomy and forcing the scientific community to find new terminology(Ransohoff, 2016, Leng and Edison, 2021). On this note, transcriptomic studies have demonstrated how microglia slowly transition from a homeostatic to

a disease-associated state while the disease progresses. The cells found in this state, which show downregulation of homeostatic genes and upregulation of genes previously associated with AD, such as *ApoE*, *TREM2* and *TYROBP*, have been named disease-associated microglia (DAM)(Keren-Shaul et al., 2017).

1.2.5.3 Cytokines and Chemokines

As mentioned above, a crucial role is played by cytokines and chemokines which are secreted by several types of cells in the CNS, including microglia, upon several stimuli. These molecules, by binding to their specific receptors, initiate cascades of intracellular events that play important roles in the initiation of immune response(Regen et al., 2017). Cytokines can broadly be classed as either pro- or anti-inflammatory, depending on the secreting cell, the target cells and the specificity of the immune response(Lehnardt, 2010, Ponomarev et al., 2007). Generally, the increase in Aβ concentration is associated with increased secretion of proinflammatory cytokines, such as TNF, IL6, IL1α and GM-CSF(Patel et al., 2005), and chemokines, such as CXCL8 (IL8), CCL2, CCL3(Savarin-Vuaillat and Ransohoff, 2007). In a similar way, Caspase 1, which is essential for the cleavage of pro-IL1β to its active form, is elevated in the brains of patients presenting mild cognitive impairment (MCI) and AD(Heneka et al., 2013). IL12 and IL23 are also secreted by microglia in a mouse model of AD, and their inhibition reduces AD pathology(Vom Berg et al., 2012). This proinflammatory environment that is established both in transgenic mouse models and patients with AD is sustained and generates a vicious circle which is extremely detrimental(Regen et al., 2017). A study conducted on 56 patients with MCI showed that the risk of conversion and worsening of the dementia stage was higher when TNF was elevated and transforming growth factor beta (TGF-β) was decreased(Tarkowski et al., 2003).

The sustained release of pro-inflammatory molecules results in by-products that are detrimental for nearby neurons and contribute to neurodegeneration by inducing synaptic dysfunction, blocking neurogenesis and promoting neuronal death(Lyman et al., 2014). For example, IL-1β has been shown to increase the

production of prostaglandin E2, which in turn drives the release of presynaptic glutamate and postsynaptic NMDA receptor activation, leading to synaptic loss(Mishra et al., 2012). TNF can cause neuronal death via activation of TNF receptor 1 and by recruiting caspase 8 upon inhibition of the nuclear factor-κB (NF-κB)(Micheau and Tschopp, 2003). Finally, Hellmann-Regen and colleagues showed that activation of murine primary microglial cells with lipopolysaccharide (LPS) induces the production of enzymes able to degrade retinoic acid, a small molecule essential in neuroprotective processes(Hellmann-Regen et al., 2013). It is clear then that the activation of microglia is combined with sustained modification in the microenvironment, which on one hand are extremely important for the successful result of the immune response, and on the other hand are dangerous for neighbouring neuronal cells(Regen et al., 2017).

There is a lot of evidence to indicate that neuroinflammation happens in early stages of the disease progression prior to amyloid plaque formation. Neuroimaging studies reported microglia activation in patients presenting MCI, in the absence of amyloid plaques(Okello et al., 2009). Similarly, animal models of AD show microglia activation in pre-plaque stages(Hanzel et al., 2014). Moreover, post-mortem tissues from young people who suffered systemic inflammation presented morphological and immunological changes in microglia cells very similar to those documented in older patients with dementia(Tischer et al., 2016). Interestingly, it has been shown that Aβ injection alone in primate brains was not able to prompt amyloid pathology. However, the simultaneous injection of Aβ together with LPS, or of Aβ in animals with chronic systemic inflammation led to the formation of amyloid plaques(Philippens et al., 2017). These studies not only show how microglial activation is present early in the disease stage, but they also demonstrate how it represents a necessary prerequisite, together with Aβ deposition, to trigger the pathology. The prevailing hypothesis is that microglia are ‘primed’ by chronic low-level stimuli, including aging and systemic inflammation, which in the preclinical stages of AD is protective against Aβ deposition. The building up of Aβ deposition, together with tau aggregation, culminates in an

excessive and damaging inflammatory response by microglia typically in clinical stages of AD(Leng and Edison, 2021, Perry and Holmes, 2014).

1.3 Induced Pluripotent Stem Cells

1.3.1 Patient-derived iPSCs generation

The generation of iPSCs was first described in 2006, when Yamanaka and colleagues screened 24 candidate genes shown to be important for the establishment and maintenance of pluripotency in embryonic stem cells (ESCs) (Takahashi and Yamanaka, 2006). ESCs are the stem cells found in the inner cell mass of blastocysts and are characterized by mainly two aspects: their ability to differentiate into any cell type from the three germ layers (ectoderm, mesoderm, endoderm), called pluripotency, and an ability to limitlessly self-renew. The list of 24 genes was narrowed down, with an exclusion approach, to 4 transcription factors, which were shown to be essential and sufficient to reprogramme mouse fibroblasts into iPSCs, which showed same capacity of differentiation and self-renewal as ESCs(Takahashi and Yamanaka, 2006). These four factors are OCT4, KLF4, c-Myc, and SOX2, referred to as OKSM(Takahashi and Yamanaka, 2006). One year later, the same group of researchers demonstrated that the same four factors are able to generate iPSCs from adult human fibroblasts(Takahashi et al., 2007).

The advent of iPSCs has completely revolutionised medical research and has had an important impact on the study of neurological disease in particular. This approach allows scientists to study live patient-derived neurons and glia cells, which are not easily accessible in humans, and deepen our understanding of the molecular mechanisms underlying these conditions. Specific genetic backgrounds can now also be studied in those cell types. Moreover, the combination of cell reprogramming, together with several genome editing technologies, such as CRISPR-Cas9, has expanded even more the possible avenues in neurodegenerative

studies. Precise genome editing offers the possibility to generate isogenic iPSC lines, genetically identical to the parental line, carrying only specific mutations of genes or knockouts (KO). All these opportunities and advantages make iPSCs an incredible tool for human disease modelling.

1.3.2 Sources of iPSCs generation

There are some challenges that still prevent the success of an easy and efficient reprogramming protocol. The two main reasons for this are the choice of the reprogramming technique, and the choice of the starting material(Raab et al., 2014).

The first type of cells used by Takahashi and colleagues were fibroblasts, as these were used in previous reprogramming experiment attempts(Takahashi and Yamanaka, 2006). The main advantage of fibroblasts is that they are easy to culture and expand quickly. The reprogramming efficiency, however, tends to be low and the collection of the samples via biopsies can be painful for the patients(Raab et al., 2014).

Other cell sources which are easier to obtain have been tested over the years; these are blood cells(Loh et al., 2009), exfoliated epithelial cells obtained from urine(Zhou et al., 2012b) and keratinocytes from hair(Aasen et al., 2008).
An easy and accessible alternative source for reprogramming purposes is blood. There are many options on how to use blood cells: they can be obtained from either peripheral blood (PB) or umbilical cord blood. In the case of PB, different subpopulations can be separated and further processed. The most common subpopulation is represented by peripheral blood mononuclear cells (PBMCs) which comprise of monocyte, T cells and B cells. PBMCs can easily be separated from plasma and red blood cells and cultivated with well-established, published protocols. Compared to fibroblasts, however, the reprogramming efficiency has been shown to be 10-50 times lower(Staerk et al., 2010) .

CD34+ hematopoietic stem cells can also be used after being mobilised in a process similar to the procedure used for stem cell donation. The donor is injected with granulocyte colony-stimulating factor (G-CSF) for 5 days(Souza et al., 1986), which lead to the increased production and mobilization (release) of CD34+ hematopoietic stem cells from the bone marrow into the PB(Raab et al., 2014). After these initial 5 days, the donor undergoes a four-hour process, named apheresis, in which stem cells are separated from the rest of the blood cells through a machine. This time-consuming, painful process can result in some side effects such as headache, bone pain, fatigue and nausea(Cashen et al., 2007). The mobilization of peripheral cells is performed in case the donor is in good health.

Endothelial cells from cord blood represent a further available source. Progenitor cell isolation from cord blood is ten times more efficient than from adult PB(Raab et al., 2014). The downside is that the harvesting and the conservation of umbilical cord blood is expensive and needs to be carried out immediately after birth.

A non-invasive procedure is the collection of exfoliated renal epithelial cells which are found in the urine. 50 to 200ml of urine are enough to isolate epithelial cells which have been shown to be able to generate iPSCs with pluripotency capacity comparable to ESCs and iPSCs derived from other types of starting material(Wang et al., 2013). Moreover, cells derived from urine can be frozen and thawed several times with no evidence of reduced reprogramming efficiency. However, once in culture, they cannot be used after five passages as the efficiency considerably decreases(Xue et al., 2013).

Finally, keratinocytes have also been described for the generation of stem cells. There are several types of keratinocyte sources in the body that can be used: from scalp hair, beard, eyebrow to hair from the nose. The main drawback in the use of keratinocytes is the need of high expertise in the first phase of sample collection. For successful reprogramming, a good amount of high quality cells is necessary, and for this reason the crucial part is plucking the hair together with the root. After this initial step, the cells can be cultured in normal DMEM medium at room

temperature (RT) for several days. The possibility to keep the cells at RT for days allows for the shipment of these cells all around the world, without the risk of loss in proliferation ability of the cells. The protocol for keratinocytes reprogramming is faster when compared to fibroblasts and blood: 1-2 weeks versus 3-4 weeks. Finally, the reprogramming efficiency reaches 1-2%, which is considerably higher than all the other sources described(Raab et al., 2014).

1.3.3 Reprogramming techniques

The majority of the studies conducted at the beginning of the reprogramming era used integrating viral vectors to transduce the reprogramming factors(Al Abbar et al., 2020). These classical methods that include retro- and lentiviruses, resulted in efficient and robust reprogramming; however, they led to permanent genomic modifications as a consequence of viral integration inside the host genome(Borgohain et al., 2019). These techniques have the potential to result in insertional mutagenesis and tumour formation, and for these reasons they are not acceptable for clinical use(Ben-David and Benvenisty, 2011).Thanks to the fast advances of technological tools in the field, reprogramming techniques are constantly evolving. To date, many non-integrative approaches have been developed in order to overcome this problem and bring iPSC technologies one step closer to biomedical applications.

Sendai Virus (SeV) is one of the systems in use today for cell reprogramming. After the first successful evidence that this viral vector could reprogram adult fibroblasts(Fusaki et al., 2009), many modifications of the system followed, mainly to achieve complete clearance of viral particles. Seki and colleagues developed a temperature-sensitive mutated virus and successfully reprogrammed T cells(Seki et al., 2010). The insertion of a point mutation in the genome of the virus allows the elimination of particles through a short temperature shift(Ban et al., 2011). Moreover, a recent study used an auto-erasable SeV vector, which responds to the microRNA-302(Nishimura et al., 2017). This specific miRNA, which is expressed at a high level in iPSCs and is completely absent in somatic cells, suppresses the viral

polymerase, which is vital for the replication of the viral genome, leading to the automatic removal from reprogrammed cells.

An alternative reprogramming technique which avoids viral vectors is the use of recombinant proteins. Bioactive forms of the reprogramming factors can be generated using both prokaryotic and eukaryotic systems in large quantities(Borgohain et al., 2019). The main limitation to this approach is the fact that the proteins have poor capacity to cross cell membranes. For this reason, the reprogramming factors need to be fused with cell-penetrating peptides. A number of studies have successfully addressed this issue, however they all show poor efficiency and kinetics of reprogramming when compared to classical viral-based techniques(Zhou et al., 2009, Kim et al., 2009, Cho et al., 2010). Nemes and colleagues overcame the problem by fusing a nuclear localization signal in order to enhance the nuclear localization of the reprogramming proteins(Nemes et al., 2014). Overall recombinant protein-based reprogramming techniques is a valid alternative to viral reprogramming methods; however low efficiency, together with the challenges of purifying a desirable amount of protein and poor *in vitro* stability, pose obstacles to the routine use of this technique(Borgohain et al., 2019).

Finally, another alternative transgene-free strategy, which enables reprogramming of somatic cells, is the use of mRNA(Steichen et al., 2014). This system does not require a clean-up phase, which is necessary with Sendai vector-based transduction to eliminate viral proteins. However, there are some disadvantages. Successful transfection is usually achieved only after multiple rounds and this is due to the short half-life of the RNA in cell culture conditions. This often results in increased cellular stress and an immune response which can in turn prevent mRNA translation. Many studies addressed these problems both by improving the synthetic mRNA structure to increase mRNA stability, and simultaneously using mechanisms to block the innate immune response(Yoshioka et al., 2013).

1.3.4 iPSC-derived Microglia

The advent of the reprogramming technique made it possible to generate all sorts of cell types from a renewable and easily manipulated source. The number of protocols to generate neurons and astrocytes quickly increased, but the production of microglia remained difficult, mainly due to their embryonic origin which was poorly understood until recently. The first microglia-dedicated protocol was published in 2016(Muffat et al., 2016), and after that, a number of independent protocols were generated(Abud et al., 2017, Haenseler et al., 2017, Takata et al., 2017, Douvaras et al., 2017). All these methods greatly vary in terms of media compositions, yields, duration, and cellular homogeneity of the derived microglia.

Abud and colleagues used a two-step maturation protocol to obtain mature microglia-like cells in around 40 days. They performed extensive characterization of the obtained cells in monoculture system, co-culture with primary rat neurons and finally in a 3d organoid model. They compare microglia cells in the monoculture versus the co-culture system, and they observed a differential behaviour. Microglia cells respond appropriately to the neuronal environment, showing an upregulation of homeostatic genes when compared to microglia in monoculture (Abud et al., 2017). Haenseler uses an embryo body based protocol, which generate MYB-independent macrophage precursors. They use IL-3 and M-CSF to drive myelopoiesis and push maturation to obtain pure microglia precursors that can be collected from the supernatant at regular intervals (usually weekly). These precursors can be terminally differentiated to microglia using IL-34 and GM-CSF. Several assays were performed to assess proper functionality of the cells among which phagocytosis of fluorescently labelled E. Coli particles, cytokine release upon LPS stimulation and migration (Haenseler et al., 2017).Douvaras et al., used instead a monolayer strategy as opposed to an EB based approach, and they obtained microglia cells in approximately 60 days. They characterized the cells

primarily in monoculture system and tested their functionality and transcriptome upon LPS stimulation (Douvaras et al., 2017). Finally, Takata and colleagues as well established a monolayer based protocol which closely recapitulate the *in vivo* hemangioblast formation. As previous studies, they highlighted the importance of neuron-microglia interaction for microglia maturation and homeostasis. The majority of their work, however was performed using mouse iPSC microglia, and only few data were generated with human iPSCs (Takata et al., 2017).

Despite the great advantages offered by iPSC-derived microglia over murine cells in the study of specific genetic risk factors for AD or other neurodegenerative disorders, the field is still facing questions and concerns. There is no complete unanimity on the genetic, proteomic, functional signature required in order to accept iPSC-derived microglia as "true" microglia cells. For this reason, *in vitro* generated cells are often referred as "microglia-like" cells. Extensive characterization is required including their morphology, gene expression profile, protein marker expression and functional activity.

One of the main problems in the use of iPSC-derived microglia resides in the fact that, as immune cells, they are extremely sensitive to *in vitro* culture conditions. This led groups to develop more complex cultures, such as co-cultures with astrocytes and neurons, as well as transplantation of progenitor cells into mouse brains. Svoboda and colleagues showed that under these circumstances, progenitor cells are able to differentiate into microglia cells, which show a morphology and gene expression signature very similar to primary microglia(Svoboda et al., 2019).

Despite the challenges and the limitations of this model, iPSC-derived microglia cells helped push forward our understanding of CNS disorders. In the future, the refinement of *in vitro* protocols, and the increasing understanding of microglia

identity, will make the iPSC-derived microglia model highly informative, also benefitting drug discovery processes.

1.4 PLCγ2

1.4.1 PLC Family

One of the most interesting discovery of recent GWAS, is the novel rare non-synonymous coding variant in the gene *PLCG2* encoding the enzyme phospholipase C-γ-2 (PLCγ2), identified in 2017 (rs72824905/P522R, P – 5.38 x 10^{-10})(Sims et al., 2017). It shows a MAF of 0.0059 for cases and 0.0093 in controls. This SNP is associated with decreased risk of late onset AD and being an enzyme, is the first classically drug-targetable molecule identified in LOAD genetic study(Sims et al., 2017).

PLCγ2 is one of 13 enzymes of the phospholipase C (PLC) family, which consists of six subtypes: β, δ, γ, ε. η and ζ. All these molecules play roles in signal transduction pathways(Kadamur and Ross, 2013); specifically they are recruited at the plasma membrane upon activation of specific receptors, such B cell receptors (BCR), T cell receptor (TCR), Fc receptors (FcRs) and G protein-coupled receptors (GPCRs)(Bill and Vines, 2020). PLC then activates a cascade event by hydrolysing phosphatidylinositol-4,5-bisphosphate (PI(4,5)P2), which is located on the plasma membrane, into two second messengers: inositol-1,2,3-trisphosphate (IP_3) and diacylglycerol (DAG). IP_3 is a crucial regulator of the release of cytoplasmic calcium (Ca^{2+}) from cell internal stores by binding its receptors located in the endoplasmic reticulum (ER)(Kurosaki and Tsukada, 2000). DAG activates protein kinase C (PKC) isozymes which regulate multiple cellular processes, including proliferation, differentiation and chemotaxis(Black and Black, 2012).

Each of the aforementioned PLC isotypes exhibits a unique expression profile in numerous cells and subcellular distribution(Kadamur and Ross, 2013). Specifically, the two PLCγ proteins (1 and 2), show highly conserved sequences but very different expression profiles. While *PLCG1* is ubiquitously expressed, *PLCG2* is

mainly expressed in myeloid cells(Wang et al., 2000), neurotrophils(Jakus et al., 2009),B cells(Hashimoto et al., 2000), and natural killer cells(Wang et al., 2000) in circulating blood; and in the brain is found predominantly in microglia(Magno et al., 2019).

1.4.2 PLCγ2 structure and mechanisms of activation

From a structural point of view, PLCγ2 shows a set of main domains, which are shared by the majority of the molecules of the family (Figure 1.4A). It consists of an N-terminal pleckstrin homology (PH) domain, followed by a series of EF-hand domains, a split triose-phosphate isomerase (TIM)-barrel catalytic domain (composed of an X and a Y domain), and finally a C2 domain (Figure 3A). The residues involved in the substrate recognition and inositol-lipid hydrolysis are located in the catalytic domains. A unique feature of the PLCγ2 isozymes is that within the X and Y domains of the TIM-barrel catalytic domain there is a large multidomain insert embedded, often called PLC-γ-specific array (γSA). This highly structured region is the core regulatory domain of the protein and it consists of a split PH (sPH) domain, two SH2 (the N-terminal Src homology 2 (nSH2) and C-terminal (cSH2)) domains and finally an SH3 domain(Magno et al., 2021, Wang et al., 2014). PLCγ2 enzyme is inhibited in basal conditions, causing the phospholipase active site to become blocked and inaccessible. There are two main regions involved in the autoinhibition of the PLCγ2 protein. Firstly, contact between the sPH domain and the TIM-like barrel, and secondly contacts between cSH2 and C2 domains(Magno et al., 2021, Gresset et al., 2010). The enzyme activation follows a two-step process (Figure 1.4B). Upon immune cell receptor stimulation, such as BCR and Fc receptors or Rac GTPase, tyrosine kinases at the plasma membrane are mobilized. These kinases will dock the nSH2 of the protein PLCγ2, recruiting the enzyme to the cell membrane. However, the engagement of the enzyme is not enough to release the auto-inhibition and promote its activity. The inhibitory interactions within the molecule are released upon phosphorylation, by the docked tyrosine kinase, of specific tyrosine within the isozyme. This engages the inhibitory cSH2 domain to interrupt the contact with the catalytic TIM barrel and

free the activation site for substrate entry. Mutations or deletions in either the cSH2 or the sPH domains are sufficient to impair the autoinhibition and lead to PLCγ2 activation(Magno et al., 2021, Gresset et al., 2010).

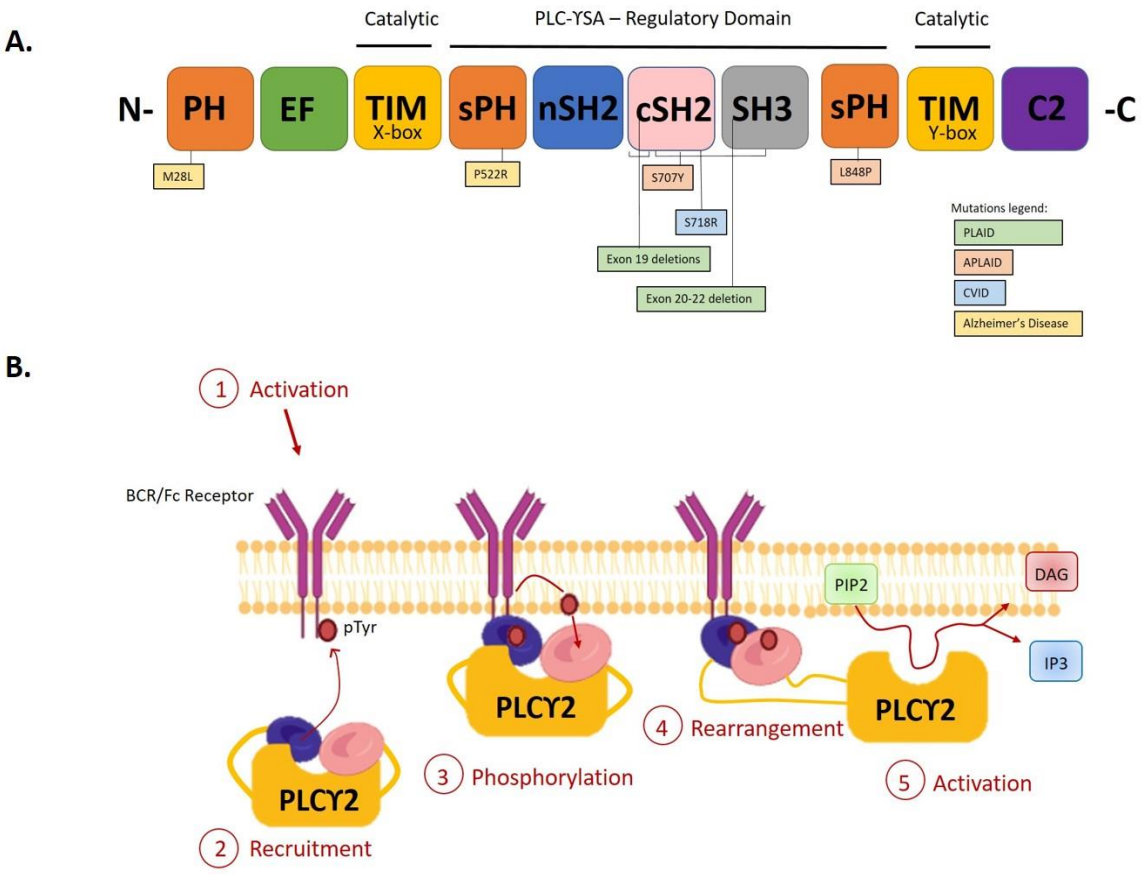

Figure 1.4 – Schematic representation of domain architecture of PLCγ2 and mechanism of enzyme recruitment and activation. A. PLCγ2 protein structure represented by domains and localization of genomic deletions, and mutations colour-coded per disease(Image adapted from Tsai et al., 2020). **B.** In the absence of stimulus, the catalytic domain (in yellow) of the enzyme is basally auto-inhibited by cSH2 (in pink). Activation of the receptor provided a phosphotyrosine (red dot) docking site for the nSH2 domain (in blue), resulting in the translocation of the enzyme from the cytoplasm to the plasma membrane. The receptor then phosphorylate PLCγ2 at a specific tyrosine, which promoted direct interactions with cSH2. engagement of this domain induces a structural rearrangements of the cSH2 domain leading to release of auto-inhibition, final activation of the enzyme and subsequent substrate hydrolysis (Image adapted from Gresset et al., 2010)

1.4.3 PLCγ2 functions

PLCγ2 is a cytoplasmic protein that, like other members of the PLC family, moves to the plasma membrane upon activation of several receptors. Specifically, PLCγ2 responds to a variety of immune cell receptors such as B cell receptor and Fc receptor(Jang et al., 2013, Driscoll, 2015), and catalyses the hydrolysis of phosphatidylinositol. In particular, the main PLC substrate is PIP_2, followed by phosphatidylinositol phosphate (PIP) and then phosphatidylinositol (PI)(Bill and Vines, 2020). The cleavage of PIP_2 leads to the generation of on one side cytosolic IP_3 and on the other DAG (Figure 1.4B). IP_3, is a small water-soluble molecule that, after being generated, diffuses away from the plasma membrane and reaches the ER where it binds IP_3 receptors. This leads to the release of Ca^{2+} from intracellular stores(Streb et al., 1983), which in turn results in the activation of several genes which control functions, such as differentiation, proliferation, degranulation(Wang et al., 2000), motility(Mueller et al., 2010), and fertilisation(Ichise et al., 2016).

In PLCγ2-deficient mouse models, two independent groups showed that this enzyme is essential in the downstream mediation of stimulus signalling through B cell receptors(Wang et al., 2000, Hashimoto et al., 2000). Specifically, the authors observed a general deficit in B cell maturation, and a decrease in the proliferation rate of the same cells in response to the engagement of the IgM antigen receptor in the PLCγ2-deficient mice. Moreover, these animals showed general lower levels of IgM, IgG2a and IgG3 in comparison to wild type (WT) in basal conditions. Finally, Wang and colleagues demonstrated a role of PLCγ2 in signalling through Fc receptors as well(Wang et al., 2000). PLCγ2-deficient mice presented reduced degranulation of mast cells, a process via which these cells are able to release a variety of mediators, such as antimicrobial molecules, from internal secretory granules. Degranulation is stimulated via binding of antigens to IgE molecules that are already bound to high affinity Fc receptors(Wang et al., 2000).

In a complex study using *ex vivo*, *in vitro* and *in vivo* models, Mueller and colleagues demonstrated a partial role of PLCγ2 in neutrophil rolling(Mueller et al., 2010). The

recruitment of leukocytes to the site of inflammation is important for host defence. Firstly, the immune cells make contact with the inflamed tissue via selectins and their counter-receptors; this is followed by rolling of the immune cell, and then integrin-mediated arrest. The rolling velocity of neutrophils with deletion of the *PLCG2* gene showed less reduction of their rolling velocity when compared to WT cells (Mueller et al., 2010).

Finally, PLCγ2 has been shown to have a crucial role in luminal expansion of clear cells in the epididymal duct; PLCγ2 deficiency in these cells resulted in male infertility caused by azoospermia(Ichise et al., 2016).

The second product of PLC activation is DAG which, after cleavage remains bound to the plasma membrane, and activates the calcium-dependent PKC(Wang et al., 2014). This activates downstream effectors by a kinase cascade, resulting in regulation of cellular functions such as cell proliferation(Ma et al., 2019), learning, memory(Sun and Alkon, 2010), and cellular cytotoxicity(Caraux et al., 2006). In a study conducted on the rat liver cell line BRL-3A, the authors showed PLCγ2 is an important regulator of cell proliferation via ERK and NF-κB(Ma et al., 2019). Specifically, targeting the gene with short-interference RNA (siRNAs) leads to the decrease of cell viability and proliferation rate, and causes significant down-regulation of the expression of genes involved in the signalling cascade, such as NFκB, FOS, JUN(Ma et al., 2019). The activation of PKC downstream of PLCγ2 has also been widely implicated in learning and memory processes(Sun and Alkon, 2010). Specifically, PKC is known to control the synthesis, vesicle-refilling, and release of many neurotransmitters, such as γ-aminobutyric acid (GABA)-ergic, cholinergic and glutamatergic systems(Nicholls, 1998, Stevens and Sullivan, 1998, Dobransky et al., 2004). Moreover, PKC regulates the phosphorylation of several substrates, such as NMDA receptors, important in the mechanisms of information storage(Sun and Alkon, 2010). Finally, PLCγ2 has also been shown to be critical for cellular cytotoxicity of natural killer (NK) cells(Caraux et al., 2006). This function of NK cells is important in the rapid response to tumour and infected cells that have

lost the expression of MHC class I molecules or have acquired the expression of stress-induced ligands. NK activity both in basal conditions and upon stimulation were undetectable in PLCγ2 KO cells(Caraux et al., 2006).

AD researchers are increasingly interested in PLCγ2 as a downstream effector of TREM2 signalling. TREM2 is a transmembrane receptor which is present in myeloid cells, including microglia, and PLCγ2 is one of its main downstream effectors. Several variants in the TREM2 gene have been described in recent years as associated with increased risk for LOAD(Sims et al., 2017, Guerreiro et al., 2013). These mutations affect TREM2 functions via several ways, such as by decreasing the ligand binding affinity (pR47H(Xiang et al., 2018), p.R62H(Song et al., 2017)), reducing cell surface expression (pT66M(Kleinberger et al., 2014)) or increasing receptor shedding (pH157Y(Thornton et al., 2017)). In turn, this leads to alterations in microglial ability, such as impairment in Aβ binding(Zhao et al., 2018), reduced proliferation(Cheng-Hathaway et al., 2018), increased expression of pro-inflammatory cytokines(Sayed et al., 2020). The discovery in recent years of several polymorphisms (rs61749044(Andy et al., 2021)rs12446759(Bellenguez et al., 2020); rs3935877(de Rojas et al., 2021)) in the *PLCG2* gene that are associated with AD has focussed attention on the function of the TREM2-PLCγ2 pathway in microglia. This pathway has already been investigated in macrophages, where it showed an involvement both in pro- and anti-inflammatory responses(Xing et al., 2015). Initial studies of this pathway in microglia cells revealed roles in the same processes(Andreone et al., 2020, Liu et al., 2020). Another important role of the TREM2-PLCγ2 axis is its involvement in lipid metabolism. TREM2 is a receptor for many ligands, but it is primarily known as a receptor for lipid molecules(Yeh et al., 2016). It is able to bind lipidated Aβ(Kober and Brett, 2017), ApoE(Atagi et al., 2015) and lipids present on the membrane of apoptotic cells(Wang et al., 2015b). Independent KO versions of the two genes in human iPSC-derived macrophages show a common downregulated pattern of genes involved in lipid processing, such as LPL, LIPA, APOC1 and PLIN2(Andreone et al., 2020). Conversely, the overexpression of the newly discovered PLCγ2^{R522} variant showed an

enhancement in the clearance of cholesterol esters, implicating again this pathway in the modulation of lipid metabolism(Andreone et al., 2020).

In addition to TREM2, PLCγ2 interacts with several other proteins expressed by genes which have been found associated with AD (Figure 1.5). Among these, the majority are expressed in microglia and are involved in innate immune pathways.

DAP12 (*TYROBP*) is an adapter protein which associate with activating receptors found on the surface of immune cells, such as TREM2. Upon ligand binding, DAP12 is phosphorylated in two tyrosine located within the immunoreceptor tyrosine-based activation motif (ITAM) and recruits kinases such as Syk which activate downstream signalling, including PLCγ2 and PI3K(Konishi and Kiyama, 2018). *TYROBP* mutations have been described in a cohort of EOAD patients(Pottier et al., 2016) and the gene has been found upregulated in LOAD. Moreover, using an integrative network-based approach, the authors identified *TYROBP* as a key regulator within the immune/microglia module(Zhang et al., 2013).

CD33 (*Siglec3*) is another innate immune receptor which is expressed on the surface of myeloid cells, specifically microglia. Two different GWAS studies in 2011, identified a SNP on the gene associated with decreased risk of developing AD(Hollingworth et al., 2011, Naj et al., 2011). Upon stimulation, the immunoreceptor tyrosine-based inhibition motif (ITIM) of the receptor acts as a docking site for tyrosine kinases of the Src family. This leads to the recruitment and activation of phosphatases, such as SH2-contaning inositol phosphatase 1 (SHIP1), among others.

SHIP1 phosphatase is encoded by *INPP5D* gene, previously found to be associated with LOAD(Lambert et al., 2013) and to be selectively expressed in plaque-associated microglia(Tsai et al., 2021). SHIP1 is able to counterbalance the proinflammatory signalling originating from ITAMs containing receptors such as TREM2-associated DAP12, by inhibiting the effector molecules among which Syk and PLCγ2, blocking the facto TREM2 downstream signalling(Wißfeld et al., 2021,

Peng et al., 2010). Moreover SHIP1 counteract PI3K activity by converting PIP_3 to PIP_2(Malik et al., 2015).

Finally, SHIP1 is able to bind to CD2AP(Bao et al., 2012), the product of another LOAD risk gene(Hollingworth et al., 2011), to form a complex with RAB5-activating guanine nucleotide exchange factor (RIN3)(Rouka et al., 2015), and BIN1(Shen et al., 2020), itself as well risk locus for LOAD(Hu et al., 2011). This complex may be able to increase uptake and degradation of Aβ by microglia cells.

PLCG2 locates then in a complex network together with several other AD risk. Understanding the role of PLCγ2 variants in the context of all these others molecules will be of benefit for the understanding of pathological mechanisms of AD.

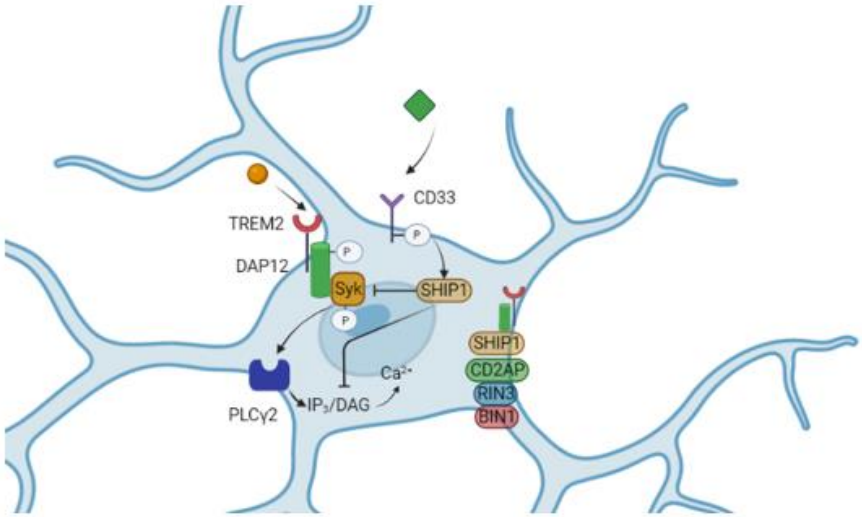

Figure 1.5 – PLCγ2 is located in a complex network of microglia signalling pathways involving several AD risk genes. Several interactions have been reported between the AD risk genes involved in innate immune responses and inflammation. Trem2 receptor signals through DAP12-Syk-PLCγ2 pathway to activate microglial phagocytosis and inflammatory response. Activated CD33 recruits

SHIP1 to inhibit Syk and PLCγ2 signalling. SHIP1 has been shown to complex with CD2AP and BIN1, other two AD associated proteins, probably to increase uptake and degradation of Aβ. Image adapted from Hodges et al., 2021 and Sierksma et al., 2020.

1.4.4 PLCγ2 deficiency disorders

Before being associated with AD, *PLCG2* mutations and deletions have been described in a series of auto-inflammatory syndromes characterized by an aberrant activation of the innate immune cells (Figure 1.4A) (Neves et al., 2018).

Ombrello and colleagues firstly described three genomic deletions, two spanning exon 19, and the third from exon 20 to 22, which all translated to complete or partial absence of the C-terminal Src-homology 2 (cSH2) domain of PLCγ2, the autoinhibitory region of the protein that prevents constitutive enzymatic function (Figure 1.4A)(Ombrello et al., 2012). All analysed subjects presented with cold-induced urticaria, and variable manifestations of immune defects such as antibody deficiency, recurrent infection and cutaneous lesions. From a molecular point of view, individuals showed reduced serum levels of IgM and IgA, as well as circulating natural killer cells and class-switched memory B cells. In vitro functional studies of cells expressing PLCγ2 protein with the pathogenic deletions revealed an elevated basal phospholipase activity when compared with WT PLCγ2. The authors proposed the term PLAID () to refer to this specific clinical, genetic and functional condition. PLCγ2-associated antibody deficiency and immune dysregulation

Zhou and colleagues identified a missense gain-of-function mutation (c. 2120C>A) [p. S707Y] that disrupts the highly conserved region in the auto inhibitory SH2 domain. The individuals described in the study presented with recurrent blistering skin lesions with inflammatory infiltrate and involvement of other tissues, such as joints, the eye and the gastrointestinal tract(Zhou et al., 2012a). Analysis of circulating lymphocytes showed a similar result seen in patients of a previous study, namely the decreased number of class-switched memory B cells and natural

killer cells. Functional studies confirmed the mutation is a hypermorphic substitution that causes an increase in the activity of the enzyme, leading to enhanced production of intracellular IP_3 and a consequent increase of intracellular Ca^{2+}. Considering the molecular similarities with the previously described disease, but also the phenotypic differences in the manifestation, the authorise suggested the name APLAID (autoinflammation and PLCγ2-associated antibody deficiency and immune dysregulation) for this disorder, to distinguish the phenotypes caused by missense mutations from phenotypes caused by genomic deletions(Zhou et al., 2012a).

Kutukculer and colleagues reported a novel missense variation (c.2152A>C) [p. S718R] in a 12-year-old girl. This mutation is also located in the autoinhibitory SH2 domain. The recurrent symptoms were consistent with common variable immunodeficiency (CVID), a symptomatic heterogeneous group of primary immunodeficiency characterized by low serum immunoglobulins and recurrent infections. No functional characterization of the protein harbouring the variant has been carried out yet(Kutukculer et al., 2021).

Despite the wide range of phenotypes, several are highly overlapping between the disorders aforementioned. Moreover, striking molecular mechanism similarities, such as impaired B cell memory and immunoglobulin production, led some authors to formulate the hypothesis that this disorder should be referred to with the unique name of “PLCγ2 deficiency” (Kutukculer et al., 2021). Notably, the majority of these mutations are located in the autoinhibitory C-terminal SH2 domain of the protein, conferring gain-of-function activity(Novice et al., 2020).

1.4.5 PLCγ2^{R522} variant in Alzheimer’s Disease

After the discovery of the newly protective variant in the *PLCγ2* gene associated with AD, a common effort in the scientific community focused on deciphering the biological meaning of this new mutation. Interestingly, Kleineidam and colleagues

showed that patients with MCI harbouring the R522 SNP have a slower cognitive decline when compared with non-carriers(Kleineidam et al., 2020)

1.4.5.1 Structural changes

This missense variant (rs72824905, OR=0.68), leads to an amino acid change at position 522, where a proline (P) is substituted by an arginine (R) (Table 1.1). From molecular dynamic modelling, Maguire and colleagues formulated several predictions on the effect of this amino acid change. Firstly, arginine is bigger than proline, and it also carries a positive charge in a predominantly electronegative region; this size and charge change may introduce an interaction between this amino acid and other domains of the protein(Maguire et al., 2021). Magno and colleagues suggested that interaction between the arginine and elements of the autoinhibitory interface may occur, causing a mild disruption in the region (Magno et al., 2021).

Secondly, although the mutation does not seem to introduce any major differences in the flexibility of the global protein, it has a great effect on the flexibility of the single amino acid in 522 position and other small areas nearby, such as the loop containing residues 643-651. This region partially constitutes the autoinhibitory cSH2 domain, which is significantly altered in position and structure when compared to the WT protein(Maguire et al., 2021). Magno and colleagues suggested classifying mutations of PLCγ2 into two main categories. The first group refers to the mutations that map in the autoinhibitory interface. The majority of these previously described mutations are involved in several inflammatory diseases and were shown to strongly activate PLCγ2 functionality. These mutations moreover can be considered disease-causing. On the other side, Magno and colleagues classify only PLCγ2^{R522} mutation that show very mild activation of PLCγ2. The mild activation can be explained by the position of the variant, which is not in the autoinhibitory interface, but on the linker in the γSA region that connect the sPH and nSH2 domains, however indirectly affecting the cSH2 domain.

1.4.5.2 Functional changes

The first functional results on the novel PLCγ2^{R522} variant in AD showed that it has a small hypermorphic effect, leading to increased activation of the enzyme in human cell lines HEK293 and COS overexpressing the polymorphism(Magno et al., 2019). Specifically, the authors quantified the production of inositol phosphates (in particular inositol phosphate 1 – IP1 – which accumulate over time and is easily measurable) and the release of intracellular Ca^{2+}. PLCγ2^{R522} displayed an increased enzyme activity in comparison to PLCγ2^{P522}. Takalo and colleagues repeated the finding using bone-marrow derived macrophages (BMDM) from mice harbouring the protective variant: a significant higher basal level of IP1 was detected in PLCγ2^{R522}(Takalo et al., 2020). This evidence was confirmed in an iPSC-derived microglia model, where intracellular Ca^{2+} was shown to be elevated following stimulation with an Fcγ activating antibody in comparison with the *PLCG2*^{P522} common SNP(Maguire et al., 2021). Moreover, mouse studies showed decreased PIP2 basal levels in mouse brains harbouring the PLCγ2^{R522} variant, which again can be explained by an increased basal activity of the enzyme(Maguire et al., 2021). As discussed above, other mutations on the *PLCG2* locus, specifically affecting the autoinhibitory interface, disrupt the regulatory domain which block enzyme inactivation, resulting in overactivation of the protein. PLCγ2^{R522} variant is located in a region that exerts regulatory functions, which might explain the hyperactivation of PLCγ2(Magno et al., 2019).

As previously stated, one of the main functions of microglia is their ability to phagocytose debris and foreign particles. Maguire et al. showed a significant reduction in the phagocytic ability of the PLCγ2^{R522} variant compared to the common variant using mouse macrophages and microglia, as well as human iPSC-derived microglia with bioparticles derived from both *E. coli* and zymosan(Maguire et al., 2021). This result is still controversial as another study showed a trend towards enhanced phagocytosis of zymosan bioparticles of the protective variant in BMDM cells(Takalo et al., 2020).

Maguire et al. also investigated the endocytic clearance ability of fluorescent oAβ_{1-42} and in all the models tested (mouse macrophages and microglia, and human iPSC-derived microglia), PLCγ2^{R522} displayed an enhanced activity(Maguire et al., 2021).

PLCγ2 has been extensively shown to signal downstream several TLRs to mediate inflammatory responses in peripheral immune cells(Chiang et al., 2012, Chae et al., 2015, Bae et al., 2017, Zhu et al., 2018). As of today, few studies have been published showing an involvement of PLCγ2 in inflammatory processes in microglia. Andreone et al. used a KO version of the gene in iPSC-derived microglia and demonstrated that upon zymosan stimulation, the response of the PLCγ2 KO was significantly downregulated in comparison to the WT when assessed via RNA Sequencing. Several genes were validated in a panel of proinflammatory cytokines and chemokines by qRTPCR mRNA analysis such as IL-6, IL1a, CXCL8 and CCL20 among others, all showing an attenuated response in PLCγ2 KO microglia. This suggests that PLCγ2 is important in zymosan-mediated inflammatory response in microglia cells, and that its signalling contributes to an enhanced proinflammatory response(Andreone et al., 2020). Moreover, PLCγ2 has been shown to induce NFκB mediated cytokine production in peripheral immune cells(Xu et al., 2009). Takalo and colleagues reported the first result regarding the role of the novel PLCγ2 protective variant following an inflammatory stimulus. They showed a significantly higher level of TNF, IL-6 and IL-1β after LPS + IFN-γ (Interferon γ) stimulus in BMDM carrying the protective polymorphism compared to the common variant(Takalo et al., 2020).

Evidence from peripheral immune cells described a role for PLCγ2 in NOD-like receptor family pyrin domain 3 (NLRP3) inflammasome activation(Chae et al., 2015). The NLRP3 inflammasome is a cytoplasmic complex made up of three main elements: the regulatory subunit NLRP3, the adaptor ASC, and then effector caspase-1 (Murakami et al., 2012). A variety of infection-related stimuli induce formation of the complex. The activation consists of two sequential signals: the

first, the priming step, is generally induced by various PAMPs and DAMPs, such as LPS or Aβ, through the activation of pattern recognition receptors (PRRs), such as TLRs and cytokine receptors, such as IL-1R(Yang et al., 2020). The priming step is important for the transcriptional up-regulation of the regulatory subunit. The activation step, is usually a signal of cellular stress, such as DAMPs, PAMPs, flux of Ca^{2+} and efflux of potassium (K^{+}) or chloride (Cl^{-}) ions(Murakami et al., 2012). Similarly, to what was observed from the broad RNASeq following the zymosan stimuli, Andreone and colleagues showed a reduction in the levels of both IL-1β and IL-18 in PLCγ2 KO microglia after applying a double stimulus (LPS + ATP) to activate the NLRP inflammasome. No evidence has been reported yet on the role of the novel protective variant on the functionality of the NLRP3 inflammasome.

Other polymorphisms in *PLCG2* have been recently identified through large-scale GWAS. Tsai and colleagues described a new rare missense variant, M28L (rs61749044; OR=1.164) which confers increased risk of AD(Andy et al., 2021). Bellenguez and colleagues have reported a new protective variant (rs12446759; OR=0.94), which is located upstream of the coding region for *PLCG2*. As yet no functional analysis has been carried out on this variant to elucidate the effect on expression levels(Bellenguez et al., 2020). Finally, a third polymorphism has been reported (rs3935877; OR=0.92). This variant maps on an intron of the gene and has not been characterized(de Rojas et al., 2021) (Table 1.1).

Table 1.1 - Summary statistics of significantly associated regions in *PLCG2* gene identified in GWAS. "AA" = aminoacid; "P" = P-value; "OR" = Odd Ratio

SNP ID	AA Change	P	OR	Notes	Reference
rs72824905	P522R	$5.38*10^{-10}$	0.68		Sims et al., 2017
rs61749044	M28L	0.047	1.164		Tsai et al., 2020
rs12446759	N/A	$1.2*10^{-13}$	0.94	Located upstream of the coding region for *PLCY2*	Bellenguez et al., 2020
rs3935877	N/A	$6.9*10^{-9}$	0.92	Located on an intron of the gene	de Rojas et al., 2021

1.

The project presented here is divided in two parts.

The first part (Chapter 3) aimed at testing several protocols to determine the most successful in order to recover the viability and cells number of a cohort of PBMCs. These samples were originally collected from individuals sampled for GWAS and

calculated to have either high or low PRS for AD. We hypothesized that subculturing and promoting proliferation of specifically T cell subpopulations, would increase the chance of successful reprogramming to iPSCs. The samples were indeed reprogrammed and PBMCs-derived iPSCs were extensively characterized.

Recent GWAS helped to uncover the strong genetic component of AD. One of the most recent discovery is the R522 protective variant found on *PLCG2* gene. The second part of the project aimed at better understanding the role of this new variant in the neuroinflammatory functions of microglia cells, in the context of Alzheimer's Disease. Chapter 4 presents a comparison between different microglia differentiation protocols and set the ground for functional studies on the novel discovered SNP. We hypothesized that cells harbouring the R522 would be able to differentiate to microglia-like cells in a similar way when compared to cells harbouring P522 variant or the KO. Moreover, we set out to confirm our hypothesis that microglia-like cells co-cultured with cortical neurons and astrocyte conditioned media show a more physiological ramified morphology when compare with microglia-like cells cultured on normal plastic plates. Finally, in chapter 5, functional assays were carried out to explore the effects on the inflammatory response of iPSCs-derived microglia carrying PLCγ2^{R522} and PLCγ2^{KO} in comparison to the common PLCγ2^{P522} variant. In the light of recent evidences showing R522 variant being a hypermorphic protective mutation, we hypothesized that the enzyme harbouring this novel protective SNP would display decreased inflammatory burden in comparison with P522 variant.

2 Materials and Methods

2.1 Materials

2.1.1 Cell Culture

2.1.1.1 Cell Culture media

Medium	Company	Catalogue Number
RPMI-1640	Gibco	#11875093
StemPro-34 SFM	Gibco	#10639011
Essential E8 Flex medium kit	Life Technologies	#A2858501
mTesr™1	StemCell Technologies	#85850
Advanced DMEM/F-12 (ADF)	Life Technologies	#12634028
Knockout DMEM/F-12	Life Technologies	#12660012
Neurobasal Medium SFM	Life Technologies	#21103049
XVIVO-15	Lonza	#BE02-060F
IMDM with Glutamax	Gibco	#31980-030
F12	Gibco	#11765- 047

2.1.1.2 Coatings

Reagent	Company	Catalogue Number
Matrigel Growth factor reduced	Corning	#354230
Mouse embryonic fibroblast (MEF) feeder layer	Invitrogen	#A24903
Human Fibronectin protein	Merck Millipore	#FC010-10MG
Poly-D-Lysine hydrobromide	Sigma-Aldrich	#P6407

2.1.1.3 Cell Culture Reagents

Reagent	Company	Catalogue Number
Bovine Serum Albumin	Sigma Aldrich	#A7888
Human TruStain FcX™ - Fc Blocking	Biolegend	#422301
Penicilin/Streptomycin (5000 U/5000 µg)	Gibco	#15070063
StemPro Accutase Cell Dissociation Reagent	Life Technologies	#A1110501
ReLeSR	Stem Cell Technologies	#05873

dPBS without CaCl and MgCl	Life Technologies	#14190250
PBS pH 7.4 without CaCl and MgCl	Gibco	#10010-023
Distilled water	Gibco	#1523-089
Y-27632 dihydrochloride (ROCK Inhibitor)	Tocris	#1254
Trypan Blue	Gibco	#15250061
Pluricin	Stem Cell Technology	#72822
Live Cell Imaging Solution	Invitrogen	#A14291DJ
Human Transferrin	Roche	#10-652-202-001
Glutamic Acid	Sigma-Aldrich	#G8415
1-Thioglycerol	Sigma-Aldrich	#M6145
CryoStore CS10	Stem Cell Technologies	#07931
Polyvinyl Alcohol (PVA)	Sigma-Aldrich	#P8136
Glucose Solution	Gibco	#15384895

2.1.1.4 Cell Culture Supplements

Supplement	Company	Catalogue Number
MACS NeuroBrew-21	Miltenyi Biotec	#130-093-566
MACS NeuroBrew-21 (w/o Vit.A)	Miltenyi Biotec	#130-097-263
Glutamax	Gibco	#25030081
N2 Supplement (100X)	Gibco	#17502-048
B27 Supplement (50X)	Gibco	#17504-001

2.1.1.5 Growth Factors for PBMC Expansion

Growth factor	Company	Catalogue Number
SCF	Miltenyi Biotec	#130-096-692
Flt-3	R&D	#308-FK
IL-3	R&D	#203-IL
IL-6	R&D	#206-IL
PHA-P	Sigma-Aldrich	#L1668
IL-2	Sigma-Aldrich	#SRP6170
IL-4	Peprotech	#200-04
IL-15	Sigma	#SRP6293

GM-CSF	Biolegend	#713604
LPS	Sigma-Aldrich	#L6529

2.1.1.6 Growth Factors for Trilienage Differentiation

Growth factor	Company	Catalogue Number
BMP-4	Peprotech	#120-05ET
VEGF-121	Peprotech	#100-20
SCF	Peprotech	#300-07
SB431542	HelloBio	#HB3555
LDN193189	HelloBio	#HB5624
CHIR99021	MiltenyiBiotec	#130-103-926
Activin A	Peprotech	#120-14E

2.1.1.7 Growth Factors for Microglia precursors Differentiation – Van Wilgenburg

Growth factor	Company	Catalogue Number
BMP-4	Peprotech	#120-05ET
VEGF-121	Peprotech	#100-20
SCF	Peprotech	#300-07
MCSF	Peprotech	#300-25
IL-3	Peprotech	#200-03

2.1.1.8 Growth Factors for Microglia precursors Differentiation – Takata

Growth factor	Company	Catalogue Number
BMP-4	R&D	#314-BP
VEGF-165	R&D	#293-VE
CHIR99021	MiltenyiBiotec	#130-103-926

FGF2	R&D	#233-FB
SCF	R&D	#255-SC
DKK-1	R&D	#5439-DK
IL-6	R&D	#206-IL
IL-3	R&D	#203-IL
MCSF	R&D	#216-MC

2.1.1.9 Growth Factors for induction of microglia-like cells

Growth factor	Company	Catalogue Number
GM-CSF	Biolegend	#572902
IL-34	Biolegend	#577906

2.1.1.10 Growth Factors for Neuronal Differentiation

Growth factor	Company	Catalogue Number
SB431542	HelloBio	#HB3555
LDN193189	HelloBio	#HB5624
IWR-1-endo	Miltenyi Biotec	#130-110-491
FGF_2	Peprotech	#100-18B
PD0332991	Tocris	#4786
DAPT	HelloBio	#HB3345
BDNF	Miltenyi Biotec	#130-93-811
Forskolin	HelloBio	#HB1348
CHIR99021	HelloBio	#HB1262
Ascorbic Acid	HelloBio	#HB1238
$CaCl_2$	Sigma	#21115
GABA	HelloBio	#HB0882

2.1.1.11 Growth Factors for Astrocyte Differentiation

Growth factor	Company	Catalogue Number
EGF	Miltenyi Biotec	#130-093825
LIF	Peprotech	#300-05
FGF_2	Peprotech	#100-18B
CNTF	Peprotech	#450-13

2.1.1.12 Media composition table

Medium name	Base Medium	Supplemented with:
Peripheral Blood Mononuclear Cells (PBMCs) culture		
Complete PBMC Medium	StemPro medium (Gibco)	**SCF** (100ng/ml); **Flt-3** (100ng/ml); **IL-3** (20ng/ml), **IL-6** (20ng/ml)
Expansion Medium A	RPMI 1640 (Gibco)	10% **FBS**; 1% **PenStrep**; **PHA-P** (10µg/ml); **IL-2** (20ng/ml), **IL-4** (20ng/ml), **IL-15** (100ng/ml), **GM-CSF** (20ng/ml); **LPS** (100µg/ml)
Expansion Medium B	RPMI 1640 (Gibco)	0% **FBS**; **IL-2** (35ng/ml)
Trilineage Differentiation		
Mesodermal induction medium	E8 flex	**VEGF-121** (50ng/ml); **BMP-4** (50ng/ml); **SCF** (20ng/ml).
Neuronal induction medium	50% Advance DMEM/F12; 50% Neurobasal medium,	**1X MACS NeuroBrew-21** (Milteny) without retinoic acid, 1x **Glutamax**, 1x **Pen/Strep**, **SB431542** (10µM), **LDN193189** (0,1 µM).
Endodermal induction medium	IMDM	1x **Glutamax**; 1x **PenStrep,** 10mM **Glucose**, 0,5% **BSA, CHIR00921** (3 µM), **Activine A** (100ng/ml).

Microglia-like cell Differentiation		
Mesodermal induction medium (Van Wilgenburg Protocol)	mTesr/E8 flex (specified in the text)	**VEGF-121** (50ng/ml); **BMP-4** (50ng/ml); **SCF** (20ng/ml).
Factory medium (Van Wilgenburg Protocol)	X-VIVO15 (Lonza)	**M-CSF (**50 ng/ml); **IL-3** (50 ng/ml)
Macrophage precursor Differentiation medium (Takata protocol) – Day 1-16	StemPro Medium	200 µg/mL **Human Transferrin;** 2 mM **Glutamic Acid**; 1x **Pen/Strep**; 0.5 mM **Ascorbic Acid**; 0.45mM **MTG** Day 0 (5 ng/mL BMP4, 50 ng/mL VEGF, and 2 uM CHIR99021), Day 2 (5 ng/mL BMP4, 50 ng/mL VEGF, and 20 ng/mL FGF2), Day 4 (15 ng/mL VEGF and 5 ng/mL FGF2), Day 6 to 10 (10 ng/mL VEGF, 10 ng/mL FGF2, 50 ng/mL SCF, 30 ng/mL DKK-1,10 ng/mL IL-6, and 20 ng/mL IL-3), Day 12 and 14 (10 ng/mL FGF2, 50 ng/mL SCF, 10 ng/mL IL-6, and 20 ng/mL IL-3)
SF-Diff Medium (Takata protocol) – From day 16	From day 16 – Serum Free Differentiation Medium: 75% IMDM with Glutamax (GIBCO), 25% F12 (GIBCO)	1x **N2 supplement;** 1x **B27 supplement;** 0.05% **BSA;** 1x **Pen/Strep**

Microglia-like cells Terminal Differentiation medium	X-VIVO15 (Lonza)	**GM-CSF** (10ng/ml); **IL-34** (100ng/ml)
Neuronal Differentiation		
SLI	ADF	1x **Pen/Strep;** 1x **Glutamax;** 1x **NeuroBrew (w/o Vit.A); SB** (10µM); **LDN** (200nM); **IWR** (1.5µM)
NB	DF	1x **Pen/Strep;** 1x **Glutamax;** 1x **NeuroBrew (w/o Vit.A);**
NF	ADF	1x **Pen/Strep;** 1x **Glutamax;** 1x **NeuroBrew (with Vit.A); FGF** (20ng/ml)
SJA	ADF	1x **Pen/Strep;** 1x **Glutamax;** x **NeuroBrew (with Vit.A); PD0332991** (2µM); **DAPT** (10µM); **BDNF** (10ng/ml) **Forskolin** (10µM); **CHIR99021** (3µM); **Ascorbic Acid** (200µM); **$CaCl_2$** (0.8mM); **GABA** (300µM)
SJB	50% Neurobasal + 50% ADF	1x **Pen/Strep;** 1x **Glutamax;** 1x **NeuroBrew (with Vit.A); PD0332991** (2µM); **Ascorbic Acid** (200µM); **$CaCl_2$** (0.4mM);
Astrocyte Differentiation		
SLI	ADF	1x **Pen/Strep;** 1x **Glutamax;** 1x **NeuroBrew (w/o Vit.A); SB** (10µM); **LDN** (200nM); **IWR** (1.5µM)
NB	ADF	1x **Pen/Strep;** 1x **Glutamax;** 1x **NeuroBrew (w/o Vit.A);**
NEL	ADF	1x **Pen/Strep;** 1x **Glutamax;** 1x **NeuroBrew (with Vit.A); EGF** (20ng/ml); **LIF** (20ng/ml)
NEF	ADF	1x **Pen/Strep;** 1x **Glutamax;** 1x **NeuroBrew (with Vit.A); FGF** (20ng/ml); **EGF** (20ng/ml)

CNTF	50% Neurobasal-A + 50% ADF	1x **Pen/Strep;** 1x **Glutamax;** 1x **NeuroBrew (with Vit.A); CNTF** (10ng/ml)
Astrocyte Conditioning Medium	ADF	1x **Pen/Strep;** 1x **Glutamax;** 1x **NeuroBrew (with Vit.A);**
Neuron-Microglia Co-culture Differentiation		
Co-culture Medium	Neurobasal A (1x Pen/Strep; 1x Glutamax) + ACM	1x **NeuroBrew (with Vit.A);** **$CaCl_2$** (0.4mM); **Fibronectin** (1µg/ml)

2.1.2 Flow Cytometry

2.1.2.1 General:

Solution	**Composition**
FACS wash	dPBS (-Ca^{2+}, -Mg^{2+}); 5mM EDTA; 2mM NaN_3; 0.5% BSA
FACS blocking buffer	FACS wash; 5% FBS

2.1.1.1 2.1.2.2 Conjugated Antibodies:

Marker	**Clone**	**Isotype Control**	**Supplier and Ref. number**
T cells characterization			
CD3 - PE-Cy7	UCHT1	Mouse IgG1, k	Invitrogen, #25-0038-42
CD14 - APC	63-D3	Mouse IgG1,k	Biolegend, #367117
Macrophage Precursors			
CD45 - FITC	2D1	Mouse IgG1κ	Biolegend, #368507
CD14 - APC	63-D3	Mouse IgG1,k	Biolegend, #367117
CD11b – BV421	ICRF44	Mouse IgG1, κ	Biolegend, #301323

CD14 – APC/Fire 750	63D3	Mouse IgG1, κ	Biolegend, #367119
Astrocyte Precursors Cells			
CD44 - FITC	REA690	Recombinant human, IgG1	Miltenyi Biotec, #130-113-903

2.1.3 Immunocytochemistry

2.1.3.1 General:

Item	**Company**	**Catalogue Number**
DAPI (4',6-diamidino-2-phenylindole)	Invitrogen	#D3571
Prolong gold antifade mountant	Invitrogen	#P36930
Solution	**Composition**	
Bocking Buffer	PBS + 3% goat/chicken serum	

2.1.3.2 Primary Antibody:

Marker	**Host and concentration**	**Supplier and Ref. number**
Sendai vector-free iPSCs check		
anti-SeV	Rabbit anti-human	MBL International Corporation; #PD029
PBMC-derived iPSCs characterization		
Sox2	Mouse anti-human 1:200	Abcam, #ab171380
Oct4	Rabbit anti-human 1:200	Abcam, #ab200834
Tra-1-60	Mouse anti-human 1:100	Abcam, #ab16288

Macrophage Precursors and Microglia		
CD11b	Rat anti-human 1:100	Abcam, #ab8878
CD45	Mouse anti-human, 1:100	Abcam, #ab30470
Runx1	Rabbit anti-human 1:100	Abcam, #ab61753
Iba1	Rabbit anti-human 1:100	Abcam, #ab178680
Tmem119	Rabbit anti-human 1:50	Abcam, #ab185333
CX3CR1	Rabbit anti-human 1:100	Bio-Rad # AHP1589
Neuronal Precursors Cells and Cortical Neurons		
βIIITub	Rabbit anti-human 1:200	Abcam, #ab18207
Pax6	Mouse anti-human 1:50	DSHB
Tbr1	Rabbit anti-human 1:500	Abcam, #ab183032
Ctip2	Rat anti-human 1:200	Abcam, # ab18465
Astrocyte Precursors Cells and Astrocyte		
Vimentin	Goat anti-human 1:500	Abcam, #ab1620
GFAP	Rabbit anti-human 1:500	Abcam, # ab33922
CD49	Rat anti-human 1:1000	Biolegend, #313602
Microglia-Neuronal co-culture		
Iba1	Goat anti-human 1:100	Abcam, #ab5076
MAP2	Rabbit anti-human 1:100	Abcam, #ab32454

2.1.3.3 Secondary Antibody:

Marker	Host and concentration	Supplier and Ref. number
AF594	Goat anti-mouse 1:500	Invitrogen, A11032
AF488	Goat anti-rabbit 1:500	Invitrogen, A11008
AF488	Goat anti-rat 1:500	Invitrogen, A11006
AF594	Goat anti-rat 1:500	Invitrogen, A11007

2.1.4 qPCR primer sequences

Gene	Forward primer	Reverse primer
Sendai vector-free iPSCs check		
SeV	GGATCACTAGGTGATATCGAGC	ACCAGACAAGAGTTTAAGAGATATGTATC
KOS	ATGCACCGCTACGACGTGAGCGC	ACCTTGACAATCCTGATGTGG
Klf4	TTCCTGCATGCCAGAGGAGCCC	AATGTATCGAAGGTGCTCAA
c-Myc	TAACTGACTAGCAGGCTTGTCG	TCCACATACAGTCCTGGATGATGATG
Trilineage Differentiation		
Oct4	AGAACCGAGTGAGAGGCAAC	ACACTCGGACCACATCCTTC
Pax6	AGGCCAGCAACACACCTAGT	GCCTCCCCTTCCAGTCTTTC
Kdr	GGCCCAATAATCAGAGTGGCA	CCAGTGTCATTTCCGATCACTTT
CD117	CATCCCCACACCCTGTTCAC	TGTACTTCATACATGGGTTTCTGT
Pluripotency Markers		
OCT4	AGAACCGAGTGAGAGGCAAC	ACACTCGGACCACATCCTTC

NANOG	ACCTCAGCTACAAACAGGTGAA	TCTGCGTCACACCATTGCTA
Macrophage Precursors and Microglia		
Brachyury	TCAGCAAAGTCAAGCTCACCA	CCCCAACTCTCACTATGTGGATT
CD34	TGGACCGCGGCTTTGCT	CCCTGGGTAGGTAACTCTGGG
Runx1	CTGCCCATCGCTTTCAAGGT	GCCGAGTAGTTTTCATCATTGCC
Kdr	GGCCCAATAATCAGAGTGGCA	CCAGTGTCATTTCCGATCACTTT
CX3CR1	TGGGGCCTTCACCATGGAT	GCCAATGGCAAAGATGACGGAG
AIF1	CTGAGCTATGAGCCAAAC	GGAATTGCTTGTTGATCTCA
P2RY12	AATGCGATCTGTATCAGCGTG	TGGTGTCGTAACAGGTGATGG
TMEM119	CTTCCTGGATGGGATAGTGGAC	GCACAGACGATGAACATCAGC
CD11b	GAAAGGCAAGGAAGCCGGAG	TGGATCTGTCCTTCTCTTAGCCG
Neuronal Precursors Cells and Cortical Neurons		
Pax6	AGGCCAGCAACACACCTAGT	GCCTCCCCTTCCAGTCTTTC
Otx1	GCCTCCCCTTCCAGTCTTTC	GGGCAGAAACACGCCAGTTA
Satb2	GTCTTCTCGGCTCTTGGTGT	GTGTCTTCTTCTGGTGCGGA
vGlut	CGACGACAGCCTTTTGTGGT	GCCGTAGACGTAGAAAACAGA
Astrocyte Precursors Cells and Astrocyte		
NFIA	TTACAGGACCCAGAGCAAGTC	TCAGGGCAGACAAGTTGGAC
Vimentin	GGCGAGGAGAGCAGGATTTC	TGGGTATCAACCAGAGGGAGT
GFAP	GAGCAGGAGGAGCGGCAC	TAGTCGTTGGCTTCGTGCTT
S100b	ATGTCTGAGCTGGAGAAGGC	TTCAAAGAACTCGTGGCAGG

2.1.5 Western Blot

Reagent	Supplier	Catalogue Number
RIPA Buffer	Sigma-Aldrich	#R0278
Mini Protease Inhibitor	Roche	#11836170001
PhosStop	Roche	#049068455001
4-12% NuPAGETM Bis-Tris plus gel	Life Tech	#NP0336PK2
Precision plus protein all blue standards	Biorad	#161-0373
Anti-PLCG2 antibody	Santa Cruz, 1:200	#sc-5283
Anti-α tubulin antibody	Abcam, 1:1000	# ab7291
RDye 800CW Goat (polyclonal) Anti-Mouse IgG (H + L)	LI-COR,	#926-32210

2.1.6 Crispr Transfection and Selection

2.1.6.1 Consumables

Consumable	Supplier	Catalogue Number
tracrRNA	IDT	#107528
Nuclease-Free Duplex buffer	IDT	#1072570
Alt-R® S.p. HiFi Cas9 Nuclease V3	IDT	#1081061
P3 Primary Cell 4D-Nucleofector TM X Kit L	Lonza	#V4XP-3024
Puromycin	Gibco	#A11138-03

2.1.6.2 CRISPR Primers

Target	Forward	Reverse
AAVS1 insert	CGGTTAATGTGGCTC	AGGATCCTCTCTGGC

2.1.6.3 PCR Reagents

Reagent	Supplier	Catalogue Number
Go Tag Polymerase	Promega	#M7801
Buffer	Promega	#M890A
MgCl2	Promega	#A351B
dNTPs	Promega	#U1240
100 bp DNA ladder	Promega	#G210A

2.1.7 Mycoplasma PCR primers sequences

Gene	Forward primer	Reverse primer
Mycoplasma Test		
Myco-5-1	CGCCTGAGTAGTACGTTCGC	
Myco-5-2	CGCCTGAGTAGTACGTACGC	
Myco-5-3	TGCCTGAGTAGTACATTCGC	
Myco-5-4	TGCCTGGGTAGTACATTCGC	
Myco-5-5	CGCCTGGGTAGTACATTCGC	
Myco-5-6	CGCCTGAGTAGTATGCTCGC	
Myco-3-1		GCGGTGTGTACAAGACCCGA
Myco-3-2		GCGGTGTGTACAAAACCCGA
Myco-3-3		GCGGTGTGTACAAACCCCGA

2.1.8 Functional stimuli

Reagent	Supplier	Catalogue Number
LPS	Sigma	#L6529
Amyloid Beta	Bachem	#4061966.1
Zymosan	Sigma	#Z4250
Nigericin	Sigma	#SML1779
ATP	Sigma	#A9187
ADP	Sigma	#A2754
Ionomycin	Merck	#407950
Edelfosine	Tocris	#3022
U73122	Sigma	#U6756
IFN-γ	Fisher Scientific Ltd	#10474733

2.1.9 Kits and probes

Kit	Supplier	Catalogue Number
CytoTune™-iPS 2.0 Sendai Reprogramming Kit	Invitrogen	#A16518
RNeasy Mini Kit	Qiagen	#74104
qScript cDNA Synthesis Kit	Quantabio	#95047
PowerUp SYBR Green Master Mix	ThermoFisher	#A25776
QIAamp DNA Mini Kit	Qiagen	#51304
LEGENDplex Custom Human: IL-6, IL-12p40, IL-10, TNF, G-CSF	Biolegend	#900000594
Human IL-1β/IL-1F2 DuoSet ELISA	R&D	#DY201
Fluo-8	Abcam	#ab142773
Griess Reagent Kit for Nitrite Determination	Life Technologies	#G-7921

2.1.10 Chemicals

Chemical	Company	Catalogue Number
PFA	Sigma	#P6148
Triton-X 100	Sigma	#93443
Tween-20	Sigma	#P7949
Ethanol	Sigma	#458600
2-Propanol	Sigma	#24137
Methanol	Sigma	#32213
DMSO	Sigma	#276855
HFPI	Sigma	#105228
β-mercaptoethanol	Sigma-Aldrich	#M3148

2.1.11 Special plastics

Consumable	Supplier	Catalogue Number
Epredia™ EZ Single Cytofunnel™ with White Filter Cards and Caps	Fisher Scientific	# 12648166
Costar Ultra Low attachment multi well plate	Corning	#CLS7007-24EA

2.1.12 Special equipments

Equipment	Company
4D-Nucleofector™	Lonza
LSRFortessa™	BD Biosciences
Leica TCS SP8	Leica Microsystems
Incucyte®	Sartorius
Opera Phenix™ high-content screening system	PerkinElmer
FLIPR® Penta High-Throughput Cellular Screening System	Molecular Devices
Odyssey® CLx	LI-COR

2.2 Methods – Part 1

2.2.1 Peripheral Blood Mononuclear Cells (PBMCs) culture and expansion

Cryopreserved PBMCs were thawed and assessed for viability at day 0. Prior to reprogramming, cells were cultured with different combinations of medium as specified in the Results section. Samples S9 and S11 were cultured with *Complete PBMC Medium* (2.1.1.12 Media composition table). Medium was changed every day. Samples S12 and S13 were cultured with *Expansion Medium A* (2.1.1.12 Media composition tables). Medium was changed every 3 days. Sample S49 was cultured with *Expansion Medium B* (2.1.1.12 Media composition tables). Sample S86, S87, S88 were cultured with a combination of Expansion Medium B and complete PBMC medium. All samples were tested for cell number and cell viability every 3 days using an automated cell counter (Olympus) and trypan blue. All samples from S12 onward where cultured in an incubator maintained at physiological oxygen levels ($physO_2$; 5%)

2.2.2 Flow Cytometry

Flow Cytometry was carried out in order to analyse cell surface molecules on expanded PBMCs. Cells were counted and fixed in fresh 4% paraformaldehyde (PFA) (pH7.6) for 10 minutes at RT. Cells were centrifuged at 200g for 3 minutes and the resulting pellet was washed three times with FACS wash (2.1.2 Flow Cytometry – General) and blocked for non-specific sites with FACS blocking buffer (2.1.2 Flow Cytometry – General) for one hour at RT. Staining was performed by incubating the cells with marker-specific conjugated antibodies or Ig isotype-matching control (with the same fluorophore, from the same manufacturer) (2.1.2 Flow Cytometry – Conjugated Antibodies) at 4° in the dark for one hour. Following primary staining, the cells were washed three times with FACS wash and centrifuged before being transferred to 5ml round bottom tubes (BD Falcon).

Fluorescence was measured using a LSRFortessa™ and data analysed using FlowJo Software.

2.2.3 Generation of iPSCs from PBMCs using Sendai Virus vector

For iPSCs derivation from PBMCs, the CytoTune 2.0 protocol from ThermoFisher was used. On the day of reprogramming, Sendai Vectors (CytoTune™-iPS 2.0 Sendai Reprogramming Kit, Invitrogen, A16518) expressing the four Yamanaka factors (OCT4, SOX2, KLF4, c-MYC) were used to transduced the PBMC population. Briefly, $4*10^5$ cells were resuspended in *Complete PBMC medium* (2.1.1.12 Media composition table) and seeded in a 12-well plate. After that, SeV were prepared at MOI 5-5-3 (KOS MOI=5, Myc MOI=5, Klf4 MOI=3) in 15-ml Falcon tube containing *Complete PBMC medium* and was added to the cells. Cell were incubated overnight at 37°C and 5% CO_2. Next day, cells were collected in a 15-ml falcon tube and washed with StemPro-34 medium (Gibco) by centrifugation at 200g for 10 min with the brake on. The transduced cell pellets were resuspended in 2ml of *Complete PBMC medium* and transferred into a well of a 12-well plate. Three days post transduction, cells from a well of a 12-well plate were transferred to a well of a Matrigel (1:100 dilution) (Corning) coated 6-well plate containing mouse embryonic fibroblast (MEF) feeder layer (Invitrogen, A24903) and cultured further for 2 days in StemPro-34 medium without cytokines. At day 7 post transduction, cells were cultured with half StemPro-34 medium and half iPSCs medium (E8 flex, Gibco) and from day 8, cells were maintained completely in E8 flex and media was changed every other day. At 15 to 21 days post transduction, the transduced cells started forming colonies with iPSCs morphology which were handpicked and transferred onto 48-well Matrigel-coated plates. Colonies of appropriate size were passaged onto 24-well Matrigel-coated plates (passage 1), subsequently onto 12-well Matrigel coated plate (passage 2) and finally onto 6-well Matrigel coated plates until passage 5 when SeV clearance was checked.

2.2.4 Maintenance and culture of iPSCs

Cell culture was performed in level 2 biosafety hood under sterile conditions. All media and solutions were pre-warmed at RT prior to use.

Reprogrammed human iPSCs were cultured in feeder-free and xeno-free conditions and maintained in Essential 8 flex (E8) medium (Gibco- ThermoFIsher) on Matrigel (Corning) coated plates. Medium was changed every other day and cells were passaged at 80% confluence. To passage, Dulbecco's PBS was added to wash the cells, ReLeSR (Stem Cell Technologies) was then added and incubated for 1 minutes at 37°C. ReLeSR activity was stopped by adding an equal volume of E8 flex and detached cell aggregates were transferred to a 15ml Falcon tube, centrifuged for 3 min at 200g and the cell pellet was then resuspended in E8 medium previously heated to 37°C, before being diluted and replated.

2.2.5 Mycoplasma test

We periodically tested all the cells used in this study for Mycoplasma contamination. 100µl of cell culture supernatant from 80-100% confluent cultures were collected and frozen at -20°. Samples were thaw and subsequently heated for 5 min at 95°C and centrifuged for 2 min at maximum speed. A PCR reaction mastermix containing the following reagents was prepared: 1x PCR buffer, 1 mM $MgCl_2$, 200 µM dNTPs, 0.2 µM of each forward and reverse primer and GoTag polymerase. The PCR was performed using the following program: 95°C for 5 min; 5 cycles of 94°C for 30 sec, 50°C for 30 sec and 72°C for 35 sec; 30 cycles of 94°C for 15 sec, 56°C for 15 sec, 72°C for 30 sec. The PCR products were run on a 1.5% gel at 80V for 40 min. A 100 bp ladder was used to detect positive products (500 bp). A positive control was run together with the samples.

2.2.6 Vector- free iPSCs control – SeV Immunofluorescence

Cells were washed twice with pre-chilled PBS, and then fixed with methanol pre-chilled for 10 minutes on ice. Cells were washed twice again with PBS for 3 minutes each. Anti-SeV (MBL, PD029) diluted in PBS was added onto the cells and incubated

for 45 minutes at 37°C. Cells were washed twice as before and FITC-conjugated anti-rabbit IgG antibody diluted in PBS was added onto the cells and incubated for 30 minutes at RT. Cells were washed with PBS and mounted on microscope slides using Prolong gold antifade mountant (ThermoScientific). Images were taken using a Leica TCS SP8 laser scanning confocal microscope.

2.2.7 Immunocytochemistry

iPSCs cells were plated on PDL- Matrigel- coated slides. iPSCs were cultured with E8 medium till 80% confluency was reached. Cells were fixed with 4% PFA (pH7.6) for 10 minutes at RT, followed by 3 washes with PBS. If intracellular staining followed, cells were incubated with PBS containing 0.1% Triton for 10 minutes at RT (for cytosolic antigen) or with ice cold absolute EtOH for 2 minutes (for nuclear antigens). Fixed cells were incubated with Blocking Buffer (2.1.3 Immunocytochemistry – General) for 1hour at RT. Overnight incubation of the primary antibody (2.1.3 – Immunocytochemistry – Primary Antibody) diluted in Blocking Buffer was performed at 4°C using a humidified chamber. Coverslips were then washed 3 times for 3 minutes, followed by 1 hour incubation with secondary antibody (2.1.3 – Immunocytochemistry – Secondary Antibody) diluted in Blocking Buffer at RT in the dark. Cells were subsequently incubated with Dapi at 1:100 in PBS and mounted on microscope slides using Prolong gold antifade mountant (ThermoScientific). Images were taken at 40x or 63x magnification using a Leica SP8 Laser scanning fluorescent microscope, using 405, 488 and 638 lasers and acquired with LAS X software

2.2.8 Trilineage Differentiation

In order to check the potential of the reprogrammed iPSCs lines to differentiate toward the three germ-layers, cells were split with RelesR into matrigel coated 12-well plates with E8 flex medium, at different densities: 150,000cells/ well for mesoderm differentiation and 600,000 cells/well for ecto- and endoderm differentiation. For mesodermal differentiation, the medium was replaced on day 1 with Mesodermal induction medium (2.1.1.12 Media composition table –

Trilienage Differentiation). Complete medium change was performed on day 3, and cells were collected on day 4 for RT-PCR analysis. For ectodermal differentiation, the medium was replaced on day 1 with Neuronal induction medium (2.1.1.12 Media composition table – Trilienage Differentiation). Complete medium change was performed every day until day 6, when cells were collected for RT-PCR analysis. For endodermal differentiation, the medium was replaced on day 1 with Endodermal induction medium (2.1.1.12 Media composition table – Trilienage Differentiation). CHIR99021 was withdrawn on day 2. Complete medium change was performed every day until day 6, when total RNA was isolated from the cells. The expression level of trilineage differentiation markers were determined via RT-PCR analysis, as described below.

2.2.9 RNA extraction and quantitative RT-PCR

Samples were harvested and lysed in RLT buffer (RNeasy Mini Kit, Qiagen), containing 10µl/ml of β-mercaptoethanol. Total RNA extraction was performed according to the manufacturer's instructions. Reverse transcription was carried out using Superscript II kit (Invitrogen), using 1 µg template RNA in a 20µl reaction volume. For each qPCR reaction, 200ng of cDNA product was used in a 20µl volume. The reaction was performed on a CFX Connect Real Time System (Bio-Rad) using PowerUp SYBR Green Master Mix (Thermo Fisher). Quantification of target gene transcripts was carried out using primers designed and validated with established efficiency between 90 and 110%. Relative gene expression values were analysed with the delta-delta CT method, with reference to β-actin. For list of primer sequences see table "2.1.4 qPCR primer sequences – Trilienage Differentiation".

2.3 Methods – Part 2

2.3.1 Microglia precursors Differentiation protocol - Van Wilgenburg Protocol.

2.3.1.1 EBs Formation Methods

Embryoid bodies (EBs) are three-dimensional structures formed by iPSCs (or ESCs), commonly used to generate specific terminally differentiated cells. Different EBs formation methods were tested for this study. Cells were cultured as described in Paragraph "2.2.4 Maintenance and culture of iPSCs". Ideal cell confluency for all the three methods described below is around 60-80% at the day of EB formation.

Self- aggregation: In order to form self-aggregate EBs, iPSCs were washed once with Dulbecco's PBS and incubated 1 minutes at 37°C with ReLeSR. The cell dissociation agent was removed and iPSCs colonies were gently detached using a 5ml stripette and 2ml of medium. Allow the EBs to complete the self-aggregation process at 37°C overnight. The following day, EBs should be in various size, and the medium was changed to Mesodermal Induction medium/E8 (2.1.1.12 Media composition table – Microglia-like cell differentiation).

Hanging Drop EBs: iPSCs were treated with ROCK Inhibitor one hour prior starting the procedure. Cells were incubated for 10 minutes with Accutase (StemCell Technology) to generate a single cell suspension and. Remaining aggregates were gently broke and Accutase activity was stopped by adding an equal volume of E8; cells were centrifuged for 3 minutes at 300g. Cells were counted and diluted to $1*10^4$ per 20µl in E8/mTesr medium containing 4 mg/ml of PVA. Single cell drops were formed on the lid of a 10cm Nunc Plate, which was then placed back on the plate. The hanging drops were cultured overnight at 37°C with ROCK Inhibitor to allow the formation of the EBs (Lin and Chen, 2008). The following day, EBs should have form with uniform size. At this point, the EBs were cultured into 3cm Nunc Plate with Mesodermal Induction medium using either E8 or mTesr (2.1.1.12 Media composition table – Microglia-like cell differentiation) for 4 days with half medium change at day 2.

Ultra low Adherence 96-well plate: iPSCs were treated with ROCK Inhibitor one hour prior starting the procedure. Cells were incubated for 1 minutes with Accutase in order to form single cells suspension. Remaining aggregates were gently broke and Accutase activity was stopped by adding an equal volume of E8. Cells were counted and diluted to $1*10^6$ per 10ml and plated with Mesodermal Induction medium/E8 (2.1.1.12 Media composition table – Microglia-like cell differentiation)containing 10 µM ROCK inhibitor in an ultra low attachment 96 well plate (Corning), 100µl per well. The plate was then centrifuged 140g for 3 minutes and cells were cultured for 4 days. Half medium change was performed on day 2.

2.3.1.2 Differentiation of iPSCs into machrophages precursors

After 4 days, the cultured EBs were further differentiated by seeding ~ 8 EBs into a well of a 6 well plate in 3ml of Factory medium (2.1.1.12 paragraph - Media composition tables – Microglia-like cell Differentiation). The medium was changed weekly and non-adherent supernatant cells were harvested once a week by centrifugation at 300g for 3 minutes, assayed for viability and prepared for downstream assays.

2.3.2 Microglia precursors Differentiation protocol – Takata protocol

Human iPSCs were cultured to 80% confluency and digested using RelesR (Stem Cell Technologies) in order to generate small aggregates and centrifuged at 200g for 5 minutes. Cells were resuspended in E8 flex and seeded at $3.3 * 10^4$ onto Matrigel-coated 12 well plate.

Starting from the next day, cells were cultured in StemPro Medium for 16 days as described in table "2.1.1.12 Media composition tables – Microglia-like cell Differentiation - Macrophage precursor Differentiation medium (Takata protocol) – Day 1-16". Starting from Day 16, cells were cultured in SF-Diff medium as described in table "2.1.1.12 Media composition table – Microglia-like cell Differentiation - SF-Diff Medium (Takata protocol) – From day 16". Full medium

change was done every 3 days. Floating cells usually appeared around Day 7 and were collected, assayed for viability and prepared for downstream assays.

2.3.3. Induction of microglia-like cells from iPSCs-derived monocytes

Macrophages precursor were seeded into fibronectin-coated (Merk Millipore) 6-well plates or 96-well plate or coverslips at a density of $5x10^5$ cells/well, $1x10^4$ and $5x10^4$ respectively. Cells were cultured with either Microglia-like cells Terminal Differentiation medium (2.1.1.12 Media composition table – Microglia-like cell Differentiation - Microglia-like cells Terminal Differentiation) or Astrocyte Conditioned Media (ACM) (Paragraph 2.3.6). The medium was changed after one week and maintained in culture for up to 14 days.

2.3.4 Cortical Neuron Differentiation Protocol

2.3.4.1 Differentiation of iPSCs into NPCs

iPSCs were differentiated to NPCs using a method adapted by Shi et al 2012. At day -1, iPSCs were treated for 1h with 10 µM ROCK inhibitor, dissociated into single cells using Accutase for 10 min at 37°C and centrifuged for 3 min at 300g. Single cells were plated into Matrigel coated (100µg/ml) 12-well plates in E8 flex containing 10 µM ROCK inhibitor to be approximately 60% confluent. The next day, cells were washed twice with dPBS-/- and cells were maintained in SLI for 7 days (2.1.1.12 Media composition table – Neuronal Differentiation – SLI), with medium changes every day. On day 8, cells were treated with ROCK inhibitor for 1h, dissociated into single cells using Accutase for 10 min at 37°C and split 1:4 into new Matrigel coated (100µg/ml) 12-well plate using NB medium containing 10µM ROCK inhibitor (2.1.1.12 Media composition table – Neuronal Differentiation – NB). The next day, ROCK inhibitor was washed off and medium changed was performed every day until day 16. If remaining iPSCs colonies appeared to be present, cultures were treated with 20µM plurisin from day 14 to day 16. On day 16, NPCs were either frozen or prepared for terminal differentiation. Cells were incubated in NF medium (2.1.1.12 Media composition table – Neuronal

Differentiation – NF) for up to 7 days in order to promote cell proliferation prior terminal differentiation.

2.3.4.2 NPCs terminal differentiation into Cortical Neurons

For terminal differentiation, NPCs were plated in PDL- (100 µg/ml) and Matrigel (100 µg/ml) coated plates. One hour prior plating, cells were treated with 10µM ROCK inhibitor. NPCs were dissociated in single cells suspension using Accutase for 10 minutes at 37°C. Cells were counted and plated using SJA medium (2.1.1.12 Media composition table – Neuronal Differentiation – SJA) for one week performing half medium change every other days. At day 7, medium was replaced with SJB (2.1.1.12 Media composition table – Neuronal Differentiation – SJB), allowing terminal maturation of the cortical neurons for two weeks.

2.3.5 Astrocyte Differentiation Protocol

2.3.5.1 Differentiation of iPSCs into astrocyte precursors cells (APCs)

iPSCs were differentiated to astrocytes using a method adapted by Serio et al., 2013. iPSCs were first differentiated to NPC till day 16 as indicated before (paragraph 2.3.4.1 – Differentiation of iPSCs into neuronal precursors cells). At day 16, NPCs were either frozen or replated into Matrigel coated (100µg/ml) T25 flask using NB medium supplemented with 20 µM plurisin in order to clean the culture from possible stem cells growing. At this point cells were expanded for 3 passage in NEL medium (2.1.1.12 Media composition table – Astrocyte Differentiation – NEL), splitting cells with a ratio of 1:5 when confluent. Cells were then sorted for the astrocyte progenitor marker CD44 using FACS and the appropriate isotype control (2.1.2 Flow Cytometry – Conjugated Antibodies). Briefly, cells were dissociated using Accutase for 10 minutes at 37°C and centrifuged at 300g for 3 minutes. 10^6 cells were resuspended and incubated with CD44 antibody (Milteny), 1:50 (or the appropriate isotype control), for 10 minutes on ice. Cells were washed and resuspended with fresh medium. Cells were sorted using the FACS Aria Fusion

and the isotype control for appropriate gating. Positive cells were collected and replated into Matrigel (50µg/ml) coated 6-well plates for proliferation in NEF medium (2.1.1.12 Media composition table – Astrocyte Differentiation – NEF). When confluent, cells were either frozen in order to build a pure APC stock or plated for terminal differentiation.

2.3.5.2 APC terminal differentiation into Astrocyte Cells

Astrocyte precursors cells were plated in Matrigel (50µg/ml)coated plated in NEF medium. When about 70% confluency was reached, cells were terminally differentiated using CNTF medium (2.1.1.12 Media composition table – Astrocyte Differentiation – CNTF) for two weeks, performing one medium change at day 7. Mature astrocytes were using in order to prepare ACM as explained below.

2.3.6 Astrocyte Conditioned Media Preparation

Terminally differentiated astrocytes were used in order to prepare ACM, important to feed Microglia both in monoculture and in co-culture with iPSCs-derived neurons. Astrocytes were fed for 48h with basal ADF medium supplemented with NeuroBrew with Vitamin A. The conditioned medium was then collected and astrocyte re-fed with fresh basal ADF medium supplemented with NeuroBrew with Vitamin A. Different ACM collections were pooled together to form appropriately labelled batches. Each batch was sterile filtered and frozen down at -80°C until further use. Moreover, CCL2 ELISA was used as housekeeping reference to quantify the mount of secreted proteins and each batch was diluted down in order to reach a final concentration of 1ng/ml of CCL2.

2.3.7 Flow Cytometry

Flow Cytometry was carried out in order to analyse cell surface molecules on non-adherent cells collected from supernatant of differentiated factories or monolayer cells as described above. Cells were counted and fixed in 4% PFA (pH7.6) for 10 minutes at RT. Cells were centrifuged at 200g for 3 minutes and the resulting pellet was washed three times with FACS wash (2.1.2 Flow Cytometry – General) and

blocked for non-specific sites with FACS blocking buffer (2.1.2 Flow Cytometry – General) for one hour at RT. Staining was performed by incubating the cells with marker-specific conjugated antibodies or Ig isotype-matching control (with the same fluorophore, from the same manufacturer) (2.1.2 Flow Cytometry – Conjugated Antibodies) at 4° in the dark for one hour. Following primary staining, the cells were washed three times with FACS wash and centrifuged before being transferred to 5ml round bottom tubes (BD Falcon). Fluorescence was measured using a LSRFortessa™ and data analysed using FlowJo Software.

2.3.8 Cytocentrifugation

Non-adherent macrophages precursor were harvested, counted and fixed in 4% PFA (pH7.6) for 10 minutes at RT. $1X10^5$ cells were spin at 800 rpm for 1 minutes through pre-wet filters onto glass slides using EZ single cytofunnel (Thermoscientific) before staining (as described below).

2.3.9 Immunocytochemistry

iPSCs cells and macrophage precursors were plated on PDL- Matrigel- coated slides. iPSCs were cultured with E8 medium till 80% confluency was reached; macrophage precursors were cultured as described above for up to 14 days allowing microglia-like differentiation. Cells were fixed with 4% PFA (pH7.6) for 10 minutes at RT, followed by 3 washes with PBS. If intracellular staining followed, cells were incubated with PBS containing 0.1% Triton for 10 minutes at RT (for cytosolic antigen) or with ice cold absolute EtOH for 2 minutes (for nuclear antigen). Fixed cells were incubated with Blocking Buffer (2.1.3 Immunocytochemistry – General) for 1hour at RT. Overnight incubation of the primary antibody (2.1.3 – Immunocytochemistry – Primary Antibody) diluted in Blocking Buffer was performed at 4°C using a humidified chamber. Coverslips were then washed 3 times for 3 minutes, followed by 1 hour incubation with secondary antibody (2.1.3 – Immunocytochemistry – Secondary Antibody) diluted in Blocking Buffer at RT in the dark. Cells were subsequently incubated with Dapi at 1:100 in PBS and mounted on microscope slides using Prolong gold antifade mountant

(ThermoScientific). Images were taken at 40x or 63x magnification using a Leica SP8 Laser scanning fluorescent microscope, 405, 488 and 638 lasers and acquired with LAS X software

2.3.10 RNA extraction and quantitative RT-PCR

Samples were harvested and lysed in RLT buffer (RNeasy Mini Kit, Qiagen), containing 10µl/ml of β-mercaptoethanol. Total RNA extraction was performed according to the manufacter's instructions. Reverse transcription was carried out using Superscript II kit (Invitrogen), using 1 µg template RNA in a 20µl reaction volume. For each qPCR reaction, 200ng of cDNA product were used in a 20µl volume. The reaction was performed on a CFX Connect Real Time System (Bio-Rad) using PowerUp SYBR Green Master Mix (Thermo Fisher). Quantification of target gene transcripts was carried out using primers designed and validated with established efficiency between 90 and 110%. Relative gene expression values were delta-delta CT method, with reference to β-actin. For list of primer sequences see table "2.1.4 qPCR primer sequences".

2.3.11 Generation of mcherry reporter cell lined using CRISPR/Cas9 system

2.3.11.1 Nucleofection

The CRISPR/Cas9 system was used to introduce the mcherry reporter into the adeno-associated virus integration site 1 (AAVS1) locus of the iPSCS. Prior to the transfection, iPSCs were incubated for 1h in E8 flex medium (Gibco) containing 10µM ROCK inhibitor. The ribonucleoprotein (RNP) complex was prepared by combining guide RNA (gRNA) and trans-activating RNA (tracrRNA) in equimolar concentration in nuclease-free duplex buffer and annealed at 95° for 2 minutes. The RNP complex was incubated together with Cas9 nuclease (6.2 µg/µl diluted in Cas9 storage buffer: 10 mM Tris-HCl, pH 7.4, 300 mM NaCl, 0.1 mM EDTA, 1mM DTT) for 20 minutes at RT. Cells where then washed with PBS and incubated with

Accutase for 10 minutes at 37°C in order to obtain a single cell suspension. The P3 Primary Cell 4D-NucleofectorTM X Kit L was used following manufacture instructions. Briefly, cells were counted and 200.000 cells were suspended in 20µl of P3 medium. RNP/Cas9 complex together with the reporter vector as well as the cells were added to the cuvette and gently mixed. The 4D-Nucleofector was used setting the CA137 program. Cells were allowed to recover for about 10 minutes after the nucleofection and then plated in Matrigel-coated 6-well plates in E8 flex medium supplemented with 10µM ROCK inhibitor and 1x Pen/Strep. On the following day, medium was changed and single cells were left growing for few days.

2.3.11.2 Selection

The transfected vector contains, besides the reporter gene, a puromycin resistance gene, giving only the transfected cells the ability to survive an incubation with puromycin. Once the single cells were grown into colonies, cells were incubated with 0.35µM puromycin in E8 flex for 3 days, followed by an incubation in 0.5µM puromycin in E8 if needed. Alive colonies were then picked into 96-well plates and imaged using the Incucyte to detect fluorescent expression of the reporter. 96-well plates were duplicated and DNA was collected as described below, in order to run a PCR for double checking the right interation site of the reporter.

2.3.11.3 DNA Extraction

iPSCs were grown to confluency in 96-well plates and DNA was extracted using QIAamp DNA Mini Kit, following manufacturer's instructions.

2.3.11.4 PCR Reactions

PCR were contacted in order to identify the right integration of the reporter gene. The PCR mix contained the following: 1x Reaction Buffer, 1 mM $MgCl_2$, 200 µM dNTPs, 0.4 µM of forward and reverse primer, 2% DMSO, 50 ng DNA sample and GoTag Polymerase. The Thermocycler was run with following conditions: 95°C for

2 min, 30 cycles of: 95°C for 30s, 61.1°C for 30s, 72°C for 30s, followed by 72°C for 5 min. The PCR product was run on an 1% agarose gel at 80 V for 45min containing SafeView reagent to visualize DNA bands.

2.3.12 Western Blot

hiPSCs-derived microglia precursors were collected, and whole-cell lysate was prepared using ice-cold RIPA buffer, supplemented with mini protease inhibitor and PhosStop reagent. Protein extracts (20µg) were denatured in loading buffer at 70°C for 10 minutes and loaded into a 4-12% NuPAGE™ Bis-Tris plus gel, and ran in MOPS SDS running buffer at 165V for 45 minutes. Gels were transferred to nitrocellulose membranes that were then blocked with 5% (w/v) skimmed milk and incubated with anti-PLCG2 antibody or anti-α-tubulin (loading control) overnight at 4°C. Membrane were washed with PBS/0.1% Tween three times and incubated for 1h at RT with IRDye 800CW Goat (polyclonal) anti-mouse IgG (H+L). Membrane were washed again three times with PBS/0.1% Tween and imaged with LI-COR Odyssey CLx imaging system. Bands were analysed and quantified using Li-COR analysis software to confirm similar expression of the PLCG2 variants and no expression in the PLCG2 KO.

2.3.13 Establishment of iPSCs derived cortical neurons-microglia co-culture system

Non-adherent macrophage precursors and NPCs were differentiated from iPSCs as indicated before. NPCs were plated at around 70/80% density on matrigel-coated plates on NB supplemented with 10µM ROCK inhibitor. The following day, terminal differentiation was started using SJA medium for 7 days, as previously described (2.3.4.2 NPCs terminal differentiation into Cortical Neurons). Non-adherent precursors were collected, centrifuged for 3 minutes and 300g, resuspended using Co-culture medium (2.1.1.12 Media composition table – Neuron-Microglia Co-culture Differentiation – Co-culture Medium) and plated on top of fully differentiated cortical neurons at 10% cell concentration (in 96 well plate: 100.000

cortical neurons and 10.000 non-adherent precursors). During the first week of co-culture, medium was topped up, in order to not disturb the non-adherent precursors and let them settle on top of the neurons. After 7 days, half medium changes were performed every other day. The co-cultures were used at day 14.

2.3.14 Cell Morphology Analysis – monoculture vs co-culture

Microglia-like cells cultured for 14 days in ACM or co-cultured with neurons as described above, were moved into the Incucyte S3 live-cell imaging system, housed inside an incubator at 37°C and 5% CO_2. Cells were imaged using the red channel and 20x magnification. Morphology was analysed using Fiji software. Manual adjustment of Brightness and Contrast was applies, followed by manual segmentation and application of the appropriate threshold. Objects smaller than 60µm and objects at the edges of the pictures were excluded. The following measurements were included in the analysis: Area, Perimeter and Shape Descriptors (which include Roundness, Aspect Ratio, Solidity and Circularity). Analysis includes three independent experiments; for each independent experiment, 2 images per clone were analysed (6 images per genotype/experiment = 18 images per genotype in total).

2.3.15 LPS and Aβ Challenges

For Aβ challenge, $Aβ_{1-42}$ (Bachem) was prepared as follow: lyophilized Aβ was dissolved in 500µl of HFIP, vortex thoroughly for 30 seconds and dried using a stream of nitrogen gas. The pellet was then resuspended again in 500µl of HFIP, sonicated for 5 minutes and dried using a SpeedVac Vacuum centrifuge. The pellet was resuspened with PBS and aliquots stored at -80°C.

For LPS and Aβ stimulations, iPSCs-derived microglia were cultured in fibronectin coated 96-well plate for 14 days. Cells were stimulated either with 100ng/ml of LPS or 5µM of Aβ and supernatant was collected and flesh frozen at determined time points. Protein levels of IL-6, IL-12p40, IL-10, TNF and G-CSF were determined using LEGENDplex Custom Human kit (Biolegend), following manufacturer's

instructions. Data were collected using a LSR Fortessa™ and analysed using LEGENDplex™ v8.0 (Biolegend). Analyses include three independent experiments; for each independent experiment, 3 clones per genotype were analysed.

2.3.16 Inflammasome activation

iPSCs-derived microglia were cultured in PDL- fibronectin-coated 96-well plate for 14 days.

For zymosan challenge, cells were treated with 50µg/ml for 24h. Then, 100µl of media was harvested, flash frozen and assayed for IL-1β levels by quantitative immunoassay (R&D), following manufacturer's instructions

For LPS + Nigericin challenge, cells were treated with 5µM of Caspase-1 inhibitor for 1h, followed by 100ng/ml of LPS for 3h, and 20uM of Nigericin for 1h. Cell culture media (100µl) was flesh frozen and subsequently assayed for IL-1β levels by quantitative immunoassay (R&D), following manufacturer's instructions. To account for differences in cell number, cells were fixed with 4% PFA, stained with DAPI and nuclei count was performed with Opera Phenix™ high-content screening system (PerkinElmer). Analyses include three independent experiments; for each independent experiment, 3 clones per genotype were analysed.

2.3.17 Nitric Oxide Assay

iPSCs-derived microglia were cultured in PDL- fibronectin-coated 96-well plate for 14 days. Cells were then treated with 100ng/ml LPS and 20ng/ml IFN-γ in live cells imaging buffer or with vehicle (PBS) for 24hs. Nitric Oxide (NO) levels were analysed using Griess Reagent Kit for Nitrite Determination (Life Technologies). To account for differences in cell number, cells were fixed with 4% PFA, stained with DAPI and nuclei count was performed with Opera Phenix™ high-content screening system (PerkinElmer). Analyses include three independent experiments; for each independent experiment, 3 clones per genotype were analysed.

2.3.18 Measurement of Ca^{2+} signalling

iPSCs-derived microglia were cultured in PDL- fibronectin-coated 96-well plate for 14 days. Cells were washed with PBS, loaded with 2µM Fluo8-AM solution (Stratech) diluted in Live Cell Imaging Buffer at RT in the dark for 1h. Cells were then washed, and imaged in live cells imaging buffer on an automated cell screening system (FLIPR Penta Molecular Devices). Cells were exposed at set time points to ATP (5µM) or ADP (5µM). This was followed by ionomycin (2 µM) as a positive control. Levels of fluorescence were detected at excitation 490nm/ emission 520nm. Cells were inhibited by pre-exposure for 2h with Edelfosine (10 µM) (Tocris) or U73122 (5 µM) (Sigma). To account for differences in cell number, cells were fixed with 4% PFA, and cell count was performed with Opera Phenix™ high-content screening system (PerkinElmer) using 488 channel. Analyses include three independent experiments; for each independent experiment, 3 clones per genotype were analysed.

2.3.19 Cell Morphology Analysis – co-culture

Microglia-like cells cultured for 14 days in co-cultured with neurons as described above (2.3.13 Establishment of iPSCs derived cortical neurons-microglia co-culture system), were moved into the Incucyte S3 live-cell imaging system, housed inside an incubator at 37°C and 5% CO_2. Cells were imaged using the red channel and 20x magnification. Four images per well were taken. The 2D tracing was analysed by Imaris and several parameters were extracted for further statistical analyses. These included: Total number of branching points and terminal points, full branch level, full branch depth and Sholl intersections.

“Total number of branching points” is defined as the number of branching points in the entire dendritic graph (Figure 2.1A). “Total number of terminal points” is defined as the number of dendrite terminal points in the entire dendritic graph (Figure 2.1A). “Full branch level” is defined as the highest value of branching level for the dendritic graph (Figure 2.1A). “Full branch depth” is defined as the number of branch points, or bifurcation in the shortest path from the beginning point to a

given point in the dendritic graph. It is the highest value of branching depth for the dendritic graph. Sholl intersections is defined as the number of dendrite intersections (branched) on concentric spheres, defining dendrite spatial distribution as a function of distance from the beginning point (Figure 2.1B).

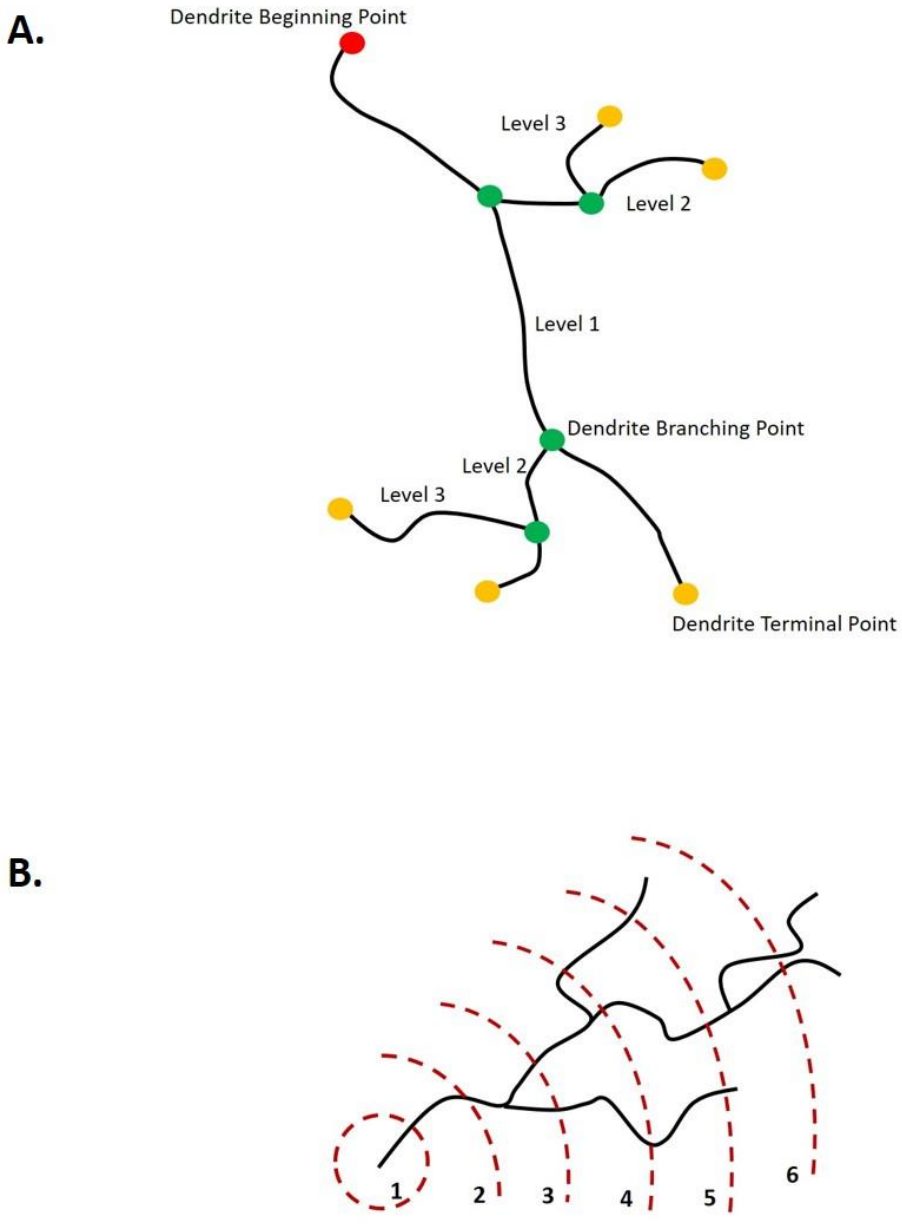

Figure 2.1 – Schematic representation of different parameters analysed using Imaris software.

2.3.20 Cell Movement Analysis

iPSCs derived cortical neurons and mcherry iPSCs derived microglia were co-cultured for 14 days as explained in paragraph 2.3.13. Mcherry signal was used to visualize microglia in co-culture using Incucyte S3 live-cell imaging system, house-inside an incubator at 37°C and 5% CO_2. Images were taken every 15 minutes for 6 hours (2 videos/well). Microglia movement was manually tracked with ImageJ and tracks were analysed with the Chemotaxis and Migration Tool Version 2.0 (Ibidi).

2.3.21 Statistical Analysis

Statistical analyses as well as graph design were carried out using GraphPad Prism (GraphPad, Software, version 9). Before statistical tests were conducted, D'Agostino-Pearson test was run to assess for normality. The Mann-Whitney test was used for comparison of two groups. One-Way ANOVA was used when three different groups (e.g. 3 different PLCG2 genotypes) were tested for a single dependent variable (e.g. level of cytokine). Two-Way ANOVA was used when three different groups (e.g. three different PLCG2 genotypes) were tested for a single dependent variable (e.g. level of cytokine) over time. Dunnet's test for multiple comparison was used when each of a number of treatments were compared with a single control. Tukey's test for multiple comparison was used when every mean is compared with every other mean. Results are resported as mean values ± SD.

3 Generation of novel iPSC lines from individuals stratified for their genetic risk for Alzheimer's disease

3.1 Introduction

Late onset Alzheimer's disease (LOAD) is the most common form of dementia and has an estimated heritability of 56-79%(Gatz et al., 2006). For many years, *APOE* has been the only genetic risk factor known for LOAD(Corder et al., 1993), with inheritance of the *APOE4* allele conferring high risk and inheritance of the *APOE2* allele being protective(Corder et al., 1993).

Rapid improvements in epidemiological and genetic analytical approaches, such as GWAS, have provided an increase in the understanding of the complex genetic

architecture of AD. The first genome-wide statistically significant associations were identified back in 2009 (Harold et al., 2009, Lambert et al., 2009), and it is now clear that AD is influenced by the additive inheritance of multiple polymorphisms(Escott-Price et al., 2015). To date, more than 75 loci associated with the disease have been identified, and more associations are expected to be found in the near future, thanks to more powerful GWAS' and bigger sample sizes(Sims et al., 2020). In addition to the common and rare single nucleotide polymorphisms (SNPs) that show genome-wide significance ($P < 5 \times 10^{-8}$), many other weak effect variants contribute to increase estimated heritability(Ridge et al., 2013). These are SNPs, which show association with the disease but do not meet the conventional P-value threshold(Lee et al., 2013).

Although the individual contribution of these disease-associated alleles is small, if they are considered collectively, the cumulative effect of common and rare SNPs allows the calculation of a personal genetic risk profile that can predict individual disease development. PRS is a powerful tool that offers many advantages for the AD research field. First, it allows the identification of people that are at the highest and lowest risk of developing the disease early in life. Identifying the population at highest risk could help advance our understanding of the initial phases of the neurodegenerative process; on the other hand, identifying people at the lowest risk may shed light on protective mechanisms that if understood could lead to the development of appropriate treatments to be used years before the onset of symptoms. Moreover, samples from individuals at the extremes of the score can be used to generate stem cell models in order to better decipher the molecular mechanisms of the disease in humans by investigating functional outcome (e.g. survival, phagocytosis, chemotaxis) of iPSCs-derived models such as microglia-like cells. This study aimed at generating iPSCs from samples of individuals at the highest and lowest PRS to elucidate the biological meaning of the genetic information.

iPSCs present a physiologically appropriate system for modelling genetic variants to study the molecular consequences in disease-relevant cell types(Hamazaki et al., 2017). The ability to reprogram somatic cells from individual patients and healthy controls, into iPSCs, provides an invaluable tool that captures complex disease-associated polygenic variation; this allows the establishment of experimentally tractable cell models to determine the impact of GWAS-identified risk on cell function. The reprogramming era began in 2006, when Yamanaka, Takahashi and colleagues described the necessary conditions to genetically reprogram somatic mouse cells into a pluripotent state(Takahashi and Yamanaka, 2006). These iPSCs, were induced by the introduction of four genes necessary for the maintenance of the pluripotent state: *OCT4, SOX2, KLF4* and *C-MYC(Takahashi and Yamanaka, 2006).*

This technology was rapidly applied to human cells(Takahashi et al., 2007) and the reprogramming technologies have been improved, since. Initially, retroviral and lentiviral vectors were used to deliver the four reprogramming factors. These genome-integrating methods, however, display some disadvantages. These include the potential of insertional mutagenesis and residual transgene expression during the differentiation process, which could negatively affect differentiation capacity(Yu et al., 2007, Okita et al., 2007). In order to overcome these problems, many different methods have been published, including the use of integration-free vectors (episomal plasmid vectors, adenoviral vectors, SeV and piggyback excision vectors), or the direct delivery of reprogramming factors, such as mRNA or protein, together with the use of small molecules that target pluripotency cell signalling and chromatin remodelling enzymes(Ye and Wang, 2018). For this study we used the negative sense, non-integrating, RNA SeV(Fusaki et al., 2009). The main advantage of this reprogramming method relies on the fact that the virus remains in the cytoplasm and therefore avoids integration into the genome reducing the risk of insertional mutagenesis associated with retrovirus and lentiviral vectors. In addition, SeV is able to infect a broad range of somatic cells with high transduction

efficiency, including neonatal and adult fibroblasts and blood cells(Fusaki et al., 2009, Seki et al., 2010, Ban et al., 2011).

The second important aspect of the reprogramming process is the choice of the starting cell type. This decision may affect the reprogramming efficiency and quality(Mishra et al., 2018). Mouse fibroblasts were initially used by Takahashi and Yamanaka in 2006(Takahashi and Yamanaka, 2006), and consequently were also the first source of cells tested for human reprogramming(Takahashi et al., 2007). However, this cell type presents some disadvantages. In the first place, the collection of the samples is painful for the donor, as a skin biopsy is needed. Moreover, it presents a risk of infection and the possible formation of scar tissue. Finally, fibroblast-derived iPSCs may contain accumulated mutations because the skin is constantly exposed to external stressors, such as UV rays. Over the years, a number of different somatic cell types have been tested and compared.

A widely accepted alternative to fibroblasts is PB. The use of PB provides a less invasive collection procedure, which offers the possibility to sample tissue from a much bigger population. It is possible to easily separate PBMCs from whole blood with the use of density gradient centrifugation. PBMCs comprise mainly lymphocytes (T- cells and B- cells) and myeloid cells. These purified cells can then be used for further reprogramming(Afshinmanesh, 2016, Ye and Wang, 2018). PBMCs have also provided the cell material processed for GWAS studies and historically, replica vials have been cryopreserved for future potential use. This study aimed to use cryopreserved PBMCs associated with previously collected GWAS data in order to generate iPSCs from high and low PRS individuals(Kunkle et al., 2019a).

Studying PBMC-derived iPSCs collected from individuals identified to have high and low PRS will help to decipher the role of complex genetic variants at a molecular and cellular level. These iPSCs with known genetic background of interest can be further differentiated into several type of cells, among which microglia-like cells that are the primary cells expressing the majority of the hit of

the genetic studies. Functional studies on these derived cells, and potential differences among genetic group (high versus low polygenic scores) would provide an invaluable tool to gain a deeper insight into the genetic architecture of AD.

3.2 Aim

Work described in this chapter aimed to test several protocols to determine the best one in order to recover the viability and cell number of a cohort of cryopreserved PBMC samples collected from individuals originally sampled for GWAS, and subsequently calculated to have either high or low PRS for AD. The samples were then reprogrammed in order to generate iPSCs which were extensively characterized.

3.3 Results

3.3.1 iPSCs generation from PBMCs

PBMCs used in this study were collected with informed consent from individuals as part of the project titled “Late Onset Alzheimer’s Disease Resource”, REC number 00/09/42. The cells were originally separated from whole blood and frozen down at a controlled rate to -80C°. They were transferred to liquid nitrogen for long-term storage more than 10 years before the start of this study. Information on the time elapsed between blood collection and PBMCs storage was not available. Likewise, no instructions about separation procedures or conservation conditions were accessible. The limited information provided about the samples included PRS, which was calculated using methods set out in Escott-Price et al., 2015(Escott-Price et al., 2015) (Table 3.1). All samples are homozygous for *APOE3* allele.

Cell viability was checked using an automated cell counter (Olympus, Model R1) and trypan blue at day of thawing; it showed a high heterogeneity in viability between samples spanning from 9% to 59% (Table 3.1).

Table 3.1 - List of samples. Samples used for the study listed in chronological order. PRS and sex are shown (1=male, 2=female). Viability calculated at day of thawing and at day of reprogramming are listed alongside the outcome of reprogramming. "N/A" identify samples that could not be reprogrammed and therefore gave no colonies. Green rows represent samples cultured in Complete PBMC medium; Yellow rows represent samples cultured in Expansion Medium A; Blue rows represent samples cultured in Expansion Medium B; Red rows represent samples cultured in Expansion Medium B + Complete PBMC Medium

Sample Name	PRS	Sex	Days kept in culture prior Reprogramming + Medium used	Viability day of thawing	Viability day of reprogramming	Number of colonies
S1: ADCAR24361UC	-0.025	1	4d - Complete PBMC Medium	23%	N/A	N/A
S2: ADANG14223UC	0.346	1	4d - Complete PBMC Medium	31%	N/A	N/A
S3: ADDUB34117UC	-1.560	1	4d - Complete PBMC Medium	10%	N/A	N/A
S4: ADANG10504CA	0.038	2	4d - Complete PBMC Medium	15%	N/A	N/A
S5: ADLON40394CA	0.852	2	4d - Complete PBMC Medium	20%	N/A	N/A
S6: ADCAR20123CA	1.258	2	4d - Complete PBMC Medium	39%	N/A	N/A
S7: ADANG14129UC	-1.220	1	4d - Complete PBMC Medium	34%	N/A	N/A
S8: ADLON40020CA	1.525	2	4d - Complete PBMC Medium	27%	N/A	N/A
S9: ADCAR24229UC	-0.518	1	4d - Complete PBMC Medium	59%	N/A	N/A
S10: ADANG14607UC	-0.920	1	1d - Complete PBMC Medium	13%	4%	0
S11: ADANG14489UC	-0.405	1	1d - Complete PBMC Medium	50%	36%	>60
S12: ADANG14359UC	-1.624	1	7d - Expansion Medium A	19%	70%	4
S13: ADLON44369UC	-0.808	1	7d - Expansion Medium A	19%	74%	1
S16: ADANG14167UC	-1.768	1	7d - Expansion Medium A	0.45	80%	N/A
S17: ADANG14245UC	-2.477	1	7d - Expansion Medium A	0.31	60%	N/A
S18: ADCAR24216UC	-0.577	1	7d - Expansion Medium A	0.125	N/A	N/A
S19: ADLON40151CA	0.319	2	7d - Expansion Medium A	0.1	N/A	N/A
S49: ADCAR24390UC	-0.952	1	8d - Expansion Medium B	17%	56%	>60
S50: ADLON44079UC	-1.033	1	8d - Expansion Medium B	10%	62%	N/A
S51: ADANG14513UC	-0.745	1	8d - Expansion Medium B	15%	N/A	N/A
S52: ADANG14251UC	-1.75	1	8d - Expansion Medium B	13%	N/A	N/A
S61: ADANG14296UC	-2.672	1	8d - Expansion Medium B	39%	76%	N/A
S86: ADANG14421UC	-2.123	1	8d - Expansion Medium B + 7d - Complete PBMC Medium	12%	60%	>20
S87: ADANG14361UC	-0.509	1	8d - Expansion Medium B + 7d - Complete PBMC Medium	18%	66%	>20
S88: ADCAR24367UC	-1.536	1	8d - Expansion Medium B + 7d - Complete PBMC Medium	9%	59%	>10
S90: ADLON44343UC	-0.127	1	8d - Expansion Medium B + 7d - Complete PBMC Medium	3%	22%	>10
S94: ADANG14281UC	-1.273	1	8d - Expansion Medium B + 7d - Complete PBMC Medium	12%	23%	N/A

3.3.1.1 Complete PBMC Medium

The initial approach used for this study aimed to follow the CytoTune 2.0 Sendai Reprogramming Kit instructions (CytoTune™-iPS 2.0 Sendai Reprogramming Kit,

Invitrogen, A16518). After thawing, PBMCs were kept for four days in Complete PBMC medium: the protocol states that this medium system aims to maintain a stable cell number but does not promote proliferation. Contrary to expected results based on the protocol instructions, the number of viable PBMCs decreased drastically during these four initial days, reaching 0% viability on the day of reprogramming for all the samples tested (S1-S9 – Table 3.1), providing no sample with which to proceed with the reprogramming.

To address this, PBMCs were reprogrammed the day after thawing in order to avoid the drastic drop in cell viability. Two samples (S10, S11 – Table 3.1) were tested, showing respectively 13% and 50% viability after thawing. The first sample did not give any colonies, but the second one was successful, giving >60 colonies. Figure 3.1 shows a schematic representation of the reprogramming protocol.

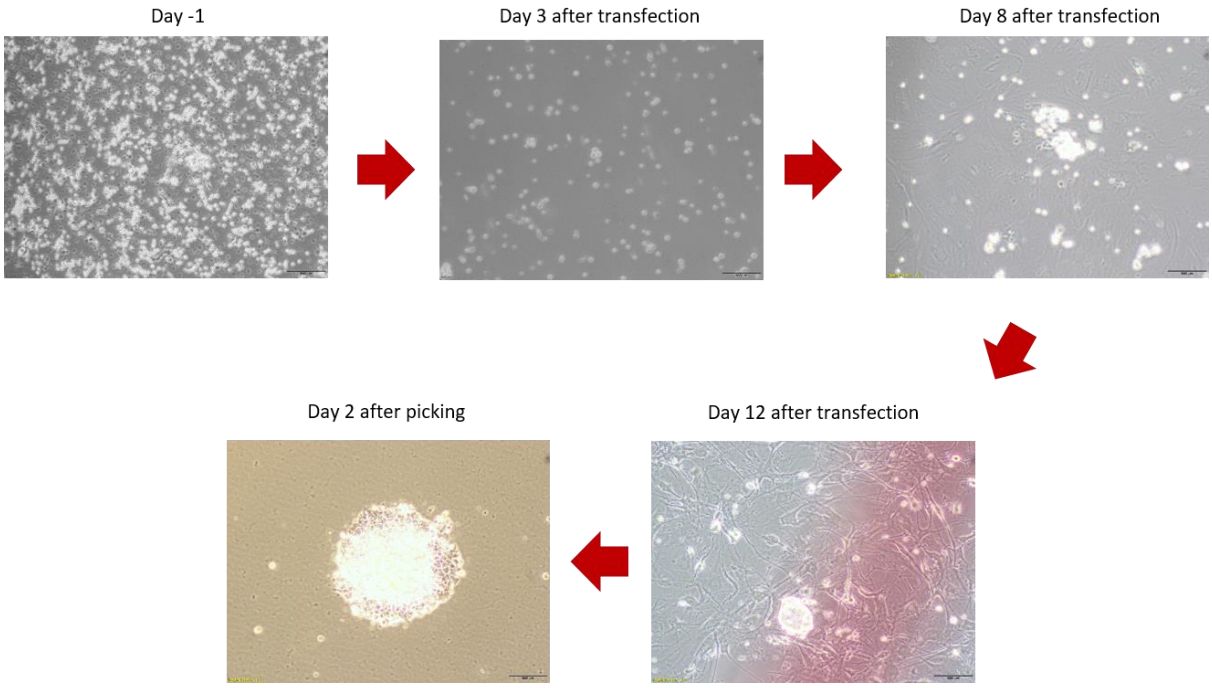

Figure 3.1 Schematic representation of colony formation for iPSCs generated from PBMCs. Cells were cultured in complete PBMC medium for 1 day before transduction. On day 0, cells were transduced overnight at an MOI 5-5-3 (KOS MOI=5, Myc MOI=5, Klf4 MOI=3). At day 3 after transduction, the cells show morphological changes indicating reprogramming and are plated on MEF feeder layer. The cells are left on MEF feeder layers in order to proliferate and colony formation is observed from day 8 till day 15. By day 15 to 21 after transduction, colonies should have grown to an appropriate size for transfer to a Matrigel coated plate. Scale bar=100µM

In order to identify stable clones, colonies were passaged at least 5 times after first picking. The size of the well increased slowly (48 well plate → 24 well plate → 12 well plate → 6 well plate) allowing the colonies to grow gradually. Some of the clones lost pluripotency during this process and underwent spontaneous differentiation.

3.3.1.2 Expansion Medium A

The day after reprogramming, PBMCs may be affected by drastic cell death (up to 60%) due to viral transduction; for this reason, cell viability is extremely important for reprogramming success. In order to overcome this problem, a cell expansion protocol was tested, in an attempt to rescue samples with very low viability. Samples were cultured in hypoxic conditions (5% O2) in Expansion Medium A, which consists of RPMI medium containing 10% FBS and a cocktail of proliferating cytokines (PHA-P, IL-2, IL-4, IL-15, GM-CSF, LPS) as suggested by Seth Brodie (NIH Bethesda, personal communication).

As shown in figure 3.2B, the response was variable depending on the sample. After an initial decrease in viability, some of the PBMC samples started proliferating and viability considerably increased over time, reaching 70%-80%. Following the same trend, cell counts drastically increased, reaching almost 2.5x 10^7 by day 22 (S12, S13, S16, S17). On the contrary, other samples (S18, S19) did not seem to respond to the treatment, showing by day 14 almost 0% viability as well as very low cell count (Figure 3.2B).

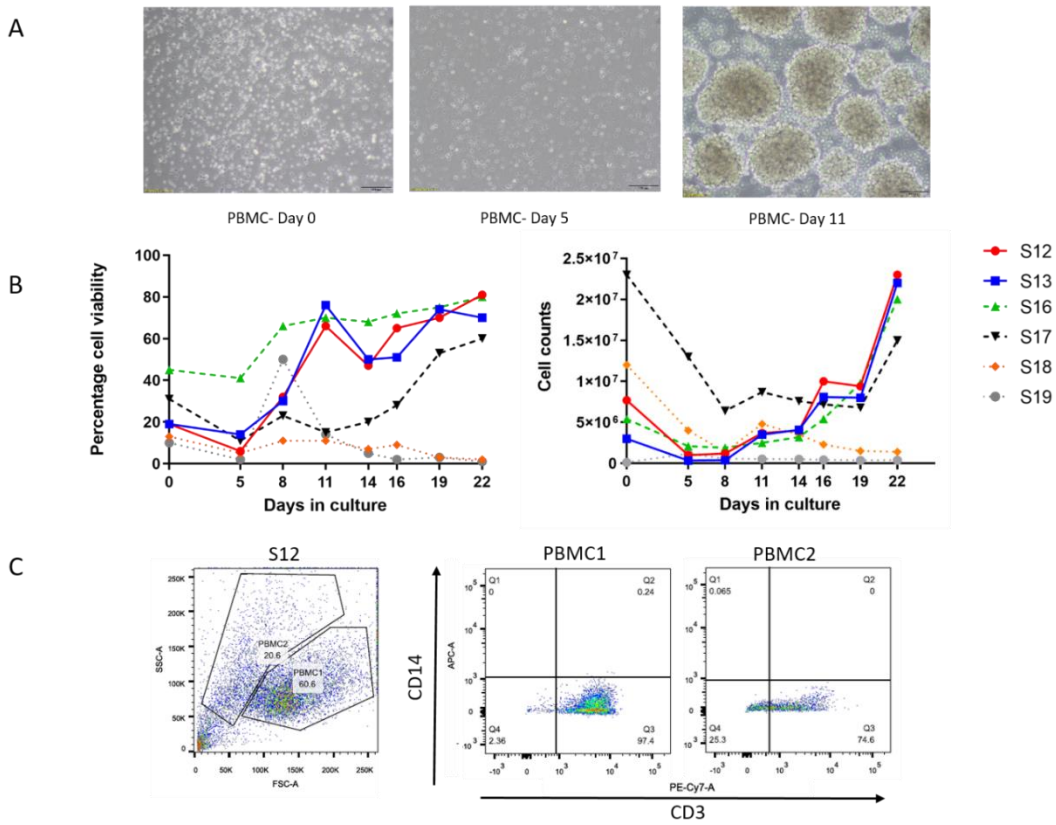

Figure 3.2 PBMCs expansion with expansion medium A. A. PBMCs at day 0 (day of thawing), at day 5 and at day 11, when clumps of cells appeared, showing proliferation. **B.** Cryopreserved PBMCs were thawed and assessed for viability at day 0. The first five days in culture resulted in drastic cell viability decrease, attributed to the unknown freezing procedure, the thawing and recovery protocol that leads to progressive cell death. After this initial period, some samples cultured in hypoxic conditions and with a cocktail of proliferative cytokines led to recovery and expansion of the cells over the course of the following weeks, whereas other samples did not show proliferation. **C.** Flow cytometry analysis of S12.

Sample 12 was also characterized by flow cytometry in order to identify the most represented PBMC subpopulation present. The first panel of figure 3.2C demonstrates how two main populations were identified by the forward and side scatter (PBMC1 & PBMC2). The PBMC1 population shows 97.4% CD3+ and the PBMC2 population a 74.6% of CD3+. A hallmark of T-cell activation is aggregation and this was observed starting around day 10 (figure 3.2A).

After this first phase in Expansion medium A, cells were reprogrammed using the CytoTune 2.0 Sendai Reprogramming Kit at day 22. As highlighted in table 3.1, despite increased viability, the reprogramming efficiency remained considerably

low. Sample 12 resulted in four colonies in total, whereas sample 13 just one. On the contrary samples 16 and 17, which showed successful expansion, did not generate any colonies.

Thirty-five samples were tested with this approach: only nine showed proliferation, of which two were successfully reprogrammed (Table 3.2).

3.3.1.3 Expansion Medium B

To test an alternative approach in order to increase reprogramming efficiency, a different expansion medium was used, Expansion Medium B, which consisted of RPMI medium containing 10% FBS and recombinant (r)IL-2 in anti-CD3 antibody coated wells. As suggested by Afshinmanesh et al.(Afshinmanesh, 2016), the cells were reprogrammed after one week of expansion (Table 3.1).

As per the previous approach, the cells went through an initial decrease in viability until day 5, before some cells started to proliferate forming the typical aggregates (figure 3.3A). However, this was not true for all the samples. As shown in figure 3.3B, S49, S50 and S61 responded to the stimulus of Expansion Medium B, whereas S51 and S52 did not. S49 and S50 were further characterized by flow cytometry, which showed positivity for anti-CD3 antibody of 85.2% and 93.2% respectively.

Despite the expansion protocol working for a few samples, only S49 was successfully reprogrammed.

Thirty-four samples were tested with this approach: only four showed proliferation of which one was successfully reprogrammed: S49 (Table 3.2).

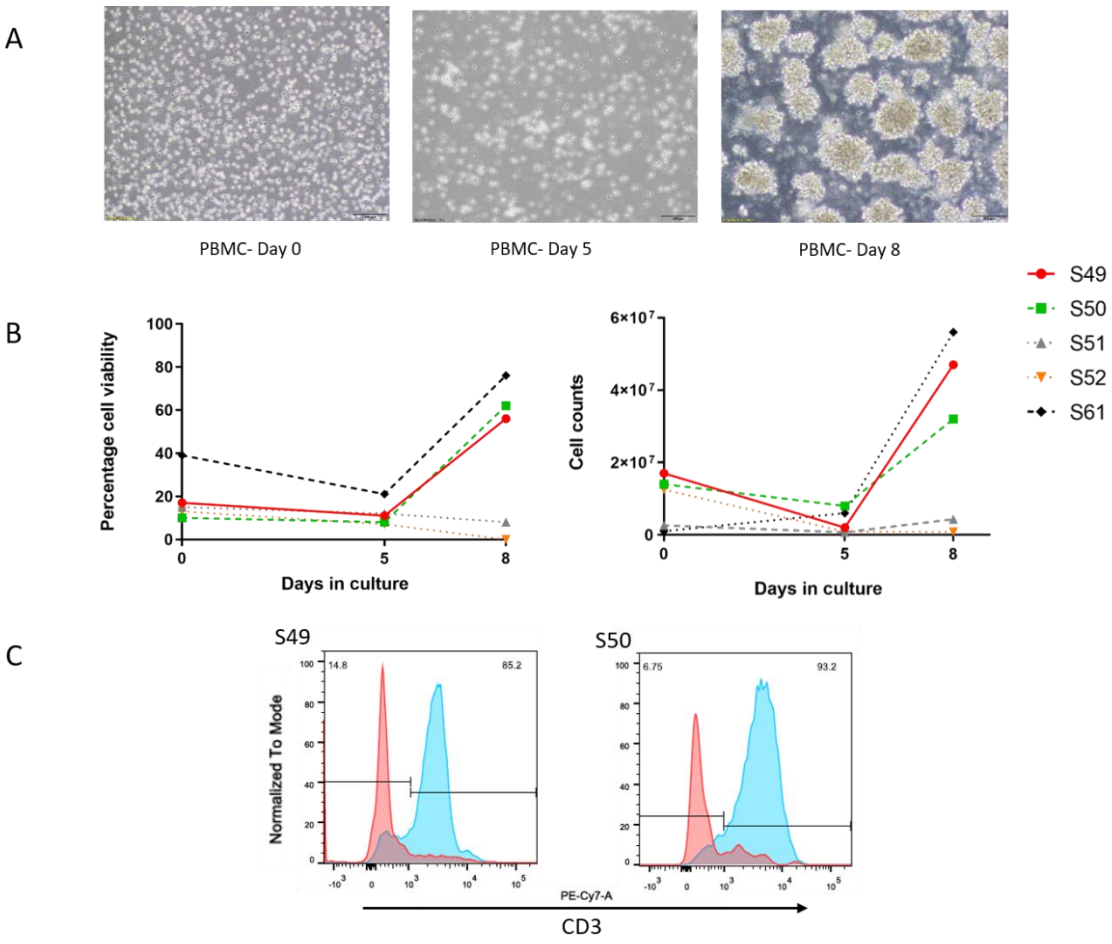

Figure 3.3 PBMCs expansion with Expansion Medium B. A. PBMCs at day 0 (day of thawing), at day 5 and at day 8, where clumps of cells appeared. **B.** Cryopreserved PBMCs were thawed and assessed for viability at day 0. The first five days in culture resulted in drastic cell viability decrease. After this initial period, some of the cells cultured with 30ng/ml of IL-2 showed recovery and expansion. **C.** Flow cytometry analysis of S49 and S50.

3.3.1.4 Expansion Medium B + Complete PBMC Medium

Finally, two of the previous approaches were combined in an attempt to obtain better results. Samples were thawed and kept for 8 days in Expansion Medium B, where they showed the pattern observed for all the other samples: low starting viability, decreased viability over the first few days followed by increased viability and expansion. Samples were then cultured for 7 days with complete PBMC complete medium, which is the medium suggested by the CytoTune 2.0 Sendai Reprogramming Kit. During this week, the cells cultured in complete PBMC medium maintained a constant cell number and viability, but stopped

proliferating. Samples were then reprogrammed using the CytoTune 2.0 Sendai Reprogramming Kit. Twenty-three samples were tested with this approach: six showed proliferation of which four were successfully reprogrammed (Table 3.2).

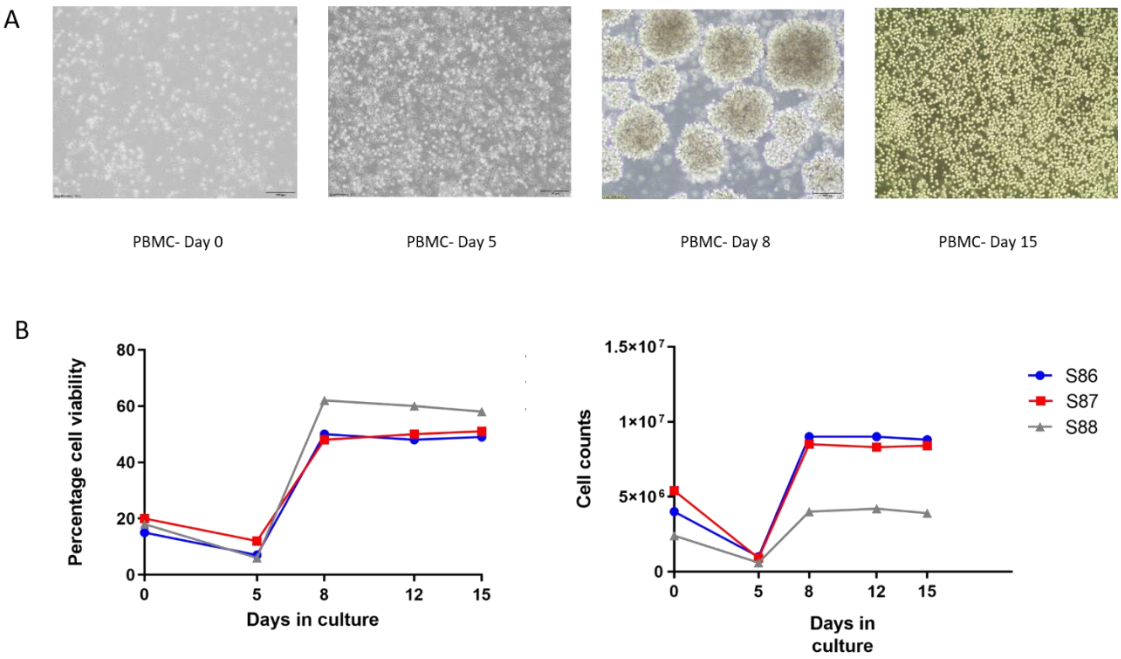

Figure 3.4 PBMCs expansion with expansion medium B + Complete PBMC medium. A. PBMCs at day 0 (day of thawing), at day 5 and at day 8, where clumps of cells appeared. PBMC at day 15, showing cells remained viable but stopped proliferating. **B.** Cryopreserved PBMCs were thawed and assessed for viability at day 0. The first five days in culture resulted in drastic cell viability decrease. After this initial period, cells cultured with 30ng/ml of IL-2 showed recovery and expansion. Viability was maintained after 7 days of cells cultured in PBMC complete medium.

Table 3.2 – Summary of Expansion Methods, Viability and % of reprogramming success per condition.

Expansion Method	Medium composition	Number of samples tried	Viability Day of Thawing (Mean)	Number of samples successfully reprogrammed	% reprogramming success
Complete PBMC Medium (4 days)	StemPro-34 + IL3, IL6, SCF, Flt3	9	29%	N/A	N/A
Complete PBMC Medium (1 day)	StemPro-34 + IL3, IL6, SCF, Flt3	2	31%	1	50%
Expansion Medium A	RMPI + FBS + PHA-P, IL-2, IL-4, IL-15, GM-CSF, LPS	35	18%	2	6%
Expansion Medium B	RPMI + FBS + IL-2	34	19%	1	3%
Expansion Medium B + Complete PBMC Medium	(RPMI + FBS + IL-2) + (StemPro-34 + IL3, IL6, SCF, Flt3)	23	13%	4	17%
Total		103		8	

Table 3.3 – Summary of generated iPSCs samples, corresponding original PBMC name, PRS and number of colonies obtained

iPSCs sample name	Original PBMC name	PRS	Number of colonies obtained
#S11	ADANG14489UC	-0.405	>60
#S12	ADANG14359UC	-1.624	4
#S13	ADLON44369UC	-0.808	1
#S49	ADCAR24390UC	-0.952	>60
#S86	ADANG14421UC	-2.123	>20
#S87	ADANG14361UC	-0.509	>20
#S88	ADCAR24367UC	-1.536	>10
#S90	ADLON44343UC	-0.127	>10

3.3.2 Characterization of iPSCs

As a consequence of the introduction of the four reprogramming factors, cells undergo a series of genetic, epigenetic and morphological changes. For this reason, variability exists between different clones derived from the same sample, and it is therefore extremely important to pick several clones and evaluate them in order to check their pluripotency and genomic integrity, to avoid any misinterpretation of data in downstream applications. In the present project, detailed characterization of clones obtained from three samples (S86, S87 and S88) was performed.

Quality control analyses carried out on iPSCs include morphological studies, integration status and clearance of reprogramming vectors, expression of pluripotency markers, *in vitro* trilineage differentiation and karyotype analysis.

3.3.2.1 Generation of vector-free iPSCs

ICC analysis was performed at different passage numbers in order to check up to which passage cells retained SeV (figure 3.5A). For all the clones analysed, cells seem to have cleared the virus by passage 10, which is in line with previous studies(Ye and Wang, 2018, Schlaeger et al., 2015).

RT-PCR using primer sets to detect the SeV genome and transgenes was performed. This confirmed clearance of all three vectors as it is shown in figure 5B.

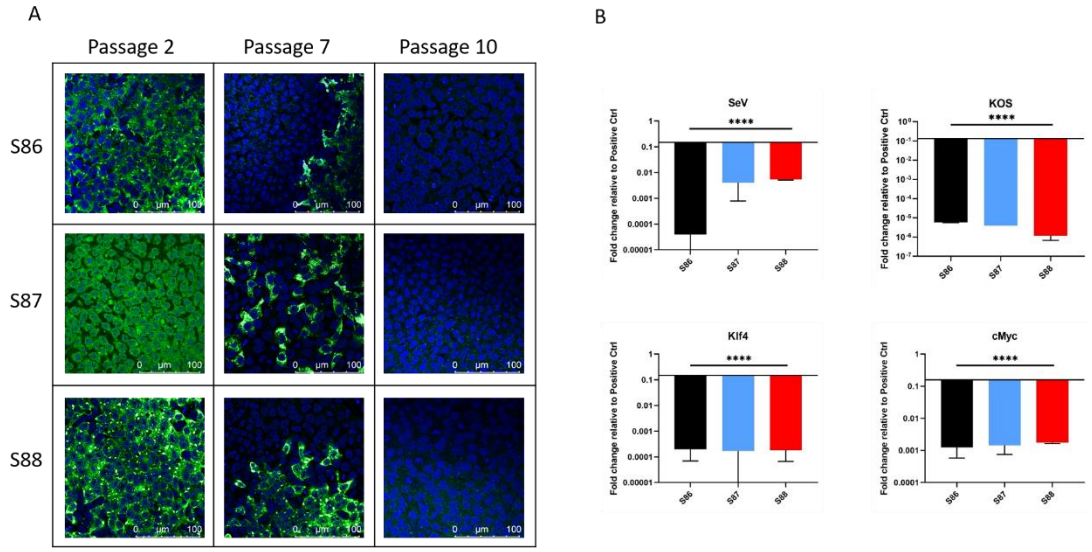

Figure 3.5 Sendai Virus clearance check – A. Immunofluorescence analysis of 4% PFA fixed iPSCs using anti SeV antibody and AlexaFluor 488 goat anti-rabbit IgG revealed positive staining for all three reprogrammed samples at passage 2. At passage 7, the virus seems be incorporated in just part of the colonies. At passage 10, the colonies of all three samples appear virus-free. **B.** RT-PCR was performed in order to confirm the clearance of the virus at passage 10. Positive control is represented by cells set aside during the reprogramming procedure. N = 3 biologically independent clones. All data are mean ± S.D.; One-way ANOVA, Dunnett's test for multiple comparison. ****p<0,0001 - relative to positive control.

3.3.2.2 Morphological analysis and pluripotency marker characterization

Morphological features were assessed on a daily basis by checking the cells with the use of a bright field microscope. iPSC colonies showed characteristic morphology being round, compact, and flat with a well-defined and smooth edge. Moreover, iPSCs showed the expected high nucleus/cytoplasm ratio (figure 3.6A).

These iPSCs also expressed the pluripotency markers Sox2, Oct4 and Tra-1-60 by ICC (figure 3.6B).

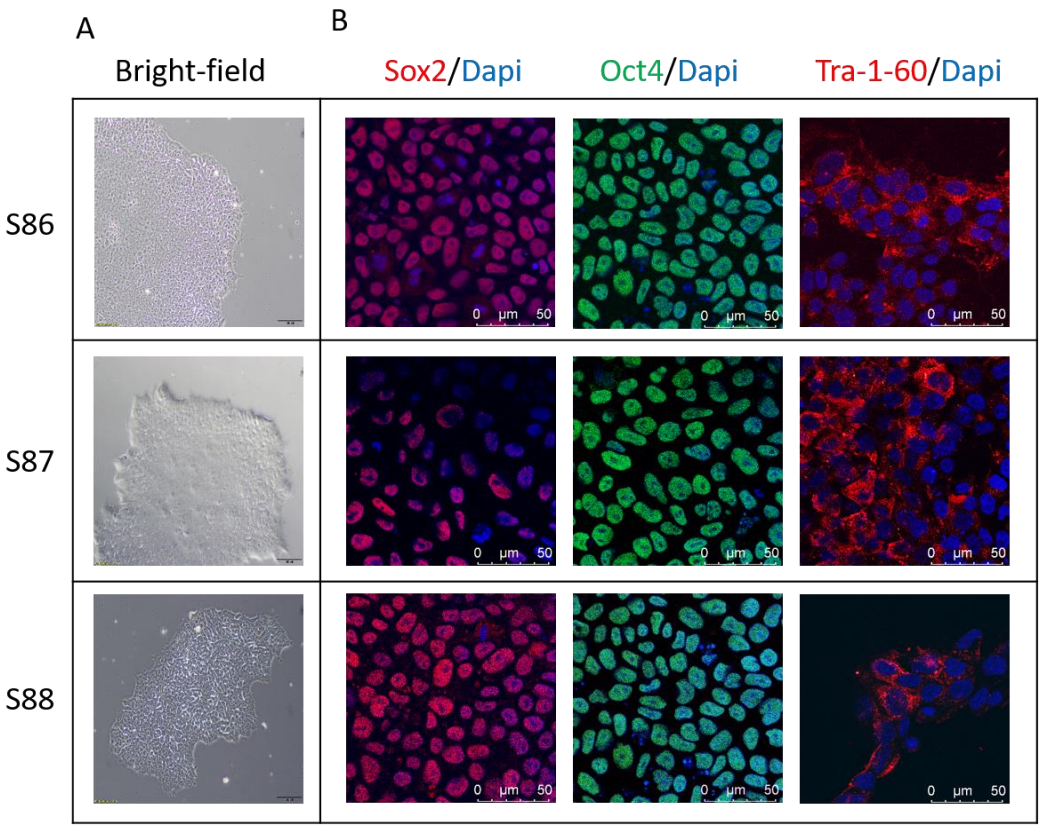

Figure 3.6 – **PBMC-derived iPSCs express characteristic pluripotency markers A)** Bright field image of iPSCs cells with typical iPSCs morphology. **B)** Fluorescent microscope analysis of the stem cell markers Sox2 (red), Oct4 (green) and Tra-1-60 (red), co-stained with Dapi (blue).

3.3.2.3 Copy Number Variation (CNV) Detection Array

CNV emerge when the number of copies of a portion of a chromosome differs from the expected number of copies. The differences could range from a few hundred base pairs to megabases(Lin et al., 2013).

Three clones per sample were genotyped using the Illumina Global Screening Array v2.0 and data was analysed alongside approximatively 500 additional samples using PennCNV with GRCh37/hg19 as a reference genome. The CNV described are limited to the regions identified by PennCNV as containing large (>100kb and spanning >10SNPs) CNVs that are subsequently confirmed by visual inspection of the LRR/BAF traces.

The only CNV to pass QC thresholds in these samples was at 2p11.2 as shown in figure 3.7, and it represents a possible deletion. Specifically, the blue dots

represent the positive correspondence of the samples with the reference genome, whereas the red dots graphically show the possible deletion. This is found in a locus immediately adjacent to the centromere. This result has to be interpreted with caution as human CNVs are significantly overrepresented close to telomeres and centromeres(Nguyen et al., 2006). No other gross structural changes have occurred due to genetic manipulation following reprogramming.

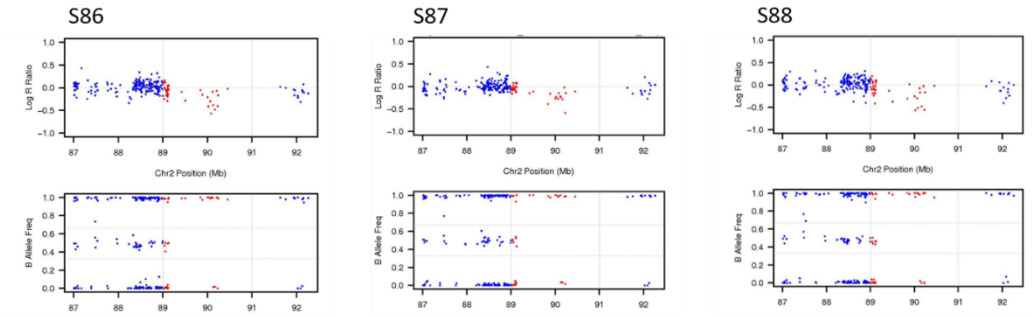

Sample ID	Signal Intensity File	CNV Locus	Approx Position	Status	Length
Elisa_86.1	/home/wptahe/iPSNOV2020_GSAv2/Nov2020v2.Elisa_86	2p11.2	chr2:89967747-90202954	Possible deletion	235,000
Elisa_86.2	/home/wptahe/iPSNOV2020_GSAv2/Nov2020v2.Elisa_86_R1	2p11.2	chr2:89967747-90202954	Possible deletion	235,000
Elisa_86.3	/home/wptahe/iPSNOV2020_GSAv2/Nov2020v2.Elisa_86_R2	2p11.2	chr2:89967747-90202954	Possible deletion	235,000
Elisa_87.1	/home/wptahe/iPSNOV2020_GSAv2/Nov2020v2.Elisa_87	2p11.2	chr2:89967747-90202954	Possible deletion	235,000
Elisa_87.2	/home/wptahe/iPSNOV2020_GSAv2/Nov2020v2.Elisa_87_R1	2p11.2	chr2:89967747-90202954	Possible deletion	235,000
Elisa_87.3	/home/wptahe/iPSNOV2020_GSAv2/Nov2020v2.Elisa_87_R2	2p11.2	chr2:89967747-90202954	Possible deletion	235,000
Elisa_88.1	/home/wptahe/iPSNOV2020_GSAv2/Nov2020v2.Elisa_88	2p11.2	chr2:89967747-90202954	Possible deletion	235,000
Elisa_88.2	/home/wptahe/iPSNOV2020_GSAv2/Nov2020v2.Elisa_88_R1	2p11.2	chr2:89967747-90202954	Possible deletion	235,000
Elisa_88.3	/home/wptahe/iPSNOV2020_GSAv2/Nov2020v2.Elisa_88_R2	2p11.2	chr2:89967747-90202954	Possible deletion	235,000

Figure 3.7 CNV Detection Array – CNV analysis detected a possible deletion at 2p11.2 in all the samples. No other CNV were detected using the Illumina Global Screening Array v2.0

3.3.2.4 Trilineage Differentiation

Directed trilineage differentiation was carried out to confirm the iPSCs potential to generate cells of the three germ layers. Three clones per sample were differentiated to the ectoderm lineage by culturing them for 6 days in order to produce neuronal progenitor cells (figure 3.8). All the samples showed a statistically significant increase in the expression of *Pax6,* neuronal progenitor cell marker(Shi et al., 2012b) (figure 3.8). The clones were also differentiated to the mesoderm lineage using an EB-based protocol as per microglia differentiation

protocol (figure 3.8); this protocol will be explained with more detail in chapter 4. The samples increased the expression of *KDR* gene, confirming mesodermal commitment. *KDR* encodes for VEGF receptor, important in the development of hematopoietic stem cells. Finally, the clones were differentiated to endodermal lineage following the protocol published by Schmid et al.(Schmid et al., 2019). The samples showed increased expression of *KIT* gene that encodes CD117, which is expressed on the early endoderm(Nostro et al., 2011).

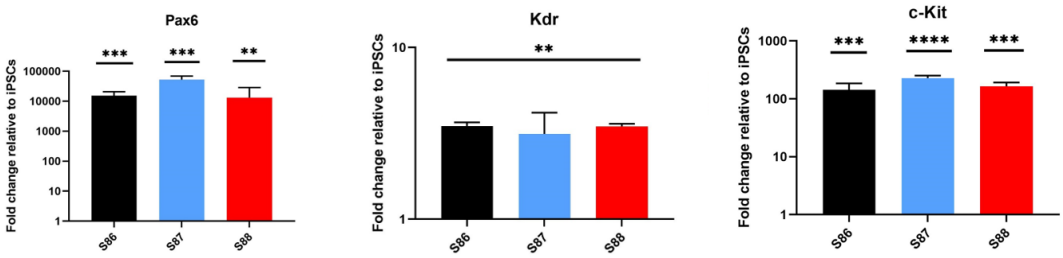

Figure 3.8 Trilineage Differentiation – RT-PCR analysis after tri-lineage differentiation detected upregulation of markers for ectodermal (*PAX6*), mesodermal (*KDR*) and endodermal lineage (*c-Kit*). Fold change is relative to undifferentiated corresponding samples. B-actin was used as a reference gene for normalization. N = 3 biologically independent clones. All data are mean ± S.D.; One-way ANOVA, Dunnett's test for multiple comparison. **p<0,005, ***p<0,0005 ****p<0,0001 – relative to iPSCs.

The reprogramming of terminally differentiated cells was described for the first time in 2006(Takahashi and Yamanaka, 2006). Despite the fact that the most popular sources of somatic cells during the last decade have been fibroblasts, PB is now a widely accepted alternative and benefits from being an easily accessible source. Fresh blood is generally desirable for reprogramming purposes, but many studies and protocols have shown easy reprogramming of frozen PBMCs(Agu et al., 2015, Ye and Wang, 2018). However, the cells used in this study proved to be particularly challenging, considering the general low viability at thawing (Table 3.2) possibly a consequence of the age of the samples and the freezing procedure, still largely unknown due to lack of information.

In consequence, while we failed to achieve the number of reprogrammed samples we desired, most of the work contained in this chapter revolves around the testing and evaluation of different strategies implemented in an attempt to overcome the

limitation imposed by the condition of the samples and to develop a protocol that could potentially be useful in similar studies in the future. Thus, the discussion of these results will be focused on the reasoning behind how we attempted to address these issues.

3.4 Discussion

3.4.1 Initial challenges of this study

The quality of the starting material for reprogramming purposes, as for any downstream applications, is of paramount importance and the steps preceding the final culturing of the cells, such as blood collection, freezing procedures and accurate tracing of sample conditions play a vital role in maintaining the good quality of the material(Betsou et al., 2019). One of the main limitations of this study was the lack of relevant information about the cohort of samples and their handling before the start of the project. This limited the option of adopting proper measures to deal with any specific handling procedures or even properly interpret and draw conclusions from the results obtained with the different samples involved in the study.

In the first instance, it is important to note that these samples were frozen down more than 10 years ago, the reprogramming technique is relatively new and the requirements would not have been known at the time of collection. The collection of the blood was intended for other purposes, for example DNA sequencing, rather than for generation of iPSCs. This is of relevance because the blood collection for consequent cell work and storage should be carried out in specialized anticoagulant-treated tubes; and the choice of the anticoagulants (EDTA, Heparin or ACD) needs to be carefully considered depending on the intended application(Betsou et al., 2019). In the same way, if the final goal was nucleic acid extraction, cells did not need to be viable and we might speculate they were left

at RT for a long time or they could have been frozen inefficiently, both of which would have dramatic effects on cell viability.

In this regard, the amount of time elapsed between the blood collection and the blood storage is critical. As Agu and colleagues show in their studies(Agu et al., 2015), blood can be kept at RT for up to 48 hours before being successfully reprogrammed. It is important to note, however, that in the *in vitro* alkaline phosphatase colony-forming cell (AP^+-CFC) assay, which is used as a mark of reprogramming efficiency, the percentage of positive colonies dropped from 0.012% of the fresh blood to 0.002% and 0.001% at 24h and 48h respectively. They addressed this problem by doubling the multiplicity of infection (MOI) of SeV from 6 to 12 which allowed the generation of some colonies per sample, although they never reached the same efficiency as with fresh blood(Agu et al., 2015).

Another important aspect to take into consideration is the freezing procedure. There is considerable divergence in the field concerning this aspect regarding PBMCs. The variation on viability at thawing could be due to mobilization strategies prior to freezing, diagnosis of the donor, number of cells frozen, concentration of cryoprotectant, temperature decrease rate and experience level of the staff members performing the cryopreservation(Majado et al., 2011, Weinberg et al., 2000). Nazarpour and colleagues tested different methods of cryopreservation, comparing centrifugation procedures, FBS and DMSO concentrations to prepare the freezing medium and the temperature of the freezing medium itself (Nazarpour et al., 2012). They did not report any differences in the centrifugation processes or the concentration of FBS in the viability of PBMCs after thawing. However, they suggested to keep DMSO concentration below 15%, to avoid cytotoxicity. Moreover, they did not observe any positive effect on cooling down the freezing medium; however, Tree and colleagues reported better functional responses of thawing PBMCs if the cold freezing medium was using before cryopreservation(Tree et al., 2004). We do not have any

information regarding the specific details of the freezing procedure in this cohort of samples.

Another parameter to be taken into consideration is the time elapsed between the storage of the samples and the thawing. Kleeberger and colleagues reported no significant loss of viable cells in a cohort of PBMCs cryopreserved for up to 12 years(Kleeberger et al., 1999). In the same way, Winter and colleagues did not see any substantial loss in PBMC subpopulation in a cohort of samples frozen down up to 15 years before the study; they observed that the major losses were attributable to cryopreservation processes, rather than length of storage(Winter et al., 2014). To our knowledge, however, there are no data available regarding the reprogramming efficiency of PBMCs stored in liquid nitrogen for more than 10 years. Agu and colleagues, showed no change in reprogramming efficiency when iPSCs where derived from samples cryopreserved 48h after collection. Their samples were stored in liquid nitrogen for only up to 4 months prior to reprogramming(Agu et al., 2015). Staerk and colleagues also used samples which were frozen and thawed between days to months after freezing, but not years(Staerk et al., 2010).

Decreased viability of cryopreserved PBMCs could also be associated with temperature variation during storage, for example if cells are stored close to the surface of the liquid nitrogen dewar or if the container is frequently removed to collect other samples(Weinberg et al., 2009).

3.4.2 Different expansion methods and media used in this study

The first approach used for reprogramming the samples followed the instructions of the CytoTune™-iPS 2.0 Sendai Reprogramming Kit, which explains how to reprogram frozen PBMCs. The media system used, consisted of StemPro®-34 SFM (Gibco) which is a serum-free medium formulated to support the development of human hematopoietic cells in culture, supplemented with four cytokines: SCF, IL-

6, IL-3 and FLT-3. As clearly stated in the protocol (CytoTune™-iPS 2.0 Sendai Reprogramming Kit), this medium targets a small subpopulation within the bigger PBMC population. Although the protocol does not specify the subpopulation in question, these cytokines are usually employed for the maintenance and proliferation of human hematopoietic cells/progenitors(Zhou et al., 2015). Specifically, SCF is known for being important in the regulation of early hematopoiesis(Galli et al., 1994). IL-6 plays a pivotal role in hematopoiesis(Heike and Nakahata, 2002) as well, and acting synergistically with IL-3, induces the proliferation of murine hematopoietic progenitors *in vitro*(Ikebuchi et al., 1987). Finally, FLT-3 works on early myeloid progenitors, bringing an addictive effect to the other three cytokines, favouring the expansion of immature cells(Broxmeyer et al., 1995).

Contradicting information about this cocktail of cytokines is found in literature. One study showed that this particular combination of cytokines leads to $CD34^+$ cell proliferation in samples of bone marrow, umbilical cord blood(Shah et al., 1996) and non-mobilized PB(Bontkes et al., 2002). On the contrary, Zhou and colleagues reported a slight increase of $CD34^+$ progenitors, whereas in the span of 4 days they showed a 80-200-fold expansion of $CD71^+$ erythroblasts. The CytoTune protocol, however, asserts that cells are not driven to proliferate but should maintain a stable number in the first few days, in order to result in a healthy and consistent culture at the day of reprogramming. Unfortunately, the situation for the first few samples tested was not as expected. Viability, already low on average at day of thawing (29%, Table 3.2) dropped down to 0% for all of the samples after four days in culture, making testing the reprogramming procedure impossible.

Considering the viability of the first nine samples after four days in culture, the number of days between thawing and reprogramming was decreased from four to one, in order to avoid the drastic drop in viability. Reprogramming was performed the day after thawing: in this case, S10 did not show any colony formation, whereas sample S11 generated a great number of iPSC colonies (Table 3.1).

It became increasingly clear that there were vast variabilities regarding the starting viability of the samples. This was a huge limitation when attempting to proceed with the reprogramming protocols, therefore we decided to attempt to rescue the cells by inducing T cell proliferation.

Thawed PBMCs were expanded using two different approaches: the first expansion protocol suggested by Seth Brodie (NIH, Bethesda) utilized a cocktail of activating cytokines. This expansion protocol was tested in 35 samples that showed 18% viability on average, ranging from 1% to 45% at day of thawing (Table 3.2), and successfully recovered a number of samples increasing both viability and number of cells.

Despite increasing viability and cell number in few cases, this protocol was not successful for the majority of the samples tested, with only 2 of them generating iPSCs colonies, having a 6% success rate (Table 3.2).

For this reason, we decided to test a published protocol of T cell expansion already demonstrated to be successful prior to reprogramming(Afshinmanesh, 2016, Seki et al., 2010). This second expansion medium consisted of RPMI containing 10% FBS and recombinant (r)IL-2 in anti-CD3 antibody coated wells. *In vivo*, the event that leads to the transition of a naïve T cell from a quiescent state to an activated one is called cell-priming(Chen and Flies, 2013). It is possible to recapitulate cell-priming *in vitro* by culturing T cells with an anti-CD3 monoclonal antibody-coated plate and rIL2(Desai-Mehta et al., 1996, Seki et al., 2010). In this particular system, T cells are selectively activated from the bigger PBMC population through the interaction of the TCR complex and the anti-CD3 antibodies used to coat the plates. This binding activates signalling pathways which are necessary in the activation of T cells(Chen and Flies, 2013), which are then able to express IL-2 and IL-2 receptors, both important for cell division(Toribio et al., 1989). The activation with this particular medium is described as effective for reprogramming of T cells as it increases the viability of the sample(Seki et al., 2010). Moreover, some studies

suggest that the activation state of T cells increases the efficiency of the SeV infection(Seki et al., 2012).

Although this was effective for a number of samples, two main problems were encountered. The first, and most striking, was that out of thirty-four samples tested, only four showed proliferation, confirming the poor quality of the starting material. Among the four expanded samples, only one was successfully reprogrammed: S49. As mentioned above, Lee and colleagues suggested that the activation of the immune system is able to enhance iPSC generation(Lee et al., 2012b). They compared efficiency of iPSC generation between two delivery methods of the reprogramming factors: retroviruses versus cell-permeant proteins. They observed that retroviral vectors, but not cell-permeant proteins, are able to activate the TLR3 pathway causing a rapid change in the expression of epigenetic modifiers. This leads to global chromatic remodelling and efficient nuclear reprogramming. The same sustained gene expression induction is observed when cell-permeant proteins carrying the reprogramming factors are combined with TLRs agonist. To confirm this finding, they knocked down the expression of TLR3 and observed little and delayed colonies appearance.

Despite the above results, contradicting evidence regarding the role of the immune system in the reprogramming mechanism exists in the literature. It is well established that IL-2 mediates immune interferon production by human T cells(Kasahara et al., 1983), and Chatterjee and colleagues showed that interferon significantly impairs susceptibility to infection by decreasing SeV-induced fusion with the plasma membrane(Chatterjee et al., 1982). Specifically, the entrance of the SeV into human cells is mediated by fusion of the viral glycoprotein with receptors located in the plasma membrane. They showed that the treatment of human cells with interferon results in decreased fluidity of the membrane, impairing the susceptibility of the cells to the fusion with the virus(Chatterjee et al., 1982).

In a different model of reprogramming strategy, Yoshioka and colleagues showed efficient generation of fibroblast-derived iPSCs with a synthetic self-replicative RNA delivered by a non-infectious Venezuelan equine encephalitis (VEE) virus. The exposure of the cells to the VEE virus harbouring the reprogramming factors induces, however, a strong interferon response, leading to low reprogramming efficiency. In order to reduce the innate immune response, the authors neutralized the interferon with B18R exposure, showing an increase in reprogramming efficiency(Yoshioka et al., 2013).

In addition, controversies also exist regarding the relationship between cellular proliferation and reprogramming success rate. Studies show that a high proliferation rate is essential for efficient reprogramming(Ruiz et al., 2011); on the other hand, others show that slowing down somatic cell proliferation is optimal for a positive reprogramming outcome(Xu et al., 2013, Gupta et al., 2015, Huangfu et al., 2008).

Exposure of the cells to the cytokine cocktails present in Expansion Medium A and Expansion Medium B induce a strong interferon immune response(Ross and Cantrell, 2018), and as shown in figure 3.2A and 3.3A, a high proliferation rate. For the reasons discussed above, the proliferation rate and activation status of T cells were controlled by moving the cells from Expansion Medium B to Complete PBMC medium. We found culturing T cells for one week in complete PBMC medium following expansion led to a decrease in the proliferation rate and resulted in successful reprogramming of 4 out of 6 expanded samples (out of 23 tested with this method, 17% of reprogramming success, Table 3.2). Considering the role of the four cytokines used in the Complete PBMC Medium (SCF, IL-3, IL-6 and Flt-3) in the maintenance of hematopoietic stem cells, it is advisable for future work involving similar samples, that T cells expanded with Expansion Medium B are moved to RPMI medium only (removing IL-2) for one week following expansion, in order to decrease innate immune state and proliferation rate.

3.4.3 Alternative PBMCs subpopulation cells as sources for reprogramming

Considering the failure of the approaches discussed above on T cells, alternative PBMC subpopulations can be considered as a source for cell reprogramming.

The PBMCs population is a mixture of different sub-groups comprising lymphocytes such as T cells (CD3+) and B cells (CD19+), macrophages (CD14+), hematopoietic stem cells (CD34+), erythroblasts (CD71+), myeloid and endothelial progenitor cells (CD13+)(. 2015).

It has been shown that the differentiation stage of the starting cells determines their susceptibility to the reprogramming procedure and consequent efficiency(Eminli et al., 2009). Specifically, pro-T cells showed 20-fold higher reprogramming efficiency when compared to immature CD4/CD8-double positive T cells, and 300-fold higher than mature peripheral T cells(Eminli et al., 2009). Likewise, myeloid progenitors demonstrated a higher reprogramming potential in comparison with macrophages and granulocytes(Eminli et al., 2009).

The first medium formulation used for this study targeted hematopoietic progenitor cells, but with no clear mention to the particular subpopulation. Zhou and colleagues specifically questioned the identity of the cells cultured in Complete PBMC medium for a 4 day period (as suggested by the Cytotune protocol) and they identified a consistent expansion in the $CD71^+$ (erythroblast) and $CD13^+$ (myeloid progenitor cells) cells, with only a slight increase in $CD34^+$ progenitors(Zhou et al., 2015). Other studies have successfully generated erythroblast-derived iPSCs(Varga et al., 2017, Yang et al., 2008, Agu et al., 2015). Erythroblast are nucleated cells arising in the red bone marrow which represent an intermediate stage in the process of red blood cell formation(Moras et al., 2017). Unfortunately, no expansion was observed in the samples tested with this media formulation.

An interesting alternative to erythroblast is represented by $CD34^+$ cells. Besides the aforementioned reason regarding the importance of the differentiation stage for reprogramming purposes, $CD34^+$ haematopoietic stem cells (HSCs) have been shown to maintain better genomic stability than differentiated somatic cells(Park and Gerson, 2005), and consequently they would represent an ideal target for cell reprogramming. The main limitation in the use of this subpopulation is in the low number in PB, representing less than 0.1% of the total PBMC population(Sekhsaria et al., 1996, Mack et al., 2011). For this reason, several studies use techniques to mobilize PB-derived $CD34^+$ in order to obtain a sufficient number of target cells(Loh et al., 2009, Ye et al., 2013). The mobilization of PB requires subcutaneous injection of Granulocyte-Colony Stimulating Factor (G-CSF) for five consecutive days(Loh et al., 2009, Raab et al., 2014). Excessive administration of this cytokine increases the production of HSCs from the bone marrow, which are then released into the PB. The isolation of these cells however is expensive, time consuming and could be painful for the donor. It takes up to four hours to separate HSCs from whole blood and this process could lead to some negative effects such as bone pain, nausea or headaches. For this reason, the mobilization of peripheral cells can only be performed if the donor is in good health. Unfortunately, we do not have any information regarding possible PB-mobilization on our samples, however chances are this was not done considering it is an unlikely procedure unless the aim of the blood collection is specifically the withdrawal of $CD34^+$ HSCs.

During the past few years different groups have tried to establish a protocol that uses non-mobilized $CD34^+$ HSCs(Merling et al., 2013, Okumura et al., 2019). Many studies conducted *ex vivo* expansion of the $CD34^+$ population in the attempt to overcome the insufficient number of cells at the steady state. Loh and colleagues showed a $CD34^+$ expanded population within 4 days of culture in RPMI medium supplemented with FBS and three of the four cytokines used in the cytotune protocol: Flt3, SCF and IL-3(Loh et al., 2009). Interestingly, Sharma and colleagues used a slightly modified version of the cytotune procedure (StemSpan SFEM II blood medium + StemSpan $CD34^+$ Expansion Supplement comprising Flt3L, SCF, IL-

3, IL-6 and Thrombopoietin (TPO)) and stated that PBMCs expanded within 10 days in culture(Sharma et al., 2018). Likewise, Mack and colleagues used the same formulation in order to culture $CD34^+$ cells previously separated from PBMC mixture, and they observed a variable expansion magnitude ranging from 3- to 83-fold after 6 days in culture(Mack et al., 2011). It is possible that in these last two mentioned studies, the presence of TPO, which was not included in the PBMC complete medium used for this study, gave the necessary boost for $CD34^+$ proliferation. TPO is able to lead to the expansion of immature myeloid and erythroid lineages, and act synergistically together with SCF and IL-3(Heike and Nakahata, 2002). None of these subpopulation markers have been tested in the samples used in the present study as viability considerably dropped after a few days in culture, and no expansion was observed.

It is of paramount importance to consider that all of these studies were conducted on fresh blood and therefore it is not possible to make a direct comparison with the samples used for this study.

A novel and recent approach shows it is possible to perform a $CD34^+$ cell-enrichment step from frozen mononuclear cell stocks(Okumura et al., 2019). Okumura and colleagues successfully reprogrammed cells from 15 patients with eight different diseases. All the samples were purified within 5h after PB collection (except for two samples which were processed after 24h) and banked in freezing medium for up to one year in liquid nitrogen before the use for iPSCs generation. Immediately after the thawing down, cells were recovered in basal medium containing SCF, FLT-3, IL-3, IL-6, TPO and G-CSF, a growth factor occasionally added to the cocktail of cytokines in order to generate committed progenitor cells(Heike and Nakahata, 2002) . The enrichment of the $CD34^+$ population was performed using immunomagnetic beads, and the cells were transduced 48h after thawing(Nishimura et al., 2017). This approach appears to be a valuable alternative to test with future samples collected for the expansion of the project.

Finally, Geti et al. showed the possibility to reprogram late-outgrowth endothelial progenitor cells (L-EPCs). These cells are described to arise from the mononuclear fraction of PB (either fresh or frozen), when cultured with endothelial-selective conditions after around 10 days(Geti et al., 2012). They appear as round, highly proliferative colonies, which can be passaged, stored and reprogrammed. This protocol was tested on a limited number of samples available for this project as well, however using this medium we were unable to establish L-EPC cultures, with all cells dying by 10 days of culture. The main difference between the study mentioned above and this present one is once again the condition of the samples. Geti et al. separated and expanded the endothelial progenitor cells from 40-80ml of PB immediately after collection; we are unable to discover the volume of blood from which the PBMCs used for this study were separated, nor the time elapsed between the collection and the freezing procedure, which might be critical in order to replicate these results.

3.4.4 Sendai Virus Reprogramming Vector

The reprogramming method selected for this study was the CytoTune 2.0 Sendai Reprogramming Kit. As already explained in the introduction, this is a non-integrating reprogramming method widely used in the field. However, new non-integrating methods are available, such as the use of episomal plasmids carrying the reprogramming factors, or mRNAs that encode OCT4, SOX2, KLF4, c-MYC. Schlaeger and colleagues compared the reprogramming efficiencies of these three methods and observed that the mRNA-based method was the most efficient(Schlaeger et al., 2015). The analysis of the karyotypes did not highlight any major differences between the methods, showing low CNVs rated across all the methods tested(Schlaeger et al., 2015). In the same way, iPSCs generated with all 3 methods showed both pluripotency marker expression and trilineage potential differentiation, with no apparent specific trend to any of the reprogramming methods.

In conclusion, no major differences were observed between the different methods. SeV is therefore a good choice being as efficient as other methods and highly reliable. One of the main limitations of this method is the dependence on one unique vendor, making it incredibly expensive(Schlaeger et al., 2015).

3.4.5 iPSCs characterization

An important step in the characterization of the iPSC lines is confirming the expression of pluripotency markers. Among the most common markers in use to characterize both ESCs and iPSCs are the cell surface epitopes SSEA-3, SSEA-4, TRA-1-60, TRA-1-81, the core pluripotency transcription factors OCT4, NANOG, SOX2, and the enzyme placental alkaline phosphatase.

Assessing differentiation potential of the generated lines is another crucial stage of the characterization process. There are many established techniques, which are used to determine the pluripotency of human iPSC lines. In this study, the cells were differentiated to the three different lineages using well established protocols. Specifically, for the ectodermal lineage, cells were differentiated for 6 days in order to produce neuronal progenitor cells(Shi et al., 2012b). For the mesodermal lineage, cells were dissociated in order to form embryo bodies (EBs) 3D structures. EBs were then cultured for 4 days with bone morphogenetic protein 4 (BMP-4, 50ng/ml, to induce mesoderm), vascular endothelial growth factor (VEGF-121, 50ng/ml endothelial precursors), and stem cell factor (SCF, 20ng/ml, hematopoietic precursor), three growth factors important for the formation of the mesodermal germ layer(van Wilgenburg et al., 2013). Finally, the protocol adapted by Schmid and colleagues(Schmid et al., 2019) was used in order to confirm the ability of the cells to generate the endodermal germ layer.

Alongside the *in vitro* techniques used for this study, a bioinformatics approach has been developed. The PluriTest® assay allows the comparison of the transcriptome of a selected cell line with the transcriptome of a big number of cells which are known to be pluripotent(Muller et al., 2011). Complementing the *in*

silico and *in vitro* approaches is the teratoma assay. A teratoma is a non-malignant tumour, which is constituted by a disorganized mixture of cells from all three embryonic germ-layers. In order to perform this assay, iPSCs are implanted into an immune compromised mouse where they can differentiate to form the teratoma(Wesselschmidt, 2011). This *in vivo* assay was considered the "gold standard" in the field for many years, and still today it is the only test which provides information not only on the pluripotency of the cells but also on their malignant potential. These two aspects are equally relevant in the pre-clinical safety assessment where PSCs are being considered for cell therapy, but not for their uses in disease modelling, so it is not relevant for this study. The international stem cell initiative suggests a strategy to analyse new human PSCs in which the method(s) is chosen based on the biological question posed and the potential future use of those cells(2018).

3.4.6 General limitations of the study

The major problem encountered from the beginning of this study was the general low viability of the cohort of the samples in use. Different attempts to rescue the cells were made, but more methods are available and could have been tested if the size of the cohort had been bigger. Unfortunately, the limited number of samples available and the impossibility of replacing most of these samples, due to their age, prevented this. Having established that HSCs appear to be more resistant to cryopreservation in comparison to fully differentiated cells, such as T- and B-cells, the different combinations of growth factors to supplement the four cytokines used in this study (SCF, FLT-3, IL-3, IL-6) could be attempted.

Unfortunately, as mentioned before, only one vial per sample was available from this cohort, making it impossible to test different protocols and conditions on the same cells. It would have been interesting to better characterize the starting population at the day of thawing to evaluate the different contribution of the

subpopulations (T cells, B cells, $CD34^+$, erythroblasts, endothelial progenitor cells). This would have helped to get a better idea on which population to focus for possible expansion. In the same way, an enrichment step for a specific subpopulation could have been helpful for the proliferation procedure.

The samples of this cohort showed better responsiveness to T cell stimulation than HSCs stimulation, resulting in lymphocyte proliferation. However, not all the samples expanded resulted in successful reprogramming, in either of the condition tested. While expensive, a possible solution to this problem would be to increase the MOI from 5, used in this study, to 12 as suggested by Agu and colleagues(Agu et al., 2015) or 20 as suggested by Seki and colleagues(Seki et al., 2012), in order to increase the chances of virus particles to infect the cells.

3.5 Conclusion

This study is the first example of a reprogramming attempt of PBMCs samples frozen for more than 10 years. This was achieved by combining several previously investigated protocols and techniques. The poor conditions of the samples became evident since the first few samples were thawed. As discussed, several factors might have contributed to the low viability of the cells, such as time elapsed between blood collections and processing, freezing procedures and temperature variation during storage. We found that the most successful protocol consisted of a first phase of T cell expansion in order to increase cell number and viability, followed by a week where cells were cultured in a specific medium formulation that slowed down cell proliferation and attenuated activation state. Samples that successfully generated iPSCs were picked and extensively characterized to check virus clearance, pluripotency marker, trilineage differentiation potential and genomic architecture.

4 Generation of novel iPSCs-derived microglia-like cells carrying the *PLCG2* Alzheimer's disease protective R522 variant, and control neurons and astrocytes

4.1 Introduction

Over the years, many different cellular and rodent models have been of invaluable help in understanding AD pathophysiological processes, but to date a definitive cure or effective treatment remains elusive. The continuous failure of therapies, tested in many different clinical trials, suggest the need to change and improve the models we use to mimic neurodegenerative disorders. New opportunities arose during the past decade with the advent of iPSCs. Human iPSCs can be differentiated into multiple cell types, including brain cells, leading to new paths of neurodegenerative disease research.

4.1.1 Alzheimer's Disease Models: Pros and Cons

A great number of cellular and animal systems have been used over the years to understand AD. Post-mortem patient brain tissue has been an invaluable tool to initially decipher the cellular and molecular alterations caused by the disease(Penney et al., 2020); however, they do not offer the possibility to intervene and try to change the development of the pathology. Moreover, many human, as well as rodent, cell lines helped uncover a role of Aβ and other molecules relevant for the disease(Penney et al., 2020). The main limit of these models lies on the fact that these are dividing cells, and thus poorly reproduce neurodegenerative mechanisms. Finally, mice represented one of the most important models of AD research for many years due to their evolutionary relationship with humans. The majority of mouse models which successfully replicate human neurodegeneration overexpress human neuronal proteins, which carry familial AD (FAD)-causing mutations at levels which are considerably higher than the endogenous analogue(Penney et al., 2020). Considering the fact that the corresponding human disease mutation in mice usually does not lead to neurodegenerative phenotypes, this is one of the main limitations of this model(Penney et al., 2020). Moreover, mice do not have a long lifespan and the over-expression of these proteins might result in artifacts that do not exist in

human disease(Esquerda-Canals et al., 2017). Alongside the FAD-models, researchers developed several sporadic AD (SAD) mouse models as well(Penney et al., 2020). The main problem with these models is that SAD mutations alone usually do not cause a neurodegenerative phenotype, which is why this is usually studied in the context of established FAD mouse models(Penney et al., 2020). This field of research is only beginning to unfold and our understanding of how SAD mutations, and more importantly each cell type, play a role in neurodegeneration is still far from complete.

4.1.2 Induced Pluripotent Stem Cells

The number of methods describing the differentiation of human iPSCs into different cell types exploded since the first publication of the initial method in 2007(Takahashi et al., 2007). Among these, several protocols have been described for the production of NPCs, different neuronal subtypes, microglia, astrocytes as well as endothelial cells, pericytes and oligodendrocyte(Penney et al., 2020). Moreover, as the understanding of the physiological mechanisms and the role of strict cell-to-cell interactions increases, so does the complexity of the culture models developed to study these factors, going from mono- and co-culture systems to 3D organoids(Haenseler and Rajendran, 2019).

4.1.3 Microglia

Microglia are the resident immune cells of the brain and although microglial-mediated neuroinflammation has long been recognized as a hallmark feature for AD, evidence suggesting a crucial role of these cells in disease pathogenesis has only emerged recently (Zhou and Verstreken, 2018). Among the GWAS-identified risk genes, many are mainly or exclusively expressed in microglia (Villegas-Llerena et al., 2016, Kunkle et al., 2019a, Sims et al., 2017).

One of the major challenges at hand is to develop new ways to interrogate the vast amount of genetic data in a cell population, such as microglia. Microglia cells, as many other tissue-resident macrophage populations, derive from yolk-sac (YS)

precursors cells that colonise the tissue during embryonic hematopoiesis, complete the differentiation process in the tissue and are self-maintained throughout life(Hoeffel and Ginhoux, 2015, Ginhoux and Guilliams, 2016). Obtaining and working with this terminally differentiated cell-type has proven to be a difficult task for the macrophage research field, mainly because microglia isolated from healthy or affected brain samples are extremely complicated to obtain; and tissues harvested post-mortem or from brain surgery may come with artifacts (Haenseler and Rajendran, 2019). Microglia-like cells have been generated from both HSC or circulating monocytes, but these populations do not share the same embryonic ontogeny of the vast majority of microglia in the brain, as explained in Chapter 1 – Introduction. For this reason, these cell models show many disadvantages, such differences with microglia cells at transcriptomic and functional levels(Hinze and Stolzing, 2011, Etemad et al., 2012). Moreover, using cells derived from animal models, such as mice and rats, very often carry species differences that may lead to results not relevant to human immunopathology(Penney et al., 2020). Finally, human myeloid cell lines, such as THP-1, are not terminally differentiated and may have abnormal karyotypes, making them not a suitable model (van Wilgenburg et al., 2013).

Because of the recent uncovering of microglia ontology, protocols for the iPSC differentiation to microglia have only recently been developed and are under constant revision and improvement(Abud et al., 2017, Douvaras et al., 2017, Haenseler et al., 2017, Muffat et al., 2016, Takata et al., 2017). Both iPSCs from healthy patients and SAD patients have already been generated, and the derived microglia have already offered a first insight into the functional differences between the two groups(Xu et al., 2019). Specifically, phagocytosis was significantly increased in microglia cells derived from SAD patients in comparison to cells derived from cognitive healthy individuals. LPS stimulus, enhanced phagocytosis ability in both groups, remaining significantly more prominent in AD-microglia. Moreover, AD-microglia cells secreted more IFN-γ, TNF, IL-6 and IL-10 than the control group when stimulated with 1µg/ml LPS.

4.1.4 Cortical Neurons

The cerebral cortex represents the executive centre of the CNS in mammals. Rodent models have been an invaluable tool to understand the developmental, physiological and pathological mechanisms of this part of the brain(Shi et al., 2012b). However, some fundamental differences between rodents' and humans' brains pose some limitations on the use of the former as research models. The first main discrepancy is the size of the cortex, which is consistently bigger in humans(Rakic, 2009). Because of this, the complexity of the developing stem cell population is also increased in humans, together with the diversity of the different neuronal layers(Shi et al., 2012b). The human cerebral cortex contains roughly 80% of excitatory glutamatergic neurons, which are generated by cortical progenitor and stem cells and 20% of GABAergic interneurons, which migrate into the cortex during embryonic development(Wonders and Anderson, 2006). Glutamatergic neurons are produced in a stereotyped temporal order, where deep layer neurons are produced first and upper layer neurons are produced last(Shi et al., 2012b). These different classes of neurons which belong to different layers can be differentiated by the expression of specific transcription factors (Figure 4.1). These cells form local microcircuits among them, as well as longer intra and extra-cortical connections(Shi et al., 2012b).

The advent of iPSCs considerably increased the possibility to decipher human cortical developmental mechanisms, circuit formation and functions. The protocol used in this work was adapted from the published method by Shi and colleagues(Shi et al., 2012b). The authors addressed a previous problem commonly observed in directed differentiation from mouse embryonic stem (ES) cells: although the production of deep layer neurons was successful, the complete cortical neurogenesis was never achieved in culture(Shi et al., 2012b). It is has been suggested that this failure arise from the ES cells inability to reproduce the intricate stem and progenitor cell populations found *in vivo*(Au and Fishell, 2008). For this reason, the monolayer protocol proposed by Shi and colleagues, aim, as first step, to differentiate iPSCs to this complex cortical stem and progenitor cells variety,

and subsequently terminally differentiate cells following the same temporal neurogenesis process that will generate neurons of all layers(Shi et al., 2012b). The differentiation of both populations was checked by the expression of specific transcription factors.

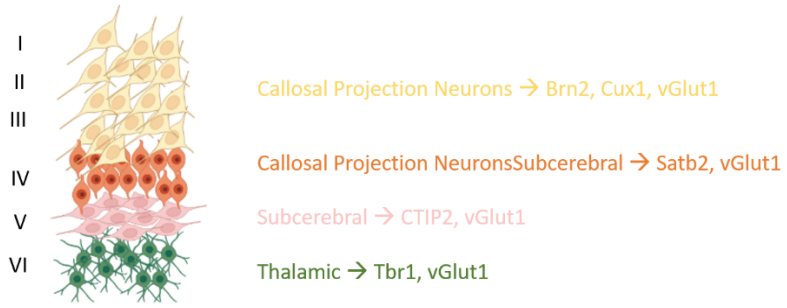

Figure 4.1 – Schematic representation of cortical neurons in the layers of the adult cortex. Each layer can be differentiated thanks to the differential expression of several transcription factors, as shown in the figure.

4.1.5 Astrocytes

Astrocytes are the most abundant glia cell type and display a high degree of morphologic and functional heterogeneity(Zhou et al., 2019). Functionally, astrocytes are able to switch to reactive states upon stimuli such as for example LPS(Liddelow and Barres, 2017). Different insults lead to different subtypes of activated astrocytes. As with the study of microglia and neurons, animal models, especially mice, contributed greatly to advance our knowledge of this cell type(Li and Shi, 2020). However, differences in morphology, function and transcriptome led to the increasing need of developing new models more representative of human astrocytes. iPSCs-derived astrocytes allowed for a better understanding of the role of these cells in neurodegenerative disorders, and in those pathologies where animal models lack disease-relevant phenotypes(Penney et al., 2020).

In this present study, we decided to use ACM generated in house, in order to better recapitulate the physiological conditions in which microglia and neurons co-exist

in the brain. Evidence suggests that astrocytes play a crucial role in microglial development and differentiation. Specifically, they have been shown to influence microglial morphology, inducing a more ramified shape in *in vitro* co-culture experiments(Tanaka and Maeda, 1996, Sievers et al., 1994, Liu et al., 1994); moreover, astrocytes are important regulators of microglia functions and immunophentoype. Not only is the physical contact between astrocytes and microglia crucial for the latter, but many studies showed that astrocyte-secreted molecules also play important roles(Jha et al., 2019). As in the case of the co-culture studies mentioned above, amoeboid microglia treated with ACM assume a more ramified morphology(Schilling et al., 2001, Eder et al., 1999).

Astrocytes were differentiated from iPSCs following the protocol by Serio et al.(Serio et al., 2013). ACM was generated and used to culture both microglia in monoculture, and in co-culture with iPSC-derived cortical neurons.

4.2 Aim

The aim of this chapter was to examine differentiation protocols for generating microglia, neurons and astrocytes from stem cells and to characterize obtained cells, to set the ground for functional studies.

4.3 Results

4.3.1 Microglia Differentiation Protocols

Disease modelling using iPSCs depends on the ability to direct their differentiation to authentic disease-relevant cell types. To establish the protocol to be used throughout the project, two different protocols were compared. Initial studies used an EB based protocol (van Wilgenburg et al., 2013) and subsequently a more recently published monolayer protocol was tested(Takata et al., 2017). Both protocols recapitulate the development of microglia cells in the embryo.

***Van Wilgenburg Embryo Body Protocol*.** This protocol was initially established using the control iPSC line KOLF2 (HPSI0114i-kolf_2, HipSci), derived from a healthy European middle-aged man, and was generated from skin tissue using SeV technology (HipSci website).

EBs are iPSC-spheroid structures, which have the ability to differentiate along the three germ lineages(Lin and Chen, 2008). During this project, different EB formation methods were tested (figure 4.2). The first method allows self-aggregation of stem cell colonies via dissociation with ReleSR, a reagent that easily detaches full size colonies. Although a quick and easy method, self-aggregation leads to the formation of EBs heterogeneous in size and with irregular shapes (figure 4.2A). This could be problematic for the differentiation of each EB, as the diffusion of the nutrients, and more importantly of the growth factors, necessary for the mesoderm commitment could be different.

To prepare EBs with consistent size and shape (10,000 cells/EB), the hanging drop method was tested(Lin and Chen, 2008). Figure 4.2B shows a schematic representation of iPSC-derived microglia protocol using the hanging drop method.

The final EBs formation method involves the use of low attachment plates (figure 4.2C) specifically design for the formation of EBs consistent in shape and size. This method will be further discussed in subsection 4.4.3.

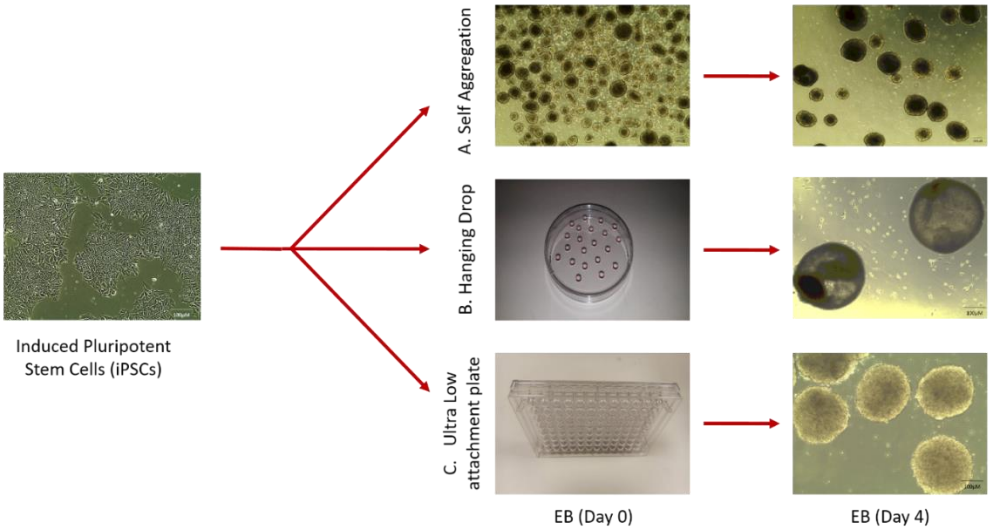

Figure 4.2 - Overview of three different EB formation methods. – The three methods tested for EB formation, represented at day 0 and day 4. **A.** Self-aggregation; **B.** hanging drop; **C.** Ultra low attachment plate.

At this stage, cells were cultured in either E8 flex (Gibco) or mTesr medium (StemCell Technology), the two most popular media in use in the field for culturing iPSCs, so that comparisons could be made between them. Media were supplemented over the first 4 days with the following growth factors: BMP-4, VEGF-121, SCF. To understand if the choice of the medium affected the commitment of the cells toward the hematopoietic lineage, qRT-PCR was performed to examine developmental markers expressed in 4-day old EBs. As shown in figure 4.3, no significant difference was detected between any of the pluripotency (*OCT4, NANOG*) and developmental (*Brachyury, CD34, RUNX1 and KDR*) markers chosen.

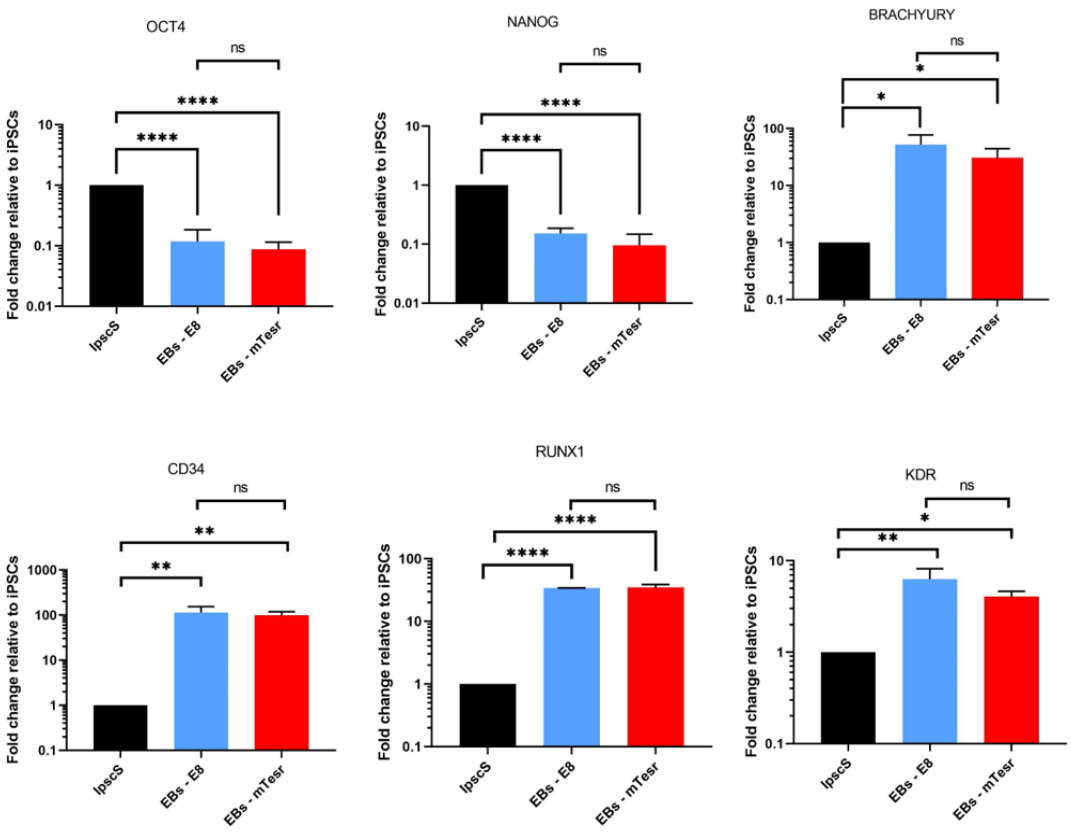

Figure 4.3 - Comparison of E8 flex and mTesr media to culture EBs - EBs cultured for 4 days were harvested and assayed by qRT-PCR for expression of developmental markers. Fold change is relative to undifferentiated Kolf2. β-actin was used as a reference gene for normalization. mRNA levels were taken from 2 technical replicates of 3 biological samples. One-way ANOVA, Tukey's test for multiple comparison. p*<0,05, **p<0,005, ****p<0,0001.

Following the Haenseler protocol(Haenseler et al., 2017), EBs were moved into flasks or 6-well plates after 4 days and cultured with XVIVO-15 medium supplemented with IL-3 and macrophage colony-stimulating factor (M-CSF), to promote monocyte differentiation. The majority of EBs adhered to the plate surface and developed cystic, yolk-sac-like structures. Non-adherent, embryonic-like macrophage precursors appeared after 4-5 weeks in the supernatant and were carefully harvested without disturbing the attached EBs (figure 4.4A).

Flow cytometry and ICC analyses were performed to assess the expression of different macrophage-precursor markers. Flow cytometry of non-adherent macrophage precursors, showed that 90% of the cells were $CD45^{+}$ and more than

60% were $CD14^+$ (figure 4.4B). For ICC, cells were cytocentrifuged onto a slide and immunolabelled for the hematopoietic surface markers CD45/CD11b, and the hematopoietic intracellular marker RUNX1. As shown in figure 4.4C, the large-nucleus cells were positive for all three markers. Taken together, these results show that iPSCs-derived macrophage precursors represent a fairly homogeneous population committed toward mesodermal lineage.

In the last step of the protocol, ramified microglia cells were induced from iPSC-derived macrophage precursors. Harvested macrophage precursors were plated in fibronectin-coated 6-well dishes or coverslips and cultured for 14 days in X-VIVO media containing IL-34 and GM-CSF (granulocyte-macrophage colony-stimulating factor), which have been shown to be essential to maintain microglial differentiation and survival(Haenseler et al., 2017).

Treatment with IL-34 and GM-CSF led to the expression of the calcium binding protein IBA-1, as shown in the ICC in figure 4.4D. IBA-1 is expressed both in microglia cells and macrophages; for this reason, microglia-derived iPSCs were also stained for TMEM119, a recently defined microglia-specific marker(Bennett et al., 2016), and for CX3CR1(Kettenmann et al., 2011).

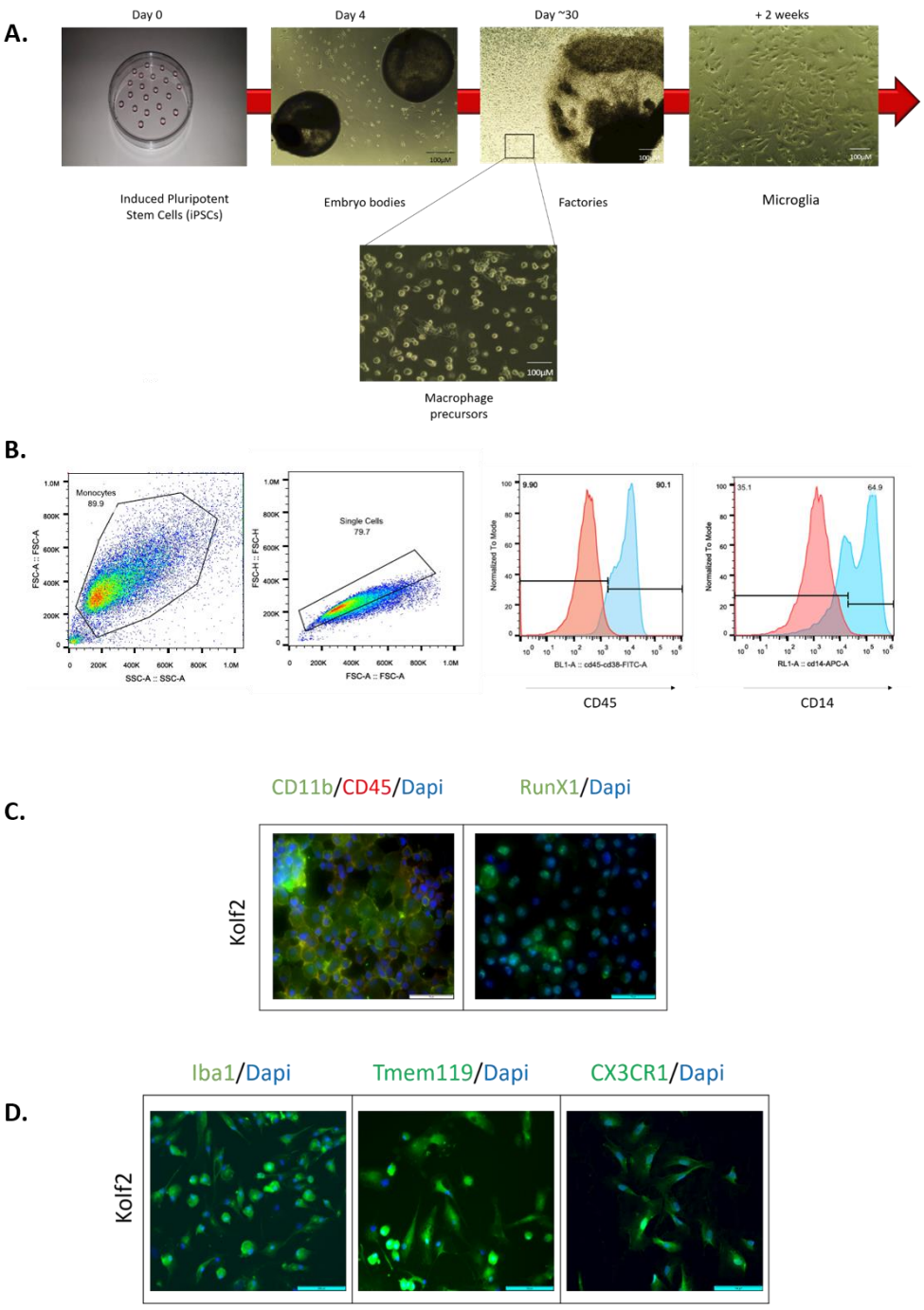

Figure 4.4 - Van Wilgenburg protocol – Differentiation and characterization of macrophage precursors and microglia-like cells generated with Hanging Drop Method. A) Schematic representation of the protocol: Kolf2 iPSCs were differentiated to microglia-like cells via EB and macrophage precursors. Macrophage precursors are produced continuously in culture and are terminally differentiated into microglia. **B)** Flow cytometry analysis revealed a large population of CD45+ cells (>90%) and CD14+ cells (64.9%). Gates were defined by using appropriate isotype controls. **C)** Immunostaining of macrophage precursors for haematopoietic markers CD11b, CD45 and Runx1. Nuclei were stained with Hoechst 33342 (Blue). Bars = 50µm. **D)** Harvested macrophage

precursors cultured in GM-CSF and IL-34 were immunostained for Iba1, Tmem119, and CX3CR1, displaying typical ramified morphology. Nuclei were stained with Hoechst 33342 (Blue). Bars = 200μm

Takata Monolayer Protocol. Monolayer differentiation has a number of advantages when compared to the EB-based method especially when differentiating multiple cell lines in parallel. Another important advantage of this more recent protocol is that it reflects more accurately the *in vivo* hemangioblast formation(Takata et al., 2017). In particular, Wnt pathway activation is important in the modulation of primitive hemangioblasts(Tsakiridis et al., 2014, Cheng et al., 2008). For this reason, iPSCs are exposed to CHIR99021, a GSK3β inhibitor (which acts as a Wnt pathway agonist) on day 0, but then from day 6 cells are exposed to Dkk1, a Wnt antagonist, to mimic the shift characteristic of the *in vivo* embryonic development. Figure 4.5A shows a schematic representation of the monolayer protocol.

At day 26, supernatant cells were collected and analysed with flow cytometry to assess expression of macrophage-precursors markers (figure 4.5B). Cells derived were positive for both CD45 and CD14 (~ 80%) macrophage surface markers as expected, of which over 96% positive for CD11b, important for adhesion and migration.

Although the macrophage precursors expressed the characteristic markers at comparable percentages with the EB-based method, once plated down for terminal differentiation they proved to be of lower quality. During the two weeks of maturation in X-VIVO with GM-CSF and IL-34, a heterogeneous population of cells appeared. As seen in figure 4.5C, the Dapi staining shows nuclei of different sizes. Upon observation, the bigger nuclei belonged to fast proliferating cells with a flat, fibroblast-like morphology. Despite showing a morphology and a behaviour different from microglia-like cells, they stained positive for Iba-1 (figure 4.5C). At the end of two weeks terminal differentiation, the culture appeared overgrown by these dividing cells making it impossible to perform any assays to test microglia

functionality. For this reason, we decided to adopt the EB-based method for further studies.

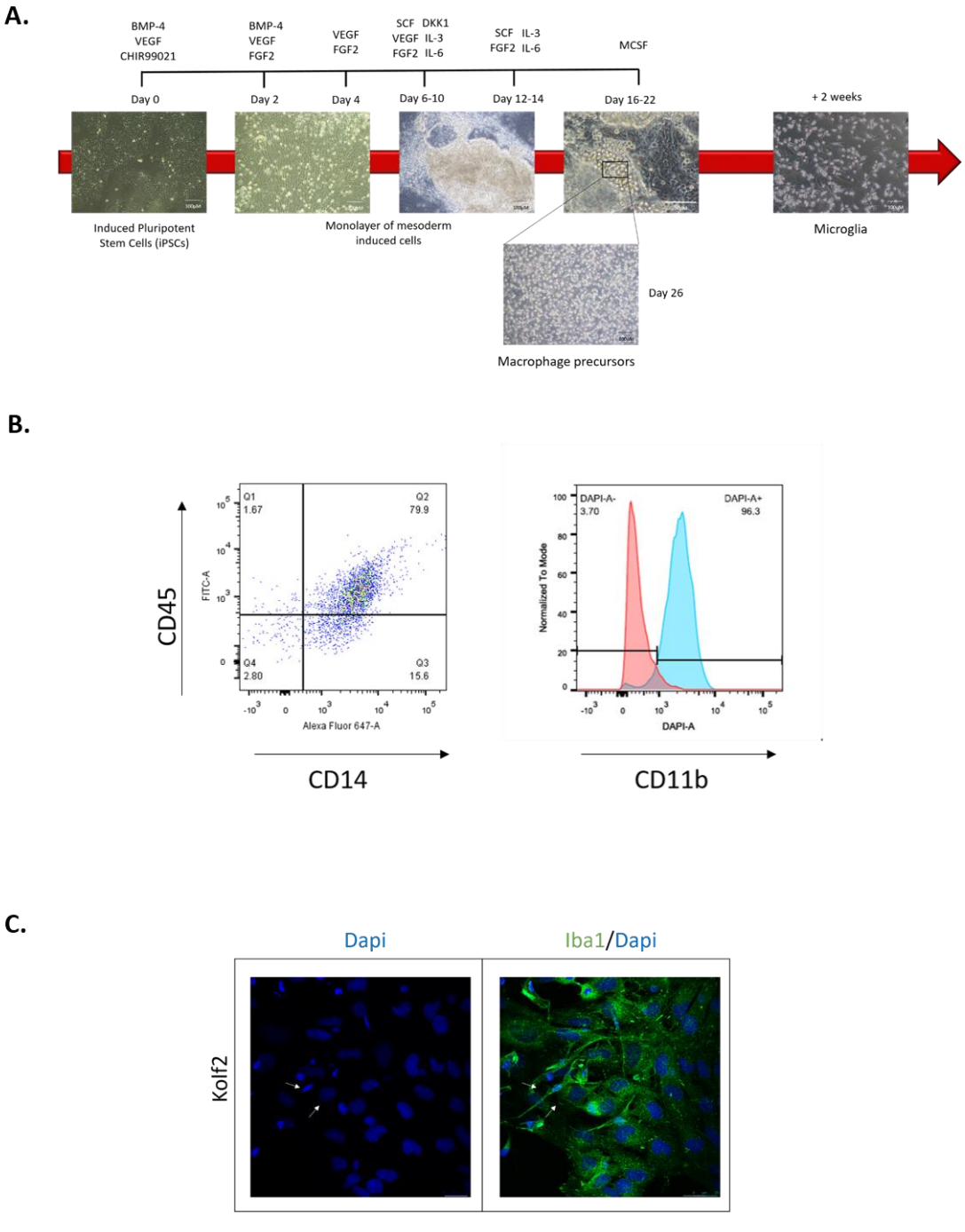

Figure 4.5 - Takata protocol – Differentiation and characterization of macrophage precursors and microglia-like cells generated with Monolayer Protocol. A) Schematic representation of the protocol: Kolf2 iPSCs were differentiated to microglia-like cells via monolayer iPSCs and macrophage precursors. Macrophage precursors are produced continuously in culture and are terminally differentiated into microglia. **B)** Flow cytometry analysis revealed a large population of

CD45+ and CD14+ cells (80%) and CD11b+ cells (90%). Gates were defined by using appropriate isotype controls. **C)** Harvested macrophage precursors cultured in GM-CSF and IL-34 were immunostained for Iba1. Results revealed that all the cells were Iba1+, including the flat, fast proliferating cells. Nuclei were stained with Dapi (Blue). Bars = 25µM. White arrows points at nuclei of different sizes, showing heterogeneity of the culture.

4.3.2 Generation of *PLCG2* cell lines expressing mcherry reporter gene

In order to investigate the role of the R522 variant of *PLCG2*(Sims et al., 2017), mutant and KO iPSC cell lines were generated in our lab. Briefly, the control iPSC line KOLF2 was nucleofected with guide RNAs, CrisprCas9 enzyme and a homology DNA template in order to insert the missense variant in chromosome 16 (reference SNP rs72824905), which encodes for the amino acid change from proline to arginine. To generate the PLCG2 knock out clones, KOLF2 was nucleofected with guide RNAs and CrisprCas9. In both cases, multiple clones were picked and screened to confirm the correct insertion of the mutation or the generation of a deletion in the gene locus. These studies were performed by Dr. Emma Cope.

To enable live cell imaging to observe the movement and behaviour of microglia cells in co-culture conditions, these cell lines were further edited to introduce fluorescent reporter transgenes. The donor plasmid, AAVS1-Pur-CAG-mCherry (AddGene), was nucleofected into iPSC cells carrying either P522, R522 or KO *PLCG2* together with two other elements: the Crispr Cas9 enzyme and a guide RNA. The former is responsible for generating the double strand break in the DNA; the second is a guide RNA, the role of which is to lead the Cas9 enzyme to the correct site where the cut is desired, in this case the AAVS1 safe harbour site(Hayashi et al., 2020). This site ensures stable expression of the fluorescent gene avoiding any random genetic disruption. The donor plasmid, specifically, is constituted of two homology arms, a puromycin cassette and the mcherry gene (figure 4.6A). The two homology arms are used as a template by the cells to repair the DNA via a homology directed repair mechanism. The puromycin cassette enables easy selection of the successful transfected cells.

Three clones per genetic condition were picked after the nucleofection and selection process, and correct integration of the mCherry reporter gene was confirmed by PCR analysis of genomic DNA (figure 4.6B). Specifically, primer pairs were designed so that the forward primer would align with the human AAV1 sequence, whereas the reverse primer aligned inside the donor plasmid (figure 4.6A). Correct site integration would give a band of around 1000bp as shown in figure 4.6B. Finally, positive expression of the mCherry reporter gene was confirmed through imaging of the cells with the Incucyte live imaging instrument (Sartorious) (figure 4.6C).

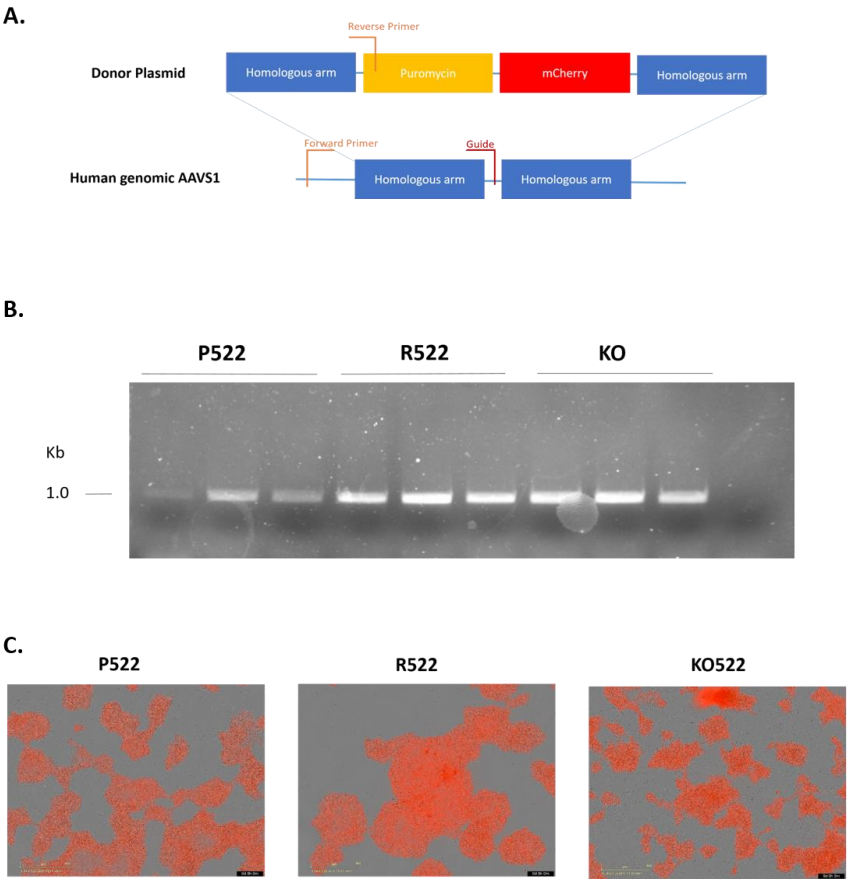

Figure 4.6 - Confirmation of integration and expression of mCherry reporter gene into PLCG2 iPSCs. A) Schematic representation of the donor plasmid structure in the upper image. Schematic representation of the integration of the donor plasmid into the human genomic AAVS1 site. The position of the forward and reverse primer, and the guide RNA are shown. **B)** The correct site of the integration was confirmed for all the 9 clones. **C)** Successful mcherry reporter gene expression was confirmed by live imaging iPSCs on Incucyte S3 incubator.

4.3.3 Microglia Differentiation and Characterization of PLCϒ2 lines using Van Wilgenburg method with ultra-low attachment plates and Astrocyte Conditioned Medium

Ultra-low attachment plates were used as a third method to prepare EBs (figure 4.2C). This last procedure proved to be the most reliable, giving EBs of homogenous size and regular shape. Three clones per genotype were routinely differentiated following the method published by Van Wilgenbur and colleagues(van Wilgenburg et al., 2013), as explained in section 4.3.1, and checked for the main macrophage precursors marker (CD45, CD14 and CD11b) in order to confirm mesoderm commitment and microglia-like cells identity (figure 4.7B). Specifically, PLCγ2^{P522} were 54% CD45^{+}CD14^{+} of which over 80% CD11b^{+}. PLCγ2^{R522} were over 61% double positive for CD45^{+}CD14^{+} of which over 87% positive for CD11b. Finally, PLCγ2^{KO} were over 67% positive for CD45^{+}CD14^{+}, of which 76% CD11b^{+}. These numbers represent the result from a representative experiment.

We introduced a modification concerning the medium used to terminally differentiate macrophage precursors into microglia-like cells during the last two weeks of the protocol. We noticed that microglia differentiated with XVIVO medium, supplemented with GM-CSF and IL-34(van Wilgenburg et al., 2013, Haenseler et al., 2017), appeared mainly bi-polar instead of ramified (figure 4.4D). We therefore supplemented the medium with ACM, as previously established in the lab (Cope Thesis), which promotes microglial differentiation, consistent with the findings of Bohlen and colleagues(Bohlen et al., 2017). Floating cells were harvested weekly and terminally differentiated using ACM. Microglia-like cells were characterized with immunostaining. ICC shows that clones of all three PLCG2 genotypes are able to produce IBA-1^{+} and TMEM119^{+} cells (figure 4.7C).

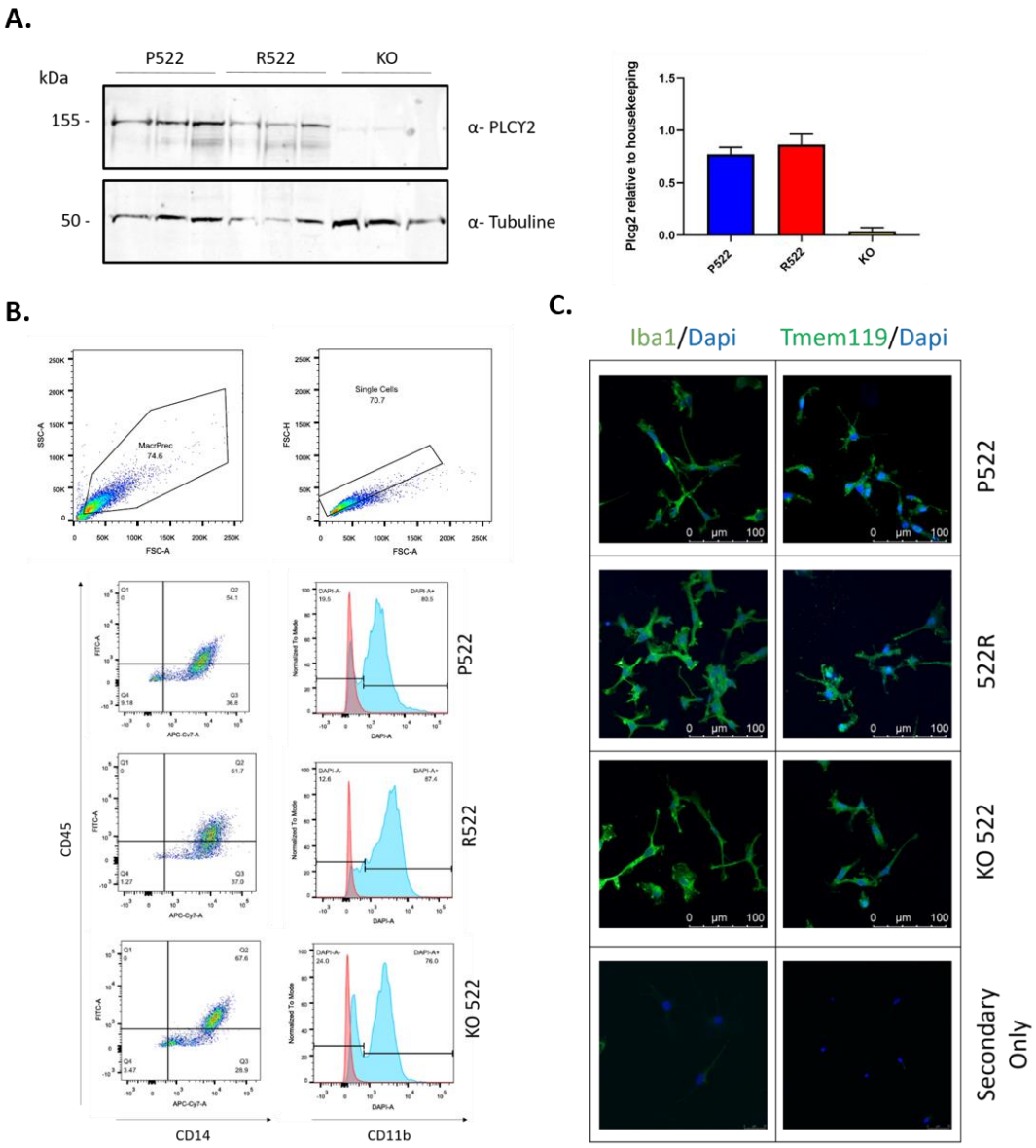

Figure 4.7 – PLCG2 clones characterization at macrophage precursors and microglia-like cells stage. A) Representative western blotting membrane (left panel) of PLCγ2 in macrophage precursor cells and relative graph (right panel) normalized to loading control of P522 (blue) control, R522 (red) variant and KO (yellow). The graph represent the mean of 3 independent experiments. **B)** Flow cytometry analysis reveals all three genotypes are able to produce a large population of CD45+, CD14+ and CD11b+ cells. Gates were defined by using appropriate isotype controls. **C)** Immunostaining of microglia-like cells differentiated with in house-produced ACM shows that all three genotypes can differentiate into Iba^{+} and Tmem119^{+} cells. Nuclei were stained with Dapi (Blue). Bars = 100µm.

4.3.4 Neuronal Differentiation Protocol

In order to establish a robust iPSC-derived microglia-cortical neuronal co-culture system, the control iPSC line KOLF2 was used to prepare cortical neurons. The

protocol used in this study is an adaptation of the one published by Shi and colleagues(Shi et al., 2012a). This is a multistep protocol, in which iPSCs are differentiated to cortical progenitor cells in the first phase, and then these are terminally differentiated to mature cortical neurons for an extended period of time which can be elongated up to 90 days(Shi et al., 2012b). Figure 4.8A displays a schematic representation of the iPSC- derived cortical neuron protocol. As used by Shi et al., dual SMAD inhibition is a fundamental step in the neuroectodermal induction(Elkabetz et al., 2008). For this reason, over the first 8 days of culture, iPSCs were treated with SB431542, a small molecule inhibitor of Smad2/3 activation and TGF-β signal transduction, and LDN193189, an inhibitor of BMP-4 mediated Smad1/5/8 phosphorylation. In addition, IWR-1 was used to potently inhibit WNT signalling. At this point, the addition of retinoic acid during the following 8 days led the cells to the formation of NPCs, as assessed by both qRT-PCR and staining. NPCs at day 16 were identified by their expression of the transcription factors *PAX6, OTX1, FOXG1* and *EMX1* (figure 4.8B)(Shi et al., 2012a). Confirmation of the neuroectodermal induction is shown in figure 4.8C with the precursors staining positive for Pax6 and BIII tubulin. After the initial induction, NPC were terminally differentiated to mature cortical neurons. For the purpose of this study, where the focus was the function of microglia cells with different PLCϒ2 variants, cortical neuron maturation went on for 21 days, before continuing in co-culture. At this point, the cells express markers such as Satb2 and vGlut (figure 4.8B), and Tbr1 and Ctip2 (figure 4.8C).

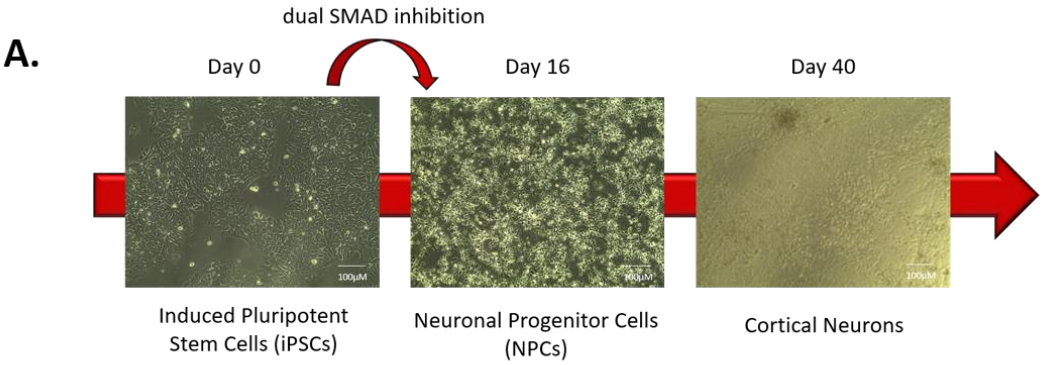
A.
dual SMAD inhibition
Day 0
Day 16
Day 40
Induced Pluripotent Stem Cells (iPSCs)
Neuronal Progenitor Cells (NPCs)
Cortical Neurons

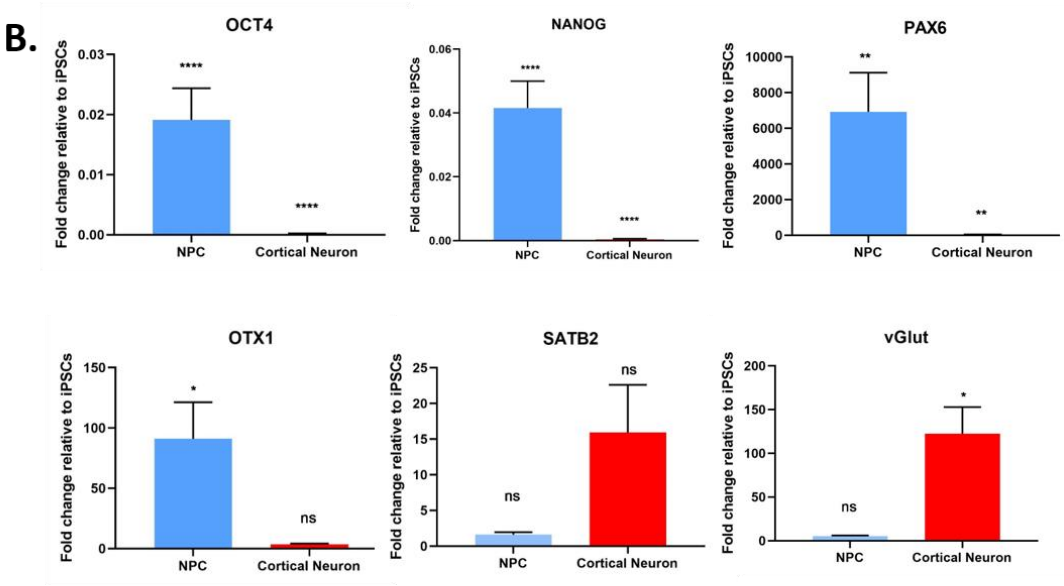
B.
OCT4
NANOG
PAX6
OTX1
SATB2
vGlut
Fold change relative to iPSCs
NPC
Cortical Neuron
ns

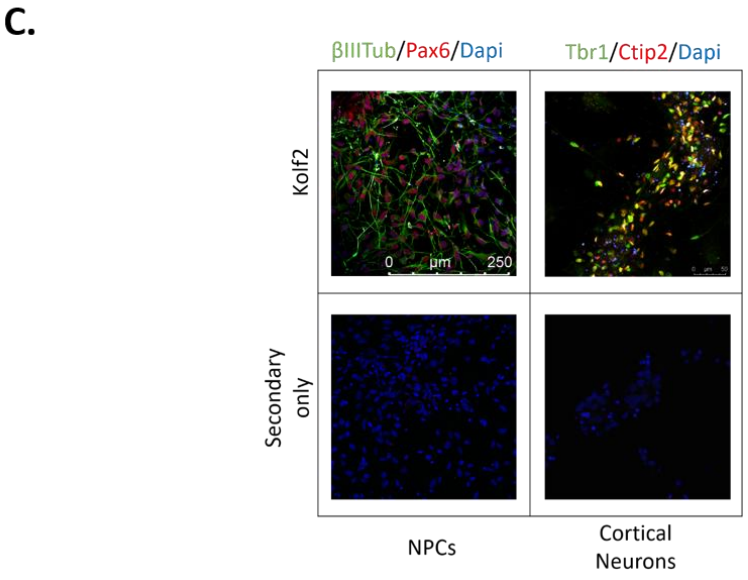
C.
βIIITub/Pax6/Dapi
Tbr1/Ctip2/Dapi
Kolf2
Secondary only
NPCs
Cortical Neurons

Figure 4.8 – Directed differentiation of human iPSCs Kolf2 to Cortical Neurons. A) Schematic representation of the protocol: Kolf2 iPSCs were differentiated to NPCs and to cortical neurons. **B)** Samples collected at day 16 (NPC, blue bars) and day 40 (cortical neurons, red bars) were assessed with RT-PCR for different developmental and terminally differentiated markers. N = 3 biologically independent differentiations. All data are mean ± S.D.; One-way ANOVA, Dunnett's test for multiple comparison. p*<0,05, **p<0,005, ****p<0,0001 - relative to iPSCs. **C)** Immunostaining of NPC at Day16 revealed positive expression of the developmental marker Pax6 and the neuronal specific marker BIII Tubuline. Immunostaining of cortical neurons at Day 40 revealed positive expression of the layer I marker TBR1 and callosal projection neurons marker Ctip2. Nuclei were stained with Dapi (Blue).

4.3.5 Astrocyte Differentiation Protocol

We decided to use the control cell line BIONi010-C-2 to generate astrocytes and produce in house astrocyte-conditioned medium. BIONi010-C-2 is part of an isogenic set of cell lines for the APOE genotype: E3/E3 (BIONi010-C-2), E4/E4 (BIONi010-C-4) and E2/E2 (BIONi010-C-6). Using the BIONi010-C-2 allowed us to set a neutral background with respect to AD which is relevant here.

NPCs were differentiated from iPSCs as described previously for the cortical neuronal protocol. At day 16, astrocytes were terminally differentiated using a protocol adapted from Serio et al., 2013(Serio et al., 2013).

Figure 4.9A displays a schematic representation of the iPSC-derived astrocyte protocol. iPSCs were differentiated to NPCs using the previously described protocol by Shi et al., followed by induction with co-application of EGF (epidermal growth factor) and LIF (leukemia inhibitory factor), which induces astrocyte differentiation of NPCs by activation of STAT3(Ito et al., 2016). At this point, the cells, which will be mainly astrocyte precursors, could present a minor contamination of neuronal cells. To enrich the astrocyte population, we sorted them for positive expression of CD44, selecting the 10% brightest cells (Figure 4.9B)(Cai et al., 2012). CD44 is a widely expressed transmembrane glycoprotein, which is involved in cell-cell and cell-matrix interactions. It has been shown that CD44+ cells are already present in the early stages of developing the mouse cerebellum and, when cultured without any factors, they expressed GFAP, a

marker of mature astrocyte. This suggests that the default program for these cells is the differentiation into astrocytes(Cai et al., 2012). The APC identity of $CD44^+$ cells was confirmed with both quantitative RT-PCR and with qualitative ICC. Expression of Nuclear factor I-A (NFIA), which is a transcription factor with a central role in astrocyte development, and Vimentin, an intermediate filament protein, were respectively 200-fold and 60000-fold higher than control iPSCs (Figure 4.9C, blue bars). Positive staining for the Vimentin marker is shown in Figure 4.10D, left panel.

CD44+ APCs were terminally differentiated to astrocytes with ciliary neurotrophic factor (CNTF) for 14 days into triple flasks. CNTF has been extensively shown to give rise to pure astrocyte populations, with minimal neuronal contamination(Johe et al., 1996).

RT-PCR showed positive expression of GFAP with a 80-fold increase when compared to control iPSCs and of S100β, a late marker of astrocyte development(Raponi et al., 2007) with a ~500-fold increase in comparison to control iPSCs (figure 4.9C, red bars). Moreover, ICC confirmed positive staining for GFAP and for CD49, a recently identified astrocytic marker(Barbar et al., 2020) (figure 9D, right panel).

RT-PCR confirmed decreased expression of pluripotency marker such as OCT4 and NANOG for both APC and astrocyte (figure 4.9C).

Mature astrocytes were kept in culture for up to three months and media was collected every 48h. Different collections were pooled together in order to produce batches of ~500ml and reduce batch variability. Each batch was filter-sterilized, aliquoted and frozen at -80°C for later use. Different batches were compared using a human CCL2 ELISA as suggested by Rushton et al., 2013(Rushton et al., 2013), and normalized to a constant final concentration of 1ng/ml.

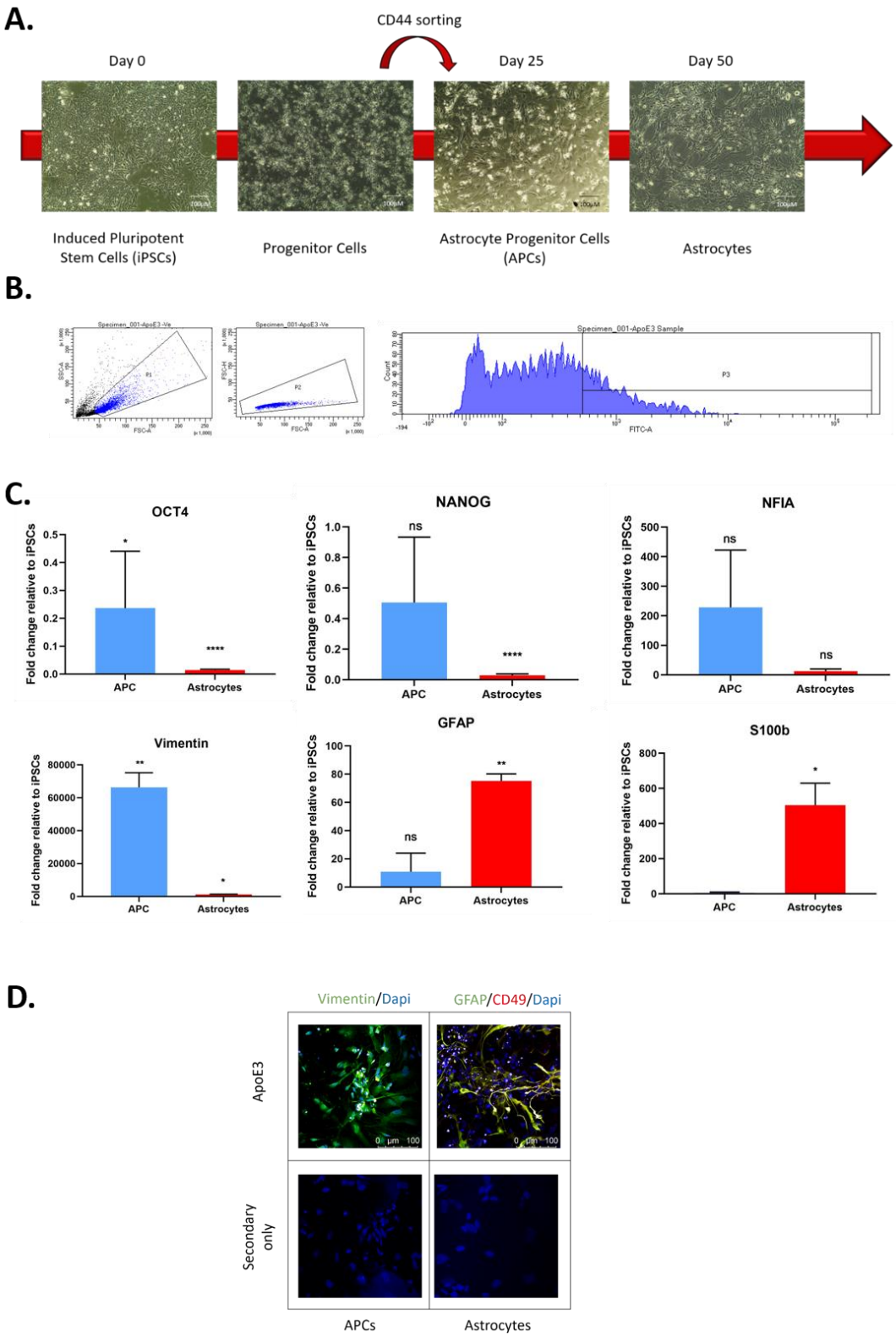

Figure 4.9 – Directed differentiation of human ApoE3/3 iPSCs to Astrocytes. A) Schematic representation of the protocol: ApoE 3/3 iPSCs were differentiated to APCs via CD44+ sorting and to astrocytes. **B)** Progenitor cells were stained with CD44 antibody and the 10% brightest cells were positively sorted for further differentiation**. C)** Samples collected at day 25 (APC, blue bars) and day

50 (astrocytes, red bars) were assessed with RT-PCR for different developmental and terminally differentiated markers. N = 3 biologically independent differentiations. All data are mean ± S.D; One-way ANOVA, Dunnett's test for multiple comparison. p*<0,05, **p<0,005, ****p<0,0001 – relative to iPSCs **D)** Immunostaining of APC at Day25 revealed positive expression of the developmental marker Vimentin Immunostaining of Astrocytes at Day 50 revealed positive expression of GFAP and nuclei were stained with Dapi (Blue). Bars =100µM

4.3.6 Establishment of iPSC-derived cortical neurons-microglia co-culture system

In order to establish a microglia-cortical neuron co-culture model, $mCherry^{+}$ macrophage precursors were cultured with unlabelled control cortical neurons and left to differentiate for 14 days (figure 4.10A). Over the first week, the precursors could be seen floating in the culture, not yet attached. Around day 7, precursor cells attached to the monolayer of neurons and began to exhibit a change in morphology, stretching out processes from their cell bodies. The three genotype were stained for IBA-1 marker with cortical neurons presenting positivity for MAP2 marker (figure 4.10B).

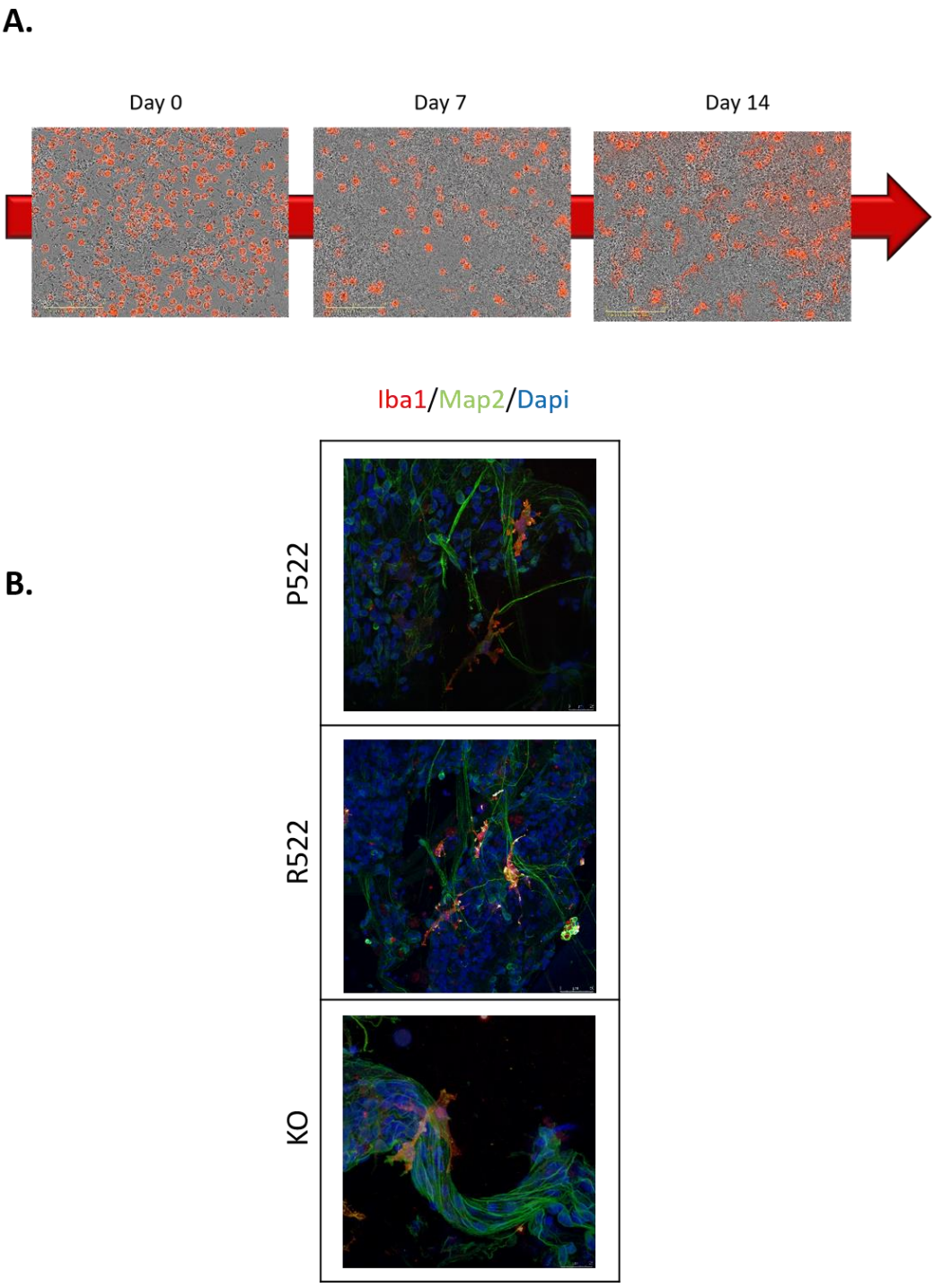

Figure 4.10 – Microglia-cortical neurons co-culture system. A) Schematic representation of seeding and differentiation of mcherry^{+} PLCG2 macrophage precursors on top of iPSC-derived cortical neurons. After 14 days of culture, precursors fully differentiate to ramified microglia-like cells. **B)** Unlabelled clones with the indicated PLCG2 genotypes were used in order to characterize both neurons and microglia in co-culture.

Ramification analysis was performed in order to compare microglia-like cells morphology in monoculture or co-culture (figure 4.11A). Ramifications are defined as multiple distally branched processes that protrude from small flat somata(Schilling et al., 2001). Different parameters were taken into consideration for the comparison (figure 4.11B, C) to establish if cells cultured in physical contact with neurons were more ramified. Specifically, area and perimeter were observed to be significantly higher in microglia co-cultured with neurons, as expected by the increase of the processes (figure 4.11B). For this analysis, PLCγ2^{P522} control cells only were used. Comparison between genotypes (in co-culture condition) will be presented in the following chapter.

Area: The area is calculated as the total number of pixels present inside a single object and is expressed in square micrometres after image calibration.

Perimeter: The perimeter is calculated based on the outside boundary of the object and is expressed in microns.

Three additional parameters were taken into consideration to analyse the complexity of the cells: circularity, roundness and solidity (figure 4.11C).

Circularity: This parameter varies from 0 to 1. A circularity value of 1 indicates a perfect circular object; the values approach 0 when the object is increasingly elongated. Co-cultured microglia-like cells were expected to be found in more physiological and homeostatic conditions, resulting in values further away from 1 when compared with monoculture microglia. As confirmed by the analysis of this parameter, circularity values were significantly decreased in co-culture microglia (figure 4.11C, left image).

Roundness: this parameter is defined by the ratio of the surface area of an object to the area of the circle whose diameter is equal to the maximum diameter of the object. Reduced roundness values suggest a more ramified morphology (figure 4.11C, middle image).

Solidity: this parameter is calculated by dividing the area of an object by its convex area. The convex area is defined as the area of the smallest polygon drawn around the object. The convex area increases as the object ramifications increases, and as a consequence giving smaller solidity values (figure 4.11C, right image).

A.

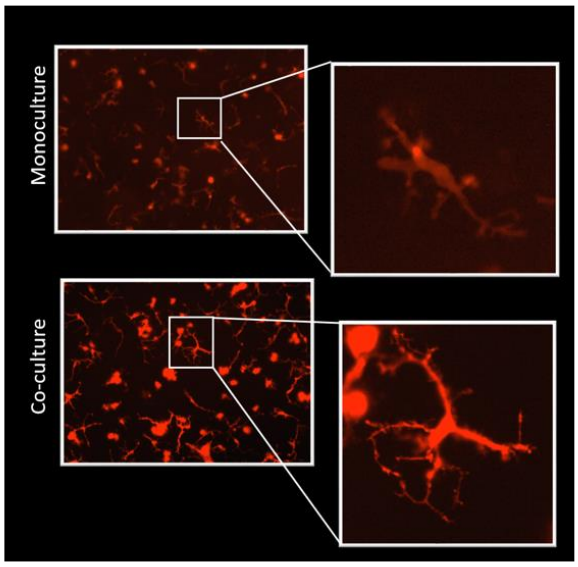

B.

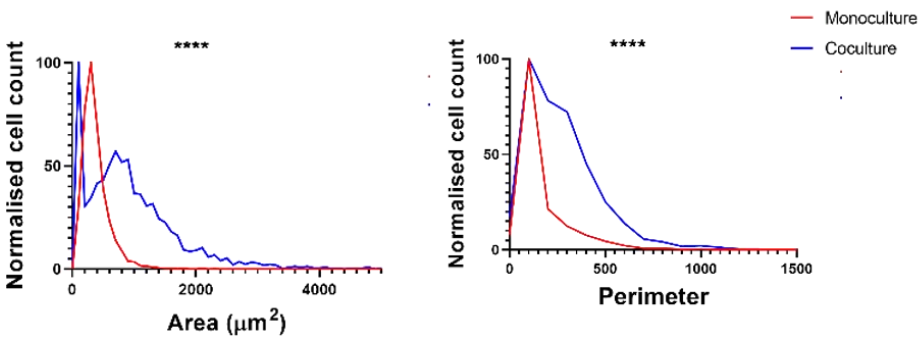

C.

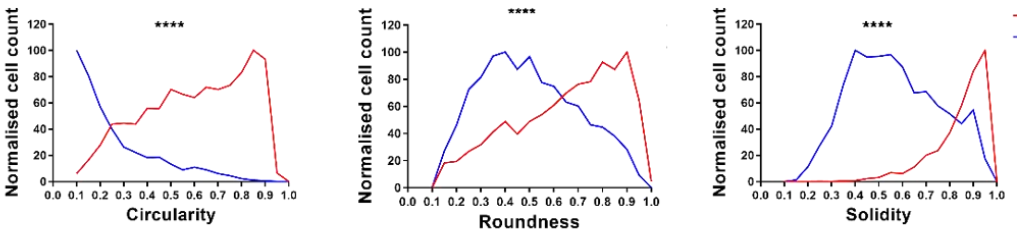

Figure 4.11 - A) Comparison of microglia-like cell morphology in monoculture and co-culture system. **B)** Comparison of Area and Perimeter between microglia-like cells in monoculture and co-culture systems. **C)** Comparison of Circularity, Roundness, Solidity between microglia-like cells in monoculture and co-culture systems. Images were analysed from three independent differentiations. N=3 independent experiments; 2 images per clone per experiment. Mann-Whitney test. ****p<0,0001.

4.4 Discussion

4.4.1 Microglia protocols

Generating microglia-like cells from iPSCs is a highly variable process that suffers from a wide range of efficiency, as demonstrated in published studies. Muffat and colleagues reported a number of macrophage precursors of 0.5- to 4- fold higher relative to input iPSCs(Muffat et al., 2016), similar to Pandaya and colleagues who observed 0.8- to 3-fold yield(Pandya et al., 2017); Haenseler et al. described instead a 10-fold yield(Haenseler et al., 2017). Finally, Abud and colleagues published a yield of precursors of 43-fold higher yield relative to input iPSCs(Abud et al., 2017). This variability could be explained by different reasons, such as the use of different differentiation protocols, genetic background of the cells, but also routine culturing and maintenance steps such as culture medium, passage number and growth rate of the starting iPSCs(Volpato and Webber, 2020). However, even the same protocol applied to the same hESC/iPSCs could show considerable variability, and this is mostly due to the fact that microglia-like cell differentiation, like many other types of iPSC differentiations, is a multistep procedure: the introduction of a small variation in any of the steps can lead to great differences in the final results(Volpato and Webber, 2020). This poses a clear problem of reproducibility and an effort to reach more standardized protocols across the wider scientific community is of paramount importance in order to generate comparable and reliable results.

In the EBs-based method, the EB formation stage is probably the most important step of the *in vitro* differentiation process, not only for microglia-like cells formation, but also for every possible type of cell(Brickman and Serup, 2017). The

quality of the EBs at its very first stages affects and determines the outcome for the rest of the differentiation(Zhou et al., 2008). For this reason, great attention should be given to the choice of the techniques, procedures and devices used in order to produce the EBs. There are many different methods described in the literature for forming these three- dimensional structures. The self-aggregation suspension technique was the first one tested in the lab. This method is successful in producing a large number of EBs, however it offers limited control regarding the size and shape of each EB, potentially affecting the diffusion of nutrients, growth factors and oxygen in the inner parts of the structure with consequences on the differentiation potential(Van Winkle et al., 2012).

The hanging drop method, which has previously been used to generate neuronal cells(He et al., 2006), hematopoietic cells(Dang et al., 2002), cardiomyocytes(Takahashi et al., 2003), renal cells(Kramer et al., 2006) and gametes(Geijsen et al., 2004) has the advantage of allowing for a better control of the number of cells in each EB when compared to the self-aggregation method(Kurosawa, 2007). However, in order to maintain the hanging drops on the lid by surface tension, the volume used to generate the drop has to be less than 50µl, limiting the amount of nutrients accessible for the EB. Another disadvantage of this method is that it is not possible to perform medium exchange while the EBs are in the hanging drop. For this reason, the EBs need to be moved into bulk suspension cultures after a couple of days of formation, where they tend to merge together and form big agglomerates. This might pose a problem for the diffusion of the growth factors in the further steps of the differentiation. Moreover, it is almost impossible to check the EB formation process using a direct bright field microscope, limiting the daily quality control check. Finally, the formation of the hanging drop is time consuming and labour-intensive, making this method not amenable to scalable cultures.

For these reasons, we decided to test a suspension culture using low-adherence plates. This type of technology has been widely used for various cells types, from

EBs of embryonal carcinoma(Martin and Evans, 1975) to neurospheres of neuronal stem cells(Suslov et al., 2002). Low-adherence plates offer a number of advantages when compared with the previous two methods. First, it allows the generation of a higher number of EBs more rapidly, facilitating the scaling up of the production. Moreover, the size and the shape of the EBs are controlled and standardized: this helps a more homogenous diffusion of the nutrients and a more consistent differentiation process. The design of the low-adherence round bottom well helps the concentration of a known number of stem cells at the centre of the well, promoting cell-cell contact and aggregation(Kurosawa, 2007). Finally, the medium can be changed when needed and the formation of the spheres can be monitored with a normal bright field microscope. The main disadvantage of the ultra-low adherence plate is that it is still not efficient enough for high throughput differentiations. This was not a problem for the aim of this study, but it should be considered not only for future applications but in the event of potential scale-up processes that attempt to reproduce these data. In order to solve this problem, a more recent technology for generating EBs has been developed: the AggreWell™ plates(Antonchuk, 2013). The principle is very similar to the ultra-low adherence plate: a suspension of single stem cells of known density is plated and centrifuged to facilitate the aggregation. The AggreWell technology has the ability to increase the throughput of the process, allowing the formation of approximately 1200 EBs of defined size simultaneously(Antonchuk, 2013). This is extremely important when working with a considerable number of clones in parallel, and when the output of cells needed is in the order of millions of precursors. Here, we did not need this magnitude of output material, so we decided to work with the ultra-low adherence plate, allowing us to keep the cost lower and avoid waste of material.

When working with multiple clones, an efficient scalable approach is needed. For this reason, we decided to test a monolayer-directed differentiation technique(Takata et al., 2017). The monolayer-based protocol closely reflects the hemangioblast formation which happens *in vivo,* as was described in detail previously. Briefly, the initial steps of primitive hematopoiesis are regulated by the

activation and following inhibition of the Wnt pathway(Tsakiridis et al., 2014, Sturgeon et al., 2014): for this reason, cells are cultured with the Wnt agonist CHIR99021 on day 0 and exposed to Dkk1, a Wnt Inhibitor, at day 6. This is of particular relevance, as the protocol published by Takata and colleagues(Takata et al., 2017) regulates more accurately the initial crucial steps of the differentiation process when compared with the EBs method previously described.

Despite the apparent advantages of this protocol, we encountered a major problem when differentiating the macrophage precursors into microglia-like cells. After a couple of days from plating macrophage precursors, a second, rapidly proliferating population appeared. At the end of the canonical 14 days differentiation used for microglia-like cells, the whole culture was overtaken by big, flat cells. This made it impossible to proceed with any type of functional experiments, considering that the culture was not pure for the cell of interest (microglia-like cells), but contaminated with a second unknown population, not relevant for our studies. In the attempt of cleaning the culture prior to macrophage precursors seeding, we sorted the cells for $CD14^{+}$ marker, however this approach did not help in eliminating the proliferating cells. We noticed that the overgrowing cell population stained positive for Iba1, the classical macrophage marker used to characterize the microglial culture. Like microglia cells, there are other cells that arises from the YS and stain positively for Iba1 marker, which are perivascular macrophages (PVMs)(Yang et al., 2019). These are brain-resident macrophages found in the perivascular space(Yang et al., 2019). Like all leukocytes, these cells express high levels of CD45, CD11b, CX3CR1 and Iba1(Yang et al., 2019). It is possible, however, to distinguish microglia-like cells from PVMs by using the purinergic receptor P2RY12, since PVMs are negative for this marker(Goldmann et al., 2016). Future studies could attempt sorting for P2RY12 in order to overcome this problem. In our case, the presence of these cells would have compromised the interpretation of any data generated from the cultures, as the purity of the cells was crucial to our objective. This is why the nature of these cell was not studied in further detail and we decided to perform all the functional studies on microglia-

like cells generated with the EB-based method, in which we did not have to deal with this issue.

4.4.2 Generation and characterization of *PLCG2* lines in mono- and co-culture

As shown by the data presented here, isogenic lines harbouring either the common *PLCγ2* variant, the novel protective R522 SNP or the deletion of the gene are still able to differentiate into microglia-like cells. All the clones were able to produce macrophage precursors expressing similar amounts of CD45, CD14 and CD11b (figure 4.7B). In the same way, all three genotypes were able to terminally differentiate to microglia-like cells showing comparable levels of key microglia markers, such as Iba1 (*AIF1*) and Tmem119, in monoculture conditions (figure 4.7C). This work expands on previous studies which used iPSC-derived microglia comparing the common variant to either the novel protective variant or the KO(Menzies G.E., 2020, Andreone et al., 2020). Our lab has previously shown equal ability of iPSCs harbouring either the common or the protective variant to differentiate to microglia-like cells, confirming the expression of microglia markers, such as Iba1 and Tmem119(Menzies G.E., 2020). Likewise, Andreone and colleagues showed similar differentiation potential between their iPSC-derived microglia model of *PLCγ2* WT and KO measuring the percentage of $PU.1^{+}$ cells(Andreone et al., 2020).

Although the study of microglia-like cell functionality is easier and more practical in monoculture conditions, it is of paramount importance to understand the interactions that occur in the CNS between the different cells. Since the normal function of the brain relies on these connections, overlooking them may lead to false conclusions or an incomplete interpretation of the pathological mechanisms of neurological diseases(Roqué and Costa, 2017). *In vitro* co-culture systems offer the possibility to tightly regulate the conditions and potentially manipulate each

cell type with the final goal of having a better understanding of their role and contribution(Roqué and Costa, 2017).

Over the years, different type of co-cultures have been established. Neuron-glia interactions have been studied by growing the two different populations in physical contact. This type of culture closely reflects the actual *in vivo* environment(Ullian et al., 2001, Christopherson et al., 2005). A valid alternative is represented by the sandwich co-culture system(Viviani, 2006) where the different populations are physically separated through membranes that however allow the diffusions of the secreted factors.

In the context of iPSC-derived models, the majority of the studies focused on microglia in monoculture, however a few complemented the results with co-cultures of microglia with neurons. Haenseler and colleagues established a microglia-cortical neurons co-culture and examined various parameters such as morphology, cytokine release, phagocytic activity and motility(Haenseler et al., 2017). They showed that co-culture microglia, upon activation, display a more anti-inflammatory type of response when compared to monoculture microglia, supporting the hypothesis that microglia acquire a less activated status when in contact with neurons(Eyo and Wu, 2013). Specifically, in the healthy brain, microglia are found in an “inactivated” state mainly by the interaction between CD200 glycoprotein, found on neuronal membranes and CD200R target receptor, present only on macrophages and microglia(Wang et al., 2007). In addition, in this particular system, microglia display the morphology and dynamic behaviour typical of these cells, sensing the surrounding neuronal environment, as shown also by Abud et al.(Abud et al., 2017), and Takata et al.(Takata et al., 2017). This is a specific consequence of the presence of neurons, as monoculture microglia did not show the same features(Haenseler et al., 2017). In the light of the above studies, we decided to culture microglia-like cells in physical contact with iPSC-derived cortical neurons in order to recreate a more relevant and physiological environment. In accordance with previous studies, microglia cells cultured

together with cortical neurons showed a more ramified morphology when compared with microglia in monoculture indicative of a higher resting state(Haenseler et al., 2017).

4.4.3 Astrocyte Conditioned Medium

In addition to neurons, we decided to study the indirect contribution of astrocytes as well, by culturing microglia both in mono- and co-culture with ACM. It is well established that *in vitro* microglia cells, when cultured with ACM, transition from an amoeboid to a more ramified morphology(Suzumura et al., 1990), and that the individual addition of astrocytic released factors, such as TGF-β, M-CSF or GM-CSF, to microglia cultures does not induce microglial branching when applied alone(Schilling et al., 2001). Moreover, recent findings showed that TGF-β produced by astrocytes is able to suppress the microglia-mediated inflammatory response, significantly decreasing the expression of TNF and IL-6 by microglia when co-cultured with astrocytes or cultured with ACM in comparison to microglia in monoculture(Zhang et al., 2020). The preparation of these media involves harvesting the secretome of live cells, which is highly variable. For this reason, we decided to establish measures that would allow us to control two essential parameters to help in ensuring the best possible quality and reproducibility of the ACM: the time span for conditioning and the percentage of conditioned medium to be added to the culture. Experience in our lab has shown that the optimal time span for conditioning the medium was 48 hours; longer time points resulted in cytotoxicity for macrophage precursors, which were not able to differentiate, and on the contrary resulted in dead cells after a few days. In order to control and keep the percentage of ACM used constant, we routinely ran ELISA to quantify CCL2 and diluted each batch to a final concentration of 1ng/ml(Rushton et al., 2013). CCL2 was previously found in our lab to be an astrocyte-secreted factor that is constitutively expressed in astrocyte culture at a good level (Dr Cope Thesis). Being a robust marker, we selected it to run the ELISAs.

Moreover, we tried to control for major batch-to-batch variability by culturing astrocytes in triple flasks, which gave us on average 150ml of medium per collection, and pooling together different collections in order to produce a consistent amount of medium per batch. We then aimed at using the same batch to complete the biological replicate of each experiment. In order to investigate further the differences between batches, and between ACM derived from genetically different astrocytes, we intended to interrogate different samples of ACM with mass spectrometry technology in collaboration with "Catapult – Medicine Discovery" Biotech. The main aim of the project was to analyse the secretome as a whole and identify potential new proteins to be used as markers to control for batch variability. Unfortunately, because of Covid-19 pandemic the collaboration could not be led forward. However, this would be an interesting and helpful step to consider in the future, in order to better understand the ACM composition and to improve future preparation of the medium.

4.5 Conclusions

This chapter set the ground for a novel approach on microglia-like cell differentiation.

Briefly, an EB-based protocol was used in order to produce macrophage precursors from iPSCs. These cells were then terminally differentiated using astrocyte-conditioned medium, produced in house from iPSC-derived astrocytes with a specific genetic background of interest. In this case, astrocytes homozygous for the APOE3 locus were chosen, in order to set a neutral background for the study of AD. To recreate a more relevant physiological environment for differentiating macrophage precursors, control iPSCs were terminally differentiated to cortical neurons, following a well-established protocol(Shi et al., 2012b). Macrophage precursors were then allowed to terminally differentiate on top of cortical neurons, in the presence of ACM. Ramification analysis confirmed the increased number and complexity of the microglia processes cultured in physical contact

with cortical neurons when compared with monoculture microglia. This suggests that the cells were in a more physiological and resting state.

5 PLCγ2^{R522} variant iPSC-microglia like cells display altered neuroinflammatory responses

5.1 Introduction

The great amount of evidence provided by recent GWAS regarding the strong genetic influence in AD has helped shape further understanding on the mechanisms of the pathology. In particular, genetic findings have, in some cases, pinpointed specific variants located in key genes involved in the neurodegenerative process. The novel protective rare coding variant R522 in the *PLCG2* gene is an example of these recent discoveries(Sims et al., 2017), which offer a new opportunity for novel approaches in drug design for AD. *PLCG2* encodes an enzyme whose function could be modulated via small molecules, and inhibitors already exist, albeit they are not monospecific. In order to identify new potential therapeutic approaches, however, it is important to understand how this protein plays a role in the disease process and how this specific variant is involved in the functionality of microglia, the primary cells expressing *PLCG2* gene in the brain.

According to previous studies, the expression of the protective variant in recombinant cell lines resulted in a slight hypermorphic effect on enzymatic function(Magno et al., 2019). This increased enzymatic activity was confirmed in mouse BMDM where the expression of the variant promoted survival, *E.coli* phagocytosis and cytokine release in response to LPS(Takalo et al., 2020). Moreover, enhanced enzyme functionality was observed in R522 human iPSCs-derived microglia-like cells, mouse microglia and macrophages demonstrated by increased Ca^{2+} release and reduced PIP_2 levels following activation. In these models the R522 variant exhibited decreased phagocytosis of fungal and bacterial particles, as opposed to previous findings in BMDMs(Takalo et al., 2020), and increased endocytosis of oAβ (Maguire et al., 2021).

Increasing interest is now focusing on deciphering the role of the R522 variant in the neuroinflammatory functions of microglia. Considering the primary role of neuroinflammation in the onset and progression of AD, understanding how to

target this enzyme in order to modulate its function in microglia would be of great benefit for the field.

Microglia express a heterogeneous group of receptors known as pattern recognition receptors (PRRs), which are crucial for triggering downstream signalling pathways that lead to the activation of the innate immune system(Venegas and Heneka, 2017). These receptors have the role of recognizing the two major damage signals which are PAMPs and DAMPs. Among the most studied PRR is the group of the TLRs, including TLR4, which is activated by LPS, a component of the outer membrane of gram-negative bacteria(Poltorak et al., 1998). TLR4 is a type I transmembrane protein, that upon LPS binding, initiates recruitment of a series of adaptor proteins and binding of lipids, among which is PIP_2(Płóciennikowska et al., 2016). This signalling cascade results in the translocation of NF-κB from the cytoplasm into the nucleus, upregulating the expression of pro-inflammatory cytokines, such as IL-6 and TNF, and chemokines such as MIP-1(Venegas and Heneka, 2017). It has been shown that the process of TLR4 activation upon LPS stimulation often requires the engagement of Syk tyrosine kinase and PLCγ2 which in turn initiates intracellular Ca^{2+} release(Chiang et al., 2012, Zanoni et al., 2011).

Misfolded, aggregated Aβ can also trigger an immune response both in its oligomer and fibril forms(Heneka et al., 2014) by binding several of these PRRs expressed in microglial cells. For example, Aβ can bind to the surface receptor CD36 leading to the formation of a TLR2-TLR6 heterodimer, which in turn activated the NF-κB pathway(Stewart et al., 2010). Moreover, Aβ aggregates activate the intracellular machinery that leads to the assembly of the NLRP3 inflammasome, which leads to an increase of IL1β in the brain(Halle et al., 2008). NLRP3 inflammasome is a multicomplex protein made of a sensor (NLRP3), an adaptor (ASC) and an effector (caspase 1)(Swanson et al., 2019). The activation of the inflammasome is, with a few exceptions(Downs et al., 2020), a two-step process: the priming step and the activation step. The priming step is essential for the upregulation of the expression

of inflammasome components, such as NLRP3 and pro-caspase 1 and substrates such as pro-IL-1β; the second step leads to complete oligomerization and full activation of the inflammasome resulting in cleavage of the pro-protein IL-1β into mature cytokine by the self-cleaved matured caspase-1(Swanson et al., 2019). Among the priming agents, LPS is one of the most used; the second hit is generated via several inducers such ATP and Nigericin, derived from S. hygroscopicus(2020;10:2869). In addition to this two-step model, usually known as "canonical pathway", the NLRP3 inflammasome can also be activated via a so called "non-canonical pathway". The non-canonical mechanism of activation involves caspases 4/5 in humans(Kayagaki et al., 2011) rather than caspase-1, and differs from the canonical pathway as it does not require a priming step for the activation of the inflammasome(Shi et al., 2014). This non-canonical pathway is activated by Gram-negative rather than Gram positive bacteria and by β-glucans, glucose polymers found in the cell walls of fungi such as zymosan(Kelley et al., 2019).

Another important aspect to be taken into consideration is the critical role played by NO in the development of AD. Evidence has shown a direct link between the overproduction of NO and neuronal cell loss and protein misfolding(Nunomura et al., 2001). In particular, animal models have demonstrated how activated microglia release NO at the pre-synapse level blocking the reuptake of glutamate. Excessive glutamate levels promotes neuronal cell death via inhibition of mitochondrial respiration(Rao et al., 2012, Bal-Price and Brown, 2001). NO is synthesized mainly by a class of enzymes called nitric oxide synthases (NOS), via conversion of L-arginine to NO and L-arginine to NO and L-citrulline(Knowles and Moncada, 1994). Three isoforms of the NOS enzyme exists in the CNS: neuronal NOS, localized mainly at synaptic spines, endothelial NOS, present in the vascular endothelial cells and inducible NOS (iNOS), induced in microglia and astrocytes following inflammatory stimuli(Yuste et al., 2015). The functional regulation of the latter takes place at the transcriptional level; in particular, NF-κB is the most important

transcription factor involved in the in the activation of the iNOS gene(Yuste et al., 2015, Davis et al., 2005).

Microglia are also equipped with another set of receptors heavily involved in their function which are the purinergic (P2) receptors(Färber and Kettenmann, 2006, Calovi et al., 2019). These receptors are classified into two categories: the ionotropic P2X ligand-gated cationic channels and the metabotropic P2Y G protein-coupled receptors(Kennedy and Burnstock, 1985). P2X receptors comprise seven isoforms, which are all primarily activated by ATP(Calovi et al., 2019). P2Y receptors are seven-membrane-spanning and comprise eight isoforms which can be activated by purines such as ATP and ADP, but also by the pyrimidines UTP and UDP(Calovi et al., 2019). These endogenous nucleotides have been described as key players in microglial activation(Davalos et al., 2005, Koizumi et al., 2007). Extracellular accumulations of these nucleotides, which are released for example from damaged or dead neuronal cells, activate purinergic receptors on the microglial surface and initiate intracellular signalling cascades(Ferrari et al., 1997). For example, ATP activates the P2X7 receptor and induces the secretion of inflammatory molecules(Bianco et al., 2005). This receptor has been found to promote neuronal death via microglia-derived IL-1β and the production of ROS, and in both AD murine and human models is consistently upregulated in microglial cells around the Aβ plaques(Lee et al., 2011, Sanz et al., 2009). Both ATP and ADP, moreover, can activate the P2Y2 receptor as well, which has been associated with microglia movement(Li et al., 2013). P2Y2 as well as P2X7 have been previously shown to signal through PLC enzyme(Meshki et al., 2006, Kopp et al., 2019). P2Y12R, another metabotropic receptor, is involved in the extension of the processes of microglial cells via the activation of both PI3K and PLC pathways(Irino et al., 2008), which allows interaction with the surrounding matrix through integrins(Ohsawa et al., 2010). Finally, P2Y13, another receptor in this family, has been suggested to play a role in the control of microglial morphology as its removal in a mouse model led to a decreased microglial ramification in comparison to their wild-type counterpart.

To address these different aspects of the neuro inflammatory response of microglia cells, and more specifically the role of R522 variant in this context, several functional assays have been performed.

5.2 Aim

This chapter aims to better understand the role of the newly discovered R522 protective variant in the *PLCG2* gene in microglia, in the context of AD. Specifically, the secretion of several cytokines such as IL-6, TNF, IL-10 upon LPS and Aβ stimuli were investigated, together with the possible role of the inflammasome. Moreover, the secretion of NO was evaluated. Taken into consideration the increased enzymatic activity previously observed, the release of Ca^{2+} upon ATP and ADP stimuli was examined. Finally, cell motility upon LPS activation was evaluated in a co-culture model.

5.3 Results

5.3.1 Cytokine Response to LPS

As previously mentioned, the PLCγ2 enzyme mediates inflammatory responses via TLRs. In order to assess if the R522 variant affects cytokine production in response to LPS stimulus, LEGENDPlex™ Multiplex Assay was used. Cytokine concentrations were measured from cell media taken from iPSCs-derived microglia either unstimulated (0h) or following exposure to LPS (100ng/ml, Figure 5.1) at 3h, 12h and 24h. Together with *PLCG2*^{P522} and *PLCG2*^{R522} expressing cells, three clones of *PLCG2*^{KO} were used to explore the effects of gene deletion (Figure 5.1). PLCγ2^{P522} microglia produce significantly more IL-6 following LPS exposure when compared to both PLCγ2^{R522} and PLCγ2^{KO} at 12h time point, and to PLCγ2^{KO} only at 24h time point (Figure 5.1A). PLCγ2^{R522} also produced less TNF at each time point compared to PLCγ2^{P522}, whereas PLCγ2^{KO} showed significant less production at 12h and 24h time points. (Figure 5.1B). IL-10 and G-CSF production was also reduced in PLCγ2^{R522} microglia, but not in PLCγ2^{KO} when compared to PLCγ2^{P522} control at 12h

(Figure 5.1 C & E). IL12p40, however, did not show any differences in secretion at any time points, among genotypes (Figure 5.1 D).

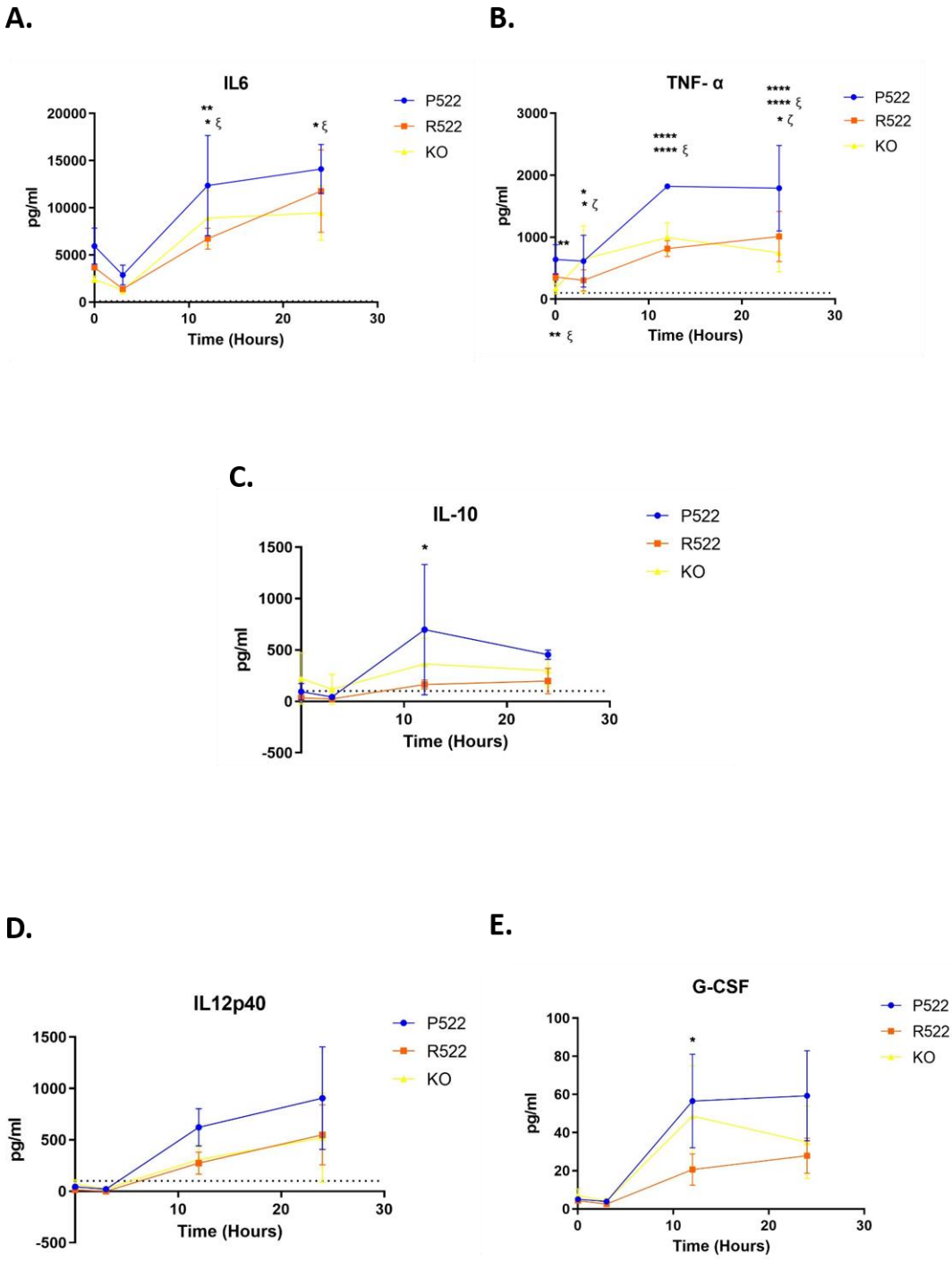

Figure 5.1 – LPS-induced secretion of inflammatory cytokines is impaired in PLCγ2^{R522} and PLCγ2^{KO} microglia-like cells. Secretion of **A.** IL-6, **B.** TNF, **C.** IL-10, **D.** IL12p40 and **E.** G-CSF in unstimulated cells (0h, control) and upon LPS stimulation (100ng/ml) at 3h, 12h, 24h. N = 3 biologically independent experiments (except for IL12p40 and GCSF N=2 biologically independent experiments). All data are mean ± S.D.; Two-way ANOVA, Holm-Šídák test for multiple comparison. p*<0,05, **p<0,005, ****p<0,0001. * = P522 vs R522, *ξ = P522 vs KO, *ζ = R522 vs KO

5.3.2 Cytokine Response to Aβ

The same LEGENDPlex™ Multiplex Assay was used to measure cytokine levels in response to oAβ 1-42 (5µM, Figure 5.2). As seen for the LPS response, PLCγ2^{P522} cells exhibited a general increase in production of IL-6 compared to PLCγ2^{R522} and PLCγ2^{KO}, which is significant at 24h in comparison to PLCγ2^{R522}. When measuring TNF, the response to oAβ 1-42 appeared to be considerably different from what seen after LPS stimulus. PLCγ2^{R522} exhibits increased cytokine release at 3h when compared to PLCγ2^{P522} and PLCγ2^{KO}. At 12h PLCγ2^{R522} shows a significant increase in TNF in comparison to PLCγ2^{KO} (Figure 5.2B). IL10 production was considerably higher at 12h within PLCγ2^{R522} in comparison to PLCγ2^{KO}, but no other significant differences were found between genotypes at any other time point. G-CSF production was decreased within PLCγ2^{R522} microglia (12h) and within PLCγ2^{KO} (3, 12h, Fig 5.2D) in comparison to PLCγ2^{P522}.

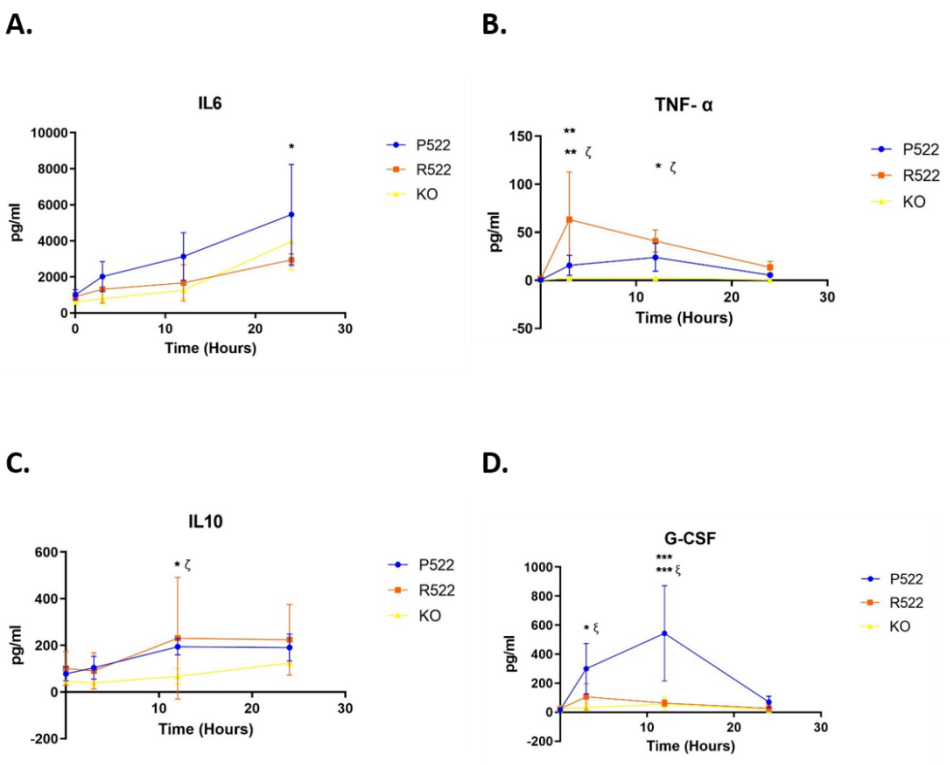

Figure 5.2 – Aβ-induced secretion of inflammatory cytokines in PLCγ2^{P522}, PLCγ2^{R522} and PLCγ2^{KO} microglia-like cells. Secretion of **A.** IL-6, **B.** TNF, **C.** IL-10, **D.** G-CSF in unstimulated cells (0h, control) and upon Aβ stimulation (5µM) at 3h, 12h, 24h. N = 3 biologically independent experiments (except

for GCSF N=2 biologically independent experiments). All data are mean ± S.D.; Two-way ANOVA, Holm-Šídák test for multiple comparison. p*<0,05, **p<0,005, ***p<0,0005. * = P522 vs R522, *ξ = P522 vs KO, *ζ = R522 vs KO

5.3.3 Inflammasome

PLCγ2 enzyme mutations have been shown to be involved in the activation of the NLRP3 inflammasome in the context of dominantly inherited autoinflammatory disease, autoinflammation and APLAID(Chae et al., 2015). To investigate if the newly recognised *PLCG2*^{R522} variant is involved in NLRP3 inflammasome activation in microglia, different stimuli were applied. In particular, zymosan is a known stimulator of the non-canonical pathway, whereas LPS and Nigericin are typical priming and activating triggers, respectively, of the canonical pathway.

5.3.3.1 Zymosan

Microglia-like cells were stimulated with 50µg/ml of Zymosan A (from *Saccharomyces cerevisiae,* Sigma) for 12h (Figure 5.3A). IL1β production showed no differences between the *PLCG2*^{P522} common SNP and *PLCG2*^{R522}. The *PLCG2*^{KO}, however, showed significant decreased production in comparison to both *PLCG2*^{P522} and *PLCG2*^{R522} variants.

5.3.3.2 LPS and Nigericin

When microglia cells were primed with LPS (3h, 100ng/ml), and activated with Nigericin (1h, 20µm), differences appeared in the response in comparison to the previous experiment (Figure 5.3B). The combination of LPS and Nigericin induced IL1β production in *PLCG2*^{P522} genotype considerably more than the novel *PLCG2*^{R522} variant and the *PLCG2*^{KO}. Moreover, no difference was detected between the production of IL1β between the protective variant and the *PLCG2*^{KO}.

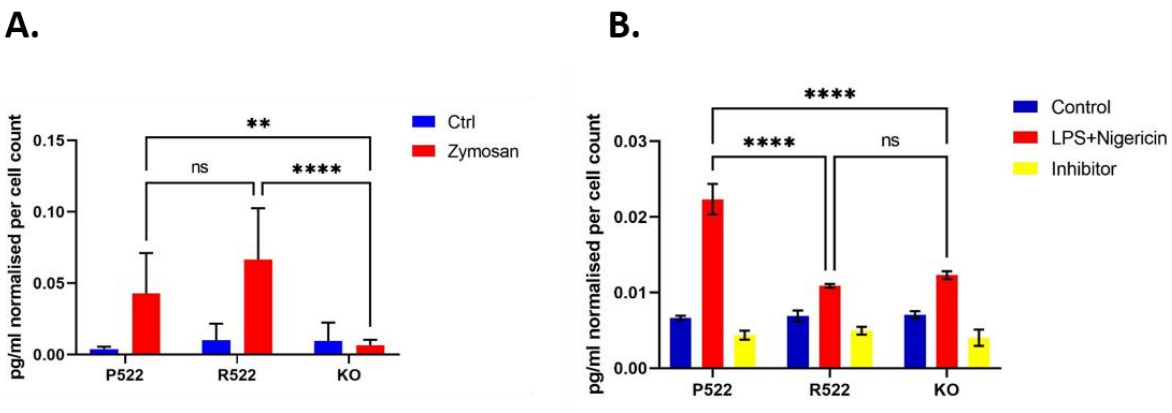

Figure 5.3 – PLCγ2^{P522}, PLCγ2^{R522} and PLCγ2^{KO} microglia-like cells display differential Inflammasome responses to different stimuli. A. NLRP3 inflammasome activation with Zymosan particles (50ug/ml, 24h) is suppressed in PLCγ2^{KO} microglia-like cells and comparable between PLCγ2^{P522} and PLCγ2^{R522}. **B.** NLRP3 inflammasome activation with LPS (100ng/ml, 3h) + Nigericin (20uM, 1h) ± Caspase 1 Inhibitor (50uM, 1h) is suppressed in both PLCγ2^{R522} and PLCγ2^{KO} microglia-like cells in comparison with PLCγ2^{P522}. N = 3 biologically independent experiment, including 3 clones per genotype in each biological experiments. Values are normalized per cell number. All data are mean ± S.D.; Two-way ANOVA, Holm-Šídák test for multiple comparison. **p<0,005, ****p<0,0001

5.3.4 Nitric Oxide

Considering the role played by NO in the development of neuroinflammatory environment in the brain, levels of this free radical were evaluated in the culture medium upon stimulation with LPS (100ng/ml) and IFN-γ (20ng/ml). Cells harbouring *PLCG2*^{P522} variant secreted significantly more NO than both *PLCG2*^{R522} and *PLCG2*^{KO} cells (Figure 5.4).

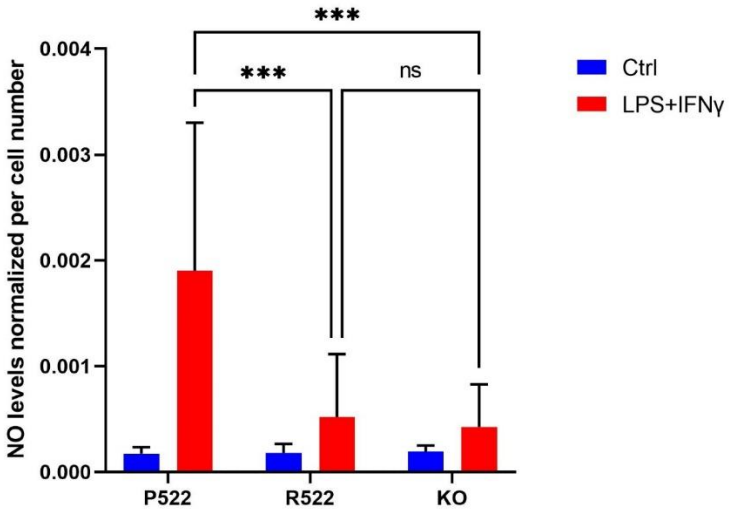

Figure 5.4 – PLCγ2^{P522}, PLCγ2^{R522} and PLCγ2^{KO} microglia-like cells display differentia NO release in response to LPS + IFN-γ. NO levels in conditioned media of PLCγ2^{P522}, PLCγ2^{R522} and PLCγ2^{KO} microglia-like cells upon 3h LPS, 100ng/ml and IFN-γ, 20ng/ml-treatment. N = 3 biologically independent experiments, including 3 clones per genotype at each biological experiment. Values are normalized per cell number. Data are mean ± S.D.; Two-way ANOVA, Holm-Šídák test for multiple comparison. p*<0,05 , **p<0,005

5.3.5 Calcium (ATP and ADP Stimulation)

Microglia can quickly react to damage signals such as ATP and ADP which are released by dying neurons by migrating to the site of damage both in the aging brain and during the neurodegenerative process(Nimmerjahn et al., 2005). *PLCG2*^{R522} variant microglia and macrophages have already been shown to be able to induce increase Ca^{2+} release from the ER when compared to *PLCG2*^{P522} common variant(Maguire et al., 2021).

When stimulated with either ATP (Figure 5.5A) or ADP (Figure 5.5B), PLCγ2^{R522} resulted in a greater cytosolic Ca^{2+} release compared to PLCγ2^{P522} control cells and to PLCγ2^{KO}. No differences were detected between PLCγ2^{P522} control cells and PLCγ2^{KO}. In order to confirm the observed Ca^{2+} increase was PLCG2-dependent, two different enzyme inhibitors were used: edelfosine (10µM) and U71322 (5µM).

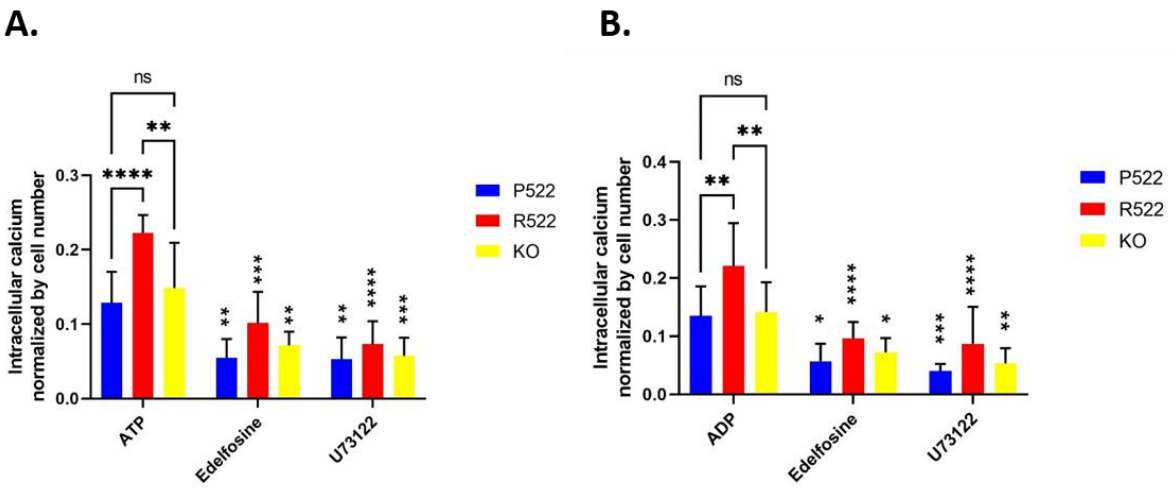

Figure 5.5 – Response of PLCγ2 to ADP and ATP. Microglia-like cells were loaded with Fluo-8 Ca^{2+} indicator and examined for peak changes in fluoresce after exposure to **A.** ATP (5µM) and **B.** ADP (5µM) with or without pre-exposure for 2 h with edelfosine (10µM) or U71322 (5µM). N = 3 biologically independent experiments, including 3 clones per genotype at each biological experiment. Values are normalized per cell number. All data are mean ± S.D.; Two-way ANOVA, Holm-Šídák test for multiple comparison. p*<0,05, **p<0,005, ***p<0,0005 ****p<0,0001. Inhibitor statistic referred to same genotype upon stimulation.

5.3.6 Morphology in co-culture

The ability of microglia to constantly scan the surrounding environment through their ramifications, is due to the highly dynamic nature of actin cytoskeleton. PIP_2 levels have been shown to be critical for actin dynamics and actin filament formation, an important step in both phagocytosis and cell migration(Botelho et al., 2000, Scott et al., 2005). Maguire and colleagues have recently demonstrated a reduction in the phagocytic ability of microglia-like cells harbouring *PLCG2*^{R522} variant, probably due to the unbalanced functionality of the enzyme and consequent reduced levels of PIP_2 at the plasma membrane(Maguire et al., 2021).

Having established a co-culture system of iPSCs-derived microglia like cells and cortical neurons, where microglia adopt a more ramified appearance than in monoculture (Chapter 2, Figure 4.11), this model was used to analyse the morphology of cells harbouring the different genotypes and their migratory ability upon LPS stimulation.

Sholl analyses of the three genotypes performed at day 14 of differentiation, at resting state, did not reveal any differences as demonstrated by comparable Sholl intersections (Figure 5.6 A-B). Moreover, similar values of total number of branching points and terminal points were observed (Figure 5.6 C-D), as well as branch level and depth (Figure 5.6 E-F).

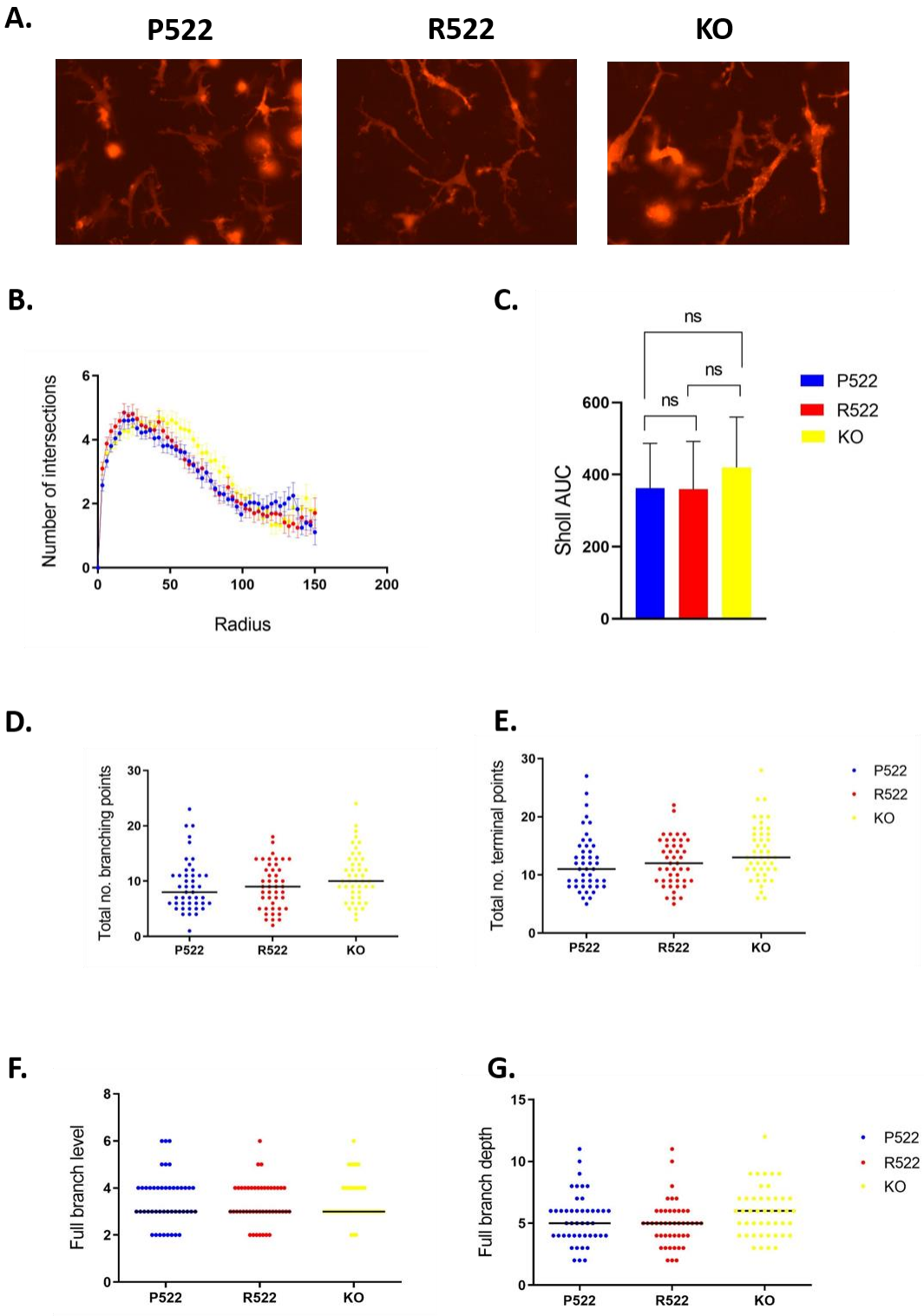

Figure 5.6 – *PLCG2*^{R522} variant and *PLCG2*^{KO} do not affect microglia ramification in a co-culture system model. A. Representative images of microglia-like cells in co-culture harbouring either P522, R522 variant or KO. Evaluation of **B.** Sholl profile and **C.**. resultant Area Under the Curve for

PLCγ2^{P522}, PLCγ2^{R522} and PLCγ2^{KO}; Evaluation of **D.** total number branching points, **E.** total number of terminal points, **F.** full branch level and **G.** full branch depth. Cells were manually traced using Imaris software. N=45 cells per genotypes. All data are mean ± S.D.; Two-way ANOVA, Holm-Šídák test for multiple comparison.

5.3.7 Movement in co-culture

In homeostatic conditions, microglia cells appear to have a generally fixed soma, but highly motile processes that continuously scan the surrounding environment(Nimmerjahn et al., 2005). Cell body migration is observed in response to several stimuli such as purinergic agonists(Honda et al., 2001), complement proteins(Yao et al., 1990), Aβ(Tiffany et al., 2001) and various chemokines(Rappert et al., 2002, Carbonell et al., 2005). Studies have shown increased migratory ability of microglia, following stimulation with LPS(Do et al., 2020, Zhao et al., 2021). In light of the differential response in cytokine secretion of the *PLCG2*^{R522} and *PLCG2*^{KO} genotypes in comparison to the *PLCG2*^{P522} upon LPS stimulation, migration of microglia cells to the same concentration of bacterial membrane component was evaluated. After 24h of LPS exposure, all three genotypes revealed a significant increase in accumulated distance, euclidean distance and velocity (Figure 5.7). However, no significant differences were observed between genotypes.

Accumulated distance is the actual path the cell travels during the set time. Euclidean distance is instead the length of the straight line between the starting and ending points (Figure 5.7B). The velocity is calculated as µm/h.

A.

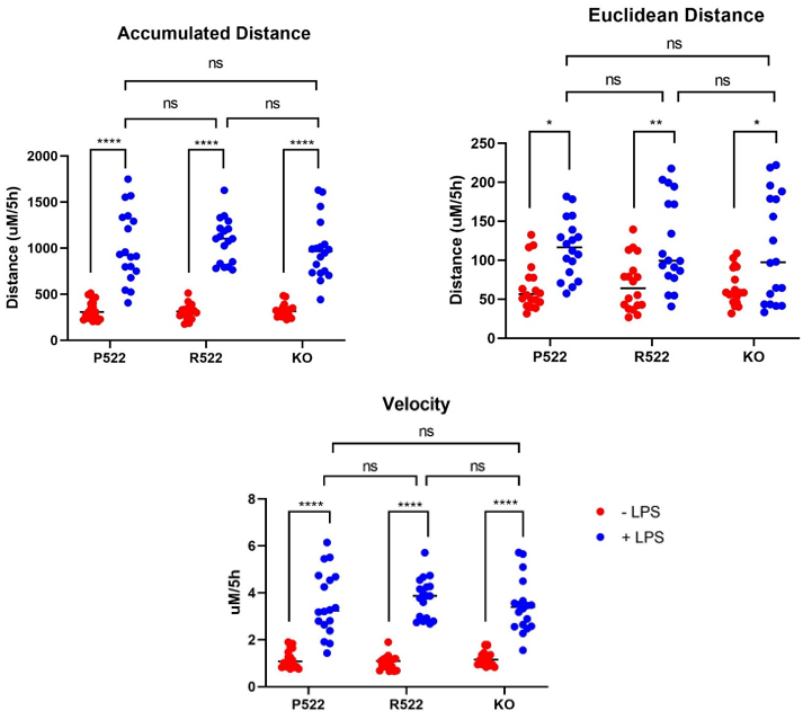
Accumulated Distance
Distance (uM/5h)
ns
ns
ns
****
****
****
P522
R522
KO
Euclidean Distance
Distance (uM/5h)
*
**
*
Velocity
uM/5h
- LPS
+ LPS

B.

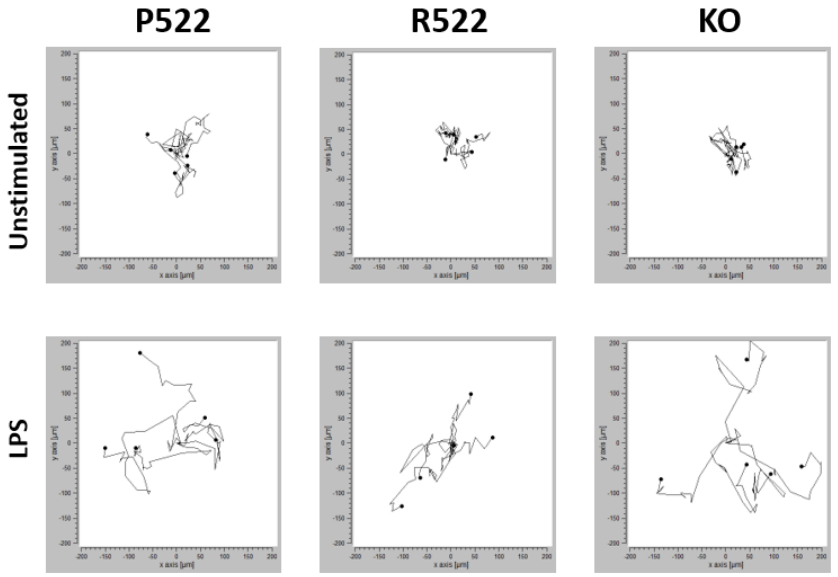
P522
R522
KO
Unstimulated
LPS

C.

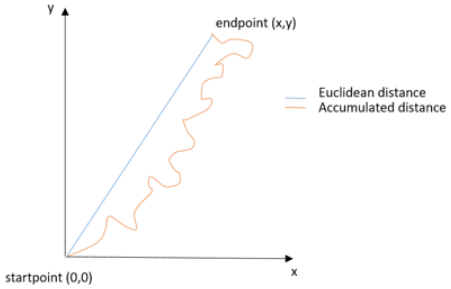
y
endpoint (x,y)
Euclidean distance
Accumulated distance
x
startpoint (0,0)

Figure 5.7 – LPS-stimulated co-culture iPSCs-derived microglia and cortical neurons do not reveal any differences between PLCγ2^{P522}, PLCγ2^{R522} and PLCγ2^{KO}. iPSCs-derived microglia-like cells expressing mcherry gene were imaged every 15 minutes for 5 hours. **A.** Parameters measured were Accumulated distance, Euclidean distance and Velocity. **B.** Representative tracks of co-culture microglia comparing unstimulated and LPS-stimulated PLCγ2^{P522}, PLCγ2^{R522} and PLCγ2^{KO}. **C.** Schematic representation of Accumulated and Euclidean distances. N = 3 biologically independent experiment, including 3 videos per genotype were analysed for each biological experiment. All data are mean ± S.D.; Two-way ANOVA, Holm-Šídák test for multiple comparison. p*<0,05, **p<0,005, ****p<0,0001

5.4 Discussion

The advent of iPSCs and microglia differentiation protocols offers a great tool to interrogate the functional consequences of AD-risk genes described in recent GWAS and will hopefully provide new opportunities for drug development. The recent discovery of a protective rare coding variant R522 in *PLCG2* gene(Sims et al., 2017) and initial functional studies in cell models are furthering our understanding of mechanisms underlying the disease. To address the potential role of the protective *PLCG2* SNP in microglial function, specifically in the context of neuro inflammation, human iPSC-derived microglia like cells were used both in monoculture and co-culture systems. Several inflammatory outputs were considered, such as cytokine and NO production, inflammasome activation and Ca^{2+} release in response to ATP and ADP; moreover, morphological and migratory changes were considered.

Several cytokines have been associated with the progression of cognitive decline and dementia(Swardfager et al., 2010). In particular, post-mortem studies on AD brain have highlighted how many cytokines, such as IL-1β, IL-6 and TGF-β accumulate around the amyloid plaques(Hüll et al., 1996, van der Wal et al., 1993). Furthermore, levels of both pro-inflammatory and anti-inflammatory cytokines are generally elevated in the cerebral spinal fluid (CSF) of subjects with either MCI or AD(Brosseron et al., 2014). Brain and plasma of AD patients revealed elevated level of TNF(Wang et al., 2015a). Moreover, a recent study demonstrated that mice

deficient in IL-12/23 p40 subunit had significantly decreased cognitive impairment and synaptic and neuronal loss was reduced together with cerebral Aβ levels(Tan et al., 2014). Contrasting evidence exists on the role of IL-10. Despite being notoriously anti-inflammatory(Lobo-Silva et al., 2016), AD patients showed increased levels of this cytokine(Guillot-Sestier et al., 2015) and animal models over expressing it revealed decreased phagocytosis of soluble Aβ by microglia together with increased Aβ deposits(Guillot-Sestier et al., 2015, Chakrabarty et al., 2015).

PLCγ2 mediates inflammatory responses through Toll-like receptors and PKC signalling pathway and leads to the production of various cytokines(Andreone et al., 2020, Xu et al., 2009). This enzyme plays a crucial role in TLR2 and TLR4-mediated Ca2+ flux and it has been shown to be necessary to produce cytokines such as IL-6 and TNF in a bone marrow macrophage model(Aki et al., 2008).

To investigate an acute response to an inflammatory stimulus, microglia-like cells were treated with 100ng/ml of LPS. Microglia cells carrying the protective *PLCG2*^{R522} variant, as well the KO cells consistently produced lower level of the cytokines analysed (Figure 5.1). Based on our observations, we speculate that the *PLCG2*^{R522} variant may in part protect against AD development by reducing levels of pro-inflammatory cytokines in the brain following activation. Our findings contrast with previously published data where BMDMs from mice carrying the PLCγ2^{R522} mutation, stimulated with LPS and IFN-γ for 3h released significantly higher levels of TNF and IL6 when compared to the common variant(Takalo et al., 2020). The discrepancy could be due to the distinct way of activation, in particular the higher LPS concentration (1ug/ml in contrast with 100ng/ml) and the addition of IFN-γ. Moreover, in our model, the PLCγ2^{KO} behaved similarly to the PLCγ2^{R522} variant, producing less cytokine than the common PLCγ2^{P522}, although statistical significance was found only for TNF and IL6 at 12h and 24h. Conversely, a recent study showed no differences in either IL6 nor TNF secretion upon LPS stimulation at 24h between *PLCG2*^{P522} SNPs and *PLCG2*^{KO} (Obst et al., 2021). This could be

explained by the fact that different cells models were used: iPSC-derived microglia as opposed to iPSC-derived macrophages.

The production of cytokines by microglia is an effective mechanism of first line of defence. This activation, although essential for carrying out scavenger functions, may cause some side effects to neighbouring cells. It is possible that, despite the gain of enzymatic function demonstrated in previous studies, the protective variant affects distal signalling and results, in some cases, in diminished PLCγ2-dependent functions. Increases in levels of the second messenger DAG reversibly recruit PKC to the plasma membrane through the zing-finger (C1) domains (Griner and Kazanietz, 2007). PKC in turn activates and regulates NF-κB pathways(Moscat et al., 2003, Lin et al., 2000) that results in the transcriptional induction of pro-inflammatory cytokines and chemokines such as IL-6, TNF, GCSF, IL8, IL2, IFN-β (Liu et al., 2017, O'Neill and Kaltschmidt, 1997). It has been previously suggested that the increased enzymatic activity within the PLCγ2^{R522} leads to depletion of the PIP_2 substrate, resulting in impaired IP_3 and DAG production(Ombrello et al., 2012, Maguire et al., 2021). It is possible that excessive substrate used prevented chronic enzyme activation which in turn would prevent prolonged long term cytokine release. Moreover, Maguire and colleagues observed significantly increased level of DAG in PLCγ2^{R522} models compared to PLCγ2^{P522} (Maguire et al., 2021). It has been shown that elevated levels of DAG molecule may lead to an increment in the basal activation of the PKC-NF-κB pathway, which finally results in a negative feedback inhibition. Specifically, Yang and colleagues demonstrated a reduced NF-κB nuclear localization in a T cell model of DGKα and ζ double KO, two members of a family of enzyme that catalyses the conversion of DAG to phosphatidic acid (PA), phospholipid important for cell signalling(Yang et al., 2016). Similarly, T cells expressing a constitutive active form of IKKβ, the kinase required for the activation of NF-κB show impairment in the nuclear translocation of NF-κB(Krishna et al., 2012).

IL-10 is a powerful anti-inflammatory cytokine, which plays a crucial role in the mitigation of inflammatory responses in the course of CNS pathologies(Porro et al., 2020). It has been shown to dampen the production of proinflammatory cytokines such as TNF, IL-6 and IFN-γ from myeloid lineage cells following TLR stimulation(de Waal Malefyt et al., 1991). Surprisingly, upon LPS stimulation, level of IL-10 where considerably higher in the PLCγ2^{P522} microglia-like cells in comparison with the protective PLCγ2^{R522} variant (Figure 5.1C). It has been demonstrated that PI3K-Akt pathway is central to IL-10 production in LPS-induced cells (Pengal et al., 2006). PI3K catalyzes the phosphorylation of PIP_2 to produce PIP_3, which then activate a variety of downstream signalling proteins(Ernest James Phillips and Maguire, 2021). It is possible that, in the PLCγ2^{R522} model, the lower level of PIP_2, substrate of the PI3K results in dampening of the pathway and decreased transcription of IL10. Another *PLCG2* hypermorphic mutation (L848P), described in an APLAID patient showed reduced production of cytokines such as IFN-y, IL-10 and IL1β upon LPS stimulation in a whole-blood cytokine production assay(Neves et al., 2018).

The build-up of amyloid plaques is a well-known hallmark of AD, and the role of microglia cells harbouring the *PLCG2*^{R522} variant in clearing oAβ has been previously investigated(Maguire et al., 2021). Maguire et al., used fluorescent oAβ to stimulate mouse macrophages and microglia and human iPSC-derived microglia and in all cases, cells harbouring the *PLCG2*^{R522} variant showed an increased ability to endocytose soluble oAβ(Maguire et al., 2021). Whilst TLR4 is the major receptor for LPS, Aβ has been shown to signal through a variety of different receptors such as complement receptors, Fc receptors, various TLRs and nucleotide-binding domain leucine-rich repeat (LRR)- containing receptors(Doens and Fernández, 2014). To investigate the inflammatory response of the *PLCG2*^{R522} variant to a more disease-relevant stimuli when compared to LPS, cells were incubated with 5μM of oAβ (Figure 5.2). The behaviour of IL-6 and GCSF is largely similar to what previously seen in response to LPS stimulation (Figure 5.2 A and D), suggesting a comparable mechanism of signal transduction by the PLCγ2 enzyme with the

different substrates. IL-10 production however, did not show any differences between PLCγ2^{P522} and PLCγ2^{R522} following stimulation with oAβ (Figure 5.1C), although we observed a trend of increased production by the cells expressing the *PLCG2*^{R522} protective variant in comparison to the *PLCG2*^{P522} SNP. Significant differences were observed between PLCγ2^{P522} and PLCγ2^{KO} at 12h time point. These findings suggest that alterative pathways are activated for the release of this cytokine following stimulation with either oAβ or LPS. Furthermore, reduced production of inflammatory cytokines by the PLCγ2^{R522} microglia in response to amyloid could further help to explain the protective effects of this variant.

TNF expression in the hippocampus of APP transgenic mice during early stages of Aβ deposition leads to a strong activation of glial cells that results in attenuation of Aβ plaques(Chakrabarty et al., 2011). The rapid increased secretion of TNF by PLCγ2^{R522} microglia cells could represent an initial protective mechanism which is enhanced in comparison to cells harbouring the common variant or the *PLCG2*^{KO}. Although the chronic activation of the *PLCG2*^{R522} variant could lead to a depletion of the PIP_2 substrate and therefore reduced functionality, the initial increased enzymatic activity within the PLCγ2^{R522} could lead to a "burst" of higher cytokine release. This result fits with the observation that PLCγ2^{R522} microglia show enhanced endocytosis of oAβ(Maguire et al., 2021). Alternatively, it is possible that the depletion of PIP_2 during Aβ endocytosis is not as substantial as during phagocytosing of larger cargos, therefore resulting in enhanced endocytosis and increased TNF release.

As previously mentioned, PLCγ2 signals downstream other important signaling receptors too, such as TREM2 and CSF1R. Andreone and colleagues identified PLCγ2 as a key signalling node in microglia cells. Specifically, they observed the enzyme to be essential for TREM2-dependent lipid metabolism, as *PLCG2*^{KO}, as well as *TREM2*^{KO} microglia showed similar defects in lipid processing(Andreone et al., 2020). The transient transgene overexpression of PLCγ2^{R522} in the PLCγ2^{KO} cells, resulted in great reduction of cholesterol accumulation, rescuing the defects of the

KO model(Andreone et al., 2020). Interestingly, they observed a hyper inflammatory state in *TREM2*^{KO} microglia cells upon TLR-dependent PLCγ2 signalling, suggesting that abnormal lipid metabolism could contribute to pro inflammatory response(Andreone et al., 2020). It would be interesting to study the possible neuroinflammatory effect of the PLCγ2^{R522} variant in *TREM2*^{KO} iPSCs-derived microglia cells, to investigate if the protective SNP would help to ameliorate the inflammatory profile. The TREM2- PLCγ2 pathway has been shown to be important for microglia survival as well: both *TREM2*^{KO} and PLCγ2^{KO} models, in fact, showed survival defects(Andreone et al., 2020). Obst and colleagues, moreover, investigated the role of PLCγ2 in the survival of iPSCs-derived macrophages as well, and reported a reduced survival rate in PLCγ2^{KO} cells, both in the presence and, for a greater extent, absence of M-CSF(Obst et al., 2021). This was not observed in *TREM2*^{KO} iPSCs-derived macrophages(Hall-Roberts et al., 2020), and suggest PLCγ2 as signalling component in the CSF1R-mediated pro survival pathway.

PLCγ2 has been described as having a role in the activation of the NLRP3 inflammasome in peripheral immune cells(Chae et al., 2015). Specifically, a novel mutation identified in the regulatory domain (Ser707Tyr) has been shown to increase PLCγ2-dependent intracellular Ca^{2+} release from the ER and increased IL-1β secretion upon stimulation(Chae et al., 2015, Zhou et al., 2012a). In order to investigate the possible role of PLCγ2^{R522} variant in the activation of this complex, iPSCs-derived microglia were stimulated 24h with zymosan particles prior to measurement of IL1β (Figure 5.3). This stimulation did not lead to any differences in IL1β secretion between PLCγ2^{P522} and PLCγ2^{R522} variants. PLCγ2^{KO} microglia however secreted significantly less IL1β in comparison to both PLCγ2^{P522} and PLCγ2^{R522} variants, confirming previously published data(Andreone et al., 2020). The absence of IL1β secretion in PLCγ2^{KO} microglia moreover, confirm the important role played by PLCγ2 in the signalling pathway of Dectin-1, a zymosan receptor(Xu et al., 2009)

Significant reduction of IL1β production by the KO genotype in comparison to the WT was also observed upon stimulation with LPS and Nigericin. In this case, however, the PLCγ2^{R522} variant behaved differently from what we previously observed with the Zymosan stimulation and led to significantly less IL1β secretion in the supernatant.

The specific roles of PLC enzyme and of Ca^{2+} mobilization in the activation of NLRP3 inflammasome remain controversial. The first implication of intracellular Ca^{2+} in ATP- and Nigericin-induced NLRP3 activation dates back to 2003(Brough et al., 2003). Since then, many studies have shown that Ca^{2+} mobilization can trigger NLRP3 either via internal ER stores, or via entry through store operated- Ca^{2+} entry (SOCE) channels from the extracellular lumen(Murakami et al., 2012). In the former case, PLC is a crucial player: Muraka and colleagues, demonstrated that PLC inhibitor U73122 blocked ATP-induced Ca^{2+} flux and IL1β processing and release into culture supernatant(Murakami et al., 2012). Conversely, the activation of PLC triggers the spontaneous activation of IL1β in the absence of NLRP3 activators(Lee et al., 2012a). Despite a lot of evidence of the involvement of Ca^{2+} in the activation of NLRP3, recent studies showed that NLRP3 inflammasome activation is Ca^{2+} independent, and that engagement of mobilizing G protein receptor actually failed to active the inflammasome(Yabal et al., 2019, Katsnelson et al., 2015).

In light of the controversial role of Ca^{2+} in the activation of the inflammasome, and the existence of several pathways (specifically “canonical” and “non-canonical”), it is possible that PLCγ2 has differing roles depending on the particular stimulus. PLCγ2^{KO} led to a significant decrease in the production of IL1β following zymosan stimulation suggesting a role of the enzyme in the inflammasome non-canonical pathway; it is possible however that this role is not affected by the presence of the R522 variant, which would explain the result in Figure 5.3A. An alternative hypothesis could be represented by the differential triggering receptors used in the recognition of stimuli in the non-canonical pathway(Kelley et al., 2019). In the case of the canonical activation of the inflammasome with LPS and Nigericin,

PLCγ2^{KO} again results in a significant decrease in the production of IL1β. However, in this case, the presence of the protective R522 variant can also be seen to significantly reduce the production of this cytokine. This is in contrast with what was previously reported on peripheral immune cells(Chae et al., 2015), where increased Ca^{2+} release correlated with increase Il1β production. However, as previously discussed, R522 variant microglia produced significantly lower levels of certain cytokines in comparison to P522 upon LPS stimulus (Figure 5.1). This could be due to a negative feedback put in place because of excess of PLC product or, as mentioned, because PIP_2 substrate depletion prevents chronic enzyme activation. It is possible, that upon addition of nigericin (second hit), the pro IL1β available for caspase 1 cleavage is reduced in the R522 model, as a consequence of reduced NF-κB signalling involved in pro-IL1β transcription. Further studies should repeat this experiment using specific PLCγ2 inhibitors alongside the caspase 1 inhibitor, and different stimulation should be tested.

To further investigate the role of PLCγ2 in the immune response of microglia-like cells, NO species were quantified following LPS + IFN-γ stimulation. Rodent microglia increase the expression of iNOS and release significant levels of NO upon LPS stimulation(Merrill et al., 1993). Several transcription factors work together in order to activate the iNOS promoter; however, the most relevant is NF-κB(Saha and Pahan, 2006), which signals downstream of PLCG2. PLCγ2^{R522} and PLCγ2^{KO} microglia appear to release significantly lower NO in response to LPS when compared to PLCγ2^{P522} (Figure 5.4). This mimics the result in Figure 5.1, where PLCγ2^{R522} microglia also secrete lower levels of cytokines such as IL6 and TNF in response to LPS. This finding supports previous studies where analysis of culture medium of BMDMs cells carrying the PLCγ2^{R522} mutation revealed significantly lower level of NO(Takalo et al., 2020). Considering the neurotoxic effect of NO, it may be that within the AD patient brain the PLCγ2^{R522} mutant lowers AD risk in part via a reduction in this compound.

Extracellular nucleotides have been reported to have an important role in the regulation of microglia functionality(Tozaki-Saitoh et al., 2011). Molecules like ATP and ADP are released by dying neurons and microglia cells are able to sense and react to these damage signals(Reich et al., 2020). Moreover, several studies have reported PLC activation downstream of purinergic signalling(Meshki et al., 2006, Kopp et al., 2019, Irino et al., 2008). Previous studies have shown a hyper activation of the PLCγ2 enzyme harbouring the R522 variant in different cell models upon stimulation with anti-CD32 antibody(Maguire et al., 2021), leading to increased Ca^{2+} release. Activation with both ATP and ADP led to a significant increase in Ca^{2+} release from the R522 microglia like cells when compared to the common PLCγ2^{P522} variant, confirming previous results. No difference in the Ca^{2+} response upon either ATP or ADP stimulation between PLCγ2^{P522} and PLCγ2^{KO} was observed (Figure 5.5 A and B) as seen in previous work(Obst et al., 2021). Two different inhibitors, Edelfosine and U71322, were used in order to confirm that the Ca^{2+} response was PLCγ2-specific. Some purinergic receptors have been implicated in neuroinflammatory processes, as previously mentioned(Rodrigues et al., 2015). Therefore, reduced purinergic signalling in the protective PLCγ2^{R522} variant could help to explain the reduced risk within humans. In the light of the LPS- and Aβ-induced cytokine release result, it would be interesting to examine the inflammatory response of microglia-like cells harbouring the PLCγ2^{R522} variant in response to ATP and ADP.

Ca^{2+} signalling is known to regulate microglial migration(Siddiqui et al., 2012, Ferreira and Schlichter, 2013), and the PLCγ2 enzyme has been previously demonstrated to have roles in regulating the migration of peripheral cells towards sites of injuries(Mueller et al., 2010). For this reason, the role of the different *PLCG2* genotypes on microglia migration was examined. It has previously been shown that microglia-like cells co-cultured together with cortical neurons behaved differently if stimulated with LPS in comparison to unstimulated cells(Haenseler et al., 2017). In particular, authors have observed a propensity of LPS-treated cells to cluster together which was not seen in unstimulated cells. There is still an open

debate on the ability of LPS to promote or suppress migration(Lively and Schlichter, 2018, Carter and Dick, 2003, Do et al., 2020, Zhao et al., 2021, Scheiblich et al., 2014) as this could depend on the LPS concentration chosen and on mediators secreted by the activated microglia(Cunha et al., 2016). In our model, iPSC-microglia cells co-cultured with cortical neurons and stimulated with 100ng/ml of LPS showed an increase in both accumulated and euclidean distance in comparison to unstimulated cells (Figure 5.7). Surprisingly, despite the same LPS concentration showing a significant difference in the acute inflammatory response between genotypes, no differences were observed between PLCγ2^{P522}, PLCγ2^{R522} and PLCγ2^{KO} cells in their migratory ability (Figure 5.7). Obst and colleagues recently observed a significant reduction in the chemotactic ability of the PLCγ2^{KO} in an iPSCs-derived macrophage-like cell model using a transwell system both in absence of stimuli and in presence of either ATP or C5a(Obst et al., 2021). The experimental setup employed in this present study, did not provide a specific chemotactic cue that would trigger the cells to directional motility, which might explain the absence of differences among the genotypes. Alternatively, the reason might be the different cell type taken into consideration. It would be interesting to repeat the experiment using ATP or C5a as a chemotactic stimulus using a transwell insert in presence or absence of LPS stimulus, to see how findings compare to those of Obst et al,.

5.5 Conclusion

The PLCγ2^{R522} variant has been associated with decreased risk of late onset AD and it represents the first classically drug-targetable molecule identified in LOAD genetic studies. Here we have shown that a model of iPSC-derived microglia-like cells harbouring the *PLCG2*^{R522} SNP display an altered neuroinflammatory response upon various stimuli. In particular, PLCγ2^{R522} microglial cells, together with PLCγ2^{KO}, produced decreased levels of cytokines such as IL-6, TNF, GCSF, IL10, IL1β

(inflammasome) and NO upon LPS stimulations. Upon oAβ stimuli, the response of these cells is more heterogeneous, suggesting differential signalling pathways involved. Specifically, IL-6 and GCSF behaviour was similar to what was seen upon LPS stimulation, hence a decrease in level in comparison to the common PLCγ2^{P522} variant. TNF and IL10 levels were instead increased in comparison to PLCγ2^{P522} microglia. The stimulation of the inflammasome with zymosan particles did not show any differences between PLCγ2^{P522} and PLCγ2^{R522} cells raising questions regarding the possible differences in PLCγ2 involvement in the activation of the canonical (stimulated by LPS + Nigericin) and non-canonical (stimulated by Nigericin) pathways, or possibly the use of different receptors. The increased levels of Ca^{2+} response to ATP and ADP stimuli confirm the hypermorphic nature of the enzyme harbouring the PLCγ2^{R522} variant, and the involvement of this enzyme in the purinergic signalling pathways. All together, these results sustain the hypothesis of a protective role of PLCγ2^{R522} variant in the context of AD, via reducing the neuro inflammatory burden in response to several stimuli. Finally, no differences in morphology or migratory activity was observed between genotypes of microglia cultured in physical contact with cortical neurons, but in the future different stimuli should be applied to evaluate the chemotactic ability of microglia cells harbouring the PLCγ2^{R522} variant.

6 Concluding remarks

AD is a multifactorial disorder and it is now clear that it cannot be explained and addressed with a unique hypothesis. Several drugs have been tested and multiple clinical trials have been carried out targeting Aβ or tau, showing only little beneficial effects. Neuroinflammation is now accepted as a key hallmark of AD. Recent GWAS have highlighted several microglia-enriched genes as risk loci associated with the disease, suggesting that targeting these cells and their functions might have important therapeutic potential in the future. The development of the PRS calculation can capture the complexity of this disorder and allow the investigation of individuals identified at the extremes of the score, by creating iPSCs from, for example, blood samples. These reprogrammed iPSCs can be further differentiated to relevant AD-cells, such as microglia, to study and compare the functionalities of the two groups (high and low PRS) to better uncover the pathological pathway. It is evident that the quality of the starting material for this type of process is of paramount importance, and for this reason the use of freshly collected blood is suggested for future study. However, it is possible that cells collected several years ago, such as the PBMCs used in this present study, and stored for long time in biobanks could be a useful source of samples considering several interesting AD SNPs are rare variants. The most successful approach in rescuing the low viability of the cells consisted of a first phase of T cell expansion in order to increase cell number and viability, followed by a week where cells were cultured in a specific medium formulation that slowed down cell proliferation and attenuated activation state. iPSCs generated from PBMCs rescued via this protocol are of good quality for further differentiations and studies.

AD research is in need of developing novel drugs for treatment of neurodegeneration and it is of great importance to choose drug targets that are well validates, meaning that they show a strong biological association with the disease. Genetic findings are helping enormously on this matter. *PLCG2*^{R522} has been found in 2017 as a novel protective variant associated with AD(Sims et al., 2017) expressed, in the CNS, selectively by microglia cells. It encodes for an enzyme, making this SNP extremely interesting for the scientific community, being

the first drug-targetable protein identified in LOAD genetic studies. Common efforts are now trying to decipher with *in vitro* and *in vivo* approaches the biological meaning of this genetic evidence; understanding how this mutation helps protecting against the development of AD might improve confidence in the target and open up new avenues for future therapies. Previous studies showed how this mutation affect the enzyme by slightly increasing its phospholipase activity, and the project presented here uncovered an altered neuroinflammatory response upon several stimuli in comparison to the common *PLCG2*^{P522} variant. In particular, several stimuli lead to a decreased secretion of cytokines, inducing to formulate the hypothesis that this novel variant protect again AD by decreasing the neuroinflammatory burden of microglia activation.

7 Reference

2015. Convergent genetic and expression data implicate immunity in Alzheimer's disease. *Alzheimers Dement,* 11**,** 658-71.

2018. Assessment of established techniques to determine developmental and malignant potential of human pluripotent stem cells. *Nat Commun,* 9**,** 1925.

2020;10:2869, M. M.

., K. C. R. 2015. *Peripheral Blood Mononuclear Cells.*

AASEN, T., RAYA, A., BARRERO, M. J., GARRETA, E., CONSIGLIO, A., GONZALEZ, F., VASSENA, R., BILIĆ, J., PEKARIK, V., TISCORNIA, G., EDEL, M., BOUÉ, S. & IZPISÚA BELMONTE, J. C. 2008. Efficient and rapid generation of induced pluripotent stem cells from human keratinocytes. *Nat Biotechnol,* 26**,** 1276-84.

ABUD, E. M., RAMIREZ, R. N., MARTINEZ, E. S., HEALY, L. M., NGUYEN, C. H. H., NEWMAN, S. A., YEROMIN, A. V., SCARFONE, V. M., MARSH, S. E., FIMBRES, C., CARAWAY, C. A., FOTE, G. M., MADANY, A. M., AGRAWAL, A., KAYED, R., GYLYS, K. H., CAHALAN, M. D., CUMMINGS, B. J., ANTEL, J. P., MORTAZAVI, A., CARSON, M. J., POON, W. W. & BLURTON-JONES, M. 2017. iPSC-Derived Human Microglia-like Cells to Study Neurological Diseases. *Neuron,* 94**,** 278-293.e9.

AFSHINMANESH, E. 2016. Reprogramming human peripheral blood mononuclear cells to inducible pluripotent stem cells (hiPSC): An examination of the efficacy of different methods.

AGU, C. A., SOARES, F. A., ALDERTON, A., PATEL, M., ANSARI, R., PATEL, S., FORREST, S., YANG, F., LINEHAM, J., VALLIER, L. & KIRTON, C. M. 2015. Successful Generation of Human Induced Pluripotent Stem Cell Lines from Blood Samples Held at Room Temperature for up to 48 hr. *Stem Cell Reports,* 5**,** 660-71.

AKI, D., MINODA, Y., YOSHIDA, H., WATANABE, S., YOSHIDA, R., TAKAESU, G., CHINEN, T., INABA, T., HIKIDA, M., KUROSAKI, T., SAEKI, K. & YOSHIMURA, A. 2008. Peptidoglycan and lipopolysaccharide activate PLCgamma2, leading to enhanced cytokine production in macrophages and dendritic cells. *Genes Cells,* 13**,** 199-208.

AKIYAMA, H. & MCGEER, P. L. 1990. Brain microglia constitutively express beta-2 integrins. *J Neuroimmunol,* 30**,** 81-93.

AL ABBAR, A., NGAI, S. C., NOGRALES, N., ALHAJI, S. Y. & ABDULLAH, S. 2020. Induced Pluripotent Stem Cells: Reprogramming Platforms and Applications in Cell Replacement Therapy. *Biores Open Access,* 9**,** 121-136.

ALLIOT, F., GODIN, I. & PESSAC, B. 1999. Microglia derive from progenitors, originating from the yolk sac, and which proliferate in the brain. *Brain Res Dev Brain Res,* 117**,** 145-52.

ANDREONE, B. J., PRZYBYLA, L., LLAPASHTICA, C., RANA, A., DAVIS, S. S., VAN LENGERICH, B., LIN, K., SHI, J., MEI, Y., ASTARITA, G., DI PAOLO, G., SANDMANN, T., MONROE, K. M. & LEWCOCK, J. W. 2020. Alzheimer's-associated PLCγ2 is a signaling node required for both TREM2 function and the inflammatory response in human microglia. *Nat Neurosci,* 23**,** 927-938.

ANDY, P. T., CHUANPENG, D., CHRISTOPH, P., MIGUEL, M., PETER BOR-CHIAN, L., NICOLE, H., JOHN, S., STEPHANIE, J. B., ADRIAN, L. O., GREGORY, W. C., YUNLONG, L., GARY, E. L., BRUCE, T. L. & KWANGSIK, N. 2021. PLCG2 as a Risk Factor for Alzheimer's Disease. *Research Square*.

ANTONCHUK, J. 2013. Formation of Embryoid Bodies from Human Pluripotent Stem Cells Using AggreWell™ Plates. *In:* HELGASON, C. D. & MILLER, C. L. (eds.) *Basic Cell Culture Protocols.* Totowa, NJ: Humana Press.

ASKEW, K., LI, K., OLMOS-ALONSO, A., GARCIA-MORENO, F., LIANG, Y., RICHARDSON, P., TIPTON, T., CHAPMAN, M. A., RIECKEN, K., BECCARI, S., SIERRA, A., MOLNÁR, Z., CRAGG, M. S., GARASCHUK, O., PERRY, V. H. & GOMEZ-NICOLA, D. 2017. Coupled Proliferation and Apoptosis Maintain the Rapid Turnover of Microglia in the Adult Brain. *Cell Rep,* 18**,** 391-405.

ATAGI, Y., LIU, C. C., PAINTER, M. M., CHEN, X. F., VERBEECK, C., ZHENG, H., LI, X., RADEMAKERS, R., KANG, S. S., XU, H., YOUNKIN, S., DAS, P., FRYER, J. D. & BU, G. 2015. Apolipoprotein E Is a Ligand for Triggering Receptor Expressed on Myeloid Cells 2 (TREM2). *J Biol Chem,* 290**,** 26043-50.

AU, E. & FISHELL, G. 2008. Cortex shatters the glass ceiling. *Cell Stem Cell,* 3**,** 472-4.

BAE, Y. S., LEE, H. Y., JUNG, Y. S., LEE, M. & SUH, P. G. 2017. Phospholipase Cγ in Toll-like receptor-mediated inflammation and innate immunity. *Adv Biol Regul,* 63**,** 92-97.

BAKER, E. & ESCOTT-PRICE, V. 2020. Polygenic Risk Scores in Alzheimer's Disease: Current Applications and Future Directions. *Front Digit Health,* 2**,** 14.

BAL-PRICE, A. & BROWN, G. C. 2001. Inflammatory neurodegeneration mediated by nitric oxide from activated glia-inhibiting neuronal respiration, causing glutamate release and excitotoxicity. *J Neurosci,* 21**,** 6480-91.

BAMBERGER, M. E., HARRIS, M. E., MCDONALD, D. R., HUSEMANN, J. & LANDRETH, G. E. 2003. A cell surface receptor complex for fibrillar beta-amyloid mediates microglial activation. *J Neurosci,* 23**,** 2665-74.

BAN, H., NISHISHITA, N., FUSAKI, N., TABATA, T., SAEKI, K., SHIKAMURA, M., TAKADA, N., INOUE, M., HASEGAWA, M., KAWAMATA, S. & NISHIKAWA, S. 2011. Efficient generation of transgene-free human induced pluripotent stem cells (iPSCs) by temperature-sensitive Sendai virus vectors. *Proc Natl Acad Sci U S A,* 108**,** 14234-9.

BAO, M., HANABUCHI, S., FACCHINETTI, V., DU, Q., BOVER, L., PLUMAS, J., CHAPEROT, L., CAO, W., QIN, J., SUN, S. C. & LIU, Y. J. 2012. CD2AP/SHIP1 complex positively

regulates plasmacytoid dendritic cell receptor signaling by inhibiting the E3 ubiquitin ligase Cbl. *J Immunol,* 189**,** 786-92.

BARBAR, L., JAIN, T., ZIMMER, M., KRUGLIKOV, I., SADICK, J. S., WANG, M., KALPANA, K., ROSE, I. V. L., BURSTEIN, S. R., RUSIELEWICZ, T., NIJSURE, M., GUTTENPLAN, K. A., DI DOMENICO, A., CROFT, G., ZHANG, B., NOBUTA, H., HÉBERT, J. M., LIDDELOW, S. A. & FOSSATI, V. 2020. CD49f Is a Novel Marker of Functional and Reactive Human iPSC-Derived Astrocytes. *Neuron,* 107**,** 436-453.e12.

BELLENGUEZ, C., KÜÇÜKALI, F., JANSEN, I., ANDRADE, V., MORENAU-GRAU, S., AMIN, N., GRENIER-BOLEY, B., BOLAND, A., KLEINEIDAM, L., HOLMANS, P., GARCIA, P., MARTIN, R. C., NAJ, A., QIONG, Y., BIS, J. C., DAMOTTE, V., LEE, S. V. D., COSTA, M., CHAPUIS, J., GIEDRAITIS, V., BULLIDO, M. J., DE MUNÁIN, A. L., PÉREZ-TUR, J., SÁNCHEZ-JUAN, P., SÁNCHEZ-VALLE, R., ÁLVAREZ, V., PASTOR, P., MEDINA, M., VAN DONGEN, J., VAN BROECKHOVEN, C., VANDENBERGHE, R., ENGELBORGHS, S., NICOLAS, G., PASQUIER, F., HANON, O., DUFOUIL, C., BERR, C., DEBETTE, S., DARTIGUES, J.-F., SPALLETTA, G., NACMIAS, B., SOLFREZZI, V., BORRONI, B., TREMOLIZZO, L., SERIPA, D., CAFFARRA, P., DANIELE, A., GALIMBERTI, D., RAINERO, I., BENUSSI, L., SQUASSINA, A., MECOCI, P., PARNETTI, L., MASULLO, C., AROSIO, B., HARDY, J., MEAD, S., MORGAN, K., HOLMES, C., KEHOE, P., WOODS, B., EADB, CHARGE, ADGC, SHA, J., ZHAO, Y., LEE, C.-Y., KUKSA, P. P., HAMILTON-NELSON, K. L., KUNKLE, B. W., BUSH, W. S., MARTIN, E. R., WANG, L.-S., MAYEUX, R., FARRER, L. A., HAINES, J. L., PERICAK-VANCE, M. A., WANG, R., SATIZABAL, C., PSATY, B., LOPEZ, O., SANCHEZ-GARCIA, F., NORDESTGAARD, B. G., TYBJÆRG-HANSEN, A., THOMASSEN, J. Q., GRAFF, C., PAPENBERG, G., SOININEN, H., KIVIPELTO, M., HAAPASALO, A., NGANDU, T., KOIVISTO, A., KUULASMAA, T., PORCEL, L. M., KORNHUBER, J., PETERS, O., SCHNEIDER, A., SCARMEAS, N., DICHGANS, M., FROELICH, L., et al. 2020. Large meta-analysis of genome-wide association studies expands knowledge of the genetic etiology of Alzheimer's disease and highlights potential translational opportunities. *medRxiv***,** 2020.10.01.20200659.

BEN-DAVID, U. & BENVENISTY, N. 2011. The tumorigenicity of human embryonic and induced pluripotent stem cells. *Nat Rev Cancer,* 11**,** 268-77.

BENNETT, M. L., BENNETT, F. C., LIDDELOW, S. A., AJAMI, B., ZAMANIAN, J. L., FERNHOFF, N. B., MULINYAWE, S. B., BOHLEN, C. J., ADIL, A., TUCKER, A., WEISSMAN, I. L., CHANG, E. F., LI, G., GRANT, G. A., HAYDEN GEPHART, M. G. & BARRES, B. A. 2016. New tools for studying microglia in the mouse and human CNS. *Proc Natl Acad Sci U S A,* 113**,** E1738-46.

BETSOU, F., GAIGNAUX, A., AMMERLAAN, W., NORRIS, P. J. & STONE, M. 2019. Biospecimen Science of Blood for Peripheral Blood Mononuclear Cell (PBMC) Functional Applications. *Current Pathobiology Reports,* 7**,** 17-27.

BHATTARAI A FAU - DEVKOTA, S., DEVKOTA S FAU - DO, H. N., DO HN FAU - WANG, J., WANG J AUID- ORCID: ---212X FAU - BHATTARAI, S., BHATTARAI S FAU - WOLFE, M. S., WOLFE MS AUID- ORCID: --- FAU - MIAO, Y. & MIAO, Y. A.-O. Mechanism of Tripeptide Trimming of Amyloid β-Peptide 49 by γ-Secretase.

BIANCO, F., PRAVETTONI, E., COLOMBO, A., SCHENK, U., MÖLLER, T., MATTEOLI, M. & VERDERIO, C. 2005. Astrocyte-derived ATP induces vesicle shedding and IL-1 beta release from microglia. *J Immunol,* 174**,** 7268-77.

BILL, C. A. & VINES, C. M. 2020. Phospholipase C. *Adv Exp Med Biol,* 1131**,** 215-242.

BISHT, K., SHARMA, K. P., LECOURS, C., SÁNCHEZ, M. G., EL HAJJ, H., MILIOR, G., OLMOS-ALONSO, A., GÓMEZ-NICOLA, D., LUHESHI, G., VALLIÈRES, L., BRANCHI, I., MAGGI, L., LIMATOLA, C., BUTOVSKY, O. & TREMBLAY, M. 2016. Dark microglia: A new phenotype predominantly associated with pathological states. *Glia,* 64**,** 826-39.

BLACK, A. R. & BLACK, J. D. 2012. Protein kinase C signaling and cell cycle regulation. *Front Immunol,* 3**,** 423.

BLACK, C. M., FILLIT, H., XIE, L., HU, X., KARIBURYO, M. F., AMBEGAONKAR, B. M., BASER, O., YUCE, H. & KHANDKER, R. K. 2018. Economic Burden, Mortality, and Institutionalization in Patients Newly Diagnosed with Alzheimer's Disease. *J Alzheimers Dis,* 61**,** 185-193.

BOHLEN, C. J., BENNETT, F. C., TUCKER, A. F., COLLINS, H. Y., MULINYAWE, S. B. & BARRES, B. A. 2017. Diverse Requirements for Microglial Survival, Specification, and Function Revealed by Defined-Medium Cultures. *Neuron,* 94**,** 759-773.e8.

BONDI, M. W., EDMONDS, E. C. & SALMON, D. P. 2017. Alzheimer's Disease: Past, Present, and Future. *J Int Neuropsychol Soc,* 23**,** 818-831.

BONTKES, H. J., DE GRUIJL, T. D., SCHUURHUIS, G. J., SCHEPER, R. J., MEIJER, C. J. & HOOIJBERG, E. 2002. Expansion of dendritic cell precursors from human CD34(+) progenitor cells isolated from healthy donor blood; growth factor combination determines proliferation rate and functional outcome. *J Leukoc Biol,* 72**,** 321-9.

BORGOHAIN, M. P., HARIDHASAPAVALAN, K. K., DEY, C., ADHIKARI, P. & THUMMER, R. P. 2019. An Insight into DNA-free Reprogramming Approaches to Generate Integration-free Induced Pluripotent Stem Cells for Prospective Biomedical Applications. *Stem Cell Rev Rep,* 15**,** 286-313.

BOTELHO, R. J., TERUEL, M., DIERCKMAN, R., ANDERSON, R., WELLS, A., YORK, J. D., MEYER, T. & GRINSTEIN, S. 2000. Localized biphasic changes in phosphatidylinositol-4,5-bisphosphate at sites of phagocytosis. *J Cell Biol,* 151**,** 1353-68.

BRADSHAW, E. M., CHIBNIK, L. B., KEENAN, B. T., OTTOBONI, L., RAJ, T., TANG, A., ROSENKRANTZ, L. L., IMBOYWA, S., LEE, M., VON KORFF, A., MORRIS, M. C., EVANS, D. A., JOHNSON, K., SPERLING, R. A., SCHNEIDER, J. A., BENNETT, D. A. & DE JAGER, P. L. 2013. CD33 Alzheimer's disease locus: altered monocyte function and amyloid biology. *Nat Neurosci,* 16**,** 848-50.

BRICKMAN, J. M. & SERUP, P. 2017. Properties of embryoid bodies. *Wiley Interdiscip Rev Dev Biol,* 6.

BROSSERON, F., KRAUTHAUSEN, M., KUMMER, M. & HENEKA, M. T. 2014. Body fluid cytokine levels in mild cognitive impairment and Alzheimer's disease: a comparative overview. *Mol Neurobiol,* 50**,** 534-44.

BROUGH, D., LE FEUVRE, R. A., WHEELER, R. D., SOLOVYOVA, N., HILFIKER, S., ROTHWELL, N. J. & VERKHRATSKY, A. 2003. Ca2+ stores and Ca2+ entry differentially contribute to the release of IL-1 beta and IL-1 alpha from murine macrophages. *J Immunol,* 170**,** 3029-36.

BROXMEYER, H. E., LU, L., COOPER, S., RUGGIERI, L., LI, Z. H. & LYMAN, S. D. 1995. Flt3 ligand stimulates/costimulates the growth of myeloid stem/progenitor cells. *Exp Hematol,* 23**,** 1121-9.

BRUTTGER, J., KARRAM, K., WÖRTGE, S., REGEN, T., MARINI, F., HOPPMANN, N., KLEIN, M., BLANK, T., YONA, S., WOLF, Y., MACK, M., PINTEAUX, E., MÜLLER, W., ZIPP, F., BINDER, H., BOPP, T., PRINZ, M., JUNG, S. & WAISMAN, A. 2015. Genetic Cell Ablation Reveals Clusters of Local Self-Renewing Microglia in the Mammalian Central Nervous System. *Immunity,* 43**,** 92-106.

BUERGER, K., EWERS, M., PIRTTILÄ, T., ZINKOWSKI, R., ALAFUZOFF, I., TEIPEL, S. J., DEBERNARDIS, J., KERKMAN, D., MCCULLOCH, C., SOININEN, H. & HAMPEL, H. 2006. CSF phosphorylated tau protein correlates with neocortical neurofibrillary pathology in Alzheimer's disease. *Brain,* 129**,** 3035-41.

C., P. 2018. World Alzheimer Report 2018. The state of the art of dementia research: New frontiers. . *London: Alzheimer's Disease International.*

CAI, N., KURACHI, M., SHIBASAKI, K., OKANO-UCHIDA, T. & ISHIZAKI, Y. 2012. CD44-positive cells are candidates for astrocyte precursor cells in developing mouse cerebellum. *Cerebellum,* 11**,** 181-93.

CALOVI, S., MUT-ARBONA, P. & SPERLÁGH, B. 2019. Microglia and the Purinergic Signaling System. *Neuroscience,* 405**,** 137-147.

CARAUX, A., KIM, N., BELL, S. E., ZOMPI, S., RANSON, T., LESJEAN-POTTIER, S., GARCIA-OJEDA, M. E., TURNER, M. & COLUCCI, F. 2006. Phospholipase C-gamma2 is essential for NK cell cytotoxicity and innate immunity to malignant and virally infected cells. *Blood,* 107**,** 994-1002.

CARBONELL, W. S., MURASE, S., HORWITZ, A. F. & MANDELL, J. W. 2005. Migration of perilesional microglia after focal brain injury and modulation by CC chemokine receptor 5: an in situ time-lapse confocal imaging study. *J Neurosci,* 25**,** 7040-7.

CARDONA, A. E., PIORO, E. P., SASSE, M. E., KOSTENKO, V., CARDONA, S. M., DIJKSTRA, I. M., HUANG, D., KIDD, G., DOMBROWSKI, S., DUTTA, R., LEE, J. C., COOK, D. N., JUNG, S., LIRA, S. A., LITTMAN, D. R. & RANSOHOFF, R. M. 2006. Control of microglial neurotoxicity by the fractalkine receptor. *Nat Neurosci,* 9**,** 917-24.

CARTER, D. A. & DICK, A. D. 2003. Lipopolysaccharide/interferon-γ and not transforming growth factor β inhibits retinal microglial migration from retinal explant. *British Journal of Ophthalmology,* 87**,** 481-487.

CASHEN, A. F., LAZARUS, H. M. & DEVINE, S. M. 2007. Mobilizing stem cells from normal donors: is it possible to improve upon G-CSF? *Bone Marrow Transplant,* 39**,** 577-88.

CHAE, J. J., PARK, Y. H., PARK, C., HWANG, I. Y., HOFFMANN, P., KEHRL, J. H., AKSENTIJEVICH, I. & KASTNER, D. L. 2015. Connecting two pathways through Ca 2+ signaling: NLRP3 inflammasome activation induced by a hypermorphic PLCG2 mutation. *Arthritis Rheumatol,* 67**,** 563-7.

CHAKRABARTY, P., HERRING, A., CEBALLOS-DIAZ, C., DAS, P. & GOLDE, T. E. 2011. Hippocampal expression of murine TNFα results in attenuation of amyloid deposition in vivo. *Mol Neurodegener,* 6**,** 16.

CHAKRABARTY, P., LI, A., CEBALLOS-DIAZ, C., EDDY, J. A., FUNK, C. C., MOORE, B., DINUNNO, N., ROSARIO, A. M., CRUZ, P. E., VERBEECK, C., SACINO, A., NIX, S., JANUS, C., PRICE, N. D., DAS, P. & GOLDE, T. E. 2015. IL-10 alters immunoproteostasis in APP mice, increasing plaque burden and worsening cognitive behavior. *Neuron,* 85**,** 519-33.

CHAN, A., HUMMEL, V., WEILBACH, F. X., KIESEIER, B. C. & GOLD, R. 2006. Phagocytosis of apoptotic inflammatory cells downregulates microglial chemoattractive function and migration of encephalitogenic T cells. *J Neurosci Res,* 84**,** 1217-24.

CHATTERJEE, S., CHEUNG, H. C. & HUNTER, E. 1982. Interferon inhibits Sendai virus-induced cell fusion: an effect on cell membrane fluidity. *Proc Natl Acad Sci U S A,* 79**,** 835-9.

CHEN, L. & FLIES, D. B. 2013. Molecular mechanisms of T cell co-stimulation and co-inhibition. *Nat Rev Immunol,* 13**,** 227-42.

CHEN, S. K., TVRDIK, P., PEDEN, E., CHO, S., WU, S., SPANGRUDE, G. & CAPECCHI, M. R. 2010. Hematopoietic origin of pathological grooming in Hoxb8 mutant mice. *Cell,* 141**,** 775-85.

CHENG-HATHAWAY, P. J., REED-GEAGHAN, E. G., JAY, T. R., CASALI, B. T., BEMILLER, S. M., PUNTAMBEKAR, S. S., VON SAUCKEN, V. E., WILLIAMS, R. Y., KARLO, J. C., MOUTINHO, M., XU, G., RANSOHOFF, R. M., LAMB, B. T. & LANDRETH, G. E. 2018. The Trem2 R47H variant confers loss-of-function-like phenotypes in Alzheimer's disease. *Mol Neurodegener,* 13**,** 29.

CHENG, X., HUBER, T. L., CHEN, V. C., GADUE, P. & KELLER, G. M. 2008. Numb mediates the interaction between Wnt and Notch to modulate primitive erythropoietic specification from the hemangioblast. *Development,* 135**,** 3447-58.

CHIANG, C. Y., VECKMAN, V., LIMMER, K. & DAVID, M. 2012. Phospholipase Cγ-2 and intracellular calcium are required for lipopolysaccharide-induced Toll-like receptor 4 (TLR4) endocytosis and interferon regulatory factor 3 (IRF3) activation. *J Biol Chem,* 287**,** 3704-9.

CHO, H. J., LEE, C. S., KWON, Y. W., PAEK, J. S., LEE, S. H., HUR, J., LEE, E. J., ROH, T. Y., CHU, I. S., LEEM, S. H., KIM, Y., KANG, H. J., PARK, Y. B. & KIM, H. S. 2010. Induction of pluripotent stem cells from adult somatic cells by protein-based reprogramming without genetic manipulation. *Blood,* 116**,** 386-95.

CHRISTOPHERSON, K. S., ULLIAN, E. M., STOKES, C. C., MULLOWNEY, C. E., HELL, J. W., AGAH, A., LAWLER, J., MOSHER, D. F., BORNSTEIN, P. & BARRES, B. A. 2005. Thrombospondins are astrocyte-secreted proteins that promote CNS synaptogenesis. *Cell,* 120**,** 421-33.

CORDER, E. H., SAUNDERS, A. M., STRITTMATTER, W. J., SCHMECHEL, D. E., GASKELL, P. C., SMALL, G. W., ROSES, A. D., HAINES, J. L. & PERICAK-VANCE, M. A. 1993. Gene dose of apolipoprotein E type 4 allele and the risk of Alzheimer's disease in late onset families. *Science,* 261**,** 921-3.

CROTTI, A. & RANSOHOFF, R. M. 2016. Microglial Physiology and Pathophysiology: Insights from Genome-wide Transcriptional Profiling. *Immunity,* 44**,** 505-515.

CUNHA, C., GOMES, C., VAZ, A. R. & BRITES, D. 2016. Exploring New Inflammatory Biomarkers and Pathways during LPS-Induced M1 Polarization. *Mediators Inflamm,* 2016**,** 6986175.

DANG, S. M., KYBA, M., PERLINGEIRO, R., DALEY, G. Q. & ZANDSTRA, P. W. 2002. Efficiency of embryoid body formation and hematopoietic development from embryonic stem cells in different culture systems. *Biotechnol Bioeng,* 78**,** 442-53.

DAVALOS, D., GRUTZENDLER, J., YANG, G., KIM, J. V., ZUO, Y., JUNG, S., LITTMAN, D. R., DUSTIN, M. L. & GAN, W. B. 2005. ATP mediates rapid microglial response to local brain injury in vivo. *Nat Neurosci,* 8**,** 752-8.

DAVIES, D. S., MA, J., JEGATHEES, T. & GOLDSBURY, C. 2017. Microglia show altered morphology and reduced arborization in human brain during aging and Alzheimer's disease. *Brain Pathol,* 27**,** 795-808.

DAVIS, R. L., SANCHEZ, A. C., LINDLEY, D. J., WILLIAMS, S. C. & SYAPIN, P. J. 2005. Effects of mechanistically distinct NF-kappaB inhibitors on glial inducible nitric-oxide synthase expression. *Nitric Oxide,* 12**,** 200-9.

DE ROJAS, I., MORENO-GRAU, S., TESI, N., GRENIER-BOLEY, B., ANDRADE, V., JANSEN, I. E., PEDERSEN, N. L., STRINGA, N., ZETTERGREN, A., HERNÁNDEZ, I., MONTRREAL, L., ANTÚNEZ, C., ANTONELL, A., TANKARD, R. M., BIS, J. C., SIMS, R., BELLENGUEZ, C., QUINTELA, I., GONZÁLEZ-PEREZ, A., CALERO, M., FRANCO-MACÍAS, E., MACÍAS, J., BLESA, R., CERVERA-CARLES, L., MENÉNDEZ-GONZÁLEZ, M., FRANK-GARCÍA, A., ROYO, J. L., MORENO, F., HUERTO VILAS, R., BAQUERO, M., DIEZ-FAIREN, M., LAGE, C., GARCÍA-MADRONA, S., GARCÍA-GONZÁLEZ, P., ALARCÓN-MARTÍN, E., VALERO, S., SOTOLONGO-GRAU, O., ULLGREN, A., NAJ, A. C., LEMSTRA, A. W., BENAQUE, A., PÉREZ-CORDÓN, A., BENUSSI, A., RÁBANO, A., PADOVANI, A., SQUASSINA, A., DE MENDONÇA, A., ARIAS PASTOR, A., KOK, A. A. L., MEGGY, A., PASTOR, A. B., ESPINOSA, A., CORMA-GÓMEZ, A., MARTÍN MONTES, A., SANABRIA, Á., DESTEFANO, A. L., SCHNEIDER, A., HAAPASALO, A., KINHULT STÅHLBOM, A.,

TYBJÆRG-HANSEN, A., HARTMANN, A. M., SPOTTKE, A., CORBATÓN-ANCHUELO, A., RONGVE, A., BORRONI, B., AROSIO, B., NACMIAS, B., NORDESTGAARD, B. G., KUNKLE, B. W., CHARBONNIER, C., ABDELNOUR, C., MASULLO, C., MARTÍNEZ RODRÍGUEZ, C., MUÑOZ-FERNANDEZ, C., DUFOUIL, C., GRAFF, C., FERREIRA, C. B., CHILLOTTI, C., REYNOLDS, C. A., FENOGLIO, C., VAN BROECKHOVEN, C., CLARK, C., PISANU, C., SATIZABAL, C. L., HOLMES, C., BUIZA-RUEDA, D., AARSLAND, D., RUJESCU, D., ALCOLEA, D., GALIMBERTI, D., WALLON, D., SERIPA, D., GRÜNBLATT, E., DARDIOTIS, E., DÜZEL, E., SCARPINI, E., CONTI, E., RUBINO, E., GELPI, E., RODRIGUEZ-RODRIGUEZ, E., et al. 2021. Common variants in Alzheimer's disease and risk stratification by polygenic risk scores. *Nat Commun,* 12**,** 3417.

DE WAAL MALEFYT, R., ABRAMS, J., BENNETT, B., FIGDOR, C. G. & DE VRIES, J. E. 1991. Interleukin 10(IL-10) inhibits cytokine synthesis by human monocytes: an autoregulatory role of IL-10 produced by monocytes. *J Exp Med,* 174**,** 1209-20.

DEL RIO-HORTEGA, P. 1932. Microglia, in Cytology and Cellular Pathology of the Nervous System. *New York: P.B. Hoerber* 50**,** 482-534.

DESAI-MEHTA, A., LU, L., RAMSEY-GOLDMAN, R. & DATTA, S. K. 1996. Hyperexpression of CD40 ligand by B and T cells in human lupus and its role in pathogenic autoantibody production. *J Clin Invest,* 97**,** 2063-73.

DIXIT, R., ROSS, J. L., GOLDMAN, Y. E. & HOLZBAUR, E. L. 2008. Differential regulation of dynein and kinesin motor proteins by tau. *Science,* 319**,** 1086-9.

DO, H. T. T., BUI, B. P., SIM, S., JUNG, J. K., LEE, H. & CHO, J. 2020. Anti-Inflammatory and Anti-Migratory Activities of Isoquinoline-1-Carboxamide Derivatives in LPS-Treated BV2 Microglial Cells via Inhibition of MAPKs/NF-κB Pathway. *Int J Mol Sci,* 21.

DOBRANSKY, T., DOHERTY-KIRBY, A., KIM, A. R., BREWER, D., LAJOIE, G. & RYLETT, R. J. 2004. Protein kinase C isoforms differentially phosphorylate human choline acetyltransferase regulating its catalytic activity. *J Biol Chem,* 279**,** 52059-68.

DOENS, D. & FERNÁNDEZ, P. L. 2014. Microglia receptors and their implications in the response to amyloid β for Alzheimer's disease pathogenesis. *J Neuroinflammation,* 11**,** 48.

DOODY, R. S., THOMAS, R. G., FARLOW, M., IWATSUBO, T., VELLAS, B., JOFFE, S., KIEBURTZ, K., RAMAN, R., SUN, X., AISEN, P. S., SIEMERS, E., LIU-SEIFERT, H. & MOHS, R. 2014. Phase 3 trials of solanezumab for mild-to-moderate Alzheimer's disease. *N Engl J Med,* 370**,** 311-21.

DOUVARAS, P., SUN, B., WANG, M., KRUGLIKOV, I., LALLOS, G., ZIMMER, M., TERRENOIRE, C., ZHANG, B., GANDY, S., SCHADT, E., FREYTES, D. O., NOGGLE, S. & FOSSATI, V. 2017. Directed Differentiation of Human Pluripotent Stem Cells to Microglia. *Stem Cell Reports,* 8**,** 1516-1524.

DOWNS, K. P., NGUYEN, H., DORFLEUTNER, A. & STEHLIK, C. 2020. An overview of the non-canonical inflammasome. *Mol Aspects Med,* 76**,** 100924.

DRISCOLL, P. C. 2015. Exposed: The Many and Varied Roles of Phospholipase C γ SH2 Domains. *J Mol Biol,* 427**,** 2731-3.

EDER, C., SCHILLING, T., HEINEMANN, U., HAAS, D., HAILER, N. & NITSCH, R. 1999. Morphological, immunophenotypical and electrophysiological properties of resting microglia in vitro. *Eur J Neurosci,* 11**,** 4251-61.

EFTHYMIOU, A. G. & GOATE, A. M. 2017. Late onset Alzheimer's disease genetics implicates microglial pathways in disease risk. *Mol Neurodegener,* 12**,** 43.

EL KHOURY, J. B., MOORE, K. J., MEANS, T. K., LEUNG, J., TERADA, K., TOFT, M., FREEMAN, M. W. & LUSTER, A. D. 2003. CD36 mediates the innate host response to beta-amyloid. *J Exp Med,* 197**,** 1657-66.

ELKABETZ, Y., PANAGIOTAKOS, G., AL SHAMY, G., SOCCI, N. D., TABAR, V. & STUDER, L. 2008. Human ES cell-derived neural rosettes reveal a functionally distinct early neural stem cell stage. *Genes Dev,* 22**,** 152-65.

EMINLI, S., FOUDI, A., STADTFELD, M., MAHERALI, N., AHFELDT, T., MOSTOSLAVSKY, G., HOCK, H. & HOCHEDLINGER, K. 2009. Differentiation stage determines potential of hematopoietic cells for reprogramming into induced pluripotent stem cells. *Nature genetics,* 41**,** 968-976.

ERNEST JAMES PHILLIPS, T. & MAGUIRE, E. 2021. Phosphoinositides: Roles in the Development of Microglial-Mediated Neuroinflammation and Neurodegeneration. *Front Cell Neurosci,* 15**,** 652593.

ESCOTT-PRICE, V., MYERS, A., HUENTELMAN, M., SHOAI, M. & HARDY, J. 2019. Polygenic Risk Score Analysis of Alzheimer's Disease in Cases without APOE4 or APOE2 Alleles. *J Prev Alzheimers Dis,* 6**,** 16-19.

ESCOTT-PRICE, V., MYERS, A. J., HUENTELMAN, M. & HARDY, J. 2017. Polygenic risk score analysis of pathologically confirmed Alzheimer disease. *Ann Neurol,* 82**,** 311-314.

ESCOTT-PRICE, V., SIMS, R., BANNISTER, C., HAROLD, D., VRONSKAYA, M., MAJOUNIE, E., BADARINARAYAN, N., MORGAN, K., PASSMORE, P., HOLMES, C., POWELL, J., BRAYNE, C., GILL, M., MEAD, S., GOATE, A., CRUCHAGA, C., LAMBERT, J. C., VAN DUIJN, C., MAIER, W., RAMIREZ, A., HOLMANS, P., JONES, L., HARDY, J., SESHADRI, S., SCHELLENBERG, G. D., AMOUYEL, P. & WILLIAMS, J. 2015. Common polygenic variation enhances risk prediction for Alzheimer's disease. *Brain,* 138**,** 3673-84.

ESQUERDA-CANALS, G., MONTOLIU-GAYA, L., GÜELL-BOSCH, J. & VILLEGAS, S. 2017. Mouse Models of Alzheimer's Disease. *J Alzheimers Dis,* 57**,** 1171-1183.

ETEMAD, S., ZAMIN, R. M., RUITENBERG, M. J. & FILGUEIRA, L. 2012. A novel in vitro human microglia model: characterization of human monocyte-derived microglia. *J Neurosci Methods,* 209**,** 79-89.

EYO, U. B. & WU, L. J. 2013. Bidirectional microglia-neuron communication in the healthy brain. *Neural Plast,* 2013**,** 456857.

FAN, Z., BROOKS, D. J., OKELLO, A. & EDISON, P. 2017. An early and late peak in microglial activation in Alzheimer's disease trajectory. *Brain,* 140**,** 792-803.

FÄRBER, K. & KETTENMANN, H. 2006. Purinergic signaling and microglia. *Pflugers Arch,* 452**,** 615-21.

FEDOROFF, S., ZHAI, R. & NOVAK, J. P. 1997. Microglia and astroglia have a common progenitor cell. *J Neurosci Res,* 50**,** 477-86.

FERRARI, D., CHIOZZI, P., FALZONI, S., DAL SUSINO, M., COLLO, G., BUELL, G. & DI VIRGILIO, F. 1997. ATP-mediated cytotoxicity in microglial cells. *Neuropharmacology,* 36**,** 1295-301.

FERREIRA, R. & SCHLICHTER, L. C. 2013. Selective activation of KCa3.1 and CRAC channels by P2Y2 receptors promotes Ca(2+) signaling, store refilling and migration of rat microglial cells. *PLoS One,* 8**,** e62345.

FROST, J. L. & SCHAFER, D. P. 2016. Microglia: Architects of the Developing Nervous System. *Trends Cell Biol,* 26**,** 587-597.

FÜGER, P., HEFENDEHL, J. K., VEERARAGHAVALU, K., WENDELN, A. C., SCHLOSSER, C., OBERMÜLLER, U., WEGENAST-BRAUN, B. M., NEHER, J. J., MARTUS, P., KOHSAKA, S., THUNEMANN, M., FEIL, R., SISODIA, S. S., SKODRAS, A. & JUCKER, M. 2017. Microglia turnover with aging and in an Alzheimer's model via long-term in vivo single-cell imaging. *Nat Neurosci,* 20**,** 1371-1376.

FUSAKI, N., BAN, H., NISHIYAMA, A., SAEKI, K. & HASEGAWA, M. 2009. Efficient induction of transgene-free human pluripotent stem cells using a vector based on Sendai virus, an RNA virus that does not integrate into the host genome. *Proc Jpn Acad Ser B Phys Biol Sci,* 85**,** 348-62.

GALLI, S. J., ZSEBO, K. M. & GEISSLER, E. N. 1994. The kit ligand, stem cell factor. *Adv Immunol,* 55**,** 1-96.

GANDY, S., SIMON, A. J., STEELE, J. W., LUBLIN, A. L., LAH, J. J., WALKER, L. C., LEVEY, A. I., KRAFFT, G. A., LEVY, E., CHECLER, F., GLABE, C., BILKER, W. B., ABEL, T., SCHMEIDLER, J. & EHRLICH, M. E. 2010. Days to criterion as an indicator of toxicity associated with human Alzheimer amyloid-beta oligomers. *Ann Neurol,* 68**,** 220-30.

GARCÍA-MARÍN, V., GARCÍA-LÓPEZ, P. & FREIRE, M. 2007. Cajal's contributions to glia research. *Trends Neurosci,* 30**,** 479-87.

GATZ, M., REYNOLDS, C. A., FRATIGLIONI, L., JOHANSSON, B., MORTIMER, J. A., BERG, S., FISKE, A. & PEDERSEN, N. L. 2006. Role of genes and environments for explaining Alzheimer disease. *Arch Gen Psychiatry,* 63**,** 168-74.

GEIJSEN, N., HOROSCHAK, M., KIM, K., GRIBNAU, J., EGGAN, K. & DALEY, G. Q. 2004. Derivation of embryonic germ cells and male gametes from embryonic stem cells. *Nature,* 427**,** 148-54.

GETI, I., ORMISTON, M. L., ROUHANI, F., TOSHNER, M., MOVASSAGH, M., NICHOLS, J., MANSFIELD, W., SOUTHWOOD, M., BRADLEY, A., RANA, A. A., VALLIER, L. & MORRELL, N. W. 2012. A practical and efficient cellular substrate for the generation of induced pluripotent stem cells from adults: blood-derived endothelial progenitor cells. *Stem Cells Transl Med,* 1**,** 855-65.

GINHOUX, F., GRETER, M., LEBOEUF, M., NANDI, S., SEE, P., GOKHAN, S., MEHLER, M. F., CONWAY, S. J., NG, L. G., STANLEY, E. R., SAMOKHVALOV, I. M. & MERAD, M. 2010. Fate mapping analysis reveals that adult microglia derive from primitive macrophages. *Science,* 330**,** 841-5.

GINHOUX, F. & GUILLIAMS, M. 2016. Tissue-Resident Macrophage Ontogeny and Homeostasis. *Immunity,* 44**,** 439-449.

GINSBERG, S. D., CHE, S., COUNTS, S. E. & MUFSON, E. J. 2006. Shift in the ratio of three-repeat tau and four-repeat tau mRNAs in individual cholinergic basal forebrain neurons in mild cognitive impairment and Alzheimer's disease. *J Neurochem,* 96**,** 1401-8.

GOEDERT, M., SPILLANTINI, M. G., JAKES, R., RUTHERFORD, D. & CROWTHER, R. A. 1989. Multiple isoforms of human microtubule-associated protein tau: sequences and localization in neurofibrillary tangles of Alzheimer's disease. *Neuron,* 3**,** 519-26.

GOLDMANN, T., WIEGHOFER, P., JORDÃO, M. J., PRUTEK, F., HAGEMEYER, N., FRENZEL, K., AMANN, L., STASZEWSKI, O., KIERDORF, K., KRUEGER, M., LOCATELLI, G., HOCHGERNER, H., ZEISER, R., EPELMAN, S., GEISSMANN, F., PRILLER, J., ROSSI, F. M., BECHMANN, I., KERSCHENSTEINER, M., LINNARSSON, S., JUNG, S. & PRINZ, M. 2016. Origin, fate and dynamics of macrophages at central nervous system interfaces. *Nat Immunol,* 17**,** 797-805.

GOMEZ-ARBOLEDAS, A., ACHARYA, M. M. & TENNER, A. J. 2021. The Role of Complement in Synaptic Pruning and Neurodegeneration. *Immunotargets Ther,* 10**,** 373-386.

GOMEZ PERDIGUERO, E., KLAPPROTH, K., SCHULZ, C., BUSCH, K., AZZONI, E., CROZET, L., GARNER, H., TROUILLET, C., DE BRUIJN, M. F., GEISSMANN, F. & RODEWALD, H. R. 2015. Tissue-resident macrophages originate from yolk-sac-derived erythro-myeloid progenitors. *Nature,* 518**,** 547-51.

GOSSELIN, D., SKOLA, D., COUFAL, N. G., HOLTMAN, I. R., SCHLACHETZKI, J. C. M., SAJTI, E., JAEGER, B. N., O'CONNOR, C., FITZPATRICK, C., PASILLAS, M. P., PENA, M., ADAIR, A., GONDA, D. D., LEVY, M. L., RANSOHOFF, R. M., GAGE, F. H. & GLASS, C. K. 2017. An environment-dependent transcriptional network specifies human microglia identity. *Science,* 356.

GRAHAM, W. V., BONITO-OLIVA, A. & SAKMAR, T. P. 2017. Update on Alzheimer's Disease Therapy and Prevention Strategies. *Annu Rev Med,* 68**,** 413-430.

GRESSET, A., HICKS, S. N., HARDEN, T. K. & SONDEK, J. 2010. Mechanism of phosphorylation-induced activation of phospholipase C-gamma isozymes. *J Biol Chem,* 285**,** 35836-47.

GRINER, E. M. & KAZANIETZ, M. G. 2007. Protein kinase C and other diacylglycerol effectors in cancer. *Nat Rev Cancer,* 7**,** 281-94.

GROZEVA, D., SAAD, S., MENZIES, G. E. & SIMS, R. 2019. Benefits and Challenges of Rare Genetic Variation in Alzheimer's Disease. *Current Genetic Medicine Reports,* 7**,** 53-62.

GUERREIRO, R., WOJTAS, A., BRAS, J., CARRASQUILLO, M., ROGAEVA, E., MAJOUNIE, E., CRUCHAGA, C., SASSI, C., KAUWE, J. S., YOUNKIN, S., HAZRATI, L., COLLINGE, J., POCOCK, J., LASHLEY, T., WILLIAMS, J., LAMBERT, J. C., AMOUYEL, P., GOATE, A., RADEMAKERS, R., MORGAN, K., POWELL, J., ST GEORGE-HYSLOP, P., SINGLETON, A. & HARDY, J. 2013. TREM2 variants in Alzheimer's disease. *N Engl J Med,* 368**,** 117-27.

GUILLOT-SESTIER, M. V., DOTY, K. R., GATE, D., RODRIGUEZ, J., JR., LEUNG, B. P., REZAI-ZADEH, K. & TOWN, T. 2015. Il10 deficiency rebalances innate immunity to mitigate Alzheimer-like pathology. *Neuron,* 85**,** 534-48.

GUPTA, M. K., TEO, A. K., RAO, T. N., BHATT, S., KLEINRIDDERS, A., SHIRAKAWA, J., TAKATANI, T., HU, J., DE JESUS, D. F., WINDMUELLER, R., WAGERS, A. J. & KULKARNI, R. N. 2015. Excessive Cellular Proliferation Negatively Impacts Reprogramming Efficiency of Human Fibroblasts. *Stem Cells Transl Med,* 4**,** 1101-8.

HAENSELER, W. & RAJENDRAN, L. 2019. Concise Review: Modeling Neurodegenerative Diseases with Human Pluripotent Stem Cell-Derived Microglia. *Stem Cells*.

HAENSELER, W., SANSOM, S. N., BUCHRIESER, J., NEWEY, S. E., MOORE, C. S., NICHOLLS, F. J., CHINTAWAR, S., SCHNELL, C., ANTEL, J. P., ALLEN, N. D., CADER, M. Z., WADE-MARTINS, R., JAMES, W. S. & COWLEY, S. A. 2017. A Highly Efficient Human Pluripotent Stem Cell Microglia Model Displays a Neuronal-Co-culture-Specific Expression Profile and Inflammatory Response. *Stem Cell Reports,* 8**,** 1727-1742.

HALL-ROBERTS, H., AGARWAL, D., OBST, J., SMITH, T. B., MONZÓN-SANDOVAL, J., DI DANIEL, E., WEBBER, C., JAMES, W. S., MEAD, E., DAVIS, J. B. & COWLEY, S. A. 2020. TREM2 Alzheimer's variant R47H causes similar transcriptional dysregulation to knockout, yet only subtle functional phenotypes in human iPSC-derived macrophages. *Alzheimers Res Ther,* 12**,** 151.

HALLE, A., HORNUNG, V., PETZOLD, G. C., STEWART, C. R., MONKS, B. G., REINHECKEL, T., FITZGERALD, K. A., LATZ, E., MOORE, K. J. & GOLENBOCK, D. T. 2008. The NALP3 inflammasome is involved in the innate immune response to amyloid-beta. *Nat Immunol,* 9**,** 857-65.

HAMAZAKI, T., EL ROUBY, N., FREDETTE, N. C., SANTOSTEFANO, K. E. & TERADA, N. 2017. Concise Review: Induced Pluripotent Stem Cell Research in the Era of Precision Medicine. *Stem Cells,* 35**,** 545-550.

HAMPEL, H., HARDY, J., BLENNOW, K., CHEN, C., PERRY, G., KIM, S. H., VILLEMAGNE, V. L., AISEN, P., VENDRUSCOLO, M., IWATSUBO, T., MASTERS, C. L., CHO, M., LANNFELT,

L., CUMMINGS, J. L. & VERGALLO, A. 2021. The Amyloid-β Pathway in Alzheimer's Disease. *Molecular Psychiatry,* 26**,** 5481-5503.

HANSEN, D. V., HANSON, J. E. & SHENG, M. 2018. Microglia in Alzheimer's disease. *J Cell Biol,* 217**,** 459-472.

HANZEL, C. E., PICHET-BINETTE, A., PIMENTEL, L. S., IULITA, M. F., ALLARD, S., DUCATENZEILER, A., DO CARMO, S. & CUELLO, A. C. 2014. Neuronal driven pre-plaque inflammation in a transgenic rat model of Alzheimer's disease. *Neurobiol Aging,* 35**,** 2249-62.

HAO, C., RICHARDSON, A. & FEDOROFF, S. 1991. Macrophage-like cells originate from neuroepithelium in culture: characterization and properties of the macrophage-like cells. *Int J Dev Neurosci,* 9**,** 1-14.

HARDY, J. & ALLSOP, D. 1991. Amyloid deposition as the central event in the aetiology of Alzheimer's disease. *Trends Pharmacol Sci,* 12**,** 383-8.

HARDY, J. & SELKOE, D. J. 2002. The amyloid hypothesis of Alzheimer's disease: progress and problems on the road to therapeutics. *Science,* 297**,** 353-6.

HAROLD, D., ABRAHAM, R., HOLLINGWORTH, P., SIMS, R., GERRISH, A., HAMSHERE, M. L., PAHWA, J. S., MOSKVINA, V., DOWZELL, K., WILLIAMS, A., JONES, N., THOMAS, C., STRETTON, A., MORGAN, A. R., LOVESTONE, S., POWELL, J., PROITSI, P., LUPTON, M. K., BRAYNE, C., RUBINSZTEIN, D. C., GILL, M., LAWLOR, B., LYNCH, A., MORGAN, K., BROWN, K. S., PASSMORE, P. A., CRAIG, D., MCGUINNESS, B., TODD, S., HOLMES, C., MANN, D., SMITH, A. D., LOVE, S., KEHOE, P. G., HARDY, J., MEAD, S., FOX, N., ROSSOR, M., COLLINGE, J., MAIER, W., JESSEN, F., SCHURMANN, B., HEUN, R., VAN DEN BUSSCHE, H., HEUSER, I., KORNHUBER, J., WILTFANG, J., DICHGANS, M., FROLICH, L., HAMPEL, H., HULL, M., RUJESCU, D., GOATE, A. M., KAUWE, J. S., CRUCHAGA, C., NOWOTNY, P., MORRIS, J. C., MAYO, K., SLEEGERS, K., BETTENS, K., ENGELBORGHS, S., DE DEYN, P. P., VAN BROECKHOVEN, C., LIVINGSTON, G., BASS, N. J., GURLING, H., MCQUILLIN, A., GWILLIAM, R., DELOUKAS, P., AL-CHALABI, A., SHAW, C. E., TSOLAKI, M., SINGLETON, A. B., GUERREIRO, R., MUHLEISEN, T. W., NOTHEN, M. M., MOEBUS, S., JOCKEL, K. H., KLOPP, N., WICHMANN, H. E., CARRASQUILLO, M. M., PANKRATZ, V. S., YOUNKIN, S. G., HOLMANS, P. A., O'DONOVAN, M., OWEN, M. J. & WILLIAMS, J. 2009. Genome-wide association study identifies variants at CLU and PICALM associated with Alzheimer's disease. *Nat Genet,* 41**,** 1088-93.

HASHIMOTO, A., TAKEDA, K., INABA, M., SEKIMATA, M., KAISHO, T., IKEHARA, S., HOMMA, Y., AKIRA, S. & KUROSAKI, T. 2000. Cutting edge: essential role of phospholipase C-gamma 2 in B cell development and function. *J Immunol,* 165**,** 1738-42.

HAYASHI, H., KUBO, Y., IZUMIDA, M. & MATSUYAMA, T. 2020. Efficient viral delivery of Cas9 into human safe harbor. *Sci Rep,* 10**,** 21474.

HE, Z., LI, J. J., ZHEN, C. H., FENG, L. Y. & DING, X. Y. 2006. Effect of leukemia inhibitory factor on embryonic stem cell differentiation: implications for supporting neuronal differentiation. *Acta Pharmacol Sin,* 27**,** 80-90.

HEFENDEHL, J. K., NEHER, J. J., SÜHS, R. B., KOHSAKA, S., SKODRAS, A. & JUCKER, M. 2014. Homeostatic and injury-induced microglia behavior in the aging brain. *Aging Cell,* 13**,** 60-9.

HEIKE, T. & NAKAHATA, T. 2002. Ex vivo expansion of hematopoietic stem cells by cytokines. *Biochim Biophys Acta,* 1592**,** 313-21.

HELLMANN-REGEN, J., KRONENBERG, G., UHLEMANN, R., FREYER, D., ENDRES, M. & GERTZ, K. 2013. Accelerated degradation of retinoic acid by activated microglia. *J Neuroimmunol,* 256**,** 1-6.

HENEKA, M. T., CARSON, M. J., EL KHOURY, J., LANDRETH, G. E., BROSSERON, F., FEINSTEIN, D. L., JACOBS, A. H., WYSS-CORAY, T., VITORICA, J., RANSOHOFF, R. M., HERRUP, K., FRAUTSCHY, S. A., FINSEN, B., BROWN, G. C., VERKHRATSKY, A., YAMANAKA, K., KOISTINAHO, J., LATZ, E., HALLE, A., PETZOLD, G. C., TOWN, T., MORGAN, D., SHINOHARA, M. L., PERRY, V. H., HOLMES, C., BAZAN, N. G., BROOKS, D. J., HUNOT, S., JOSEPH, B., DEIGENDESCH, N., GARASCHUK, O., BODDEKE, E., DINARELLO, C. A., BREITNER, J. C., COLE, G. M., GOLENBOCK, D. T. & KUMMER, M. P. 2015. Neuroinflammation in Alzheimer's disease. *Lancet Neurol,* 14**,** 388-405.

HENEKA, M. T., KUMMER, M. P. & LATZ, E. 2014. Innate immune activation in neurodegenerative disease. *Nat Rev Immunol,* 14**,** 463-77.

HENEKA, M. T., KUMMER, M. P., STUTZ, A., DELEKATE, A., SCHWARTZ, S., VIEIRA-SAECKER, A., GRIEP, A., AXT, D., REMUS, A., TZENG, T. C., GELPI, E., HALLE, A., KORTE, M., LATZ, E. & GOLENBOCK, D. T. 2013. NLRP3 is activated in Alzheimer's disease and contributes to pathology in APP/PS1 mice. *Nature,* 493**,** 674-8.

HICKMAN, S. E., ALLISON, E. K. & EL KHOURY, J. 2008. Microglial dysfunction and defective beta-amyloid clearance pathways in aging Alzheimer's disease mice. *J Neurosci,* 28**,** 8354-60.

HICKMAN, S. E., KINGERY, N. D., OHSUMI, T. K., BOROWSKY, M. L., WANG, L. C., MEANS, T. K. & EL KHOURY, J. 2013. The microglial sensome revealed by direct RNA sequencing. *Nat Neurosci,* 16**,** 1896-905.

HINZE, A. & STOLZING, A. 2011. Differentiation of mouse bone marrow derived stem cells toward microglia-like cells. *BMC Cell Biol,* 12**,** 35.

HOEFFEL, G., CHEN, J., LAVIN, Y., LOW, D., ALMEIDA, F. F., SEE, P., BEAUDIN, A. E., LUM, J., LOW, I., FORSBERG, E. C., POIDINGER, M., ZOLEZZI, F., LARBI, A., NG, L. G., CHAN, J. K., GRETER, M., BECHER, B., SAMOKHVALOV, I. M., MERAD, M. & GINHOUX, F. 2015. C-Myb(+) erythro-myeloid progenitor-derived fetal monocytes give rise to adult tissue-resident macrophages. *Immunity,* 42**,** 665-78.

HOEFFEL, G. & GINHOUX, F. 2015. Ontogeny of Tissue-Resident Macrophages. *Front Immunol,* 6**,** 486.

HOEK, R. M., RUULS, S. R., MURPHY, C. A., WRIGHT, G. J., GODDARD, R., ZURAWSKI, S. M., BLOM, B., HOMOLA, M. E., STREIT, W. J., BROWN, M. H., BARCLAY, A. N. &

SEDGWICK, J. D. 2000. Down-regulation of the macrophage lineage through interaction with OX2 (CD200). *Science,* 290**,** 1768-71.

HOLLINGWORTH, P., HAROLD, D., SIMS, R., GERRISH, A., LAMBERT, J. C., CARRASQUILLO, M. M., ABRAHAM, R., HAMSHERE, M. L., PAHWA, J. S., MOSKVINA, V., DOWZELL, K., JONES, N., STRETTON, A., THOMAS, C., RICHARDS, A., IVANOV, D., WIDDOWSON, C., CHAPMAN, J., LOVESTONE, S., POWELL, J., PROITSI, P., LUPTON, M. K., BRAYNE, C., RUBINSZTEIN, D. C., GILL, M., LAWLOR, B., LYNCH, A., BROWN, K. S., PASSMORE, P. A., CRAIG, D., MCGUINNESS, B., TODD, S., HOLMES, C., MANN, D., SMITH, A. D., BEAUMONT, H., WARDEN, D., WILCOCK, G., LOVE, S., KEHOE, P. G., HOOPER, N. M., VARDY, E. R., HARDY, J., MEAD, S., FOX, N. C., ROSSOR, M., COLLINGE, J., MAIER, W., JESSEN, F., RUTHER, E., SCHURMANN, B., HEUN, R., KOLSCH, H., VAN DEN BUSSCHE, H., HEUSER, I., KORNHUBER, J., WILTFANG, J., DICHGANS, M., FROLICH, L., HAMPEL, H., GALLACHER, J., HULL, M., RUJESCU, D., GIEGLING, I., GOATE, A. M., KAUWE, J. S., CRUCHAGA, C., NOWOTNY, P., MORRIS, J. C., MAYO, K., SLEEGERS, K., BETTENS, K., ENGELBORGHS, S., DE DEYN, P. P., VAN BROECKHOVEN, C., LIVINGSTON, G., BASS, N. J., GURLING, H., MCQUILLIN, A., GWILLIAM, R., DELOUKAS, P., AL-CHALABI, A., SHAW, C. E., TSOLAKI, M., SINGLETON, A. B., GUERREIRO, R., MUHLEISEN, T. W., NOTHEN, M. M., MOEBUS, S., JOCKEL, K. H., KLOPP, N., WICHMANN, H. E., PANKRATZ, V. S., SANDO, S. B., AASLY, J. O., BARCIKOWSKA, M., WSZOLEK, Z. K., DICKSON, D. W., GRAFF-RADFORD, N. R., PETERSEN, R. C., et al. 2011. Common variants at ABCA7, MS4A6A/MS4A4E, EPHA1, CD33 and CD2AP are associated with Alzheimer's disease. *Nat Genet,* 43**,** 429-35.

HONDA, S., SASAKI, Y., OHSAWA, K., IMAI, Y., NAKAMURA, Y., INOUE, K. & KOHSAKA, S. 2001. Extracellular ATP or ADP Induce Chemotaxis of Cultured Microglia through G_{i/o}-Coupled P2Y Receptors. *The Journal of Neuroscience,* 21**,** 1975-1982.

HONG, S., DISSING-OLESEN, L. & STEVENS, B. 2016. New insights on the role of microglia in synaptic pruning in health and disease. *Curr Opin Neurobiol,* 36**,** 128-34.

HONIG, L. S., VELLAS, B., WOODWARD, M., BOADA, M., BULLOCK, R., BORRIE, M., HAGER, K., ANDREASEN, N., SCARPINI, E., LIU-SEIFERT, H., CASE, M., DEAN, R. A., HAKE, A., SUNDELL, K., POOLE HOFFMANN, V., CARLSON, C., KHANNA, R., MINTUN, M., DEMATTOS, R., SELZLER, K. J. & SIEMERS, E. 2018. Trial of Solanezumab for Mild Dementia Due to Alzheimer's Disease. *N Engl J Med,* 378**,** 321-330.

HSIEH, C. L., KOIKE, M., SPUSTA, S. C., NIEMI, E. C., YENARI, M., NAKAMURA, M. C. & SEAMAN, W. E. 2009. A role for TREM2 ligands in the phagocytosis of apoptotic neuronal cells by microglia. *J Neurochem,* 109**,** 1144-56.

HU, X., PICKERING, E., LIU, Y. C., HALL, S., FOURNIER, H., KATZ, E., DECHAIRO, B., JOHN, S., VAN EERDEWEGH, P. & SOARES, H. 2011. Meta-analysis for genome-wide association study identifies multiple variants at the BIN1 locus associated with late-onset Alzheimer's disease. *PLoS One,* 6**,** e16616.

HUANG, Y., XU, Z., XIONG, S., SUN, F., QIN, G., HU, G., WANG, J., ZHAO, L., LIANG, Y. X., WU, T., LU, Z., HUMAYUN, M. S., SO, K. F., PAN, Y., LI, N., YUAN, T. F., RAO, Y. & PENG, B.

2018. Repopulated microglia are solely derived from the proliferation of residual microglia after acute depletion. *Nat Neurosci,* 21**,** 530-540.

HUANGFU, D., MAEHR, R., GUO, W., EIJKELENBOOM, A., SNITOW, M., CHEN, A. E. & MELTON, D. A. 2008. Induction of pluripotent stem cells by defined factors is greatly improved by small-molecule compounds. *Nat Biotechnol,* 26**,** 795-7.

HÜLL, M., BERGER, M., VOLK, B. & BAUER, J. 1996. Occurrence of interleukin-6 in cortical plaques of Alzheimer's disease patients may precede transformation of diffuse into neuritic plaques. *Ann N Y Acad Sci,* 777**,** 205-12.

ICHISE, H., ICHISE, T. & YOSHIDA, N. 2016. Phospholipase Cγ2 Is Required for Luminal Expansion of the Epididymal Duct during Postnatal Development in Mice. *PLoS One,* 11**,** e0150521.

IKEBUCHI, K., WONG, G. G., CLARK, S. C., IHLE, J. N., HIRAI, Y. & OGAWA, M. 1987. Interleukin 6 enhancement of interleukin 3-dependent proliferation of multipotential hemopoietic progenitors. *Proc Natl Acad Sci U S A,* 84**,** 9035-9.

IQBAL, K., LIU, F. & GONG, C. X. 2016. Tau and neurodegenerative disease: the story so far. *Nat Rev Neurol,* 12**,** 15-27.

IRINO, Y., NAKAMURA, Y., INOUE, K., KOHSAKA, S. & OHSAWA, K. 2008. Akt activation is involved in P2Y12 receptor-mediated chemotaxis of microglia. *J Neurosci Res,* 86**,** 1511-9.

ITAGAKI, S., MCGEER, P. L., AKIYAMA, H., ZHU, S. & SELKOE, D. 1989. Relationship of microglia and astrocytes to amyloid deposits of Alzheimer disease. *J Neuroimmunol,* 24**,** 173-82.

ITO, K., SANOSAKA, T., IGARASHI, K., IDETA-OTSUKA, M., AIZAWA, A., UOSAKI, Y., NOGUCHI, A., ARAKAWA, H., NAKASHIMA, K. & TAKIZAWA, T. 2016. Identification of genes associated with the astrocyte-specific gene Gfap during astrocyte differentiation. *Sci Rep,* 6**,** 23903.

IWATSUBO, T., ODAKA, A., SUZUKI, N., MIZUSAWA, H., NUKINA, N. & IHARA, Y. 1994. Visualization of A beta 42(43) and A beta 40 in senile plaques with end-specific A beta monoclonals: evidence that an initially deposited species is A beta 42(43). *Neuron,* 13**,** 45-53.

JAGANNATHAN-BOGDAN, M. & ZON, L. I. 2013. Hematopoiesis. *Development,* 140**,** 2463-7.

JAKUS, Z., SIMON, E., FROMMHOLD, D., SPERANDIO, M. & MÓCSAI, A. 2009. Critical role of phospholipase Cgamma2 in integrin and Fc receptor-mediated neutrophil functions and the effector phase of autoimmune arthritis. *J Exp Med,* 206**,** 577-93.

JANG, H. J., YANG, Y. R., KIM, J. K., CHOI, J. H., SEO, Y. K., LEE, Y. H., LEE, J. E., RYU, S. H. & SUH, P. G. 2013. Phospholipase C-γ1 involved in brain disorders. *Adv Biol Regul,* 53**,** 51-62.

JANSEN, I. E., SAVAGE, J. E., WATANABE, K., BRYOIS, J., WILLIAMS, D. M., STEINBERG, S., SEALOCK, J., KARLSSON, I. K., HÄGG, S., ATHANASIU, L., VOYLE, N., PROITSI, P., WITOELAR, A., STRINGER, S., AARSLAND, D., ALMDAHL, I. S., ANDERSEN, F., BERGH, S., BETTELLA, F., BJORNSSON, S., BRÆKHUS, A., BRÅTHEN, G., DE LEEUW, C., DESIKAN, R. S., DJUROVIC, S., DUMITRESCU, L., FLADBY, T., HOHMAN, T. J., JONSSON, P. V., KIDDLE, S. J., RONGVE, A., SALTVEDT, I., SANDO, S. B., SELBÆK, G., SHOAI, M., SKENE, N. G., SNAEDAL, J., STORDAL, E., ULSTEIN, I. D., WANG, Y., WHITE, L. R., HARDY, J., HJERLING-LEFFLER, J., SULLIVAN, P. F., VAN DER FLIER, W. M., DOBSON, R., DAVIS, L. K., STEFANSSON, H., STEFANSSON, K., PEDERSEN, N. L., RIPKE, S., ANDREASSEN, O. A. & POSTHUMA, D. 2019. Genome-wide meta-analysis identifies new loci and functional pathways influencing Alzheimer's disease risk. *Nat Genet,* 51**,** 404-413.

JHA, M. K., JO, M., KIM, J. H. & SUK, K. 2019. Microglia-Astrocyte Crosstalk: An Intimate Molecular Conversation. *Neuroscientist,* 25**,** 227-240.

JOHE, K. K., HAZEL, T. G., MULLER, T., DUGICH-DJORDJEVIC, M. M. & MCKAY, R. D. 1996. Single factors direct the differentiation of stem cells from the fetal and adult central nervous system. *Genes Dev,* 10**,** 3129-40.

KADAMUR, G. & ROSS, E. M. 2013. Mammalian phospholipase C. *Annu Rev Physiol,* 75**,** 127-54.

KASAHARA, T., HOOKS, J. J., DOUGHERTY, S. F. & OPPENHEIM, J. J. 1983. Interleukin 2-mediated immune interferon (IFN-gamma) production by human T cells and T cell subsets. *J Immunol,* 130**,** 1784-9.

KATSNELSON, M. A., RUCKER, L. G., RUSSO, H. M. & DUBYAK, G. R. 2015. K+ efflux agonists induce NLRP3 inflammasome activation independently of Ca2+ signaling. *J Immunol,* 194**,** 3937-52.

KATSUMOTO, A., TAKEUCHI, H., TAKAHASHI, K. & TANAKA, F. 2018. Microglia in Alzheimer's Disease: Risk Factors and Inflammation. *Front Neurol,* 9**,** 978.

KAYAGAKI, N., WARMING, S., LAMKANFI, M., VANDE WALLE, L., LOUIE, S., DONG, J., NEWTON, K., QU, Y., LIU, J., HELDENS, S., ZHANG, J., LEE, W. P., ROOSE-GIRMA, M. & DIXIT, V. M. 2011. Non-canonical inflammasome activation targets caspase-11. *Nature,* 479**,** 117-21.

KELLEY, N., JELTEMA, D., DUAN, Y. & HE, Y. 2019. The NLRP3 Inflammasome: An Overview of Mechanisms of Activation and Regulation. *Int J Mol Sci,* 20.

KENNEDY, C. & BURNSTOCK, G. 1985. Evidence for two types of P2-purinoceptor in longitudinal muscle of the rabbit portal vein. *Eur J Pharmacol,* 111**,** 49-56.

KEREN-SHAUL, H., SPINRAD, A., WEINER, A., MATCOVITCH-NATAN, O., DVIR-SZTERNFELD, R., ULLAND, T. K., DAVID, E., BARUCH, K., LARA-ASTAISO, D., TOTH, B., ITZKOVITZ, S., COLONNA, M., SCHWARTZ, M. & AMIT, I. 2017. A Unique Microglia Type Associated with Restricting Development of Alzheimer's Disease. *Cell,* 169**,** 1276-1290.e17.

KETTENMANN, H., HANISCH, U. K., NODA, M. & VERKHRATSKY, A. 2011. Physiology of microglia. *Physiol Rev,* 91**,** 461-553.

KETTENMANN, H., KIRCHHOFF, F. & VERKHRATSKY, A. 2013. Microglia: new roles for the synaptic stripper. *Neuron,* 77**,** 10-8.

KIERDORF, K., ERNY, D., GOLDMANN, T., SANDER, V., SCHULZ, C., PERDIGUERO, E. G., WIEGHOFER, P., HEINRICH, A., RIEMKE, P., HÖLSCHER, C., MÜLLER, D. N., LUCKOW, B., BROCKER, T., DEBOWSKI, K., FRITZ, G., OPDENAKKER, G., DIEFENBACH, A., BIBER, K., HEIKENWALDER, M., GEISSMANN, F., ROSENBAUER, F. & PRINZ, M. 2013. Microglia emerge from erythromyeloid precursors via Pu.1- and Irf8-dependent pathways. *Nat Neurosci,* 16**,** 273-80.

KIM, D., KIM, C. H., MOON, J. I., CHUNG, Y. G., CHANG, M. Y., HAN, B. S., KO, S., YANG, E., CHA, K. Y., LANZA, R. & KIM, K. S. 2009. Generation of human induced pluripotent stem cells by direct delivery of reprogramming proteins. *Cell Stem Cell,* 4**,** 472-6.

KITAMURA, T., MIYAKE, T. & FUJITA, S. 1984. Genesis of resting microglia in the gray matter of mouse hippocampus. *J Comp Neurol,* 226**,** 421-33.

KLEEBERGER, C. A., LYLES, R. H., MARGOLICK, J. B., RINALDO, C. R., PHAIR, J. P. & GIORGI, J. V. 1999. Viability and recovery of peripheral blood mononuclear cells cryopreserved for up to 12 years in a multicenter study. *Clin Diagn Lab Immunol,* 6**,** 14-9.

KLEINBERGER, G., YAMANISHI, Y., SUÁREZ-CALVET, M., CZIRR, E., LOHMANN, E., CUYVERS, E., STRUYFS, H., PETTKUS, N., WENNINGER-WEINZIERL, A., MAZAHERI, F., TAHIROVIC, S., LLEÓ, A., ALCOLEA, D., FORTEA, J., WILLEM, M., LAMMICH, S., MOLINUEVO, J. L., SÁNCHEZ-VALLE, R., ANTONELL, A., RAMIREZ, A., HENEKA, M. T., SLEEGERS, K., VAN DER ZEE, J., MARTIN, J. J., ENGELBORGHS, S., DEMIRTAS-TATLIDEDE, A., ZETTERBERG, H., VAN BROECKHOVEN, C., GURVIT, H., WYSS-CORAY, T., HARDY, J., COLONNA, M. & HAASS, C. 2014. TREM2 mutations implicated in neurodegeneration impair cell surface transport and phagocytosis. *Sci Transl Med,* 6**,** 243ra86.

KLEINEIDAM, L., CHOURAKI, V., PRÓCHNICKI, T., VAN DER LEE, S. J., MADRID-MÁRQUEZ, L., WAGNER-THELEN, H., KARACA, I., WEINHOLD, L., WOLFSGRUBER, S., BOLAND, A., MARTINO ADAMI, P. V., LEWCZUK, P., POPP, J., BROSSERON, F., JANSEN, I. E., HULSMAN, M., KORNHUBER, J., PETERS, O., BERR, C., HEUN, R., FRÖLICH, L., TZOURIO, C., DARTIGUES, J. F., HÜLL, M., ESPINOSA, A., HERNÁNDEZ, I., DE ROJAS, I., ORELLANA, A., VALERO, S., STRINGA, N., VAN SCHOOR, N. M., HUISMAN, M., SCHELTENS, P., RÜTHER, E., DELEUZE, J. F., WILTFANG, J., TARRAGA, L., SCHMID, M., SCHERER, M., RIEDEL-HELLER, S., HENEKA, M. T., AMOUYEL, P., JESSEN, F., BOADA, M., MAIER, W., SCHNEIDER, A., GONZÁLEZ-PÉREZ, A., VAN DER FLIER, W. M., WAGNER, M., LAMBERT, J. C., HOLSTEGE, H., SÁEZ, M. E., LATZ, E., RUIZ, A. & RAMIREZ, A. 2020. PLCG2 protective variant p.P522R modulates tau pathology and disease progression in patients with mild cognitive impairment. *Acta Neuropathol,* 139**,** 1025-1044.

KNOWLES, R. G. & MONCADA, S. 1994. Nitric oxide synthases in mammals. *Biochem J,* 298 (Pt 2)**,** 249-58.

KOBER, D. L. & BRETT, T. J. 2017. TREM2-Ligand Interactions in Health and Disease. *J Mol Biol,* 429**,** 1607-1629.

KOIZUMI, S., SHIGEMOTO-MOGAMI, Y., NASU-TADA, K., SHINOZAKI, Y., OHSAWA, K., TSUDA, M., JOSHI, B. V., JACOBSON, K. A., KOHSAKA, S. & INOUE, K. 2007. UDP acting at P2Y6 receptors is a mediator of microglial phagocytosis. *Nature,* 446**,** 1091-5.

KONISHI, H. & KIYAMA, H. 2018. Microglial TREM2/DAP12 Signaling: A Double-Edged Sword in Neural Diseases. *Front Cell Neurosci,* 12**,** 206.

KOPP, R., KRAUTLOHER, A., RAMÍREZ-FERNÁNDEZ, A. & NICKE, A. 2019. P2X7 Interactions and Signaling - Making Head or Tail of It. *Front Mol Neurosci,* 12**,** 183.

KRAMER, J., STEINHOFF, J., KLINGER, M., FRICKE, L. & ROHWEDEL, J. 2006. Cells differentiated from mouse embryonic stem cells via embryoid bodies express renal marker molecules. *Differentiation,* 74**,** 91-104.

KRISHNA, S., XIE, D., GORENTLA, B., SHIN, J., GAO, J. & ZHONG, X. P. 2012. Chronic activation of the kinase IKKβ impairs T cell function and survival. *J Immunol,* 189**,** 1209-19.

KUMAR, A., SINGH, A. & EKAVALI 2015. A review on Alzheimer's disease pathophysiology and its management: an update. *Pharmacol Rep,* 67**,** 195-203.

KUNKLE, B. W., GRENIER-BOLEY, B., SIMS, R., BIS, J. C., DAMOTTE, V., NAJ, A. C., BOLAND, A., VRONSKAYA, M., VAN DER LEE, S. J., AMLIE-WOLF, A., BELLENGUEZ, C., FRIZATTI, A., CHOURAKI, V., MARTIN, E. R., SLEEGERS, K., BADARINARAYAN, N., JAKOBSDOTTIR, J., HAMILTON-NELSON, K. L., MORENO-GRAU, S., OLASO, R., RAYBOULD, R., CHEN, Y., KUZMA, A. B., HILTUNEN, M., MORGAN, T., AHMAD, S., VARDARAJAN, B. N., EPELBAUM, J., HOFFMANN, P., BOADA, M., BEECHAM, G. W., GARNIER, J. G., HAROLD, D., FITZPATRICK, A. L., VALLADARES, O., MOUTET, M. L., GERRISH, A., SMITH, A. V., QU, L., BACQ, D., DENNING, N., JIAN, X., ZHAO, Y., DEL ZOMPO, M., FOX, N. C., CHOI, S. H., MATEO, I., HUGHES, J. T., ADAMS, H. H., MALAMON, J., SANCHEZ-GARCIA, F., PATEL, Y., BRODY, J. A., DOMBROSKI, B. A., NARANJO, M. C. D., DANIILIDOU, M., EIRIKSDOTTIR, G., MUKHERJEE, S., WALLON, D., UPHILL, J., ASPELUND, T., CANTWELL, L. B., GARZIA, F., GALIMBERTI, D., HOFER, E., BUTKIEWICZ, M., FIN, B., SCARPINI, E., SARNOWSKI, C., BUSH, W. S., MESLAGE, S., KORNHUBER, J., WHITE, C. C., SONG, Y., BARBER, R. C., ENGELBORGHS, S., SORDON, S., VOIJNOVIC, D., ADAMS, P. M., VANDENBERGHE, R., MAYHAUS, M., CUPPLES, L. A., ALBERT, M. S., DE DEYN, P. P., GU, W., HIMALI, J. J., BEEKLY, D., SQUASSINA, A., HARTMANN, A. M., ORELLANA, A., BLACKER, D., RODRIGUEZ-RODRIGUEZ, E., LOVESTONE, S., GARCIA, M. E., DOODY, R. S., MUNOZ-FERNADEZ, C., SUSSAMS, R., LIN, H., FAIRCHILD, T. J., BENITO, Y. A., et al. 2019a. Genetic meta-analysis of diagnosed Alzheimer's disease identifies new risk loci and implicates Abeta, tau, immunity and lipid processing. *Nat Genet,* 51**,** 414-430.

KUNKLE, B. W., GRENIER-BOLEY, B., SIMS, R., BIS, J. C., DAMOTTE, V., NAJ, A. C., BOLAND, A., VRONSKAYA, M., VAN DER LEE, S. J., AMLIE-WOLF, A., BELLENGUEZ, C., FRIZATTI, A., CHOURAKI, V., MARTIN, E. R., SLEEGERS, K., BADARINARAYAN, N., JAKOBSDOTTIR,

J., HAMILTON-NELSON, K. L., MORENO-GRAU, S., OLASO, R., RAYBOULD, R., CHEN, Y., KUZMA, A. B., HILTUNEN, M., MORGAN, T., AHMAD, S., VARDARAJAN, B. N., EPELBAUM, J., HOFFMANN, P., BOADA, M., BEECHAM, G. W., GARNIER, J. G., HAROLD, D., FITZPATRICK, A. L., VALLADARES, O., MOUTET, M. L., GERRISH, A., SMITH, A. V., QU, L., BACQ, D., DENNING, N., JIAN, X., ZHAO, Y., DEL ZOMPO, M., FOX, N. C., CHOI, S. H., MATEO, I., HUGHES, J. T., ADAMS, H. H., MALAMON, J., SANCHEZ-GARCIA, F., PATEL, Y., BRODY, J. A., DOMBROSKI, B. A., NARANJO, M. C. D., DANIILIDOU, M., EIRIKSDOTTIR, G., MUKHERJEE, S., WALLON, D., UPHILL, J., ASPELUND, T., CANTWELL, L. B., GARZIA, F., GALIMBERTI, D., HOFER, E., BUTKIEWICZ, M., FIN, B., SCARPINI, E., SARNOWSKI, C., BUSH, W. S., MESLAGE, S., KORNHUBER, J., WHITE, C. C., SONG, Y., BARBER, R. C., ENGELBORGHS, S., SORDON, S., VOIJNOVIC, D., ADAMS, P. M., VANDENBERGHE, R., MAYHAUS, M., CUPPLES, L. A., ALBERT, M. S., DE DEYN, P. P., GU, W., HIMALI, J. J., BEEKLY, D., SQUASSINA, A., HARTMANN, A. M., ORELLANA, A., BLACKER, D., RODRIGUEZ-RODRIGUEZ, E., LOVESTONE, S., GARCIA, M. E., DOODY, R. S., MUNOZ-FERNADEZ, C., SUSSAMS, R., LIN, H., FAIRCHILD, T. J., BENITO, Y. A., et al. 2019b. Genetic meta-analysis of diagnosed Alzheimer's disease identifies new risk loci and implicates Aβ, tau, immunity and lipid processing. *Nat Genet,* 51**,** 414-430.

KUROSAKI, T. & TSUKADA, S. 2000. BLNK: connecting Syk and Btk to calcium signals. *Immunity,* 12**,** 1-5.

KUROSAWA, H. 2007. Methods for inducing embryoid body formation: in vitro differentiation system of embryonic stem cells. *J Biosci Bioeng,* 103**,** 389-98.

KUTUKCULER, N., TOPYILDIZ, E., BERDELI, A., GUVEN BILGIN, B., AYKUT, A., DURMAZ, A., COGULU, O., AKSU, G. & EDEER KARACA, N. 2021. Four diseases, PLAID, APLAID, FCAS3 and CVID and one gene (PHOSPHOLIPASE C, GAMMA-2; PLCG2): Striking clinical phenotypic overlap and difference. *Clin Case Rep,* 9**,** 2023-2031.

LAMBERT, J. C., HEATH, S., EVEN, G., CAMPION, D., SLEEGERS, K., HILTUNEN, M., COMBARROS, O., ZELENIKA, D., BULLIDO, M. J., TAVERNIER, B., LETENNEUR, L., BETTENS, K., BERR, C., PASQUIER, F., FIEVET, N., BARBERGER-GATEAU, P., ENGELBORGHS, S., DE DEYN, P., MATEO, I., FRANCK, A., HELISALMI, S., PORCELLINI, E., HANON, O., DE PANCORBO, M. M., LENDON, C., DUFOUIL, C., JAILLARD, C., LEVEILLARD, T., ALVAREZ, V., BOSCO, P., MANCUSO, M., PANZA, F., NACMIAS, B., BOSSU, P., PICCARDI, P., ANNONI, G., SERIPA, D., GALIMBERTI, D., HANNEQUIN, D., LICASTRO, F., SOININEN, H., RITCHIE, K., BLANCHE, H., DARTIGUES, J. F., TZOURIO, C., GUT, I., VAN BROECKHOVEN, C., ALPEROVITCH, A., LATHROP, M. & AMOUYEL, P. 2009. Genome-wide association study identifies variants at CLU and CR1 associated with Alzheimer's disease. *Nat Genet,* 41**,** 1094-9.

LAMBERT, J. C., IBRAHIM-VERBAAS, C. A., HAROLD, D., NAJ, A. C., SIMS, R., BELLENGUEZ, C., DESTAFANO, A. L., BIS, J. C., BEECHAM, G. W., GRENIER-BOLEY, B., RUSSO, G., THORTON-WELLS, T. A., JONES, N., SMITH, A. V., CHOURAKI, V., THOMAS, C., IKRAM, M. A., ZELENIKA, D., VARDARAJAN, B. N., KAMATANI, Y., LIN, C. F., GERRISH, A., SCHMIDT, H., KUNKLE, B., DUNSTAN, M. L., RUIZ, A., BIHOREAU, M. T., CHOI, S. H., REITZ, C., PASQUIER, F., CRUCHAGA, C., CRAIG, D., AMIN, N., BERR, C., LOPEZ, O. L., DE JAGER, P. L., DERAMECOURT, V., JOHNSTON, J. A., EVANS, D., LOVESTONE, S., LETENNEUR, L., MORON, F. J., RUBINSZTEIN, D. C., EIRIKSDOTTIR, G., SLEEGERS, K.,

GOATE, A. M., FIEVET, N., HUENTELMAN, M. W., GILL, M., BROWN, K., KAMBOH, M. I., KELLER, L., BARBERGER-GATEAU, P., MCGUINESS, B., LARSON, E. B., GREEN, R., MYERS, A. J., DUFOUIL, C., TODD, S., WALLON, D., LOVE, S., ROGAEVA, E., GALLACHER, J., ST GEORGE-HYSLOP, P., CLARIMON, J., LLEO, A., BAYER, A., TSUANG, D. W., YU, L., TSOLAKI, M., BOSSU, P., SPALLETTA, G., PROITSI, P., COLLINGE, J., SORBI, S., SANCHEZ-GARCIA, F., FOX, N. C., HARDY, J., DENIZ NARANJO, M. C., BOSCO, P., CLARKE, R., BRAYNE, C., GALIMBERTI, D., MANCUSO, M., MATTHEWS, F., MOEBUS, S., MECOCCI, P., DEL ZOMPO, M., MAIER, W., HAMPEL, H., PILOTTO, A., BULLIDO, M., PANZA, F., CAFFARRA, P., NACMIAS, B., GILBERT, J. R., MAYHAUS, M., LANNEFELT, L., HAKONARSON, H., PICHLER, S., et al. 2013. Meta-analysis of 74,046 individuals identifies 11 new susceptibility loci for Alzheimer's disease. *Nat Genet,* 45**,** 1452-8.

LANE, C. A., HARDY, J. & SCHOTT, J. M. 2018. Alzheimer's disease. *Eur J Neurol,* 25**,** 59-70.

LAWSON, L. J., PERRY, V. H., DRI, P. & GORDON, S. 1990. Heterogeneity in the distribution and morphology of microglia in the normal adult mouse brain. *Neuroscience,* 39**,** 151-70.

LAWSON, L. J., PERRY, V. H. & GORDON, S. 1992. Turnover of resident microglia in the normal adult mouse brain. *Neuroscience,* 48**,** 405-15.

LEE, G., NEVE, R. L. & KOSIK, K. S. 1989. The microtubule binding domain of tau protein. *Neuron,* 2**,** 1615-24.

LEE, G. S., SUBRAMANIAN, N., KIM, A. I., AKSENTIJEVICH, I., GOLDBACH-MANSKY, R., SACKS, D. B., GERMAIN, R. N., KASTNER, D. L. & CHAE, J. J. 2012a. The calcium-sensing receptor regulates the NLRP3 inflammasome through Ca2+ and cAMP. *Nature,* 492**,** 123-7.

LEE, H. G., WON, S. M., GWAG, B. J. & LEE, Y. B. 2011. Microglial $P2X_7$ receptor expression is accompanied by neuronal damage in the cerebral cortex of the APPswe/PS1dE9 mouse model of Alzheimer's disease. *Exp Mol Med,* 43**,** 7-14.

LEE, J., SAYED, N., HUNTER, A., AU, K. F., WONG, W. H., MOCARSKI, E. S., PERA, R. R., YAKUBOV, E. & COOKE, J. P. 2012b. Activation of innate immunity is required for efficient nuclear reprogramming. *Cell,* 151**,** 547-58.

LEE, S., VARVEL, N. H., KONERTH, M. E., XU, G., CARDONA, A. E., RANSOHOFF, R. M. & LAMB, B. T. 2010. CX3CR1 deficiency alters microglial activation and reduces beta-amyloid deposition in two Alzheimer's disease mouse models. *Am J Pathol,* 177**,** 2549-62.

LEE, S. H., HAROLD, D., NYHOLT, D. R., GODDARD, M. E., ZONDERVAN, K. T., WILLIAMS, J., MONTGOMERY, G. W., WRAY, N. R. & VISSCHER, P. M. 2013. Estimation and partitioning of polygenic variation captured by common SNPs for Alzheimer's disease, multiple sclerosis and endometriosis. *Hum Mol Genet,* 22**,** 832-41.

LEHNARDT, S. 2010. Innate immunity and neuroinflammation in the CNS: the role of microglia in Toll-like receptor-mediated neuronal injury. *Glia,* 58**,** 253-63.

LENG, F. & EDISON, P. 2021. Neuroinflammation and microglial activation in Alzheimer disease: where do we go from here? *Nat Rev Neurol,* 17**,** 157-172.

LESNÉ, S., KOTILINEK, L. & ASHE, K. H. 2008. Plaque-bearing mice with reduced levels of oligomeric amyloid-beta assemblies have intact memory function. *Neuroscience,* 151**,** 745-9.

LI, L. & SHI, Y. 2020. When glia meet induced pluripotent stem cells (iPSCs). *Mol Cell Neurosci,* 109**,** 103565.

LI, Z., LI, W., LI, Q. & TANG, M. 2013. Extracellular nucleotides and adenosine regulate microglial motility and their role in cerebral ischemia. *Acta Pharmaceutica Sinica B,* 3**,** 205-212.

LIDDELOW, S. A. & BARRES, B. A. 2017. Reactive Astrocytes: Production, Function, and Therapeutic Potential. *Immunity,* 46**,** 957-967.

LIN, C. F., NAJ, A. C. & WANG, L. S. 2013. Analyzing copy number variation using SNP array data: protocols for calling CNV and association tests. *Curr Protoc Hum Genet,* 79**,** Unit 1.27.

LIN, X., O'MAHONY, A., MU, Y., GELEZIUNAS, R. & GREENE, W. C. 2000. Protein kinase C-theta participates in NF-kappaB activation induced by CD3-CD28 costimulation through selective activation of IkappaB kinase beta. *Mol Cell Biol,* 20**,** 2933-40.

LIN, Y. & CHEN, G. 2008. Embryoid body formation from human pluripotent stem cells in chemically defined E8 media. *StemBook.* Cambridge (MA): Harvard Stem Cell Institute

LIU, C. C., LIU, C. C., KANEKIYO, T., XU, H. & BU, G. 2013. Apolipoprotein E and Alzheimer disease: risk, mechanisms and therapy. *Nat Rev Neurol,* 9**,** 106-18.

LIU, T., ZHANG, L., JOO, D. & SUN, S. C. 2017. NF-κB signaling in inflammation. *Signal Transduct Target Ther,* 2**,** 17023-.

LIU, W., BROSNAN, C. F., DICKSON, D. W. & LEE, S. C. 1994. Macrophage colony-stimulating factor mediates astrocyte-induced microglial ramification in human fetal central nervous system culture. *Am J Pathol,* 145**,** 48-53.

LIU, W., TASO, O., WANG, R., BAYRAM, S., GRAHAM, A. C., GARCIA-REITBOECK, P., MALLACH, A., ANDREWS, W. D., PIERS, T. M., BOTIA, J. A., POCOCK, J. M., CUMMINGS, D. M., HARDY, J., EDWARDS, F. A. & SALIH, D. A. 2020. Trem2 promotes anti-inflammatory responses in microglia and is suppressed under pro-inflammatory conditions. *Hum Mol Genet,* 29**,** 3224-3248.

LIU, Y., WALTER, S., STAGI, M., CHERNY, D., LETIEMBRE, M., SCHULZ-SCHAEFFER, W., HEINE, H., PENKE, B., NEUMANN, H. & FASSBENDER, K. 2005. LPS receptor (CD14): a receptor for phagocytosis of Alzheimer's amyloid peptide. *Brain,* 128**,** 1778-89.

LIVELY, S. & SCHLICHTER, L. C. 2018. Microglia Responses to Pro-inflammatory Stimuli (LPS, IFNγ+TNFα) and Reprogramming by Resolving Cytokines (IL-4, IL-10). *Front Cell Neurosci,* 12**,** 215.

LOBO-SILVA, D., CARRICHE, G. M., CASTRO, A. G., ROQUE, S. & SARAIVA, M. 2016. Balancing the immune response in the brain: IL-10 and its regulation. *J Neuroinflammation,* 13**,** 297.

LOH, Y. H., AGARWAL, S., PARK, I. H., URBACH, A., HUO, H., HEFFNER, G. C., KIM, K., MILLER, J. D., NG, K. & DALEY, G. Q. 2009. Generation of induced pluripotent stem cells from human blood. *Blood,* 113**,** 5476-9.

LORD, J., LU, A. J. & CRUCHAGA, C. 2014. Identification of rare variants in Alzheimer's disease. *Frontiers in Genetics,* 5.

LYMAN, M., LLOYD, D. G., JI, X., VIZCAYCHIPI, M. P. & MA, D. 2014. Neuroinflammation: the role and consequences. *Neurosci Res,* 79**,** 1-12.

MA, D., LIAN, F. & WANG, X. 2019. PLCG2 promotes hepatocyte proliferation in vitro via NF-κB and ERK pathway by targeting bcl2, myc and ccnd1. *Artif Cells Nanomed Biotechnol,* 47**,** 3786-3792.

MACK, A. A., KROBOTH, S., RAJESH, D. & WANG, W. B. 2011. Generation of induced pluripotent stem cells from CD34+ cells across blood drawn from multiple donors with non-integrating episomal vectors. *PLoS One,* 6**,** e27956.

MAGNO, L., BUNNEY, T. D., MEAD, E., SVENSSON, F. & BICTASH, M. N. 2021. TREM2/PLCγ2 signalling in immune cells: function, structural insight, and potential therapeutic modulation. *Mol Neurodegener,* 16**,** 22.

MAGNO, L., LESSARD, C. B., MARTINS, M., LANG, V., CRUZ, P., ASI, Y., KATAN, M., BILSLAND, J., LASHLEY, T., CHAKRABARTY, P., GOLDE, T. E. & WHITING, P. J. 2019. Alzheimer's disease phospholipase C-gamma-2 (PLCG2) protective variant is a functional hypermorph. *Alzheimers Res Ther,* 11**,** 16.

MAGUIRE, E., MENZIES, G. E., PHILLIPS, T., SASNER, M., WILLIAMS, H. M., CZUBALA, M. A., EVANS, N., COPE, E. L., SIMS, R., HOWELL, G. R., LLOYD-EVANS, E., WILLIAMS, J., ALLEN, N. D. & TAYLOR, P. R. 2021. PIP2 depletion and altered endocytosis caused by expression of Alzheimer's disease-protective variant PLCγ2 R522. *Embo j***,** e105603.

MAJADO, M. J., SALGADO-CECILIA, G., BLANQUER, M., FUNES, C., GONZÁLEZ-GARCÍA, C., INSAUSTI, C. L., PARRADO, A., MORALES, A., MINGUELA, A. & MORALEDA, J. M. 2011. Cryopreservation impact on blood progenitor cells: influence of diagnoses, mobilization treatments, and cell concentration. *Transfusion,* 51**,** 799-807.

MALIK, M., PARIKH, I., VASQUEZ, J. B., SMITH, C., TAI, L., BU, G., LADU, M. J., FARDO, D. W., REBECK, G. W. & ESTUS, S. 2015. Genetics ignite focus on microglial inflammation in Alzheimer's disease. *Mol Neurodegener,* 10**,** 52.

MARTIN, G. R. & EVANS, M. J. 1975. Differentiation of clonal lines of teratocarcinoma cells: formation of embryoid bodies in vitro. *Proc Natl Acad Sci U S A,* 72**,** 1441-5.

MASS, E., BALLESTEROS, I., FARLIK, M., HALBRITTER, F., GÜNTHER, P., CROZET, L., JACOME-GALARZA, C. E., HÄNDLER, K., KLUGHAMMER, J., KOBAYASHI, Y., GOMEZ-PERDIGUERO, E., SCHULTZE, J. L., BEYER, M., BOCK, C. & GEISSMANN, F. 2016. Specification of tissue-resident macrophages during organogenesis. *Science,* 353.

MENZIES G.E., P. T., MAGUIRE E., SASNER M, WILLIAMS H. M., CZUBALA M. A., EVANS N., COPE E.L., SIMS R., HOWELL G.R., LLOYD-EVANS E., WILLIAMS J., ALLEN N.D. AND TAYLOR P.R. 2020. Protective coding variant for Alzheimer's disease in PLCG2 shows consistently enhanced PLCγ2 activation in microglia.

MERLING, R. K., SWEENEY, C. L., CHOI, U., DE RAVIN, S. S., MYERS, T. G., OTAIZO-CARRASQUERO, F., PAN, J., LINTON, G., CHEN, L., KOONTZ, S., THEOBALD, N. L. & MALECH, H. L. 2013. Transgene-free iPSCs generated from small volume peripheral blood nonmobilized CD34+ cells. *Blood,* 121**,** e98-107.

MERRILL, J. E., IGNARRO, L. J., SHERMAN, M. P., MELINEK, J. & LANE, T. E. 1993. Microglial cell cytotoxicity of oligodendrocytes is mediated through nitric oxide. *J Immunol,* 151**,** 2132-41.

MESHKI, J., TULUC, F., BREDETEAN, O., GARCIA, A. & KUNAPULI, S. P. 2006. Signaling pathways downstream of P2 receptors in human neutrophils. *Purinergic Signal,* 2**,** 537-44.

MICHEAU, O. & TSCHOPP, J. 2003. Induction of TNF receptor I-mediated apoptosis via two sequential signaling complexes. *Cell,* 114**,** 181-90.

MISHRA, A., KIM, H. J., SHIN, A. H. & THAYER, S. A. 2012. Synapse loss induced by interleukin-1β requires pre- and post-synaptic mechanisms. *J Neuroimmune Pharmacol,* 7**,** 571-8.

MISHRA, S., KACIN, E., STAMATIADIS, P., FRANCK, S., VAN DER JEUGHT, M., MERTES, H., PENNINGS, G., DE SUTTER, P., SERMON, K., HEINDRYCKX, B. & GEENS, M. 2018. The role of the reprogramming method and pluripotency state in gamete differentiation from patient-specific human pluripotent stem cells. *Mol Hum Reprod,* 24**,** 173-184.

MONSELL, S. E., KUKULL, W. A., ROHER, A. E., MAAROUF, C. L., SERRANO, G., BEACH, T. G., CASELLI, R. J., MONTINE, T. J. & REIMAN, E. M. 2015. Characterizing Apolipoprotein E ε4 Carriers and Noncarriers With the Clinical Diagnosis of Mild to Moderate Alzheimer Dementia and Minimal β-Amyloid Peptide Plaques. *JAMA Neurol,* 72**,** 1124-31.

MORAS, M., LEFEVRE, S. D. & OSTUNI, M. A. 2017. From Erythroblasts to Mature Red Blood Cells: Organelle Clearance in Mammals. *Front Physiol,* 8**,** 1076.

MOSCAT, J., DIAZ-MECO, M. T. & RENNERT, P. 2003. NF-kappaB activation by protein kinase C isoforms and B-cell function. *EMBO Rep,* 4**,** 31-6.

MUELLER, H., STADTMANN, A., VAN AKEN, H., HIRSCH, E., WANG, D., LEY, K. & ZARBOCK, A. 2010. Tyrosine kinase Btk regulates E-selectin-mediated integrin activation and neutrophil recruitment by controlling phospholipase C (PLC) gamma2 and PI3Kgamma pathways. *Blood,* 115**,** 3118-27.

MUFFAT, J., LI, Y., YUAN, B., MITALIPOVA, M., OMER, A., CORCORAN, S., BAKIASI, G., TSAI, L. H., AUBOURG, P., RANSOHOFF, R. M. & JAENISCH, R. 2016. Efficient derivation of microglia-like cells from human pluripotent stem cells. *Nat Med,* 22**,** 1358-1367.

MULLER, F. J., SCHULDT, B. M., WILLIAMS, R., MASON, D., ALTUN, G., PAPAPETROU, E. P., DANNER, S., GOLDMANN, J. E., HERBST, A., SCHMIDT, N. O., ALDENHOFF, J. B., LAURENT, L. C. & LORING, J. F. 2011. A bioinformatic assay for pluripotency in human cells. *Nat Methods,* 8**,** 315-7.

MURABE, Y. & SANO, Y. 1983. Morphological studies on neuroglia. VII. Distribution of "brain macrophages" in brains of neonatal and adult rats, as determined by means of immunohistochemistry. *Cell Tissue Res,* 229**,** 85-95.

MURAKAMI, T., OCKINGER, J., YU, J., BYLES, V., MCCOLL, A., HOFER, A. M. & HORNG, T. 2012. Critical role for calcium mobilization in activation of the NLRP3 inflammasome. *Proc Natl Acad Sci U S A,* 109**,** 11282-7.

NAJ, A. C., JUN, G., BEECHAM, G. W., WANG, L. S., VARDARAJAN, B. N., BUROS, J., GALLINS, P. J., BUXBAUM, J. D., JARVIK, G. P., CRANE, P. K., LARSON, E. B., BIRD, T. D., BOEVE, B. F., GRAFF-RADFORD, N. R., DE JAGER, P. L., EVANS, D., SCHNEIDER, J. A., CARRASQUILLO, M. M., ERTEKIN-TANER, N., YOUNKIN, S. G., CRUCHAGA, C., KAUWE, J. S., NOWOTNY, P., KRAMER, P., HARDY, J., HUENTELMAN, M. J., MYERS, A. J., BARMADA, M. M., DEMIRCI, F. Y., BALDWIN, C. T., GREEN, R. C., ROGAEVA, E., ST GEORGE-HYSLOP, P., ARNOLD, S. E., BARBER, R., BEACH, T., BIGIO, E. H., BOWEN, J. D., BOXER, A., BURKE, J. R., CAIRNS, N. J., CARLSON, C. S., CARNEY, R. M., CARROLL, S. L., CHUI, H. C., CLARK, D. G., CORNEVEAUX, J., COTMAN, C. W., CUMMINGS, J. L., DECARLI, C., DEKOSKY, S. T., DIAZ-ARRASTIA, R., DICK, M., DICKSON, D. W., ELLIS, W. G., FABER, K. M., FALLON, K. B., FARLOW, M. R., FERRIS, S., FROSCH, M. P., GALASKO, D. R., GANGULI, M., GEARING, M., GESCHWIND, D. H., GHETTI, B., GILBERT, J. R., GILMAN, S., GIORDANI, B., GLASS, J. D., GROWDON, J. H., HAMILTON, R. L., HARRELL, L. E., HEAD, E., HONIG, L. S., HULETTE, C. M., HYMAN, B. T., JICHA, G. A., JIN, L. W., JOHNSON, N., KARLAWISH, J., KARYDAS, A., KAYE, J. A., KIM, R., KOO, E. H., KOWALL, N. W., LAH, J. J., LEVEY, A. I., LIEBERMAN, A. P., LOPEZ, O. L., MACK, W. J., MARSON, D. C., MARTINIUK, F., MASH, D. C., MASLIAH, E., MCCORMICK, W. C., MCCURRY, S. M., MCDAVID, A. N., MCKEE, A. C., MESULAM, M., MILLER, B. L., et al. 2011. Common variants at MS4A4/MS4A6E, CD2AP, CD33 and EPHA1 are associated with late-onset Alzheimer's disease. *Nat Genet,* 43**,** 436-41.

NAJ, A. C., LEONENKO, G., JIAN, X., GRENIER-BOLEY, B., DALMASSO, M. C., BELLENGUEZ, C., SHA, J., ZHAO, Y., VAN DER LEE, S. J., SIMS, R., CHOURAKI, V., BIS, J. C., KUNKLE, B. W., HOLMANS, P., LEUNG, Y. Y., FARRELL, J. J., CHESI, A., CHEN, H.-H., VARDARAJAN, B., BENCHEK, P., BARRAL, S., LEE, C.-Y., KUKSA, P., HAUT, J., LEE, E. B., LI, M., ZHANG, Y., GRANT, S., PHILLIPS-CREMINS, J. E., COMIC, H., PITSILLIDES, A., XIA, R., HAMILTON-NELSON, K. L., KUZMA, A., VALLADARES, O., FULTON-HOWARD, B.,

DUPUIS, J., BUSH, W. S., WANG, L.-S., BELOW, J. E., FARRER, L. A., VAN DUIJN, C., MAYEUX, R., HAINES, J. L., DESTEFANO, A. L., PERICAK-VANCE, M. A., RAMIREZ, A., SESHADRI, S., AMOUYEL, P., WILLIAMS, J., LAMBERT, J.-C. & SCHELLENBERG, G. D. 2021. Genome-Wide Meta-Analysis of Late-Onset Alzheimer's Disease Using Rare Variant Imputation in 65,602 Subjects Identifies Novel Rare Variant Locus NCK2: The International Genomics of Alzheimer's Project (IGAP). *medRxiv***,** 2021.03.14.21253553.

NASERI, N. N., WANG, H., GUO, J., SHARMA, M. & LUO, W. 2019. The complexity of tau in Alzheimer's disease. *Neurosci Lett,* 705**,** 183-194.

NAZARPOUR, R., ZABIHI, E., ALIJANPOUR, E., ABEDIAN, Z., MEHDIZADEH, H. & RAHIMI, F. 2012. Optimization of Human Peripheral Blood Mononuclear Cells (PBMCs) Cryopreservation. *Int J Mol Cell Med,* 1**,** 88-93.

NEMES, C., VARGA, E., POLGAR, Z., KLINCUMHOM, N., PIRITY, M. K. & DINNYES, A. 2014. Generation of mouse induced pluripotent stem cells by protein transduction. *Tissue Eng Part C Methods,* 20**,** 383-92.

NEVES, J. F., DOFFINGER, R., BARCENA-MORALES, G., MARTINS, C., PAPAPIETRO, O., PLAGNOL, V., CURTIS, J., MARTINS, M., KUMARARATNE, D., CORDEIRO, A. I., NEVES, C., BORREGO, L. M., KATAN, M. & NEJENTSEV, S. 2018. Novel PLCG2 Mutation in a Patient With APLAID and Cutis Laxa. *Front Immunol,* 9**,** 2863.

NGUYEN, D. Q., WEBBER, C. & PONTING, C. P. 2006. Bias of selection on human copy-number variants. *PLoS Genet,* 2**,** e20.

NICHOLLS, D. G. 1998. Presynaptic modulation of glutamate release. *Prog Brain Res,* 116**,** 15-22.

NIMMERJAHN, A., KIRCHHOFF, F. & HELMCHEN, F. 2005. Resting microglial cells are highly dynamic surveillants of brain parenchyma in vivo. *Science,* 308**,** 1314-8.

NISHIMURA, K., OHTAKA, M., TAKADA, H., KURISAKI, A., TRAN, N. V. K., TRAN, Y. T. H., HISATAKE, K., SANO, M. & NAKANISHI, M. 2017. Simple and effective generation of transgene-free induced pluripotent stem cells using an auto-erasable Sendai virus vector responding to microRNA-302. *Stem Cell Res,* 23**,** 13-19.

NOSTRO, M. C., SARANGI, F., OGAWA, S., HOLTZINGER, A., CORNEO, B., LI, X., MICALLEF, S. J., PARK, I. H., BASFORD, C., WHEELER, M. B., DALEY, G. Q., ELEFANTY, A. G., STANLEY, E. G. & KELLER, G. 2011. Stage-specific signaling through TGFβ family members and WNT regulates patterning and pancreatic specification of human pluripotent stem cells. *Development,* 138**,** 861-71.

NOVICE, T., KARIMINIA, A., DEL BEL, K. L., LU, H., SHARMA, M., LIM, C. J., READ, J., LUGT, M. V., HANNIBAL, M. C., O'DWYER, D., HOSLER, M., SCHARNITZ, T., RIZZO, J. M., ZACUR, J., PRIATEL, J., ABDOSSAMADI, S., BOHM, A., JUNKER, A., TURVEY, S. E., SCHULTZ, K. R. & ROZMUS, J. 2020. A Germline Mutation in the C2 Domain of PLCγ2 Associated with Gain-of-Function Expands the Phenotype for PLCG2-Related Diseases. *J Clin Immunol,* 40**,** 267-276.

NUNOMURA, A., PERRY, G., ALIEV, G., HIRAI, K., TAKEDA, A., BALRAJ, E. K., JONES, P. K., GHANBARI, H., WATAYA, T., SHIMOHAMA, S., CHIBA, S., ATWOOD, C. S., PETERSEN, R. B. & SMITH, M. A. 2001. Oxidative damage is the earliest event in Alzheimer disease. *J Neuropathol Exp Neurol,* 60**,** 759-67.

O'BRIEN, R. J. & WONG, P. C. 2011. Amyloid precursor protein processing and Alzheimer's disease. *Annu Rev Neurosci,* 34**,** 185-204.

O'NEILL, L. A. & KALTSCHMIDT, C. 1997. NF-kappa B: a crucial transcription factor for glial and neuronal cell function. *Trends Neurosci,* 20**,** 252-8.

OBST, J., HALL-ROBERTS, H. L., SMITH, T. B., KREUZER, M., MAGNO, L., DI DANIEL, E., DAVIS, J. B. & MEAD, E. 2021. PLCγ2 regulates TREM2 signalling and integrin-mediated adhesion and migration of human iPSC-derived macrophages. *Sci Rep,* 11**,** 19842.

OHSAWA, K., IRINO, Y., SANAGI, T., NAKAMURA, Y., SUZUKI, E., INOUE, K. & KOHSAKA, S. 2010. P2Y12 receptor-mediated integrin-beta1 activation regulates microglial process extension induced by ATP. *Glia,* 58**,** 790-801.

OKELLO, A., EDISON, P., ARCHER, H. A., TURKHEIMER, F. E., KENNEDY, J., BULLOCK, R., WALKER, Z., KENNEDY, A., FOX, N., ROSSOR, M. & BROOKS, D. J. 2009. Microglial activation and amyloid deposition in mild cognitive impairment: a PET study. *Neurology,* 72**,** 56-62.

OKITA, K., ICHISAKA, T. & YAMANAKA, S. 2007. Generation of germline-competent induced pluripotent stem cells. *Nature,* 448**,** 313-7.

OKUMURA, T., HORIE, Y., LAI, C. Y., LIN, H. T., SHODA, H., NATSUMOTO, B., FUJIO, K., KUMAKI, E., OKANO, T., ONO, S., TANITA, K., MORIO, T., KANEGANE, H., HASEGAWA, H., MIZOGUCHI, F., KAWAHATA, K., KOHSAKA, H., MORITAKE, H., NUNOI, H., WAKI, H., TAMARU, S. I., SASAKO, T., YAMAUCHI, T., KADOWAKI, T., TANAKA, H., KITANAKA, S., NISHIMURA, K., OHTAKA, M., NAKANISHI, M. & OTSU, M. 2019. Robust and highly efficient hiPSC generation from patient non-mobilized peripheral blood-derived CD34(+) cells using the auto-erasable Sendai virus vector. *Stem Cell Res Ther,* 10**,** 185.

OMBRELLO, M. J., REMMERS, E. F., SUN, G., FREEMAN, A. F., DATTA, S., TORABI-PARIZI, P., SUBRAMANIAN, N., BUNNEY, T. D., BAXENDALE, R. W., MARTINS, M. S., ROMBERG, N., KOMAROW, H., AKSENTIJEVICH, I., KIM, H. S., HO, J., CRUSE, G., JUNG, M. Y., GILFILLAN, A. M., METCALFE, D. D., NELSON, C., O'BRIEN, M., WISCH, L., STONE, K., DOUEK, D. C., GANDHI, C., WANDERER, A. A., LEE, H., NELSON, S. F., SHIANNA, K. V., CIRULLI, E. T., GOLDSTEIN, D. B., LONG, E. O., MOIR, S., MEFFRE, E., HOLLAND, S. M., KASTNER, D. L., KATAN, M., HOFFMAN, H. M. & MILNER, J. D. 2012. Cold urticaria, immunodeficiency, and autoimmunity related to PLCG2 deletions. *N Engl J Med,* 366**,** 330-8.

PANDYA, H., SHEN, M. J., ICHIKAWA, D. M., SEDLOCK, A. B., CHOI, Y., JOHNSON, K. R., KIM, G., BROWN, M. A., ELKAHLOUN, A. G., MARIC, D., SWEENEY, C. L., GOSSA, S., MALECH, H. L., MCGAVERN, D. B. & PARK, J. K. 2017. Differentiation of human and

murine induced pluripotent stem cells to microglia-like cells. *Nat Neurosci,* 20**,** 753-759.

PARESCE, D. M., GHOSH, R. N. & MAXFIELD, F. R. 1996. Microglial cells internalize aggregates of the Alzheimer's disease amyloid beta-protein via a scavenger receptor. *Neuron,* 17**,** 553-65.

PARK, Y. & GERSON, S. L. 2005. DNA repair defects in stem cell function and aging. *Annu Rev Med,* 56**,** 495-508.

PARONI, G., BISCEGLIA, P. & SERIPA, D. 2019. Understanding the Amyloid Hypothesis in Alzheimer's Disease. *J Alzheimers Dis,* 68**,** 493-510.

PATEL, N. S., PARIS, D., MATHURA, V., QUADROS, A. N., CRAWFORD, F. C. & MULLAN, M. J. 2005. Inflammatory cytokine levels correlate with amyloid load in transgenic mouse models of Alzheimer's disease. *J Neuroinflammation,* 2**,** 9.

PENG, Q., MALHOTRA, S., TORCHIA, J. A., KERR, W. G., COGGESHALL, K. M. & HUMPHREY, M. B. 2010. TREM2- and DAP12-dependent activation of PI3K requires DAP10 and is inhibited by SHIP1. *Sci Signal,* 3**,** ra38.

PENGAL, R. A., GANESAN, L. P., WEI, G., FANG, H., OSTROWSKI, M. C. & TRIDANDAPANI, S. 2006. Lipopolysaccharide-induced production of interleukin-10 is promoted by the serine/threonine kinase Akt. *Mol Immunol,* 43**,** 1557-64.

PENNEY, J., RALVENIUS, W. T. & TSAI, L. H. 2020. Modeling Alzheimer's disease with iPSC-derived brain cells. *Mol Psychiatry,* 25**,** 148-167.

PERRY, V. H. & HOLMES, C. 2014. Microglial priming in neurodegenerative disease. *Nat Rev Neurol,* 10**,** 217-24.

PERRY, V. H., HUME, D. A. & GORDON, S. 1985. Immunohistochemical localization of macrophages and microglia in the adult and developing mouse brain. *Neuroscience,* 15**,** 313-26.

PHILIPPENS, I. H., ORMEL, P. R., BAARENDS, G., JOHANSSON, M., REMARQUE, E. J. & DOVERSKOG, M. 2017. Acceleration of Amyloidosis by Inflammation in the Amyloid-Beta Marmoset Monkey Model of Alzheimer's Disease. *J Alzheimers Dis,* 55**,** 101-113.

PŁÓCIENNIKOWSKA, A., HROMADA-JUDYCKA, A., DEMBIŃSKA, J., ROSZCZENKO, P., CIESIELSKA, A. & KWIATKOWSKA, K. 2016. Contribution of CD14 and TLR4 to changes of the PI(4,5)P2 level in LPS-stimulated cells. *J Leukoc Biol,* 100**,** 1363-1373.

POLTORAK, A., HE, X., SMIRNOVA, I., LIU, M. Y., VAN HUFFEL, C., DU, X., BIRDWELL, D., ALEJOS, E., SILVA, M., GALANOS, C., FREUDENBERG, M., RICCIARDI-CASTAGNOLI, P., LAYTON, B. & BEUTLER, B. 1998. Defective LPS signaling in C3H/HeJ and C57BL/10ScCr mice: mutations in Tlr4 gene. *Science,* 282**,** 2085-8.

PONOMAREV, E. D., MARESZ, K., TAN, Y. & DITTEL, B. N. 2007. CNS-derived interleukin-4 is essential for the regulation of autoimmune inflammation and induces a state of alternative activation in microglial cells. *J Neurosci,* 27**,** 10714-21.

PORRO, C., CIANCIULLI, A. & PANARO, M. A. 2020. The Regulatory Role of IL-10 in Neurodegenerative Diseases. *Biomolecules,* 10.

POTTIER, C., RAVENSCROFT, T. A., BROWN, P. H., FINCH, N. A., BAKER, M., PARSONS, M., ASMANN, Y. W., REN, Y., CHRISTOPHER, E., LEVITCH, D., VAN BLITTERSWIJK, M., CRUCHAGA, C., CAMPION, D., NICOLAS, G., RICHARD, A. C., GUERREIRO, R., BRAS, J. T., ZUCHNER, S., GONZALEZ, M. A., BU, G., YOUNKIN, S., KNOPMAN, D. S., JOSEPHS, K. A., PARISI, J. E., PETERSEN, R. C., ERTEKIN-TANER, N., GRAFF-RADFORD, N. R., BOEVE, B. F., DICKSON, D. W. & RADEMAKERS, R. 2016. TYROBP genetic variants in early-onset Alzheimer's disease. *Neurobiol Aging,* 48**,** 222.e9-222.e15.

PRINZ, M., JUNG, S. & PRILLER, J. 2019. Microglia Biology: One Century of Evolving Concepts. *Cell,* 179**,** 292-311.

RAAB, S., KLINGENSTEIN, M., LIEBAU, S. & LINTA, L. 2014. A Comparative View on Human Somatic Cell Sources for iPSC Generation. *Stem Cells Int,* 2014**,** 768391.

RAJENDRAN, L. & PAOLICELLI, R. C. 2018. Microglia-Mediated Synapse Loss in Alzheimer's Disease. *J Neurosci,* 38**,** 2911-2919.

RAKIC, P. 2009. Evolution of the neocortex: a perspective from developmental biology. *Nat Rev Neurosci,* 10**,** 724-35.

RAMESH, M., GOPINATH, P. & GOVINDARAJU, T. 2020. Role of Post-translational Modifications in Alzheimer's Disease. *Chembiochem,* 21**,** 1052-1079.

RAMIREZ-EXPOSITO, M. J. & MARTINEZ-MARTOS, J. M. 1998. [Structure and functions of the macroglia in the central nervous system. Response to degenerative disorders]. *Rev Neurol,* 26**,** 600-11.

RANSOHOFF, R. M. 2016. A polarizing question: do M1 and M2 microglia exist? *Nat Neurosci,* 19**,** 987-91.

RAO, J. S., KELLOM, M., KIM, H. W., RAPOPORT, S. I. & REESE, E. A. 2012. Neuroinflammation and synaptic loss. *Neurochem Res,* 37**,** 903-10.

RAPONI, E., AGENES, F., DELPHIN, C., ASSARD, N., BAUDIER, J., LEGRAVEREND, C. & DELOULME, J. C. 2007. S100B expression defines a state in which GFAP-expressing cells lose their neural stem cell potential and acquire a more mature developmental stage. *Glia,* 55**,** 165-77.

RAPPERT, A., BIBER, K., NOLTE, C., LIPP, M., SCHUBEL, A., LU, B., GERARD, N. P., GERARD, C., BODDEKE, H. W. & KETTENMANN, H. 2002. Secondary lymphoid tissue chemokine (CCL21) activates CXCR3 to trigger a Cl- current and chemotaxis in murine microglia. *J Immunol,* 168**,** 3221-6.

REGEN, F., HELLMANN-REGEN, J., COSTANTINI, E. & REALE, M. 2017. Neuroinflammation and Alzheimer's Disease: Implications for Microglial Activation. *Curr Alzheimer Res,* 14**,** 1140-1148.

REICH, M., PARIS, I., EBELING, M., DAHM, N., SCHWEITZER, C., REINHARDT, D., SCHMUCKI, R., PRASAD, M., KÖCHL, F., LEIST, M., COWLEY, S. A., ZHANG, J. D., PATSCH, C., GUTBIER, S. & BRITSCHGI, M. 2020. Alzheimer's Risk Gene TREM2 Determines Functional Properties of New Type of Human iPSC-Derived Microglia. *Front Immunol,* 11**,** 617860.

RICCIARELLI, R. & FEDELE, E. 2017. The Amyloid Cascade Hypothesis in Alzheimer's Disease: It's Time to Change Our Mind. *Curr Neuropharmacol,* 15**,** 926-935.

RIDGE, P. G., MUKHERJEE, S., CRANE, P. K. & KAUWE, J. S. 2013. Alzheimer's disease: analyzing the missing heritability. *PLoS One,* 8**,** e79771.

RODRIGUES, R. J., TOMÉ, A. R. & CUNHA, R. A. 2015. ATP as a multi-target danger signal in the brain. *Front Neurosci,* 9**,** 148.

ROQUÉ, P. J. & COSTA, L. G. 2017. Co-Culture of Neurons and Microglia. *Curr Protoc Toxicol,* 74**,** 11.24.1-11.24.17.

ROSS, S. H. & CANTRELL, D. A. 2018. Signaling and Function of Interleukin-2 in T Lymphocytes. *Annu Rev Immunol,* 36**,** 411-433.

ROUKA, E., SIMISTER, P. C., JANNING, M., KUMBRINK, J., KONSTANTINOU, T., MUNIZ, J. R., JOSHI, D., O'REILLY, N., VOLKMER, R., RITTER, B., KNAPP, S., VON DELFT, F., KIRSCH, K. H. & FELLER, S. M. 2015. Differential Recognition Preferences of the Three Src Homology 3 (SH3) Domains from the Adaptor CD2-associated Protein (CD2AP) and Direct Association with Ras and Rab Interactor 3 (RIN3). *J Biol Chem,* 290**,** 25275-92.

RUIZ, S., PANOPOULOS, A. D., HERRERÍAS, A., BISSIG, K. D., LUTZ, M., BERGGREN, W. T., VERMA, I. M. & IZPISUA BELMONTE, J. C. 2011. A high proliferation rate is required for cell reprogramming and maintenance of human embryonic stem cell identity. *Curr Biol,* 21**,** 45-52.

RUSHTON, D. J., MATTIS, V. B., SVENDSEN, C. N., ALLEN, N. D. & KEMP, P. J. 2013. Stimulation of GABA-induced Ca2+ influx enhances maturation of human induced pluripotent stem cell-derived neurons. *PLoS One,* 8**,** e81031.

SAHA, R. N. & PAHAN, K. 2006. Regulation of inducible nitric oxide synthase gene in glial cells. *Antioxid Redox Signal,* 8**,** 929-47.

SALLOWAY, S., SPERLING, R., FOX, N. C., BLENNOW, K., KLUNK, W., RASKIND, M., SABBAGH, M., HONIG, L. S., PORSTEINSSON, A. P., FERRIS, S., REICHERT, M., KETTER, N., NEJADNIK, B., GUENZLER, V., MILOSLAVSKY, M., WANG, D., LU, Y., LULL, J., TUDOR, I. C., LIU, E., GRUNDMAN, M., YUEN, E., BLACK, R. & BRASHEAR, H. R. 2014. Two phase 3 trials of bapineuzumab in mild-to-moderate Alzheimer's disease. *N Engl J Med,* 370**,** 322-33.

SANZ, J. M., CHIOZZI, P., FERRARI, D., COLAIANNA, M., IDZKO, M., FALZONI, S., FELLIN, R., TRABACE, L. & DI VIRGILIO, F. 2009. Activation of microglia by amyloid {beta} requires P2X7 receptor expression. *J Immunol,* 182**,** 4378-85.

SAVARIN-VUAILLAT, C. & RANSOHOFF, R. M. 2007. Chemokines and chemokine receptors in neurological disease: raise, retain, or reduce? *Neurotherapeutics,* 4**,** 590-601.

SAYED, F. A., KODAMA, L., UDEOCHU, J. C., FAN, L., CARLING, G. K., LE, D., LI, Q., ZHOU, L., MATHYS, H., WANG, M., NIU, X., MAZUTIS, L., JIANG, X., WANG, X., WONG, M. Y., GAO, F., TELPOUKHOVSKAIA, M., TRACY, T. E., FROST, G., ZHOU, Y., LI, Y., BRENDEL, M., QIU, Y., CHENG, Z., YU, G., HARDY, J., COPPOLA, G., GONG, S., WANG, F., DETURE, M. A., ZHANG, B., XIE, L., DICKSON, D. W., LUO, W. & GAN, L. 2020. AD-linked R47H-TREM2 mutation induces disease-enhancing proinflammatory microglial states in mice and humans. *bioRxiv***,** 2020.07.24.218719.

SCHAFER, D. P., LEHRMAN, E. K., KAUTZMAN, A. G., KOYAMA, R., MARDINLY, A. R., YAMASAKI, R., RANSOHOFF, R. M., GREENBERG, M. E., BARRES, B. A. & STEVENS, B. 2012. Microglia sculpt postnatal neural circuits in an activity and complement-dependent manner. *Neuron,* 74**,** 691-705.

SCHEIBLICH, H., ROLOFF, F., SINGH, V., STANGEL, M., STERN, M. & BICKER, G. 2014. Nitric oxide/cyclic GMP signaling regulates motility of a microglial cell line and primary microglia in vitro. *Brain Res,* 1564**,** 9-21.

SCHILLING, T., NITSCH, R., HEINEMANN, U., HAAS, D. & EDER, C. 2001. Astrocyte-released cytokines induce ramification and outward K+ channel expression in microglia via distinct signalling pathways. *Eur J Neurosci,* 14**,** 463-73.

SCHLAEGER, T. M., DAHERON, L., BRICKLER, T. R., ENTWISLE, S., CHAN, K., CIANCI, A., DEVINE, A., ETTENGER, A., FITZGERALD, K., GODFREY, M., GUPTA, D., MCPHERSON, J., MALWADKAR, P., GUPTA, M., BELL, B., DOI, A., JUNG, N., LI, X., LYNES, M. S., BROOKES, E., CHERRY, A. B., DEMIRBAS, D., TSANKOV, A. M., ZON, L. I., RUBIN, L. L., FEINBERG, A. P., MEISSNER, A., COWAN, C. A. & DALEY, G. Q. 2015. A comparison of non-integrating reprogramming methods. *Nat Biotechnol,* 33**,** 58-63.

SCHMID, B., PREHN, K. R., NIMSANOR, N., GARCIA, B. I. A., POULSEN, U., JORRING, I., RASMUSSEN, M. A., CLAUSEN, C., MAU-HOLZMANN, U. A., RAMAKRISHNA, S., MUDDASHETTY, R., STEEG, R., BRUCE, K., MACKINTOSH, P., EBNETH, A., HOLST, B. & CABRERA-SOCORRO, A. 2019. Generation of a set of isogenic, gene-edited iPSC lines homozygous for all main APOE variants and an APOE knock-out line. *Stem Cell Res,* 34**,** 101349.

SCHULZ, C., GOMEZ PERDIGUERO, E., CHORRO, L., SZABO-ROGERS, H., CAGNARD, N., KIERDORF, K., PRINZ, M., WU, B., JACOBSEN, S. E., POLLARD, J. W., FRAMPTON, J., LIU, K. J. & GEISSMANN, F. 2012. A lineage of myeloid cells independent of Myb and hematopoietic stem cells. *Science,* 336**,** 86-90.

SCOTT, C. C., DOBSON, W., BOTELHO, R. J., COADY-OSBERG, N., CHAVRIER, P., KNECHT, D. A., HEATH, C., STAHL, P. & GRINSTEIN, S. 2005. Phosphatidylinositol-4,5-

bisphosphate hydrolysis directs actin remodeling during phagocytosis. *J Cell Biol,* 169**,** 139-49.

SEKHSARIA, S., FLEISHER, T. A., VOWELLS, S., BROWN, M., MILLER, J., GORDON, I., BLAESE, R. M., DUNBAR, C. E., LEITMAN, S. & MALECH, H. L. 1996. Granulocyte colony-stimulating factor recruitment of CD34+ progenitors to peripheral blood: impaired mobilization in chronic granulomatous disease and adenosine deaminase--deficient severe combined immunodeficiency disease patients. *Blood,* 88**,** 1104-12.

SEKI, T., YUASA, S. & FUKUDA, K. 2012. Generation of induced pluripotent stem cells from a small amount of human peripheral blood using a combination of activated T cells and Sendai virus. *Nat Protoc,* 7**,** 718-28.

SEKI, T., YUASA, S., ODA, M., EGASHIRA, T., YAE, K., KUSUMOTO, D., NAKATA, H., TOHYAMA, S., HASHIMOTO, H., KODAIRA, M., OKADA, Y., SEIMIYA, H., FUSAKI, N., HASEGAWA, M. & FUKUDA, K. 2010. Generation of induced pluripotent stem cells from human terminally differentiated circulating T cells. *Cell Stem Cell,* 7**,** 11-4.

SENGUPTA, U., NILSON, A. N. & KAYED, R. 2016. The Role of Amyloid-β Oligomers in Toxicity, Propagation, and Immunotherapy. *EBioMedicine,* 6**,** 42-49.

SERIO, A., BILICAN, B., BARMADA, S. J., ANDO, D. M., ZHAO, C., SILLER, R., BURR, K., HAGHI, G., STORY, D., NISHIMURA, A. L., CARRASCO, M. A., PHATNANI, H. P., SHUM, C., WILMUT, I., MANIATIS, T., SHAW, C. E., FINKBEINER, S. & CHANDRAN, S. 2013. Astrocyte pathology and the absence of non-cell autonomy in an induced pluripotent stem cell model of TDP-43 proteinopathy. *Proc Natl Acad Sci U S A,* 110**,** 4697-702.

SHAH, A. J., SMOGORZEWSKA, E. M., HANNUM, C. & CROOKS, G. M. 1996. Flt3 ligand induces proliferation of quiescent human bone marrow CD34+CD38- cells and maintains progenitor cells in vitro. *Blood,* 87**,** 3563-70.

SHARMA, A., MUCKE, M. & SEIDMAN, C. E. 2018. Human Induced Pluripotent Stem Cell Production and Expansion from Blood using a Non-Integrating Viral Reprogramming Vector. *Curr Protoc Mol Biol,* 122**,** e58.

SHEN, R., ZHAO, X., HE, L., DING, Y., XU, W., LIN, S., FANG, S., YANG, W., SUNG, K., SPENCER, B., RISSMAN, R. A., LEI, M., DING, J. & WU, C. 2020. Upregulation of RIN3 induces endosomal dysfunction in Alzheimer's disease. *Transl Neurodegener,* 9**,** 26.

SHENG, J., RUEDL, C. & KARJALAINEN, K. 2015. Most Tissue-Resident Macrophages Except Microglia Are Derived from Fetal Hematopoietic Stem Cells. *Immunity,* 43**,** 382-93.

SHENG, M., SABATINI, B. L. & SÜDHOF, T. C. 2012. Synapses and Alzheimer's disease. *Cold Spring Harbor perspectives in biology,* 4**,** a005777.

SHI, J., ZHAO, Y., WANG, Y., GAO, W., DING, J., LI, P., HU, L. & SHAO, F. 2014. Inflammatory caspases are innate immune receptors for intracellular LPS. *Nature,* 514**,** 187-92.

SHI, Y., KIRWAN, P. & LIVESEY, F. J. 2012a. Directed differentiation of human pluripotent stem cells to cerebral cortex neurons and neural networks. *Nat Protoc,* 7**,** 1836-46.

SHI, Y., KIRWAN, P., SMITH, J., ROBINSON, H. P. & LIVESEY, F. J. 2012b. Human cerebral cortex development from pluripotent stem cells to functional excitatory synapses. *Nat Neurosci,* 15**,** 477-86, s1.

SIDDIQUI, T. A., LIVELY, S., VINCENT, C. & SCHLICHTER, L. C. 2012. Regulation of podosome formation, microglial migration and invasion by Ca(2+)-signaling molecules expressed in podosomes. *J Neuroinflammation,* 9**,** 250.

SIERRA, A., ENCINAS, J. M., DEUDERO, J. J., CHANCEY, J. H., ENIKOLOPOV, G., OVERSTREET-WADICHE, L. S., TSIRKA, S. E. & MALETIC-SAVATIC, M. 2010. Microglia shape adult hippocampal neurogenesis through apoptosis-coupled phagocytosis. *Cell Stem Cell,* 7**,** 483-95.

SIEVERS, J., PARWARESCH, R. & WOTTGE, H. U. 1994. Blood monocytes and spleen macrophages differentiate into microglia-like cells on monolayers of astrocytes: morphology. *Glia,* 12**,** 245-58.

SIMS, R., HILL, M. & WILLIAMS, J. 2020. The multiplex model of the genetics of Alzheimer's disease. *Nat Neurosci,* 23**,** 311-322.

SIMS, R., VAN DER LEE, S. J., NAJ, A. C., BELLENGUEZ, C., BADARINARAYAN, N., JAKOBSDOTTIR, J., KUNKLE, B. W., BOLAND, A., RAYBOULD, R., BIS, J. C., MARTIN, E. R., GRENIER-BOLEY, B., HEILMANN-HEIMBACH, S., CHOURAKI, V., KUZMA, A. B., SLEEGERS, K., VRONSKAYA, M., RUIZ, A., GRAHAM, R. R., OLASO, R., HOFFMANN, P., GROVE, M. L., VARDARAJAN, B. N., HILTUNEN, M., NOTHEN, M. M., WHITE, C. C., HAMILTON-NELSON, K. L., EPELBAUM, J., MAIER, W., CHOI, S. H., BEECHAM, G. W., DULARY, C., HERMS, S., SMITH, A. V., FUNK, C. C., DERBOIS, C., FORSTNER, A. J., AHMAD, S., LI, H., BACQ, D., HAROLD, D., SATIZABAL, C. L., VALLADARES, O., SQUASSINA, A., THOMAS, R., BRODY, J. A., QU, L., SANCHEZ-JUAN, P., MORGAN, T., WOLTERS, F. J., ZHAO, Y., GARCIA, F. S., DENNING, N., FORNAGE, M., MALAMON, J., NARANJO, M. C. D., MAJOUNIE, E., MOSLEY, T. H., DOMBROSKI, B., WALLON, D., LUPTON, M. K., DUPUIS, J., WHITEHEAD, P., FRATIGLIONI, L., MEDWAY, C., JIAN, X., MUKHERJEE, S., KELLER, L., BROWN, K., LIN, H., CANTWELL, L. B., PANZA, F., MCGUINNESS, B., MORENO-GRAU, S., BURGESS, J. D., SOLFRIZZI, V., PROITSI, P., ADAMS, H. H., ALLEN, M., SERIPA, D., PASTOR, P., CUPPLES, L. A., PRICE, N. D., HANNEQUIN, D., FRANK-GARCIA, A., LEVY, D., CHAKRABARTY, P., CAFFARRA, P., GIEGLING, I., BEISER, A. S., GIEDRAITIS, V., HAMPEL, H., GARCIA, M. E., WANG, X., LANNFELT, L., MECOCCI, P., EIRIKSDOTTIR, G., CRANE, P. K., PASQUIER, F., BOCCARDI, V., et al. 2017. Rare coding variants in PLCG2, ABI3, and TREM2 implicate microglial-mediated innate immunity in Alzheimer's disease. *Nat Genet,* 49**,** 1373-1384.

SIMS, R. & WILLIAMS, J. 2016. Defining the Genetic Architecture of Alzheimer's Disease: Where Next. *Neurodegener Dis,* 16**,** 6-11.

SONDAG, C. M., DHAWAN, G. & COMBS, C. K. 2009. Beta amyloid oligomers and fibrils stimulate differential activation of primary microglia. *J Neuroinflammation,* 6**,** 1.

SONG, W., HOOLI, B., MULLIN, K., JIN, S. C., CELLA, M., ULLAND, T. K., WANG, Y., TANZI, R. E. & COLONNA, M. 2017. Alzheimer's disease-associated TREM2 variants exhibit either decreased or increased ligand-dependent activation. *Alzheimers Dement,* 13**,** 381-387.

SOUZA, L. M., BOONE, T. C., GABRILOVE, J., LAI, P. H., ZSEBO, K. M., MURDOCK, D. C., CHAZIN, V. R., BRUSZEWSKI, J., LU, H., CHEN, K. K., BARENDT, J., PLATZER, E., MOORE, M. A. S., MERTELSMANN, R. & WELTE, K. 1986. Recombinant human granulocyte colony-stimulating factor: effects on normal and leukemic myeloid cells. *Science,* 232**,** 61-5.

SPITTAU, B. 2017. Aging Microglia-Phenotypes, Functions and Implications for Age-Related Neurodegenerative Diseases. *Front Aging Neurosci,* 9**,** 194.

SQUARZONI, P., OLLER, G., HOEFFEL, G., PONT-LEZICA, L., ROSTAING, P., LOW, D., BESSIS, A., GINHOUX, F. & GAREL, S. 2014. Microglia modulate wiring of the embryonic forebrain. *Cell Rep,* 8**,** 1271-9.

STAERK, J., DAWLATY, M. M., GAO, Q., MAETZEL, D., HANNA, J., SOMMER, C. A., MOSTOSLAVSKY, G. & JAENISCH, R. 2010. Reprogramming of human peripheral blood cells to induced pluripotent stem cells. *Cell Stem Cell,* 7**,** 20-4.

STEICHEN, C., LUCE, E., MALUENDA, J., TOSCA, L., MORENO-GIMENO, I., DESTERKE, C., DIANAT, N., GOULINET-MAINOT, S., AWAN-TOOR, S., BURKS, D., MARIE, J., WEBER, A., TACHDJIAN, G., MELKI, J. & DUBART-KUPPERSCHMITT, A. 2014. Messenger RNA-versus retrovirus-based induced pluripotent stem cell reprogramming strategies: analysis of genomic integrity. *Stem Cells Transl Med,* 3**,** 686-91.

STEVENS, C. F. & SULLIVAN, J. M. 1998. Regulation of the readily releasable vesicle pool by protein kinase C. *Neuron,* 21**,** 885-93.

STEWART, C. R., STUART, L. M., WILKINSON, K., VAN GILS, J. M., DENG, J., HALLE, A., RAYNER, K. J., BOYER, L., ZHONG, R., FRAZIER, W. A., LACY-HULBERT, A., EL KHOURY, J., GOLENBOCK, D. T. & MOORE, K. J. 2010. CD36 ligands promote sterile inflammation through assembly of a Toll-like receptor 4 and 6 heterodimer. *Nat Immunol,* 11**,** 155-61.

STREB, H., IRVINE, R. F., BERRIDGE, M. J. & SCHULZ, I. 1983. Release of Ca2+ from a nonmitochondrial intracellular store in pancreatic acinar cells by inositol-1,4,5-trisphosphate. *Nature,* 306**,** 67-9.

STURGEON, C. M., DITADI, A., AWONG, G., KENNEDY, M. & KELLER, G. 2014. Wnt signaling controls the specification of definitive and primitive hematopoiesis from human pluripotent stem cells. *Nat Biotechnol,* 32**,** 554-61.

SUN, M. K. & ALKON, D. L. 2010. Pharmacology of protein kinase C activators: cognition-enhancing and antidementic therapeutics. *Pharmacol Ther,* 127**,** 66-77.

SUSLOV, O. N., KUKEKOV, V. G., IGNATOVA, T. N. & STEINDLER, D. A. 2002. Neural stem cell heterogeneity demonstrated by molecular phenotyping of clonal neurospheres. *Proc Natl Acad Sci U S A,* 99**,** 14506-11.

SUZUMURA, A., SAWADA, M., YAMAMOTO, H. & MARUNOUCHI, T. 1990. Effects of colony stimulating factors on isolated microglia in vitro. *J Neuroimmunol,* 30**,** 111-20.

SVOBODA, D. S., BARRASA, M. I., SHU, J., RIETJENS, R., ZHANG, S., MITALIPOVA, M., BERUBE, P., FU, D., SHULTZ, L. D., BELL, G. W. & JAENISCH, R. 2019. Human iPSC-derived microglia assume a primary microglia-like state after transplantation into the neonatal mouse brain. *Proc Natl Acad Sci U S A,* 116**,** 25293-25303.

SWANSON, K. V., DENG, M. & TING, J. P. 2019. The NLRP3 inflammasome: molecular activation and regulation to therapeutics. *Nat Rev Immunol,* 19**,** 477-489.

SWARDFAGER, W., LANCTÔT, K., ROTHENBURG, L., WONG, A., CAPPELL, J. & HERRMANN, N. 2010. A meta-analysis of cytokines in Alzheimer's disease. *Biol Psychiatry,* 68**,** 930-41.

SZEPESI, Z., MANOUCHEHRIAN, O., BACHILLER, S. & DEIERBORG, T. 2018. Bidirectional Microglia–Neuron Communication in Health and Disease. *Frontiers in Cellular Neuroscience,* 12.

TAKAHASHI, K., TANABE, K., OHNUKI, M., NARITA, M., ICHISAKA, T., TOMODA, K. & YAMANAKA, S. 2007. Induction of pluripotent stem cells from adult human fibroblasts by defined factors. *Cell,* 131**,** 861-72.

TAKAHASHI, K. & YAMANAKA, S. 2006. Induction of pluripotent stem cells from mouse embryonic and adult fibroblast cultures by defined factors. *Cell,* 126**,** 663-76.

TAKAHASHI, T., LORD, B., SCHULZE, P. C., FRYER, R. M., SARANG, S. S., GULLANS, S. R. & LEE, R. T. 2003. Ascorbic acid enhances differentiation of embryonic stem cells into cardiac myocytes. *Circulation,* 107**,** 1912-6.

TAKALO, M., WITTRAHM, R., WEFERS, B., PARHIZKAR, S., JOKIVARSI, K., KUULASMAA, T., MÄKINEN, P., MARTISKAINEN, H., WURST, W., XIANG, X., MARTTINEN, M., POUTIAINEN, P., HAAPASALO, A., HILTUNEN, M. & HAASS, C. 2020. The Alzheimer's disease-associated protective Plcγ2-P522R variant promotes immune functions. *Mol Neurodegener,* 15**,** 52.

TAKATA, K., KOZAKI, T., LEE, C. Z. W., THION, M. S., OTSUKA, M., LIM, S., UTAMI, K. H., FIDAN, K., PARK, D. S., MALLERET, B., CHAKAROV, S., SEE, P., LOW, D., LOW, G., GARCIA-MIRALLES, M., ZENG, R., ZHANG, J., GOH, C. C., GUL, A., HUBERT, S., LEE, B., CHEN, J., LOW, I., SHADAN, N. B., LUM, J., WEI, T. S., MOK, E., KAWANISHI, S., KITAMURA, Y., LARBI, A., POIDINGER, M., RENIA, L., NG, L. G., WOLF, Y., JUNG, S., ONDER, T., NEWELL, E., HUBER, T., ASHIHARA, E., GAREL, S., POULADI, M. A. & GINHOUX, F. 2017. Induced-Pluripotent-Stem-Cell-Derived Primitive Macrophages Provide a Platform for Modeling Tissue-Resident Macrophage Differentiation and Function. *Immunity,* 47**,** 183-198.e6.

TAN, M. S., YU, J. T., JIANG, T., ZHU, X. C., GUAN, H. S. & TAN, L. 2014. IL12/23 p40 inhibition ameliorates Alzheimer's disease-associated neuropathology and spatial memory in SAMP8 mice. *J Alzheimers Dis,* 38**,** 633-46.

TANAKA, J. & MAEDA, N. 1996. Microglial ramification requires nondiffusible factors derived from astrocytes. *Exp Neurol,* 137**,** 367-75.

TAPIA-ROJAS, C., CABEZAS-OPAZO, F., DEATON, C. A., VERGARA, E. H., JOHNSON, G. V. W. & QUINTANILLA, R. A. 2019. It's all about tau. *Prog Neurobiol,* 175**,** 54-76.

TARKOWSKI, E., ANDREASEN, N., TARKOWSKI, A. & BLENNOW, K. 2003. Intrathecal inflammation precedes development of Alzheimer's disease. *J Neurol Neurosurg Psychiatry,* 74**,** 1200-5.

TELLECHEA, P., PUJOL, N., ESTEVE-BELLOCH, P., ECHEVESTE, B., GARCIA-EULATE, M. R., ARBIZU, J. & RIVEROL, M. 2018. Early- and late-onset Alzheimer disease: Are they the same entity? *Neurologia,* 33**,** 244-253.

TERRY, R. D., MASLIAH, E., SALMON, D. P., BUTTERS, N., DETERESA, R., HILL, R., HANSEN, L. A. & KATZMAN, R. 1991. Physical basis of cognitive alterations in Alzheimer's disease: synapse loss is the major correlate of cognitive impairment. *Ann Neurol,* 30**,** 572-80.

THORNTON, P., SEVALLE, J., DEERY, M. J., FRASER, G., ZHOU, Y., STÅHL, S., FRANSSEN, E. H., DODD, R. B., QAMAR, S., GOMEZ PEREZ-NIEVAS, B., NICOL, L. S., EKETJÄLL, S., REVELL, J., JONES, C., BILLINTON, A., ST GEORGE-HYSLOP, P. H., CHESSELL, I. & CROWTHER, D. C. 2017. TREM2 shedding by cleavage at the H157-S158 bond is accelerated for the Alzheimer's disease-associated H157Y variant. *EMBO Mol Med,* 9**,** 1366-1378.

TIFFANY, H. L., LAVIGNE, M. C., CUI, Y. H., WANG, J. M., LETO, T. L., GAO, J. L. & MURPHY, P. M. 2001. Amyloid-beta induces chemotaxis and oxidant stress by acting at formylpeptide receptor 2, a G protein-coupled receptor expressed in phagocytes and brain. *J Biol Chem,* 276**,** 23645-52.

TISCHER, J., KRUEGER, M., MUELLER, W., STASZEWSKI, O., PRINZ, M., STREIT, W. J. & BECHMANN, I. 2016. Inhomogeneous distribution of Iba-1 characterizes microglial pathology in Alzheimer's disease. *Glia,* 64**,** 1562-72.

TORIBIO, M. L., DE LA HERA, A., MARCOS, M. A., MARQUEZ, C. & MARTINEZ, C. 1989. Activation of the interleukin 2 pathway precedes CD3-T cell receptor expression in thymic development. Differential growth requirements of early and mature intrathymic subpopulations. *Eur J Immunol,* 19**,** 9-15.

TOZAKI-SAITOH, H., TSUDA, M. & INOUE, K. 2011. Role of purinergic receptors in CNS function and neuroprotection. *Adv Pharmacol,* 61**,** 495-528.

TREE, T. I., ROEP, B. O. & PEAKMAN, M. 2004. Enhancing the sensitivity of assays to detect T cell reactivity: the effect of cell separation and cryopreservation media. *Ann N Y Acad Sci,* 1037**,** 26-32.

TREMBLAY, M., STEVENS, B., SIERRA, A., WAKE, H., BESSIS, A. & NIMMERJAHN, A. 2011. The role of microglia in the healthy brain. *J Neurosci,* 31**,** 16064-9.

TSAI, A. P., LIN, P. B., DONG, C., MOUTINHO, M., CASALI, B. T., LIU, Y., LAMB, B. T., LANDRETH, G. E., OBLAK, A. L. & NHO, K. 2021. INPP5D expression is associated with risk for Alzheimer's disease and induced by plaque-associated microglia. *Neurobiol Dis,* 153**,** 105303.

TSAKIRIDIS, A., HUANG, Y., BLIN, G., SKYLAKI, S., WYMEERSCH, F., OSORNO, R., ECONOMOU, C., KARAGIANNI, E., ZHAO, S., LOWELL, S. & WILSON, V. 2014. Distinct Wnt-driven primitive streak-like populations reflect in vivo lineage precursors. *Development,* 141**,** 1209-21.

ULLIAN, E. M., SAPPERSTEIN, S. K., CHRISTOPHERSON, K. S. & BARRES, B. A. 2001. Control of synapse number by glia. *Science,* 291**,** 657-61.

VAN CAUWENBERGHE, C., VAN BROECKHOVEN, C. & SLEEGERS, K. 2016. The genetic landscape of Alzheimer disease: clinical implications and perspectives. *Genet Med,* 18**,** 421-30.

VAN DER WAL, E. A., GÓMEZ-PINILLA, F. & COTMAN, C. W. 1993. Transforming growth factor-beta 1 is in plaques in Alzheimer and Down pathologies. *Neuroreport,* 4**,** 69-72.

VAN WILGENBURG, B., BROWNE, C., VOWLES, J. & COWLEY, S. A. 2013. Efficient, long term production of monocyte-derived macrophages from human pluripotent stem cells under partly-defined and fully-defined conditions. *PLoS One,* 8**,** e71098.

VAN WINKLE, A. P., GATES, I. D. & KALLOS, M. S. 2012. Mass transfer limitations in embryoid bodies during human embryonic stem cell differentiation. *Cells Tissues Organs,* 196**,** 34-47.

VARGA, E., HANSEN, M., WÜST, T., VON LINDERN, M. & VAN DEN AKKER, E. 2017. Generation of human erythroblast-derived iPSC line using episomal reprogramming system. *Stem Cell Res,* 25**,** 30-33.

VENEGAS, C. & HENEKA, M. T. 2017. Danger-associated molecular patterns in Alzheimer's disease. *J Leukoc Biol,* 101**,** 87-98.

VILLEGAS-LLERENA, C., PHILLIPS, A., GARCIA-REITBOECK, P., HARDY, J. & POCOCK, J. M. 2016. Microglial genes regulating neuroinflammation in the progression of Alzheimer's disease. *Curr Opin Neurobiol,* 36**,** 74-81.

VIVIANI, B. 2006. Preparation and coculture of neurons and glial cells. *Curr Protoc Cell Biol,* Chapter 2**,** Unit 2.7.

VOLPATO, V. & WEBBER, C. 2020. Addressing variability in iPSC-derived models of human disease: guidelines to promote reproducibility. *Dis Model Mech,* 13.

VOM BERG, J., PROKOP, S., MILLER, K. R., OBST, J., KÄLIN, R. E., LOPATEGUI-CABEZAS, I., WEGNER, A., MAIR, F., SCHIPKE, C. G., PETERS, O., WINTER, Y., BECHER, B. & HEPPNER, F. L. 2012. Inhibition of IL-12/IL-23 signaling reduces Alzheimer's disease-like pathology and cognitive decline. *Nat Med,* 18**,** 1812-9.

WAKE, H., MOORHOUSE, A. J., MIYAMOTO, A. & NABEKURA, J. 2013. Microglia: actively surveying and shaping neuronal circuit structure and function. *Trends Neurosci,* 36**,** 209-17.

WANG, D., FENG, J., WEN, R., MARINE, J. C., SANGSTER, M. Y., PARGANAS, E., HOFFMEYER, A., JACKSON, C. W., CLEVELAND, J. L., MURRAY, P. J. & IHLE, J. N. 2000. Phospholipase Cgamma2 is essential in the functions of B cell and several Fc receptors. *Immunity,* 13**,** 25-35.

WANG, J., SOHN, H., SUN, G., MILNER, J. D. & PIERCE, S. K. 2014. The autoinhibitory C-terminal SH2 domain of phospholipase C-γ2 stabilizes B cell receptor signalosome assembly. *Sci Signal,* 7**,** ra89.

WANG, L., WANG, L., HUANG, W., SU, H., XUE, Y., SU, Z., LIAO, B., WANG, H., BAO, X., QIN, D., HE, J., WU, W., SO, K. F., PAN, G. & PEI, D. 2013. Generation of integration-free neural progenitor cells from cells in human urine. *Nat Methods,* 10**,** 84-9.

WANG, W. Y., TAN, M. S., YU, J. T. & TAN, L. 2015a. Role of pro-inflammatory cytokines released from microglia in Alzheimer's disease. *Ann Transl Med,* 3**,** 136.

WANG, X. J., YE, M., ZHANG, Y. H. & CHEN, S. D. 2007. CD200-CD200R regulation of microglia activation in the pathogenesis of Parkinson's disease. *J Neuroimmune Pharmacol,* 2**,** 259-64.

WANG, Y., CELLA, M., MALLINSON, K., ULRICH, J. D., YOUNG, K. L., ROBINETTE, M. L., GILFILLAN, S., KRISHNAN, G. M., SUDHAKAR, S., ZINSELMEYER, B. H., HOLTZMAN, D. M., CIRRITO, J. R. & COLONNA, M. 2015b. TREM2 lipid sensing sustains the microglial response in an Alzheimer's disease model. *Cell,* 160**,** 1061-71.

WEINBERG, A., SONG, L. Y., WILKENING, C., SEVIN, A., BLAIS, B., LOUZAO, R., STEIN, D., DEFECHEREUX, P., DURAND, D., RIEDEL, E., RAFTERY, N., JESSER, R., BROWN, B., KELLER, M. F., DICKOVER, R., MCFARLAND, E. & FENTON, T. 2009. Optimization and limitations of use of cryopreserved peripheral blood mononuclear cells for functional and phenotypic T-cell characterization. *Clin Vaccine Immunol,* 16**,** 1176-86.

WEINBERG, A., ZHANG, L., BROWN, D., ERICE, A., POLSKY, B., HIRSCH, M. S., OWENS, S. & LAMB, K. 2000. Viability and functional activity of cryopreserved mononuclear cells. *Clin Diagn Lab Immunol,* 7**,** 714-6.

WEINGARTEN, M. D., LOCKWOOD, A. H., HWO, S. Y. & KIRSCHNER, M. W. 1975. A protein factor essential for microtubule assembly. *Proc Natl Acad Sci U S A,* 72**,** 1858-62.

WESSELSCHMIDT, R. L. 2011. The teratoma assay: an in vivo assessment of pluripotency. *Methods Mol Biol,* 767**,** 231-41.

WIGHTMAN, D. P., JANSEN, I. E., SAVAGE, J. E., SHADRIN, A. A., BAHRAMI, S., HOLLAND, D., RONGVE, A., BØRTE, S., WINSVOLD, B. S., DRANGE, O. K., MARTINSEN, A. E., SKOGHOLT, A. H., WILLER, C., BRÅTHEN, G., BOSNES, I., NIELSEN, J. B., FRITSCHE, L. G., THOMAS, L. F., PEDERSEN, L. M., GABRIELSEN, M. E., JOHNSEN, M. B., MEISINGSET, T. W., ZHOU, W., PROITSI, P., HODGES, A., DOBSON, R., VELAYUDHAN, L., SEALOCK, J. M., DAVIS, L. K., PEDERSEN, N. L., REYNOLDS, C. A., KARLSSON, I. K., MAGNUSSON, S., STEFANSSON, H., THORDARDOTTIR, S., JONSSON, P. V., SNAEDAL, J., ZETTERGREN, A., SKOOG, I., KERN, S., WAERN, M., ZETTERBERG, H., BLENNOW, K., STORDAL, E., HVEEM, K., ZWART, J. A., ATHANASIU, L., SELNES, P., SALTVEDT, I., SANDO, S. B., ULSTEIN, I., DJUROVIC, S., FLADBY, T., AARSLAND, D., SELBÆK, G., RIPKE, S., STEFANSSON, K., ANDREASSEN, O. A. & POSTHUMA, D. 2021. A genome-wide association study with 1,126,563 individuals identifies new risk loci for Alzheimer's disease. *Nat Genet,* 53**,** 1276-1282.

WINGO, T. S., LAH, J. J., LEVEY, A. I. & CUTLER, D. J. 2012. Autosomal recessive causes likely in early-onset Alzheimer disease. *Arch Neurol,* 69**,** 59-64.

WINTER, J. M., JACOBSON, P., BULLOUGH, B., CHRISTENSEN, A. P., BOYER, M. & REEMS, J. A. 2014. Long-term effects of cryopreservation on clinically prepared hematopoietic progenitor cell products. *Cytotherapy,* 16**,** 965-75.

WIßFELD, J., MATHEWS, M., MOSSAD, O., PICARDI, P., CINTI, A., REDAELLI, L., PRADIER, L., BRÜSTLE, O. & NEUMANN, H. 2021. Reporter cell assay for human CD33 validated by specific antibodies and human iPSC-derived microglia. *Sci Rep,* 11**,** 13462.

WITOELAR, A., RONGVE, A., ALMDAHL, I. S., ULSTEIN, I. D., ENGVIG, A., WHITE, L. R., SELBÆK, G., STORDAL, E., ANDERSEN, F., BRÆKHUS, A., SALTVEDT, I., ENGEDAL, K., HUGHES, T., BERGH, S., BRÅTHEN, G., BOGDANOVIC, N., BETTELLA, F., WANG, Y., ATHANASIU, L., BAHRAMI, S., LE HELLARD, S., GIDDALURU, S., DALE, A. M., SANDO, S. B., STEINBERG, S., STEFANSSON, H., SNAEDAL, J., DESIKAN, R. S., STEFANSSON, K., AARSLAND, D., DJUROVIC, S., FLADBY, T. & ANDREASSEN, O. A. 2018. Meta-analysis of Alzheimer's disease on 9,751 samples from Norway and IGAP study identifies four risk loci. *Sci Rep,* 8**,** 18088.

WONDERS, C. P. & ANDERSON, S. A. 2006. The origin and specification of cortical interneurons. *Nat Rev Neurosci,* 7**,** 687-96.

XIANG, X., PIERS, T. M., WEFERS, B., ZHU, K., MALLACH, A., BRUNNER, B., KLEINBERGER, G., SONG, W., COLONNA, M., HERMS, J., WURST, W., POCOCK, J. M. & HAASS, C. 2018. The Trem2 R47H Alzheimer's risk variant impairs splicing and reduces Trem2 mRNA and protein in mice but not in humans. *Mol Neurodegener,* 13**,** 49.

XING, J., TITUS, A. R. & HUMPHREY, M. B. 2015. The TREM2-DAP12 signaling pathway in Nasu-Hakola disease: a molecular genetics perspective. *Res Rep Biochem,* 5**,** 89-100.

XU, M., ZHANG, L., LIU, G., JIANG, N., ZHOU, W. & ZHANG, Y. 2019. Pathological Changes in Alzheimer's Disease Analyzed Using Induced Pluripotent Stem Cell-Derived Human Microglia-Like Cells. *J Alzheimers Dis,* 67**,** 357-368.

XU, S., HUO, J., LEE, K. G., KUROSAKI, T. & LAM, K. P. 2009. Phospholipase Cgamma2 is critical for Dectin-1-mediated Ca2+ flux and cytokine production in dendritic cells. *J Biol Chem,* 284**,** 7038-46.

XU, Y., WEI, X., WANG, M., ZHANG, R., FU, Y., XING, M., HUA, Q. & XIE, X. 2013. Proliferation rate of somatic cells affects reprogramming efficiency. *J Biol Chem,* 288**,** 9767-9778.

XUE, Y., CAI, X., WANG, L., LIAO, B., ZHANG, H., SHAN, Y., CHEN, Q., ZHOU, T., LI, X., HOU, J., CHEN, S., LUO, R., QIN, D., PEI, D. & PAN, G. 2013. Generating a non-integrating human induced pluripotent stem cell bank from urine-derived cells. *PLoS One,* 8**,** e70573.

YABAL, M., CALLEJA, D. J., SIMPSON, D. S. & LAWLOR, K. E. 2019. Stressing out the mitochondria: Mechanistic insights into NLRP3 inflammasome activation. *J Leukoc Biol,* 105**,** 377-399.

YANG, J., WISE, L. & FUKUCHI, K. I. 2020. TLR4 Cross-Talk With NLRP3 Inflammasome and Complement Signaling Pathways in Alzheimer's Disease. *Front Immunol,* 11**,** 724.

YANG, J., ZHANG, P., KRISHNA, S., WANG, J., LIN, X., HUANG, H., XIE, D., GORENTLA, B., HUANG, R., GAO, J., LI, Q. J. & ZHONG, X. P. 2016. Unexpected positive control of NFκB and miR-155 by DGKα and ζ ensures effector and memory CD8+ T cell differentiation. *Oncotarget,* 7**,** 33744-64.

YANG, T., GUO, R. & ZHANG, F. 2019. Brain perivascular macrophages: Recent advances and implications in health and diseases. *CNS Neurosci Ther,* 25**,** 1318-1328.

YANG, W., MILLS, J. A., SULLIVAN, S., LIU, Y., FRENCH, D. L. & GADUE, P. 2008. iPSC Reprogramming from Human Peripheral Blood Using Sendai Virus Mediated Gene Transfer. *StemBook.* Cambridge (MA): Harvard Stem Cell Institute

YAO, J., HARVATH, L., GILBERT, D. L. & COLTON, C. A. 1990. Chemotaxis by a CNS macrophage, the microglia. *J Neurosci Res,* 27**,** 36-42.

YE, H. & WANG, Q. 2018. Efficient Generation of Non-Integration and Feeder-Free Induced Pluripotent Stem Cells from Human Peripheral Blood Cells by Sendai Virus. *Cell Physiol Biochem,* 50**,** 1318-1331.

YE, L., MUENCH, M. O., FUSAKI, N., BEYER, A. I., WANG, J., QI, Z., YU, J. & KAN, Y. W. 2013. Blood cell-derived induced pluripotent stem cells free of reprogramming factors generated by Sendai viral vectors. *Stem Cells Transl Med,* 2**,** 558-66.

YEH, F. L., WANG, Y., TOM, I., GONZALEZ, L. C. & SHENG, M. 2016. TREM2 Binds to Apolipoproteins, Including APOE and CLU/APOJ, and Thereby Facilitates Uptake of Amyloid-Beta by Microglia. *Neuron,* 91**,** 328-40.

YOSHIOKA, N., GROS, E., LI, H. R., KUMAR, S., DEACON, D. C., MARON, C., MUOTRI, A. R., CHI, N. C., FU, X. D., YU, B. D. & DOWDY, S. F. 2013. Efficient generation of human iPSCs by a synthetic self-replicative RNA. *Cell Stem Cell,* 13**,** 246-54.

YU, J., VODYANIK, M. A., SMUGA-OTTO, K., ANTOSIEWICZ-BOURGET, J., FRANE, J. L., TIAN, S., NIE, J., JONSDOTTIR, G. A., RUOTTI, V., STEWART, R., SLUKVIN, II & THOMSON, J. A. 2007. Induced pluripotent stem cell lines derived from human somatic cells. *Science,* 318**,** 1917-20.

YUSTE, J. E., TARRAGON, E., CAMPUZANO, C. M. & ROS-BERNAL, F. 2015. Implications of glial nitric oxide in neurodegenerative diseases. *Front Cell Neurosci,* 9**,** 322.

ZANONI, I., OSTUNI, R., MAREK, L. R., BARRESI, S., BARBALAT, R., BARTON, G. M., GRANUCCI, F. & KAGAN, J. C. 2011. CD14 controls the LPS-induced endocytosis of Toll-like receptor 4. *Cell,* 147**,** 868-80.

ZHANG, B., GAITERI, C., BODEA, L. G., WANG, Z., MCELWEE, J., PODTELEZHNIKOV, A. A., ZHANG, C., XIE, T., TRAN, L., DOBRIN, R., FLUDER, E., CLURMAN, B., MELQUIST, S., NARAYANAN, M., SUVER, C., SHAH, H., MAHAJAN, M., GILLIS, T., MYSORE, J., MACDONALD, M. E., LAMB, J. R., BENNETT, D. A., MOLONY, C., STONE, D. J., GUDNASON, V., MYERS, A. J., SCHADT, E. E., NEUMANN, H., ZHU, J. & EMILSSON, V. 2013. Integrated systems approach identifies genetic nodes and networks in late-onset Alzheimer's disease. *Cell,* 153**,** 707-20.

ZHANG, J., ZHANG, L., YI, S., JIANG, X., QIAO, Y., ZHANG, Y., XIAO, C. & ZHOU, T. 2020. Mouse Astrocytes Promote Microglial Ramification by Releasing TGF-β and Forming Glial Fibers. *Front Cell Neurosci,* 14**,** 195.

ZHANG, Y. W., THOMPSON, R., ZHANG, H. & XU, H. 2011. APP processing in Alzheimer's disease. *Mol Brain,* 4**,** 3.

ZHAO, Y., WU, X., LI, X., JIANG, L. L., GUI, X., LIU, Y., SUN, Y., ZHU, B., PIÑA-CRESPO, J. C., ZHANG, M., ZHANG, N., CHEN, X., BU, G., AN, Z., HUANG, T. Y. & XU, H. 2018. TREM2 Is a Receptor for β-Amyloid that Mediates Microglial Function. *Neuron,* 97**,** 1023-1031.e7.

ZHAO, Y., YI, W., LU, Y., LI, W. & WANG, H. 2021. Lipopolysaccharide induces BV2 microglial cell migration via a decrease in SET8 expression. *Can J Physiol Pharmacol,* 99**,** 667-675.

ZHOU, B., ZUO, Y. X. & JIANG, R. T. 2019. Astrocyte morphology: Diversity, plasticity, and role in neurological diseases. *CNS Neurosci Ther,* 25**,** 665-673.

ZHOU, H., MARTINEZ, H., SUN, B., LI, A., ZIMMER, M., KATSANIS, N., DAVIS, E. E., KURTZBERG, J., LIPNICK, S., NOGGLE, S., RAO, M. & CHANG, S. 2015. Rapid and Efficient Generation of Transgene-Free iPSC from a Small Volume of Cryopreserved Blood. *Stem Cell Rev Rep,* 11**,** 652-65.

ZHOU, H., WU, S., JOO, J. Y., ZHU, S., HAN, D. W., LIN, T., TRAUGER, S., BIEN, G., YAO, S., ZHU, Y., SIUZDAK, G., SCHOLER, H. R., DUAN, L. & DING, S. 2009. Generation of induced pluripotent stem cells using recombinant proteins. *Cell Stem Cell,* 4**,** 381-4.

ZHOU, J. M., XING, F. Y., SHI, J. J., FANG, Z. F., CHEN, X. J. & CHEN, F. 2008. Quality of embryonic bodies and seeding density effects on neural differentiation of mouse embryonic stem cells. *Cell Biol Int,* 32**,** 1169-75.

ZHOU, L. & VERSTREKEN, P. 2018. Reprogramming neurodegeneration in the big data era. *Curr Opin Neurobiol,* 48**,** 167-173.

ZHOU, Q., LEE, G. S., BRADY, J., DATTA, S., KATAN, M., SHEIKH, A., MARTINS, M. S., BUNNEY, T. D., SANTICH, B. H., MOIR, S., KUHNS, D. B., LONG PRIEL, D. A., OMBRELLO, A., STONE, D., OMBRELLO, M. J., KHAN, J., MILNER, J. D., KASTNER, D. L. & AKSENTIJEVICH, I. 2012a. A hypermorphic missense mutation in PLCG2, encoding phospholipase Cγ2, causes a dominantly inherited autoinflammatory disease with immunodeficiency. *Am J Hum Genet,* 91**,** 713-20.

ZHOU, T., BENDA, C., DUNZINGER, S., HUANG, Y., HO, J. C., YANG, J., WANG, Y., ZHANG, Y., ZHUANG, Q., LI, Y., BAO, X., TSE, H. F., GRILLARI, J., GRILLARI-VOGLAUER, R., PEI, D. & ESTEBAN, M. A. 2012b. Generation of human induced pluripotent stem cells from urine samples. *Nat Protoc,* 7**,** 2080-9.

ZHU, L., JONES, C. & ZHANG, G. 2018. The Role of Phospholipase C Signaling in Macrophage-Mediated Inflammatory Response. *J Immunol Res,* 2018**,** 5201759.

ZHU, X. C., TAN, L., WANG, H. F., JIANG, T., CAO, L., WANG, C., WANG, J., TAN, C. C., MENG, X. F. & YU, J. T. 2015. Rate of early onset Alzheimer's disease: a systematic review and meta-analysis. *Ann Transl Med,* 3**,** 38.